This electronic thesis or dissertation has been downloaded from the King's Research Portal at https://kclpure.kcl.ac.uk/portal/



The Role of Fascin and Drebrin in Neuroblast Migration in the Postnatal Brain

Sonego, Martina

Awarding institution:
King's College London

The copyright of this thesis rests with the author and no quotation from it or information derived from it may be published without proper acknowledgement.

END USER LICENCE AGREEMENT



Unless another licence is stated on the immediately following page this work is licensed

under a Creative Commons Attribution-NonCommercial-NoDerivatives 4.0 International

licence. https://creativecommons.org/licenses/by-nc-nd/4.0/

You are free to copy, distribute and transmit the work

Under the following conditions:

- Attribution: You must attribute the work in the manner specified by the author (but not in any way that suggests that they endorse you or your use of the work).
- Non Commercial: You may not use this work for commercial purposes.
- No Derivative Works - You may not alter, transform, or build upon this work.

Any of these conditions can be waived if you receive permission from the author. Your fair dealings and other rights are in no way affected by the above.

Take down policy

If you believe that this document breaches copyright please contact librarypure@kcl.ac.uk providing details, and we will remove access to the work immediately and investigate your claim.

Download date: 08. Oct. 2023

THE ROLE OF FASCIN AND DREBRIN

IN NEUROBLAST MIGRATION

IN THE POSTNATAL BRAIN

Martina Sonego

Thesis presented for the degree of Doctor of Philosophy

Wolfson Centre for Age-Related Diseases

King's College London

To Nonna Tona

whose life continues to inspire mine

Abstract

After birth, stem cells in the subventricular zone (SVZ) generate neuroblasts that migrate along the rostral migratory stream (RMS) to become interneurons in the olfactory bulb (OB). This migration is a fundamental event controlling the proper integration of new neurons in a pre-existing synaptic network. Many regulators of neuroblast migration have been identified; however, still very little is known about the intracellular molecular mechanisms controlling this process. We have investigated the function of fascin and drebrin, two actin-binding proteins highly expressed by RMS neuroblasts in the postnatal mammalian brain.

We show that *fascin-1* ko mice display an abnormal RMS and a smaller OB. Bromodeoxyuridine labeling experiments show that lack of fascin significantly impairs neuroblast migration, but does not affect cell proliferation. Moreover, fascin depletion alters the polarized morphology of rat neuroblasts. Protein kinase C (PKC)-dependent phosphorylation of fascin on Ser39 regulates its actin-bundling function. Postnatal electroporation of phosphomimetic (S39D) or nonphosphorylatable (S39A) fascin variants followed by time-lapse imaging of brain slices demonstrates that the phospho-dependent modulation of fascin function ensures efficient neuroblast migration. Fluorescence lifetime imaging microscopy (FLIM) studies in rat neuroblasts reveal that the interaction between fascin and PKC can be modulated by cannabinoid signaling, which controls neuroblast migration *in vivo*. These findings identify fascin as a crucial regulator of neuroblast motility. We propose that a tightly regulated phospho/dephospho-fascin cycle modulated by extracellular signals is required for the polarized migration of stem cell-derived neuroblasts.

Depletion of drebrin using different RNAi approaches affects neuroblast morphology and impairs neuroblast migration both *in vitro* and *in vivo*. Drebrin phosphorylation on Ser142 by Cdk5 promotes actin bundling and microtubule binding. Electroporation of phosphomimetic (S142D) or non-phosphorylatable (S142A) drebrin followed by time-lapse imaging shows decreased neuroblast migration compared to control. Our findings demonstrate that drebrin is necessary for efficient neuroblast migration and suggest that its phosphorylation on Ser142 plays an important role in regulating neuroblast orientation along the RMS.

Publications arising from this thesis

Fascin Regulates the Migration of Subventricular Zone-Derived Neuroblasts in the Postnatal Brain. The Journal of Neuroscience, July 2013, 33 (30): 12171–12185
Sonego M., Gajendra S., Parsons M., Ma Y., Hobbs C., Zentar M. P., Williams G., Machesky M. L., Doherty P., and Lalli G.

In vivo Postnatal Electroporation and Time-lapse Imaging of Neuroblast Migration in Mouse Acute Brain Slices. Journal of Visualized Experiments, e50905, doi:10.3791/50905 (2013).
Sonego M. *, Zhou Y. *, Oudin M.J., Doherty P., Lalli G.

Nucleofection of Rodent Neuroblasts to Study Neuroblast Migration In vitro. Journal of Visualized Experiments (81), e50989, doi:10.3791/50989 (2013).
Falenta K., Gajendra S., **Sonego M.**, Doherty P., Lalli G.

Transcriptional Basis for the Inhibition of Neural Stem Cell Proliferation and Migration by the TGFβ-Family Member GDF11. PLoS One, November 2013, 8 (11): e78478, doi: 10.1371/journal.pone.0078478.
Williams G., Zentar M.P., Gajendra S., **Sonego M.**, Doherty P., Lalli G.

Regional effects of endocannabinoid, BDNF and FGF receptor signalling on neuroblast motility and guidance along the rostral migratory stream. Submitted.
Zhou Y., Oudin M.J., Gajendra S., **Sonego M.**, Falenta K., Williams G., Lalli G., Doherty P.

Drebrin Regulates the Migration of Subventricular Zone-Derived Neuroblasts in the Postnatal Brain. In preparation.
Sonego M., Oberoi M., Gajendra S., Hendricusdottir R., Eickholt B.J., Worth D., Gordon-Weeks P., Doherty P., Lalli G.

Acknowledgements

First and foremost I would like to express my deep gratitude to Dr. Giovanna Lalli for the opportunity to work in her lab and for the constant support and endless time she dedicated to my research project. I thank her for giving me the freedom and space to find my own path. I am especially grateful that she shared with me her passion for science, and I am convinced that many of the things she taught me will continue to serve me in the future. I would like to thank Prof. Pat Doherty for his contributions to the big picture of my project, providing valuable intellectual support. I am grateful for his advice in challenging moments. I would like to thank Carl Hobbs for his wisdom in immunohistochemistry and for the numerous times he helped me with microscopy and technical issues, often at short notice and without hesitation. I would like to thank John Chesson, Brenda Williams and Ralph Wilson for their constant helpfulness, competence, reliability and kindness. I would like to thank Sangeetha Gajendra and Prav Singh for their friendship, which has manifested itself during numerous challenges and difficulties over the past four years. I also thank them for proofreading this thesis. I would like to thank Fiona Howell, Kasia Falenta, Zhou Ya and Rachel Markwick for their warm welcome to the office and for contributing to an enjoyable work environment. I would like to thank past and present members of the third floor of the Wolfson Centre for Age-Related Diseases, in particular Pippa, Rie, Ariana, Tom, Amelie, Merrick, Patricia, Olivia, Clare, Federica, Elisa, Lorenzo, Andrew, Sean, Katia, Melina, Madeleine and Umut. I would like to thank David Andersson for his extreme patience and advice teaching me calcium imaging. I would like to thank Hannes Kiesewetter for his precious friendship, for always being available and for his knowledgable help with the RT-PCR experiments. I would like to give special thanks to Gianluca Bello for accompanying me on our PhD adventure and for his help, especially during the first month. I would like to thank Cristina Trento and Laura Paneghetti for sharing both the good and the bad times. I would like to thank Bernie Keating and Valerie Ryan for being my Irish family in London, for giving me much useful advice, great support and friendship. I would like to thank Piero Savaris for sharing and preparing many a lunch during the writing of this thesis. I would like to thank Federica and Andrea for being my second home in London. I would like to thank my Italian friends Federica, Giada, Irene, Firi,

Davide, Luca, Tommaso, Michele, Lorenzo, Alessandro, Mauro and Thomas, who, though overseas, have been constantly present and have made it easier to be away from home. I would like to give a big thank you to my parents Caterina and Luciano for having supported my choices and for their precious advice and help. I would like to thank my brother Matteo for his multiple visits and always interesting and stimulating company. I would like to thank my relatives Vittorina, Orietta and Flavio for having been a close and supportive family. Finally, I would like to give my deepest thanks to Bertram Neurohr not only for having proof-read every single line of this manuscript, but especially for having closely supported me, always with a critical and clever view that has challenged and helped me throughout these years.

Contributors

All studies described in the thesis were conducted by myself with the following exceptions:

- Carl Hobbs performed the immunohistochemistry of paraffin-embedded sections in Chapter 3 and 4.
- Maddy Parsons performed the Fluorescence Life-time Imaging Microscopy analysis described in Chapter 3.
- Laura Machesky and Yafeng Ma provided the brains from wild type, heterozygous and *fascin-1* ko mice for the experiments described in Chapter 3.

I am very grateful to these collaborators for their invaluable help and expertise.

Table of Contents

Abstract **3**

Publications arising from this thesis **4**

Acknowledgements **5**

Contributors **7**

Table of Contents **8**

Table of Figures **13**

Table of Tables **15**

Supplementary movies on accompanying CD (Full description of legends for movies available on the CD) **15**

Abbreviations **17**

Chapter 1 Introduction **23**

1.1 Postnatal Neurogenesis **23**

1.1.1 History 23

1.1.2 The neurogenic niches in the Central Nervous System (CNS) 24

1.1.3 SVZ neurogenesis 29

1.1.4 Function of SVZ neurogenesis 33

1.1.5 Neurogenesis in the human brain 38

1.2 Neural progenitor migration **40**

1.2.1 RMS neuroblast migration 40

1.2.2 What regulates migration in the RMS 43

1.2.3 Radial migration in the OB 56

1.2.4 Intracellular regulation of neuroblast migration 57

1.2.5 Neuroblast migration in the injured brain 64

1.3 Fascin 66

1.3.1 History, molecular structure and expression 66

1.3.2 Biological functions 69

1.3.3 Fascin regulators 74

1.4 Drebrin 77

1.4.1 History, molecular structure and expression 77

1.4.2 Drebrin regulators 79

1.4.3 Biological function 83

1.5 Aim: investigation of intracellular mechanisms regulating neuroblast migration in the postnatal RMS 86

Chapter 2 Materials and Methods 87

2.1 Materials 87

2.1.1 Animals 87

2.1.2 Cell culture 87

2.1.3 Tissue culture 88

2.1.4 Immunohistochemistry 88

2.1.5 Immunocytochemistry 90

2.1.6 Molecular biology 90

2.1.7 Western Blotting 92

2.1.8 Compounds 94

2.1.9 Antibodies and dyes 95

2.2 Methods 97

2.2.1 Cell culture 97

2.2.2 Nucleofection 97

2.2.3 Electroporation 98

2.2.4 Brain slice culture 100
2.2.5 3-D Matrigel migration assay using RMS explants or aggregates 100
2.2.6 Time-lapse imaging 100
2.2.7 Analysis of migration 101
2.2.8 Bromodeoxyuridine injections 102
2.2.9 Counting of BrdU positive cells 102
2.2.10 Immunohistochemistry 103
2.2.11 Immunocytochemistry 104
2.2.12 Fluorescence lifetime imaging microscopy (FLIM) 105
2.2.13 Western Blotting 108
2.2.14 Statistical Analysis 108

Chapter 3 Fascin regulates neuroblast migration 110

3.1 Introduction 110

3.2 Results 112

3.2.1 Fascin is expressed along the rostral migratory stream (RMS) of postnatal and adult mouse brains 112
3.2.2 Genetic deletion of *fascin-1* affects brain and olfactory bulb (OB) size 112
3.2.3 *Fascin-1* ko mice show a smaller and thinner RMS 118
3.2.4 *Fascin-1* ko mice show abnormal neuroblast chain organization 121
3.2.5 Genetic deletion of fascin does not affect proliferation in the subventricular zone (SVZ) 124
3.2.6 Genetic deletion of fascin affects RMS neuroblast migration 126
3.2.7 Fascin is upregulated in migrating neuroblasts 129
3.2.8 Fascin is expressed in filopodia of RMS migrating neuroblasts 131
3.2.9 Fascin knockdown impairs RMS neuroblast morphology *in vitro* 133
3.2.10 siRNA-mediated fascin knockdown impairs neuroblast migration *in vitro* 136

3.2.11 shRNA-mediated fascin knockdown impairs neuroblast migration 141
3.2.12 Fascin knockdown impairs RMS neuroblast migration *ex vivo* 146
3.2.13 Fascin phosphorylation on Ser39 regulates neuroblast migration *in vitro* 153
3.2.14 Phosphorylation of fascin on Ser39 regulates *ex vivo* RMS neuroblast migration 158
3.2.15 Fascin overexpression and its phosphorylation at Ser39 influence neuroblast morphology and orientation 163
3.2.16 Fascin and PKC interact in RMS migrating neuroblasts 168
3.2.17 Fascin/PKC interaction depends on PKC activity 172
3.2.18 Cannabinoid signalling regulates fascin/PKC interaction in RMS migrating neuroblasts 175
3.2.19 Fascin may act as a downstream mediator of CB-promoted neuroblast migration. 179
3.3 Discussion 182
3.3.1 Fascin: a novel marker for RMS migrating neuroblasts 182
3.3.2 The role of Ser39 phosphorylation in regulating neuroblast migration 185
3.3.3 Signals regulating fascin in neuroblast migration 187
Chapter 4 Drebrin regulates RMS neuroblast migration 190
4.1 Introduction 190
4.2 Results 192
4.2.1 Drebrin is expressed in the RMS 192
4.2.2 Drebrin is upregulated in migrating neuroblasts 192
4.2.3 Drebrin is expressed in RMS migrating neuroblasts in primary cultures 195
4.2.4 Pharmacological inhibition of drebrin impairs neuroblast migration *in vitro* .. 197
4.2.5 Pharmacological inhibition of drebrin impairs neuroblast migration *ex vivo* .. 199
4.2.6 Drebrin knockdown impairs RMS neuroblast migration *in vitro* 201

4.2.7 shRNA-mediated drebrin knockdown impairs neuroblast migration 204

4.2.8 Drebrin regulates neuroblast morphology 209

4.2.9 Drebrin knockdown impairs RMS neuroblast migration *ex vivo* 212

4.2.10 Drebrin knockdown affects neuroblast morphology *ex vivo* 215

4.2.11 Regulation of drebrin by phosphorylation 218

4.2.12 Drebrin phosphorylation on S142 regulates neuroblast morphology *in vitro* 222

4.2.13 Drebrin phosphorylation on S142 regulates neuroblast migration *ex vivo* ... 228

4.2.14 Drebrin phosphorylation on S142 regulates neuroblast orientation *in vivo* . 231

4.2.15 Investigating the regulation of drebrin phosphorylation on S142 234

4.3 Discussion 237

4.3.1 Drebrin expression in migrating neuroblasts 237

4.3.2 Drebrin function in migrating neuroblasts 238

4.3.3 Ser142 function in migrating neuroblasts 239

Chapter 5 General Discussion 242

5.1 The importance of studying migration in neurogenesis 242

5.2 RMS migration *in vitro* and *ex vivo* 243

5.3 Fascin and drebrin in neuroblast migration 247

5.3.1 Fascin in neuroblast migration 248

5.3.2 Drebrin in neuroblast migration 251

Table of Figures

Figure 1-1. The neurogenic niche in the SVZ. 26

Figure 1-2. The neurogenic niche in the SGZ. 28

Figure 1-3. Olfactory bulb (OB) layers. 36

Figure 1-4. OB structure. 37

Figure 1-5. The rostral migratory stream (RMS). 42

Figure 1-6. Steps of the neuroblast migration cycle. 59

Figure 1-7. Molecular regulators of neuroblast migration. 63

Figure 1-8. The molecular structure of fascin. 68

Figure 1-9. Fascin in filopodia assembly. 73

Figure 1-10. Fascin regulators. 76

Figure 1-11. Molecular structure of drebrin. 78

Figure 1-12. Cdk5-dependent regulation of drebrin. 82

Figure 2-1. Electroporation. 99

Figure 2-2. Fluorescent life-time imaging microscopy. 107

Figure 3-1. Fascin is expressed in the postnatal and adult mammalian brain 114

Figure 3-2. *Fascin-1* ko mice show a smaller OB. 116

Figure 3-3. *Fascin-1* ko mice show an intact organization of the OB. 117

Figure 3-4. *Fascin-1* ko mice show an abnormal RMS. 120

Figure 3-5. *Fascin-1* ko mice show abnormal neuroblast chain organization in the RMS. 123

Figure 3-6. Genetic deletion of fascin does not affect SVZ cell proliferation. 125

Figure 3-7. Genetic deletion of fascin affects neuroblast migration. 128

Figure 3-8. Fascin is upregulated in RMS migrating neuroblasts. 130

Figure 3-9. Fascin is expressed by RMS migrating neuroblasts. 132

Figure 3-10. Fascin can be knocked down in RMS migrating neuroblasts using RNAi. 134

Figure 3-11. Fascin knockdown disrupts neuroblast morphology. 135

Figure 3-12. Fascin regulates RMS neuroblast migration *in vitro*. 138

Figure 3-13. Tracking analysis of fascin-depleted cells shows impairment in RMS neuroblast migration 140

Figure 3-14. shRNA-mediated fascin depletion in RMS neuroblasts. 143

Figure 3-15. shRNA-mediated fascin knockdown impairs neuroblast migration *in vitro*. 145

Figure 3-16. *In vivo* postnatal electroporation in mouse SVZ. 149

Figure 3-17. Fascin regulates neuroblast morphology *in vivo*. 150

Figure 3-18. Fascin is necessary for efficient neuroblast migration *ex vivo*. 152

Figure 3-19. Fascin phosphorylation site Ser39 regulates neuroblast migration *in vitro*. 155

Figure 3-20. Tracking analysis shows that fascin phosphorylation site Ser39 regulates neuroblast migration *in vitro*. 157

Figure 3-21. Phosphorylation of fascin on Ser39 regulates neuroblast migration *ex vivo*. 160

Figure 3-22. Fascin phosphorylation on Ser39 regulates neuroblast directionality *ex vivo*. 162

Figure 3-23. Fascin phosphorylation site Ser39 regulates neuroblast morphology and orientation *in vivo*. 166

Figure 3-24. Phosphorylation of fascin at Ser39 reduces the number of filopodia in RMS migrating neuroblasts *in vitro*. 167

Figure 3-25. The interaction between fascin and PKC γ or PKC α can be detected by FLIM analysis in migrating neuroblasts. 171

Figure 3-26. The interaction between fascin and PKC γ detected by FLIM in migrating neuroblasts depends on PKC activity. 174

Figure 3-27. Cannabinoid signalling regulates the interaction between PKC and fascin. 178

Figure 3-28. Fascin is a downstream mediator of CB-promoted migration *in vitro*. 181

Figure 4-1. Drebrin is expressed in the postnatal and adult mammalian brain. 193

Figure 4-2. Drebrin is upregulated in RMS migrating neuroblasts. 194

Figure 4-3. Drebrin is highly expressed by RMS migrating neuroblasts. 196

Figure 4-4. BTP treatment impairs neuroblast migration *in vitro*. 198

Figure 4-5. BTP decreases migration of neuroblasts *ex vivo*. 200

Figure 4-6. Drebrin can be knocked down in RMS migrating neuroblasts using siRNA. 202

Figure 4-7. Drebrin regulates RMS neuroblast migration *in vitro*. 203

Figure 4-8. shRNA-mediated drebrin depletion in RMS neuroblasts. 206

Figure 4-9. Drebrin regulates RMS neuroblast migration *in vitro*. 207

Figure 4-10. Drebrin shRNA has a specific effect in impairing neuroblast migration......208

Figure 4-11. Drebrin knockdown disrupts neuroblast morphology. 211

Figure 4-12. Drebrin is necessary for efficient neuroblast migration *ex vivo*......214

Figure 4-13. Drebrin regulates neuroblast morphology *in vivo*. 217

Figure 4-14. Drebrin is phosphorylated on S142 in RMS migrating neuroblasts. 221

Figure 4-15. Altering the phosphorylation state of drebrin on S142 does not affect RMS neuroblast migration *in vitro*. 225

Figure 4-16. Drebrin pS142 regulates RMS neuroblast morphology *in vitro*......227

Figure 4-17. Drebrin phosphorylation on Ser142 regulates neuroblast migration *ex vivo*......230

Figure 4-18. Drebrin phosphorylation on S142 regulates neuroblast morphology and orientation *in vivo*. 233

Figure 4-19. Endocannabinoid signalling and FGF-2 do not appear to regulate phosphorylation of drebrin on S142 in migrating neuroblasts. 236

Figure 5-1. The role of fascin and drebrin in RMS migrating neuroblasts......255

Table of Tables

Table 1-1. List of factors that regulate neuroblast migration in the RMS......54

Supplementary movies on accompanying CD (Full description of legends for movies available on the CD)

Supplementary movie 1 – Neuroblast migrating in 3D Matrigel 20X

Supplementary movie 2 – Control siRNA aggregate in 3D Matrigel 20X

Supplementary movie 3 – Fascin siRNA aggregate in 3D Matrigel 20X

Supplementary movie 4 – GFP aggregate in 3D Matrigel 20X

Supplementary movie 5 – Fascin S39A aggregate in 3D Matrigel 20X

Supplementary movie 6 – Fascin S39D aggregate in 3D Matrigel 20X

Supplementary movie 7 – GFP labelled neuroblasts in mouse brain slice

Supplementary movie 8 – Fascin S39A labelled neuroblasts in mouse brain slice

Supplementary movie 9 – Fascin S39D labelled neuroblasts in mouse brain slice

Supplementary movie 10 – YFP labelled neuroblasts in mouse brain slice

Supplementary movie 11 – Drebrin WT labelled neuroblasts in mouse brain slice

Supplementary movie 12 – Drebrin S142A labelled neuroblasts in mouse brain slice

Supplementary movie 13 – Drebrin S142D labelled neuroblasts in mouse brain slice

Abbreviations

2/3D	2/3-dimensional
2-AG	2-arachidonoylglycerol
6-OHDA	6-hydroxydopamine
aa	Aminoacid
ADF-H	Actin-depolymerising factor homology
AhR	Aryl hydrocarbon receptor
AMPA	α-Amino-3-hydroxy-5-methyl-4-isoxazolepropionic acid
Ang1	Angiopoietin1
aPKC	Atypical protein kinase C
ApoER2	Apolipoprotein E receptor 2
Arp2/3	Actin-related protein 2/3
ATPase	Adenyltriphosphatase
BB	Blue box
BDNF	Brain derived neurotrophic factor
bHLH-PAS	Basic helix-loop-helix PAS
BL	Basal Lamina
BMP	Bone Morphogenetic Protein
BrdU	Bromodeoxy-Uridine
BTP	3,5-bis(trifluoromethyl)pyrazole
C	Carboxyl
Ca2+	Calcium
CAM	Cell adhesion molecule
cAMP	Cyclic adenosine monophosphate
CalB	Calbindin
CalR	Calretinin
CB	Cannabinoid
CB1	Cannabinoid receptor 1
CB2	Cannabinoid receptor 2
CC	Coiled-coil
CCR2	C-C chemokine receptor type 2
Cdc42	Cell division control protein 42 homolog

Cdk5	Cyclin-Dependent Kinase 5
cDNA	Complementary deoxyribonucleic acid
CNS	Central nervous system
CP	Choroid plexus
Cre	Cyclic Recombinase
CREB	cAMP response element binding protein
CSF	Cerebrospinal Fluid
CXCR4	C-X-C chemokine receptor type 4
DAG	Diacylglycerol
DAG-L	Diacylglycerol lipase
DCX	Doublecortin (human)
Dcx	Doublecortin (mouse)
DG	Dentate Gyrus
Dlx2	Distal-Less Homeobox 2
DMEM	Dulbecco's modified eagle medium
DNA	Deoxyribonucleic Acid
Drebrin	Developmentally regulated brain protein
E	Embryonic day
EB3	End-binding protein 3
eCB	Endocannabinoid
ECL	Enhanced chemiluminescence
ECM	Extracellular Matrix
EGF	Epidermal growth factor
EGFP	Enhanced green fluorescent protein
EGFR	Epidermal growth factor receptor
ENA/VASP	Enabled/vasodilator-stimulated phosphoprotein
EPL	External plexiform layer
EV	Empty vector
FAK	Focal adhesion kinase
FCS	Foetal calf serum
FGF	Fibroblast growth factor
FLIM	Fluorescence life-time imaging microscopy

FRET	Fluorescence resonance energy transfer
GABA	γ-Aminobutyric acid
GAT4	GABA transporter 4
GC	Granule cell
GCL	Granule cell layer
GDF11	Growth and differentiation factor-11
GDNF	Glial cell line derived neurotrophic factor
GFAP	Glial fibrilliary astrocyte protein
GFP	Green fluorescent protein
GL	Granular layer
Glu	Glutamate
GPCR	G-Protein Coupled Receptor
GPR55	G-protein coupled receptor 55
GSK3β	Glycogen Synthase Kinase3β
GTP	Guanosine triphosphate
GTPases	(GTP)-binding proteins
Hel	Helical
HGF	Hepatocyte growth factor
IGF	Insulin growth factor
IRES	Internal ribosome entry site
IRSp53	Insulin-receptor substrate p53
LIMK	p-Lin-11/Isl-1/Mec-3 kinases
LV	Lateral ventricle
Map2/4	Mitogen-Activated Protein 2/4
MAPK	Mitogen-Activated Protein Kinase
MARK2	MAP/microtubule affinity-regulating kinase 2
MC	Mitral cell
MCL	Mitral cell Layer
MCP1	Monocyte chemoattractant protein 1
mDia	Mammalian Diaphanous
mGluR	Metabotropic glutamate receptor
miRNA	micro-RNA

MLC	Myosin light chain
ML	Molecular layer
MMPs	Matrix metalloproteinases
MRI	Magnetic Resonance Imaging
mRNA	Messenger RNA
N	Amino
NCAM	Neural cell adhesion molecule
NGF	Nerve growth factor
NMDA	N-methyl-D-aspartate
NS	Neural stem
Nudel	NudE-like 1
OB	Olfactory bulb
OD	Optical density
OE	Olfactory Epithelia
OPCs	Olfactory precursor cells
OSN	Olfactory Sensory Neuron
P	Postnatal day
$p75^{NTR}$	p75 neutrophin receptor
PAK	p21-activated kinase
PAK1	p21-activated kinase 1
PAR	Partitioning defective
PBS	Phosphate buffered saline
PDK1	Phosphoinositide-dependent protein kinase 1
PCNA	Proliferating cell nuclear antigen
PCR	Polymerase Chain Reaction
PDGF	Platelet-Derived Growth Factor
PET	Positron emission tomography
PGC	Periglomerular cell
PI	Phosphatidylinositol
PIP2	Phosphatidylinositol 4,5-bisphosphate
PI3K	Phosphatidylinositol-3 kinase
PKA	Protein kinase A

PKC	Protein kinase C
PLC	Phospholipase C
PLD	Phospholipase D
PP	Proline-rich
PSA	Polysialic Acid
PSA-NCAM	Polysialylated neural cell adhesion molecule
PSD-95	Post-synaptic density 95
PTEN	Phosphatase and tension homolog
Ral	Ras-like GTPase
Ral-GDS	Ral guanine nucleotide dissociation stimulator
RG	Radial glia
RMS	Rostral migratory stream
RNA	Ribonucleic Acid
Robo	Roundabout
RRP	Readily releasable pool
S	Serine
SDF1	Stromal cell-derived factor
Ser	Serine
SGZ	Subgranular zone
Shh	Sonic Hedgehog
shRNA	Small hairpin ribonucleic acid
siRNA	Short interfering ribonucleic acid
SVZ	Subventricular zone
TBS	Tris-Buffer Saline
TCF	T cell factor
TGFα	Transforming growth factor α
TH	Tyrosine hydroxylase
THBS-1	Thrombospondin-1
ΔTHC	Δ-tetrahydrocannabinol
Tie2	Tyrosine protein kinase receptor 2
Toca-1	Transducer of Cdc42-dependent actin assembly
VEGF	Vascular endothelial growth factor

VEGFR	Vascular endothelial growth factor receptor
VLDLR	Very-low density lipoprotein receptor
VZ	Ventricular zone
WASP/WAVE	Wiskott-Aldrich syndrome protein/ verprolin-homologous protein
WT	Wild type
YFP	Yellow fluorescent protein

Chapter 1 Introduction

1.1 Postnatal Neurogenesis

1.1.1 History

For a long time it was believed that the brain does not regenerate. Regeneration did not seem plausible since neurons are highly differentiated cells with complex dendrites and multiple synapses. Moreover, it seemed implausible to achieve the structural reorganisation required for new neurons to be integrated into the complex network of dendrites, axons and synapses (Gage, 2002). This view changed with the emergence of the concepts of plasticity and adaptability of the synapses (Hebb, 1949) and the discovery of neurogenesis (Altman, 1962).

It was in the early sixties when Altman used injections of the cell proliferation marker thymidine-H(3) into injured brains of adult rats combined with autoradiography to discover the presence of labelled neurons and neuroblasts in the hippocampus, thus indicating the presence of a pool of undifferentiated cells capable of proliferation (Altman, 1962). This was the first evidence that neurogenesis, a fundamental process in brain embryonic development, still occurs after birth and, specifically, in the adult brain. Subsequent investigations provided even stronger evidence of adult neurogenesis observed in different species including rabbits, rats, mice, songbirds, cats and non-human primates (Altman, 1963, Altman and Das, 1965, Altman, 1969, Kaplan and Hinds, 1977, Goldman and Nottebohm, 1983, Rakic, 1985, Alvarez-Buylla and Nottebohm, 1988).

In the 1990s further reports continued to highlight the existence of neural stem cells in the adult brain capable of self-renewal and differentiation into astrocytes, oligodendrocytes and neurons (Reynolds and Weiss, 1992, Gage et al., 1995, Palmer et al., 1997). Moreover, it was during these years that Eriksson et al. (1998) published the first evidence of neurogenesis in the human brain. He found that cancer patients injected with bromodeoxyuridine (BrdU), a marker for proliferative cells, had labeled newborn neurons in the dentate gyrus of the hippocampus (Eriksson et al., 1998). Altogether, these discoveries marked a new era of acceptance of neurogenesis and its recognition as scientific dogma.

1.1.2 The neurogenic niches in the Central Nervous System (CNS)

In the adult brain neural stem cells can be found in three germinal regions: the subventricular zone (SVZ) of the lateral ventricle (LV) wall (Reynolds and Weiss 1992; Richards et al., 1992), the dentate gyrus subgranular zone (SGZ) of the hippocampus (Gage et al. 1995; Palmer et al., 1997) and the hypothalamic subependymal zone of the third ventricle (Kokoeva et al., 2005, Yuan and Arias-Carrion, 2011, Cheng, 2013).

Similar to stem cells in the gonads, skin, and gut, neural stem cells also live in a micro-environment, called "niche", formed by different cell types and specialized extracellular matrix (ECM), and capable of controlling stem cell renewal and differentiation (Spradling et al., 2001).

SVZ niche

The SVZ is located along the LV walls and is the area that hosts the biggest pool of proliferative cells in the brain (Doetsch and Alvarez-Buylla, 1996). The SVZ contains four different cell types: neuroblasts (type A cells), astrocytes (type B cells), transit amplifying cells (type C cells), and ependymal cells (type E cells) (Doetsch et al., 1997). These cell types, their interactions and epigenetic state, the blood vessels with their specialised basal lamina, the cerebrospinal fluid in contact with the LV and the ECM constitute the architecture of the SVZ niche and the environment that supports neurogenesis (Doetsch, 2003). The cells of the SVZ niche are distinguishable from each other for the following reasons: they have different characteristic shapes, express specific subsets of markers (Figure 1-1) and have different behaviours.

1) **Ependymal ciliated cells** are a monolayer of cells that separate the LV from the SVZ and that circulate the cerebrospinal fluid.
2) **Neural stem cells** are SVZ astrocytes which self-renew and proliferate slowly, giving rise to transit amplifying cells. Neural stem cells surround the neuroblasts. Type B1 cells make contact with the LV with an apical primary cilium and reach the blood vessels using a basal process; they encase neuroblasts, separating them from the ependymal cells. Type B2 cells are astrocytes without stem cell properties; they

encase neuroblasts separating them from the striatum and reach with the tip of their process the blood vessels (Doetsch et al., 1997).

SVZ astrocytes express specific markers such as the Glial Fibrilliary Acidic Protein (GFAP) (Bignami and Dahl, 1974), the neural precursor marker vimentin (Cochard and Paulin, 1984, Alvarez-Buylla et al., 1987, Sancho-Tello et al., 1995), and the intermediate filament protein nestin (Lendahl et al., 1990, Doetsch et al., 1997).

3) **Transit amplifying cells** are the most actively proliferative population in the SVZ and they give rise to neuroblasts. Transit amplifying cells are large, spherical, immature cells that can aggregate and form contacts with neuroblasts (Doetsch et al., 1997), mainly located along the LV in the SVZ (Porteus et al., 1994, Doetsch et al., 1997).

   Transit amplifying cells are positive for nestin (Doetsch et al., 1997), for distal-less homeobox 2 (Dlx2), a transcription factor identified in embryonic developing γ-Aminobutyric acid (GABA)ergic neurons also necessary for SVZ neurogenesis (Porteus et al., 1994, Doetsch et al., 2002, Panganiban and Rubenstein, 2002, Suh et al., 2009), and the transcription factor Mash1 (Casarosa et al., 1999).

4) **Neuroblasts** have an elongated shape (Doetsch et al., 1997). They organise themselves in chains and migrate, sliding against each other along a specific route, called the rostral migratory stream (RMS), towards the olfactory bulb (OB), where they finally differentiate into interneurons (Doetsch and Alvarez-Buylla, 1996).

   Neuroblasts show positive immunoreactivity for Dlx2 (Doetsch et al., 2002), polysialylated neuronal cell adhesion molecule (PSA-NCAM), a cell-adhesion marker, (Rousselot et al., 1995, Doetsch and Alvarez-Buylla, 1996), β-lll tubulin, a specific marker for immature neurons (Easter et al., 1993) and doublecortin (Dcx), a microtubule-associated protein (Gleeson et al., 1999).

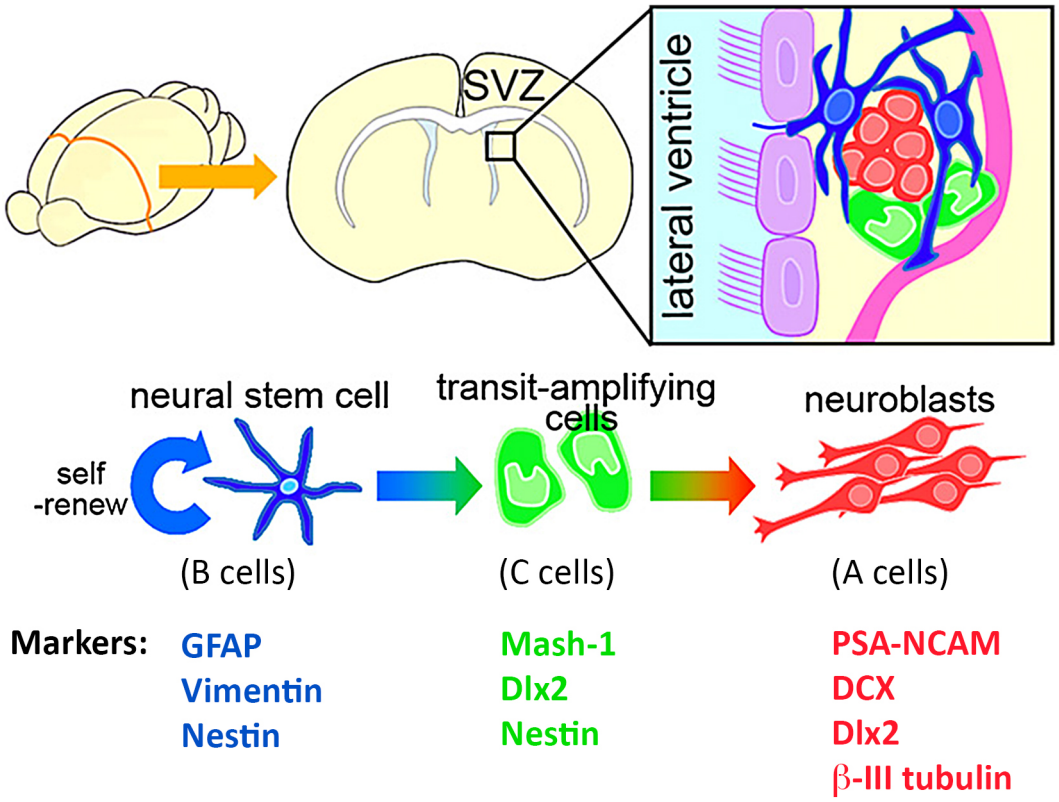


Figure 1-1. The neurogenic niche in the SVZ.

(Top) Schematic coronal brain section (in rodents) showing the organization of the ependymal cells (purple), astrocytes or B cells (blue), neural progenitors or C cells (green) and migrating neuroblasts or A cells (red) in relation to the lateral ventricles and blood vessels (pink) in the SVZ. (Middle) Schematic drawing showing neural stem cells becoming transit amplifying cells which divide quickly to become neuroblasts. (Bottom) List of markers for the different cell types. Adapted from Kaneko and Sawamoto, 2009.

SGZ niche

The SGZ is the other major neurogenic niche in the brain and is located between the hilus and the granule cell layer (GCL) in the dentate gyrus of the hippocampus (Seri et al., 2001) (Figure 1-2, top panel). In this area there are 2 cell types: neural stem cells or astrocytes (B cells) and neuronal precursors or immature granule cells (D cells) (Figure 1-2, bottom panel).

SGZ neural stem cells have a complex morphology with multiple radial processes that infiltrate the GCL and reach the molecular layer (ML). They are mitotically active and can give rise to immature granule cells, which move small distances to reach the GCL (Seri et al., 2001, Seri et al., 2004). Once in the GCL, immature granule cells differentiate into mature granule cells that extend dendrites towards the ML and axons (mossy fibers) towards the CA3 region of the hippocampus, integrating into the synaptic circuit (van Praag et al., 2002).

The cells in this niche, like the cells in the SVZ, express specific markers; the neural stem cells are positive for the glial marker GFAP, while immature granule cells show positivity for PSA-NCAM (Seri et al., 2001, Seri et al., 2004). Like the transit amplifying cells in the SVZ, immature granule cells serve as intermediate neuronal precursors, however they are smaller and do not proliferate at such a high rate pointing towards a higher similarity to RMS migrating neuroblasts (Seri et al., 2001).

In the SGZ, as in the SVZ, blood vessels are intimately associated with the cellular components of the niche, supporting a fundamental role for endothelial cells in regulating neurogenesis (Palmer et al., 2000, Doetsch, 2003).

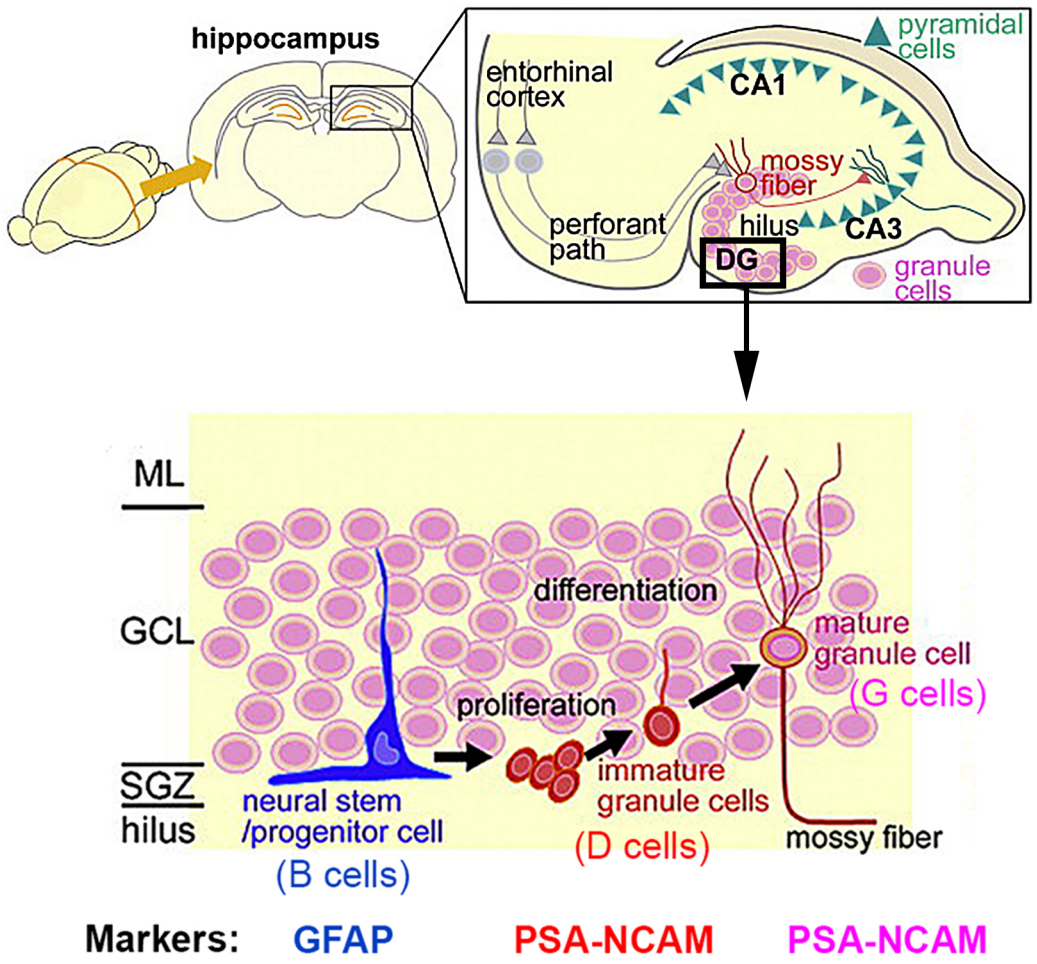


Figure 1-2. The neurogenic niche in the SGZ.

(Top) Schematic coronal brain section (in rodents) showing the hippocampus: the pyramidal cells in the CA1 and CA3 regions (green), the hilus, the granule cells in the dentate gyrus (DG) (pink) and the mature granule cells forming dendrites and mossy fibers (red). (Middle) Schematic drawing showing an enlargement of the DG, which is divided into different layers: subgranular zone (SGZ), granule cell layer (GCL) and molecular layer (ML). The neurogenic niche is in the SGZ between the hilus and the GCL. Neural stem cells (B cells) (blue) become immature granule cells (D cells) (dark red) in the SGZ. D cells migrate in the GCL where they become mature granule cells (G cells) (red) extending dendrites into the ML and mossy fibers connecting to the hippocampal synaptic circuit. (Bottom) List of markers of the different cell types. Adopted from Kaneko and Sawamoto, 2009.

1.1.3 SVZ neurogenesis

Identity of the neural stem (NS) cells

The presence of a quiescent pool of cells that can self-renew and generate neurons, astrocytes and oligodendrocytes has directed the interest of the neuro-scientific community towards the following question: which are the true "stem cells" in the adult brain?

An early attempt in trying to identify the nature of the NS cells was made by Johansson in 1999. Using BrdU injections, he observed that most of the BrdU incorporation was occurring in the ependymal layer, from which he concluded that ependymal cells might have the self-renewal property (Johansson et al., 1999). This hypothesis was soon rejected by Doetsch et al (1999), who monitored BrdU+ cells in the LV wall using electron microscopy but did not detect any proliferation in ependymal cells (Doetsch et al., 1999). Moreover, using antimitotic drugs that are capable of eliminating neuroblasts and transit amplifying precursors, the authors showed that SVZ astrocytes were still able to make new neurons through generation of the transit amplifying cells (Doetsch et al., 1999). Interestingly, specific labelling of SVZ astrocytes using retrovirus showed that these cells gave rise to neuroblasts migrating along the RMS and integrating into the OB (Doetsch et al., 1999).

There are two types of GFAP+ neural stem cells in the SVZ: active proliferating astrocytes, which express Epidermal Growth Factor Receptor (EGFR), and quiescent niche astrocytes, which are EGFR negative (Doetsch et al., 2002). Treatment with antimitotic drugs destroys the proliferating, but not the quiescent GFAP+ astrocytes. The latter are able to recreate the active proliferative GFAP+ astrocytic population within 12 hours (Pastrana et al., 2009). Importantly, GFAP+ astrocytes are also able to grow *in vitro*, forming neurospheres (Doetsch et al., 1999; Pastrana et al., 2009).

Additional evidence that GFAP+ astrocytes are the neural stem cells in the brain came from two studies of transgenic mice expressing the herpes simplex virus thymidine kinase from the GFAP promoter (GFAP-TK). Treatment with the antiviral agent ganciclovir killed the GFAP-expressing cells, resulting in a dramatic NS cell reduction (Imura et al., 2003, Morshead et al., 2003). Another study in GFAP-TK

transgenic mice using targeted ablation and fate-mapping strategies showed that new neurons in the adult OB are generated from GFAP-expressing cells (Garcia et al., 2004). Altogether, these findings strongly point to the astrocytic nature of NS cells in the SVZ.

Origin of the NS cells

The fact that NS cells in the SVZ are cells with astrocytic properties challenged the previously established concept that astrocytes are terminally differentiated glial cells, distinct from the neuronal lineage (Alvarez-Buylla et al., 2001). Moreover, this gave rise to questions about the origin of NS cells in the adult SVZ.

During embryonic development, NS cells constitute the neuroepithelium that sits within the ventricular zone (VZ), between the LVs and the pial surface (Noctor et al., 2001). During cortical neurogenesis NS cells have been identified as radial glia (RG) cells (Noctor et al., 2007). After birth, the VZ becomes the ependymal layer of the SVZ and RG cells become the astrocytes that populate this layer (Schmechel and Rakic, 1979). The idea that astrocytes are descendants of RG cells was supported by subsequent studies demonstrating that RG cells transform into astrocytes (Voigt, 1989) and ependymal cells (Spassky et al., 2005) soon after birth. The connection between RG cells and astrocytes was further supported by the expression of common markers such as RC1 (Mission et al., 1991). The hypothesis that astrocytes derive from RG cells was finally supported by fate mapping experiments, in which specifically labelled RG cells gave rise to SVZ astrocytes and migratory neuroblasts in the RMS (Merkle et al., 2004).

Several studies have pointed out similarities between RG cells and SVZ niche astrocytes. During developmental neurogenesis, RG cells extend a short apical process towards the ventricular surface and a long process towards the pial membrane contacting the blood vessels (Noctor et al., 2001). Similarly, the B1 astrocytes found in the postnatal SVZ have an apical surface in contact with the ventricle (Doetsch et al., 1999) and a long basal process that ensheathes neuroblast chains and ends on niche blood vessels (Mirzadeh et al., 2008). It is therefore evident that, in a similar way, RG cells and B1 cells are important for transferring signals from the ventricles and the blood vessels to the VZ or SVZ, respectively, and

for creating a scaffold for neuroblast migration in developmental or adult neurogenesis, respectively.

The architecture of the neurogenic niche

Transplantation of NS cells in heterotypic neurogenic regions in the brain showed that the environment plays a role in determining their fate. For example, hippocampal NS cells transplanted in either the SGZ or the SVZ differentiate according to the new environment. In particular, hippocampal NS cells transplanted in the SVZ generate neuroblasts migrating along the RMS and differentiate into tyrosine hydroxylase-positive interneurons in the OB (Suhonen et al., 1996). Within the niche there are several components that can maintain or activate the NS cell population: cell-cell interactions, blood vessels, ECM and basal lamina (Doetsch, 2003, Zhao et al., 2008).

Cell-cell interactions

Contrary to other astrocytes from non-neurogenic regions, astrocytes from neurogenic niches regulate adult neurogenesis by secreting factors that lead to proliferation or differentiation of NS cells. This indicates that hippocampal and subventricular astrocytes are specialized cells capable of providing signals necessary to maintain the SGZ and SVZ niches, respectively (Lim and Alvarez-Buylla, 1999, Song et al., 2002). Moreover, interactions between astrocytes via gap junctions are required for adult neurogenesis to occur as growing astrocytes in an astrocyte-conditioned medium by itself is insufficient to support proliferation of neural precursors (Lim and Alvarez-Buylla, 1999). Thanks to their stellate shape, astrocytes are capable of making contacts with all the different cells and tissues residing in the SVZ niche (Doetsch, 2003). While the apical processes of the astrocytes lying along the LV wall sense and translate signals from the cerebrospinal fluid, the long basal processes make contacts with the basal lamina of the blood vessels (Doetsch, 2003, Mirzadeh et al., 2008). Additionally, the ependymal cells make contact with astrocytes and the choroid plexus (Doetsch, 2003, Mirzadeh et al., 2008). In particular, they promote neurogenesis and neuronal differentiation by producing

Noggin, an antagonist of the bone morphogenetic proteins (BMPs) known to inhibit neurogenesis (Lim et al., 2000).

Vasculature

The vasculature is a fundamental component of neurogenic niches (Palmer et al., 2000, Alvarez-Buylla and Lim, 2004). Blood vessels are in close proximity to NS cells and secrete growth factors such as vascular endothelial growth factor, VEGF, and brain-derived neurotrophic factor, BDNF, increasing neurogenesis (Leventhal et al., 1999, Palmer et al., 2000, Alvarez-Buylla and Lim, 2004, Cao et al., 2004). Moreover, both VEGF and BDNF are upregulated in testosterone-induced angiogenesis, which has been linked to increased neurogenesis in the songbird brain (Louissaint et al., 2002). Interestingly, in a co-culture system, endothelial cells promote NS cell self-renewal while maintaining their multipotency and preventing their differentiation (Shen et al., 2004). The close association between angiogenesis and neurogenesis was further explored in irradiated brains. The radiation-induced ablation of neurogenesis induces changes in the microenvironment of the neurogenic niche disrupting angiogenesis and increasing microglia activation. Interestingly, transplant of non-irradiated NS cells in the SGZ of irradiated brains cannot induce neurogenesis (Monje et al., 2002), suggesting that the microvasculature in the niche is a prerequisite for neurogenesis.

ECM and the basal lamina

The basal lamina, surrounding the endothelial cells, separates the blood vessels from the brain tissue. Moreover, this specialized basal lamina extends within the neurogenic niche surrounding all cell types and ending in structures called “bulbs” in the subependymal layer (Mercier et al., 2002). The basal lamina and ECM function as support for cells and as storage for factors (Doetsch, 2003). The basal lamina has been identified as “mats” of ECM with a role in cell proliferation, differentiation and morphogenesis (Halfter et al., 1998, Iozzo, 2005). In the neurogenic niche, several ECM components like collagen I, heparan sulphate proteoglycans and laminins were found in close association with the basal lamina (Mercier et al., 2002, Kerever et al., 2007, Mercier and Arikawa-Hirasawa, 2012). In

particular, N-sulphate heparin sulphate proteoglycans were able to localize fibroblast growth factor 2 (FGF-2), a factor promoting cell proliferation in the niche (Kerever et al., 2007, Mercier and Arikawa-Hirasawa, 2012). Consistent with this, the most mitotically active progenitors were found close to the basal lamina (Kerever et al., 2007). Interestingly, NS cells express receptors for the surrounding components of the ECM. For instance, NS cells, which are surrounded by a laminin-rich ECM, express low levels of laminin receptor α6β1 that becomes upregulated in mitotically active NS cells during regeneration of the niche (Kazanis et al., 2010). These evidences show that ECM composition of the niche exerts a crucial role in regulating neurogenesis.

1.1.4 Function of SVZ neurogenesis

The OB is the final destination of new generated SVZ-derived neuroblasts. After having migrated along the RMS, neuroblasts differentiate into neurons and integrate into the pre-existing synaptic circuit in the OB (Alvarez-Buylla et al., 2001).

OB cellular composition

The first synaptic contact responsible for olfaction occurs in the OB. The olfactory sensory neurons (OSNs) have their cell body in the olfactory epithelium and project their axons into the glomeruli in the glomerular layer (GL) of the OB. Glomeruli are round structures where the OSN axons make synapses with the apical dendrites of mitral cells (MCs) and tufted cells, both projecting axons towards the cortex where the olfactory sensations are processed (Shepherd, 1972). MCs and tufted cells make synapses also with inhibitory interneurons, which constitute a fundamental part of the neural activity in the olfactory synaptic system considering the fact that the ratio between them and the excitatory neurons is 100 to 1 (Shepherd, 2004). While OSNs, MCs and tufted cells establish a fixed circuit, inhibitory interneurons are replaced throughout life (Lledo et al., 2008). There are two types of inhibitory neurons in the OB: granule cells (GCs) in the granule cell layer (GCL) and periglomerular cells (PGCs) in the GL (Belluzzi et al., 2003, Carleton et al., 2003). Two other layers are been characterized in the OB: the internal plexiform layer (IPL), between the GCL and the mitral cell layer (MCL), and the external plexiform layer

(EPL), between the MCL and the GL (Lazarini and Lledo, 2011) (Figure 1-3, Figure 1-4).

GCs have a short process oriented towards the GCL and a longer one extending towards the EPL, with more complex branching occurring in parallel with maturation (Shepherd, 1972). GCs can be classified as superficial or deep depending on the level at which they make "dendro-dendritic" synapses with either tufted or MCs. Superficial GCs make synapses with tufted cell dendrites in the superficial lamina of the EPL, while deep GCs make synapses with MC dendrites in the deep lamina of the EPL (Orona et al., 1983) (Figure 1-4). These GCs are GABAergic (Shepherd, 2004). Recently, Merkle and collegues found 4 types of unknown interneurons, which resemble the previously characterised GCs but differ in morphology and cell body position in the OB layers. Type 1 cells have the cell body in the superficial part of GCL, similarly to the superficial GCs, but their dendrites only reach the IPL. Type 2 cells have the cell body in the ML and display only apical dendrites, which extend into the EPL. Type 3 cells also have their cell bodies in the MCL but extend their processes into the MCL and the IPL. Type 4 cells have their soma located throughout the EPL and extend their dendrites radially within the EPL. A substantial percentage of these type 1-4 cells are positive for calretinin (CalR) (Merkle et al., 2014). Parvalbumin-positive interneurons are also present in the EPL (Batista-Brito et al., 2008).

PGCs make synapses with the apical dendrites of MCs and tufted cells in the glomeruli, but they can also extend to make synapses between different glomeruli (Kosaka and Kosaka, 2005) (Figure 1-4). PGCs can be classified into three different types depending on the expression of tyrosine hydroxylase (TH), calbindin (CalB), or CalR. TH is an enzyme for dopamine production, while CalB and CalR are both calcium-binding proteins (Parrish-Aungst et al., 2007). PGCs can be either GABAergic or dopaminergic (Shepherd, 2004).

Although in a smaller percentage, excitatory neurons were also recently reported to be present in the OB. Fate mapping studies revealed that glutamatergic juxtaglomerular neurons, which project their dendritic arbors into the adjacent glomeruli in the OB, derive from neural progenitors located in the SVZ (Brill et al., 2009).

Several thousands of neurons migrate everyday from the SVZ to the OB (Lois and Alvarez-Buylla, 1994), but only 50% of these integrate into the OB synaptic circuit, where they remain for a longer period (up to 19 months) if they have survived the first 3 months (Petreanu and Alvarez-Buylla, 2002, Winner et al., 2002). The function of this continuous replacement is still a point of controversy.

By recruiting newborn neurons, adult neurogenesis contributes to the maintenance of the OB circuit. Reducing the SVZ proliferation rate by genetic depletion of new neurons leads to a decrease in the GC population in the OB (Imayoshi et al., 2008). Moreover, irradiation of the SVZ has a similar effect to naris closure leading to a decrease in new neuron recruitment in the OB (Frazier-Cierpial and Brunjes, 1989, Lazarini et al., 2009).

Although controversial, a mutual relationship exists between SVZ neurogenesis and olfactory abilities (Lledo et al., 2006). SVZ disruption and the subsequent decrease of GC in the OB showed a decrease in fear responses after exposure to conditioned odours (Valley et al., 2009). In NCAM knockout mice, the reduction of newborn neurons reaching the OB affects odour discrimination (Gheusi et al., 2000), but not odour sensitivity or memory. Other reports, instead, have found association between SVZ neurogenesis and olfactory memory, but not with odour discrimination (Lazarini et al., 2009, Sultan et al., 2010). The use of anti-mitotic drugs or the focal irradiation of the SVZ to block the arrival of new neurons into the OB has been proven to affect only long-term memory in some cases (Lazarini et al., 2009, Sultan et al., 2010), or only short-term memory in others (Breton-Provencher et al., 2009).

Finally, SVZ neurogenesis has a function in perceptual learning (Moreno et al., 2009, Alonso et al., 2012). Interestingly, odour discrimination improvements are inhibited if neurogenesis has been blocked before or during odour enrichment (Moreno et al., 2009). Similarly, activation of new neurons in the OB is capable of improving odour discrimination learning as well as memory formation. More precisely, only activation of adult born neurons, but not early postnatal born neurons, facilitates learning difficult tasks (Alonso et al., 2012), showing that the high synaptic plasticity of new neurons allows for better transduction of information compared to mature neurons.

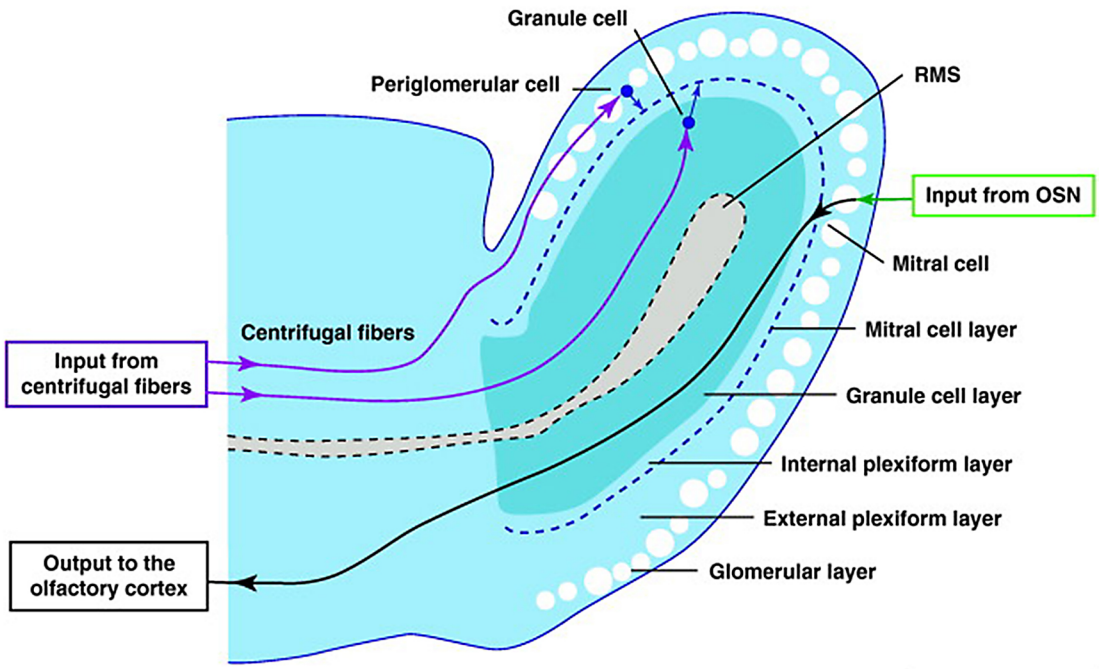


Figure 1-3. Olfactory bulb (OB) layers.

Six layers are recognisable from the outside to the inside: glomerular layer (GL), external plexiform layer (EPL), mitral cell layer (ML), internal plexiform layer (IPL), granule cell layer (GCL), and the rostral migratory stream (RMS) at the core of the OB. The olfactory outputs are transmitted by the olfactory sensory neurons (OSNs) to the glomeruli (white circles), which activate the mitral cells (MCs) projecting information to the olfactory cortex. Inputs from the centrifugal fibres terminate to granule cells (GCs) and perigranule cells (PGCs), which modulate MC activities. Adapted from Lazarini et al., 2011.

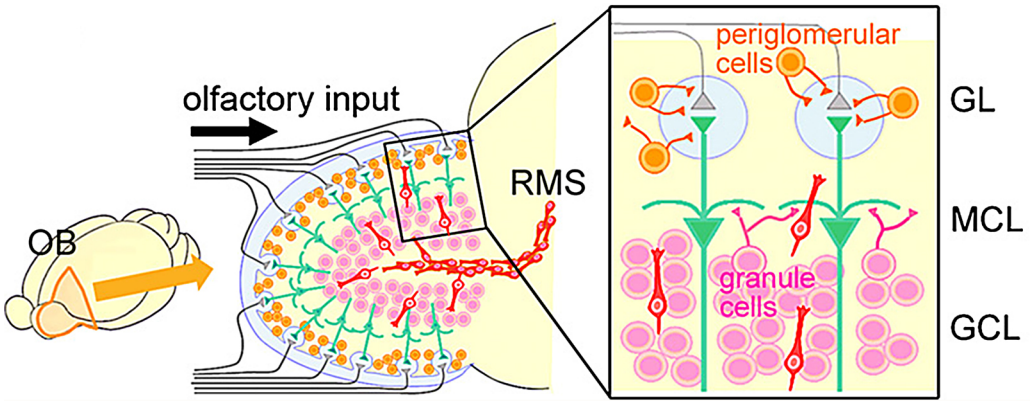


Figure 1-4. OB structure.

Olfactory inputs are perceived by OSNs in the olfactory epithelium (not shown). OSNs extend an axon (grey) that forms synapses inside one or more glomeruli (blue circle) in the GL with the apical dendrites of MCs (green), which have their cell body in the MCL. MCs have axons projecting towards the olfactory cortex, where the sensory input is processed. The SVZ-derived cells are the PGCs (orange) and GCs (pink). Both PGCs and GCs are responsible for the inhibitory activity in the OB. PGCs form synapses in the glomeruli in the GL, while GCs form dendro-dendritic synapses with MCs in the MCL. Adapted from Kaneko and Sawamoto, 2009.

1.1.5 Neurogenesis in the human brain

Adult neurogenesis has been very well characterised in rodents. For obvious reasons, this is not the case in humans although progress has been made in the last decade. The first evidence of human neurogenesis was provided by Eriksson and colleagues, who discovered proliferating cells in the adult human hippocampus analysing post-mortem tissues from cancer patients that had been injected with BrdU for diagnostic purposes (Eriksson et al., 1998). Sanai (2004) reported the discovery of an astrocytic "ribbon" lying along the human LV, and isolation of these cells showed their stem cell multipotent properties as well as high proliferation rate *in vitro* (Sanai et al., 2004). In the same year it was shown that human OBs in the granular and glomerular layers have newborn cells positive for proliferative cell markers such as Ki67 and the proliferating cell nuclear antigen (PCNA) (Bedard and Parent, 2004). These cells also show positivity for migrating neuroblast markers like DCX and Nestin (Bedard and Parent, 2004). A subsequent study has described the architecture of the SVZ in humans as a structure with 4 different layers: an ependymal cell layer (layer 1), a hypocellular gap layer (layer 2), an astrocytic ribbon layer (layer 3) and a transitional layer (layer 4) before the striatum (Quinones-Hinojosa et al., 2006). This report also speculates on a proliferation rate based on the expression of Ki67 and PCNA in the GFAP-positive astrocytes along the LV (Quinones-Hinojosa et al., 2006).

In a following report, a structure resembling the rodent RMS called "RMS-like pathway", was described in the adult human brain (Curtis et al., 2007). This became a point of controversy (Sanai et al., 2007, Kam et al., 2009) and only recently a detailed study showed convincing evidence of the existence of a corridor of migrating neurons from the LV to the olfactory peduncle (the human OB) until 18 months of age (Sanai et al., 2011).

Studies on human neurogenesis using a retrospective birth dating technique measuring the incorporation levels of ^{14}C to calculate the age of the cell population (Spalding et al., 2005) showed that there is a minimal (1% in the entire life) presence of newborn neurons in the OB (Bergmann et al., 2012), but a high proliferative rate in the hippocampus (1.75% per annum, 700 new neurons per day) (Spalding et al., 2013) and in the SVZ of the lateral ventricle (2.7% per annum in

adulthood) (Ernst et al., 2014). Interestingly, using carbon-dating studies, thymidine analog IdU injections in patients and immunohistochemistry, Ernst et collegues (2014) showed that DCX and PSA-NCAM postive neuroblasts are not confined in the SVZ but they are also present in the adjacent striatum where they can differentiate into NeuN, MAP2 and/or CalR-positive interneurons (Ernst et al., 2014).

Neurogenesis is a fundamental process during brain embryonic development and, although at the birth it is largely complete, there is evidence that shows a continuous generation of newborn neurons after birth in the SVZ of rodents and humans. Neurogenesis in the SVZ-RMS-OB is a process that involves cell proliferation (SVZ), migration (RMS) and differentiation (OB) (Mackowiak et al., 2004). In this study we focused on the tangential migration of newborn neurons along the RMS.

1.2 Neural progenitor migration

Neuronal progenitor migration is a highly regulated process that is crucial for the development of the brain architecture, allowing the correct formation of the complex glia and neuronal networks in the nervous system (Cayre et al., 2009, Valiente and Marin, 2010). Neuroblast migration relies on both intracellular signalling and cytoskeletal components involved in cell-cell and cell-matrix interactions and on extracellular cues acting as chemoattractants or chemorepellants (Schaar and McConnell, 2005, Cayre et al., 2009). In the CNS neuroblast migration occurs not only during embryonic development, but also after birth (Lois and Alvarez-Buylla, 1994). There are two main types of glia-independent migration through which neuroblasts reach their final destinations: radial migration, (meaning here perpendicular to the main brain axis), and tangential migration, which is parallel to the main brain axis (Lois et al., 1996, Park et al., 2002). Neuroblasts adopt these two forms of migration during development (for instance in cortical neurogenesis) but also during adulthood. In the postnatal brain neuroblasts first migrate tangentially from the SVZ to the OB along the RMS and then radially from the OB core towards the different OB layers, where they will finally differentiate into interneurons.

1.2.1 RMS neuroblast migration

The evidence of a long migratory path (5 to 8 mm) from the SVZ to the OB was found using injections of a retroviral vector containing the reporter gene LacZ in the rat neonatal SVZ and using transplantation of adult SVZ cells carrying a neuronal-specific transgene into the adult SVZ of another mouse as well as injecting dye DiI in the SVZ to label endogenous neural precursors (Luskin, 1993, Lois and Alvarez-Buylla, 1994). The LacZ-positive cells in the postnatal rats as well as the transgenic cells and the DiI-labelled cells in the adult mice were detected out of the SVZ and distributed along a well-defined path called RMS, migrating tangentially towards the OB. These cells possess a morphology similar to migrating neurons, with an elongated cell body and a leading process oriented towards the direction of the migration and tipped with a small growth cone (Luskin, 1993, Lois and Alvarez-

Buylla, 1994). Subsequent experiments showed that neuroblasts have a main leading process that can branch while testing the environment during migration as well as a trailing process (Schaar and McConnell, 2005, Nam et al., 2007).

The RMS containing chains of migrating neuroblasts extends from the SVZ to the OB (Figure 1-5). In contrast to other types of neuronal migration where either glial or axonal support is needed, neuroblasts in the RMS migrate in chains, sliding against each other without any extra glial/axonal support (Doetsch and Alvarez-Buylla, 1996, Lois et al., 1996). GFAP+ astrocytes surround the RMS neuroblasts, forming a scaffold (or "glial tube") supporting their migration, and creating an environment separated from the parenchyma, which provides cues regulating neuroblast motility (Figure 1-5) (Lois et al., 1996, Doetsch et al., 1997, Bozoyan et al., 2012). Although the astrocytes forming the glial tube are considered fundamental structures for the organization of the RMS, neuroblasts retain an intrinsic migratory ability, since they can migrate without the astrocytic scaffold *in vitro* (Wichterle et al., 1997).

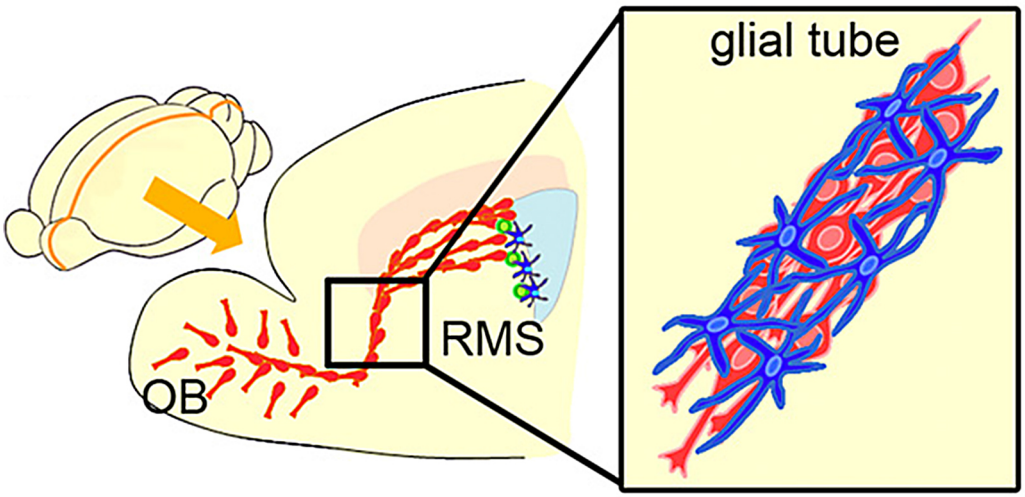


Figure 1-5. The rostral migratory stream (RMS).

Schematic sagittal section of a rodent brain showing the organisation in chains of the migrating neuroblasts. Neuroblasts (red) generated in the SVZ migrate in chains to the OB along the rostrocaudal axis forming the RMS. (Enlarged picture) Neuroblast chains are ensheathed by astrocytes (blue) in a structure called the glial tube. Adapted from Kaneko and Sawamoto, 2009.

1.2.2 What regulates migration in the RMS

The RMS is a complex environment, where neuroblasts migrate long distances to reach their final destination, the OB. In the last decade several studies have identified molecules acting as chemoattractant, chemorepulsive, or motogenic factors that cooperatively regulate the directed migration of neuroblasts along the RMS (Cayre et al., 2009).

The following section gives a detailed presentation of the key extracellular signals regulating neuroblast migration in the postnatal RMS. A list of the regulators can be found at the end of this subchapter (Table 1-1).

1.2.2.1 Structural guides

Cerebrospinal fluid (CSF)

The CSF, which is especially secreted by the choroid plexus in the LV, is in contact with the cilia of the ependymal cell layer. The beating of the ependymal cell cilia controls the currents of the CSF close to the LV wall. The orientation of the neuroblast chains has been suggested to be influenced by the CSF flow and not by the anatomical location of the RMS or OB (Sawamoto et al., 2006). Transgenic mice with impaired ciliogenesis showed a strong misorientation of neuroblast chains in the SVZ, leading to a much lower number of neuroblasts migrating along the RMS (Sawamoto et al., 2006). Interestingly, the neuroblasts that enter the RMS were correctly oriented towards the OB, indicating that the CSF plays a role in neuroblast chain orientation only in the SVZ (Sawamoto et al., 2006). Moreover, the choroid plexus secretes several molecules that have a chemorepellent effect on SVZ migration, such as Slit proteins (Hu, 1999). Sawamoto and his colleagues (2006) also showed that CSF flow is necessary for the creation of a Slit2 gradient, promoting the migration of neuroblasts from the SVZ (Sawamoto et al., 2006).

The vasculature

A higher concentration of blood vessels has been detected along the RMS compared to other areas in the CNS (Whitman et al., 2009). In the RMS, blood vessels are mainly oriented longitudinally, parallel to the neuroblast chains and the long astrocytic processes (Snapyan et al., 2009, Whitman et al., 2009). This vascular

structure creates a physical support that can guide neuroblast migration to the OB. Interestingly, blood vessels start to align along the stream of migrating neuroblasts already at E14 (Nie et al., 2010) and appear to progressively form a scaffold that is completed within a few days after birth (P7-P14), when also the glial tube starts to assume its tunnel shape (Peretto et al., 2005). During this process astrocytes release VEGF, which is necessary for the formation of parallel blood vessels (Bozoyan et al., 2012). The fact that blood vessels are useful structures for the stimulation of efficient migration is supported also by the difference in the speed of migration between the early postnatal stages, when the scaffold of blood vessels is not completely formed (slower) and the adult stages (faster) (Bozoyan et al., 2012).

Besides being physically supportive structures, blood vessels control neuroblast migration by releasing BDNF, which acts on the p75 neutrophin receptor ($p75^{NTR}$) expressed by neuroblasts, facilitating their migration (Snapyan et al., 2009). Interestingly, astrocytes express the receptor TrkB, capable of sequestering BDNF, thus making neuroblasts enter a "stationary phase" (Snapyan et al., 2009).

Astrocytes

Astrocytes in the RMS have long, multiple GFAP+ processes that run longitudinally and parallel to the PSA-NCAM+ neuroblast chains and blood vessels, creating a physically restricted environment that supports RMS migration (Lois et al., 1996, Whitman et al., 2009). Although astrocytes are not required for *in vitro* neuroblast chain migration (Wichterle et al., 1997), several groups have reported a connection between the astrocytic scaffold and neuroblast migration *in vivo*. For instance, NCAM knockout mice show a reduction in neuroblast migration due to a loss of the cross-talk interactions between astrocytes and neuroblasts (Chazal et al., 2000). A similar phenotype is shown by the β1 integrin knockout mice, where the integrity of the glial tube is compromised and leads to an ectopic migration of neuroblasts towards the striatum (Belvindrah et al., 2007). Moreover, mice carrying mutations for the receptor tyrosine kinase ErbB4 or Galectin-3 show an abnormal glial tube and disrupted neuroblast migration (Anton et al., 2004, Comte et al., 2011). Interestingly, while astrocytes express the Roundabout (Robo) receptor, neuroblasts express its ligand Slit1, a diffusible protein known to act as a

chemorepellent (Kaneko et al., 2010). Slit1 knockout mice show a morphological disorganization of the astrocytic tube, pointing to a specific role for the Robo-Slit1 pathway, and thus astrocyte-neuroblast interactions in the maintenance of RMS structure and migration (Kaneko et al., 2010). The physical support offered by the astrocytic tube is combined with a regulated secretion of guidance cues by the astrocytes to promote efficient neuroblast migration. Astrocytes are capable of controlling the RMS microenviroment by regulating GABA secretion (Bolteus and Bordey, 2004) and glutamate (Glu) levels that activate $GABA_A$, Glu_{K5} and N-methyl-D-aspartate (NMDA) receptors on neuroblasts, thus regulating their speed (Platel et al., 2007, Platel et al., 2008b, Platel et al., 2010).

Electric currents

A recent report shows that there is an endogenous electric current along the RMS (Cao et al., 2013). In the SVZ the electric field is created by Na^+/K^+ - ATPase pumps expressed on the basal lamina, which produces a flow of positive charges inwards, forming a positive potential of 7.9 ± 5.3 mV. In the OB instead, Na^+/K^+ - ATPase pumps are expressed on the apical surface and create a flow of positive charge outwards, forming a voltage hole with a negative potential of -2.0 ± 5.6 mV. Considering the length of the RMS, the difference between the two potentials comes to about 3.3 mV/mm (Cao et al., 2013).

Several studies have shown that electric fields can have an effect on cell growth, division, polarization and migration (McCaig et al., 2005). Experiments using either neuroblast cultures or acute brain slices show that in an electric field RMS neuroblasts migrate towards the cathode and have a better directionality, indicating that neuroblasts are directed in their movement towards the OB by the electric gradient in the RMS (Cao et al., 2013). Interestingly, the guidance by the electric field in the RMS is perceived through the purinergic receptor P2Y1, transiently expressed by the neuroblasts exiting the SVZ (Cao et al., 2013).

1.2.2.2 Growth factors

In the past few years several growth factors have been identified to act as regulators either with motogenic or chemoattractant properties at different levels of the SVZ-RMS-OB system.

Insulin-like growth factor-1 (IGF-1)

IGF-1 has recently been identified as a stimulator of neuroblast migration. It is released by the choroid plexus and it stimulates migration in culture. Moreover, IGF-1 knockout mice show a clear defect in neuroblast migration, having a smaller OB and progenitor cell accumulation in the caudal part of the RMS (Hurtado-Chong et al., 2009).

Vascular endothelial growth factor (VEGF)

VEGF, a glycoprotein that stimulates vasculogenesis and angiogenesis, increases neurogenesis in the SVZ (Jin et al., 2002). It also acts as a chemoattractant, stimulating neuroblast migration through its receptor VEGF receptor 2, whose expression is increased by the presence of FGF-2 (Zhang et al., 2003).

Knockout mice for VEGF receptor 1 show lower numbers of BrdU+ cells along the RMS and higher number of BrdU+ cells differentiating in the OB compared to wild type animals. Interestingly, deleting VEGF receptor 1 increases the level of VEGF-A. Moreover, infusion of VEGF-A in wild type mice shows the same phenotype as VEGF receptor 1 knockout mice as well as higher levels of phosphorylated VEGF receptor 2. Importantly, VEGF receptor 2 loses its phosphorylation once the neuroblasts detach from the chains in the OB, supporting the idea that VEGF-A and VEGF receptor 2 regulate tangential neuroblast migration in the RMS (Wittko et al., 2009).

Brain derived neurotrophic factor (BDNF)

BDNF was initially identified as a regulator of neuron cortical tangential migration in embryonic development (Polleux et al., 2002) and, subsequently, of tangential neuroblast migration in the postnatal RMS (Chiaramello et al., 2007, Snapyan et al., 2009). BDNF is highly expressed along the RMS, but it has an even higher concentration in the OB (Chiaramello et al., 2007, Snapyan et al., 2009).

Interestingly, BDNF was seen to have a motogenic effect on RMS neuroblast migration by increasing the number of migrating neuroblasts *in vitro* and *in vivo*, but not their migration distance (Zigova et al., 1998, Chiaramello et al., 2007, Grade et al., 2013). Moreover, removal of BDNF by injection of TrkB receptor or genetic deletion of one allele (BDNF heterozygous mice) drastically decreases the number of BrdU+ cells reaching the OB (Bath et al., 2008, Snapyan et al., 2009). BDNF is secreted by the blood vessels surrounding the glial tube and acts on the $p75^{NTR}$ expressed by migrating neuroblasts, thereby modulating their migration (Snapyan et al., 2009).

Hepatocyte growth factor (HGF)

HGF is a paracrine growth factor playing a role through its tyrosine kinase receptor Met in migration and morphogenesis during development (Birchmeier and Gherardi, 1998). HGF as well as its receptor Met are highly expressed along the RMS (Garzotto et al., 2008). This high expression correlates with a double function of HGF *in vitro*. Exposure of RMS explants to HGF increases the number of neuroblasts migrating from the explants, thus showing a motogenic function for HGF (Garzotto et al., 2008). Moreover, experiments using Boyden chambers show that the number of migrated OB interneuron precursors responds to HGF treatment in a dose-dependent manner, thus indicating a chemoattractant function for this factor (Garzotto et al., 2008). HGF stimulation of neuroblast migration signals through the mitogen-activated protein (MAP) kinase pathway and RMS explants from mice mutated for the Met receptor, impairing MAP kinase signalling, show reduced neuroblast migration (Garzotto et al., 2008).

Glial cell derived neurotrophic factor (GDNF)

The neurotrophic factor GDNF as well as its receptor GDNF family receptor alpha-1 (GFRα1) are expressed throughout the RMS in a rostral-caudal gradient. GDNF seems to be produced in the OB, acting as a chemoattractant for migrating neuroblasts (Paratcha et al., 2006). *In vitro* experiments show that GDNF attracts neuroblasts isolated from the RMS, but not neuroblasts isolated from the SVZ (Paratcha et al., 2006). Moreover, GDNF promotes neuroblast migration through

cyclin dependent kinase 5 (Cdk5), since treatment with the Cdk5 inhibitor roscovitine impairs the GDNF chemoattractive effect (Paratcha et al., 2006).

Epidermal growth factor (EGF)

The receptor for EGF (EGFR) is expressed by NS cells and transit amplifying cells in the SVZ (Doetsch et al., 2002). EGF has been shown to stimulate NS cell proliferation *in vitro* (using neurosphere assays) and *in vivo* by injection in the LV (Craig et al., 1996, Doetsch et al., 2002). Recently, low expression of EGFR ($EGFR^{low}$) was detected in neuroblasts, which is inversely correlated with the expression of migrating neuroblast markers such as PSA-NCAM, Dcx and βIII tubulin (Kim et al., 2009), probably characterising cells in the transition state from transit amplifying cells to neuroblasts. Indeed, neuroblasts showing $EGFR^{low}$ migrate slower and in a more random manner compared to neuroblasts negative for EGFR expression (Kim et al., 2009). Moreover, time-lapse imaging on brain slices reveals that treatment with transforming growth factor alpha (TGFα) (a selective EGFR agonist) decreases neuroblast migration, thus reinforcing the concept that EGFR stimulation negatively regulates neuroblast migration (Kim et al., 2009). Interestingly, EGF has been shown to regulate the cell population in the SVZ by transforming transit amplifying cells (C cells) into a more immature state (glial-cell type C^{*}) (Doetsch et al., 2002). Further investigations are needed to clarify whether the EGFR negative effect on neuroblast migration is directly linked to the migration or whether this is the result of a change in cell fate (non motile transit amplifying cells express high levels of EGFR).

Fibroblast growth factor (FGF)

FGFs are a family of growth factors involved in several processes during embryonic development (Mason, 2007). FGF-2 shows expression along the RMS in a caudal-rostral gradient, with a particularly high concentration in the SVZ. FGF-2 enhances astrocytic proliferation in the SVZ and acts as a motogenic cue, increasing the number of migrating neuroblasts out of SVZ explants in early postnatal stages (P5-P15) (Garcia-Gonzalez et al., 2010). In time-lapse imaging of SVZ explants (from P5-P15) treated with FGF-2, at the constant concentration of 20 ng/ml, it was evident that FGF-2 also increases neuroblast migration distance and speed. The effect of

FGF-2 on migration is promoted through its receptor FGFR1, which is expressed by migrating neuroblasts (Garcia-Gonzalez et al., 2010). Anosmin-1, an ECM glycoprotein involved in axon guidance and neuronal migration, also promotes neuroblast migration through FGFR1, acting as a chemoattractant cue (Garcia-Gonzalez et al., 2010). This indicates that simultaneous effects of FGF-2 and Anosmin-1 on FGFR1 help SVZ-derived neuroblasts to migrate along the first tract of the RMS during the initial stages of postnatal development, when the glial tube is not yet completely shaped (Garcia-Gonzalez et al., 2010).

1.2.2.3 Neurotransmitters

GABA is the major inhibitory neurotransmitter in the CNS regulating neural excitability. Although neuroblasts do not form synapses, GABA is present in the SVZ, regulating proliferation of neuronal precursors (Nguyen et al., 2003). Moreover, migrating neuroblasts express the $GABA_A$ receptor and a smaller percentage also expresses glutamate receptors, such as either metabotropic glutamate receptor 5 (mGluR5) or GLU_{K5} or both (Stewart et al., 2002, Nguyen et al., 2003, Platel et al., 2008b), whereas astrocytic processes ensheathing neuroblasts express GABA transporter 4 (GAT4), the high affinity GABA transporter (Bolteus and Bordey, 2004). GABA infusion on acute brain slices reduces neuroblast migration by acting through the $GABA_A$ receptor on neuroblasts, while treatment with the $GABA_A$ antagonist reverses this effect, suggesting the existence of a GABA tone regulating neuroblast migration (Bolteus and Bordey, 2004). Interestingly, migrating neuroblasts also contain GABA, which can activate $GABA_A$ receptors, thereby interfering with the release of intracellular calcium, making them capable of auto-controlling their migration (Bolteus and Bordey, 2004).

Although activation of either mGluR5 or GLU_{K5} receptors leads to an increase of calcium in neuroblasts, only GLU_{K5} receptors contribute towards the regulation of neuroblast migration (GLU_{K5} activation reduces migration, while inactivation using a GLU_{K5} antagonist increases migration) (Platel et al., 2008b). GABA and glutamate therefore regulate the migration of neuroblasts in a controlled environment where crosstalk between neuroblasts and between neuroblasts and astrocytes plays a fundamental role.

1.2.2.4 Axon guidance molecules

Slit/Robo

Slits are diffusible proteins that act through Robo receptors. They act as guidance cues during brain development (Brose et al., 1999, Nguyen Ba-Charvet et al., 1999, Wu et al., 1999, Nguyen-Ba-Charvet et al., 2002, Marin et al., 2003). Slit1 is secreted by migrating neuroblasts exiting the SVZ (Kaneko et al., 2010), while Slit2 is produced by the choroid plexus (Nguyen-Ba-Charvet et al., 2004) and transported to the SVZ by the CSF (Sawamoto et al., 2006). Both Slits, acting as chemorepellents, play a role in promoting neuroblast migration out of the SVZ. The Slit chemorepellent activity was also detected *in vitro*, where neuroblasts reverse their migration in response to an increased Slit concentration (Ward et al., 2003). Investigations in Slit knockout mice show that neuroblasts migrate out of their native route towards the corpus callosum, supporting their role in orienting migration (Nguyen-Ba-Charvet et al. 2004). In a following study, Slit1 knockout mice show a decrease in neuroblast migration speed (Kaneko et al., 2010). Moreover, astrocytes as well as neuroblasts express Slits receptors, Robo2 and Robo3. Interestingly, Slits secreted by neuroblasts causes a Robo-dependent rearrangement of surrounding astrocytic processes, favouring neuroblast migration through the glial tunnel (Kaneko et al., 2010).

1.2.2.5 Adhesion molecules

PSA-NCAM

The neural cell adhesion molecule (NCAM) is a homophilic receptor expressed by neurons and glia involved in cell adhesion and neurite outgrowth (Doherty et al., 1990). NCAM can be post-translationally modified by the addition of polysialic acid (PSA), reducing its homophilic binding and thus adhesiveness, thereby regulating cell migration during embryonic brain development (Rutishauser et al., 1985). PSA-NCAM is expressed in the adult brain in migrating neuroblasts (Seki and Arai, 1993). Although NCAM knockout mice maintain the neuroblast chain structure, they have a smaller OB and a build-up of neuroblasts in the RMS, indicating that NCAM plays a role in neuroblast migration (Tomasiewicz et al., 1993, Cremer et al., 1994, Chazal et al., 2000). Moreover, NCAM knockout mice show impairment in astrocyte-

neuroblast interactions. Interestingly, a similar phenotype was seen in mice where PSA was enzymatically removed by injection of neuraminidase (Ono et al., 1994), indicating that NCAM glycosylation is necessary for NCAM-dependent regulation of neuroblast migration. This suggests that reduction in neuroblast adhesion promoted by PSA may help SVZ-derived neuroblasts to migrate through the surrounding glial tube.

Integrins

Integrins are heterodimeric transmembrane receptors consisting of two subunits, α and β, and are responsible for mediating information between cells or between cells and the ECM (Hynes, 2002).

Several integrins are expressed along the RMS at different developmental stages. α1 is expressed by neonates, but its level decreases during postnatal development, while αv, β3, β6 are expressed in early postnatal development and in adulthood (Murase and Horwitz 2002). On the other hand, β8 is expressed during development and also in adult stages (Mobley and McCarty, 2011). Interestingly, knockout mice for β8 integrin show impairment in neuroblast chain formation (Mobley and McCarty, 2011). Integrins when dimerised form receptors for laminins, which are also expressed in the SVZ-RMS (Kazanis et al., 2010). β1 integrin is highly expressed in RMS migrating neuroblasts as are the α1, α2 and α4 subunits, with which β1 forms laminin receptors (Belvindrah et al., 2007). Although neuroblasts are still capable of migration, genetic deletion or blockade of β1 disrupts neuroblast chains in the glial tube, indicating that β1 controls neuroblast migration by regulating intercellular contacts (Belvindrah et al., 2007, Kazanis et al., 2010). A similar phenotype was observed in α2 and α4 knockout mice, where neuroblast chains are loose and disorganised (Belvindrah et al., 2007), indicating that the interaction between integrins and their ligands, laminins, is important to regulate chain organisation in the RMS.

Galectin-3

At the intracellular level, Galectin-3 has a cytoplasmic function by interacting with integrins, thus regulating adhesion to the ECM, and a nuclear function regulating

cell survival (Elola et al., 2007). In the SVZ, galectin-3 is expressed by ependymal cells and astrocytes and its genetic deletion leads to an abnormal phenotype of these cells (Comte et al., 2011). This may indicate that galectin-3 could have a role in maintaining the ependymal cilia beating and thus CSF flow, which contributes to regulate the directed migration of neuroblasts (Sawamoto et al., 2006), as well as in maintaining the structure of the astrocytic tunnel (Comte et al., 2011). While cell proliferation and cell death were not affected by lack of galectin-3, neuroblast migration was slower with a higher number of stationary cells (Comte et al., 2011). Interestingly, RMS explants from *gal-3* knockout mice show an increase in cells migrating individually. Moreover, inhibiting galectin-3 with blocking antibodies leads to a dramatic decrease of neuroblast chains. This suggests that galectin-3 might regulate neuroblast migration by maintaining neuroblast chains during migration along the RMS (Comte et al., 2011). Finally, loss of galectin-3 leads to an increased level of phosphorylated EGFR, a negative regulator of neuroblast migration (see above) (Kim et al., 2009, Comte et al., 2011). Therefore, galectin-3 seems to play a series of different roles in controlling neuroblast migration, including antagonising signalling from factors (i.e. EGF) that inhibit migration (Comte et al., 2011).

Thrombospondin-1

Thrombospondins are secreted proteins widely expressed in the CNS where they promote neurite outgrowth in cultured neurons and migration of cerebellar granule cells (O'Shea et al., 1990, O'Shea et al., 1991). Thrombospondin-1 (THBS-1) is involved in inter-cell and cell-ECM interactions (Lawler, 2000). Interestingly, THBS-1 is expressed in the SVZ and along the RMS of postnatal mice and binds to two important neuroblast chain regulators, apolipoprotein E receptor 2 (ApoER2) and very-low density lipoprotein receptor (VLDLR) (Andrade et al., 2007, Blake et al., 2008). THBS-1 genetic deletion leads to an abnormal RMS morphology and decreased neuroblast migration as well as integration in the OB (Blake et al., 2008). THBS-1 regulates neuroblast migration by stabilizing neuroblast chains; indeed, in cultured RMS explants THBS-1 addition leads to longer neuroblast chains while its

depletion causes an increase of neuroblasts migrating as single cells (Blake et al., 2008).

1.2.2.6 Endocannabinoid signalling

The main endocannabinoids (eCBs) in the brain are two lipids, 2-arachidonyl-glycerol (2-AG) (Sugiura et al., 1995) and anandamide (Devane et al., 1992), which activate the cannabinoid receptors CB1 and CB2 (Matsuda et al., 1990, Munro et al., 1993). Endocannabinoids play regulatory functions in the CNS during development and adult stages (Harkany et al., 2007, Mechoulam and Parker, 2013). Interestingly, endocannabinoid signalling also controls adult neurogenesis. In both the hippocampus and the SVZ, NS cell proliferation was impaired after treatment with CB1 or CB2 antagonists (Jin et al., 2004, Aguado et al., 2006, Palazuelos et al., 2006, Goncalves et al., 2008). Similarly, inhibition or genetic deletion of diacylglycerol lipases, DAGLα or DAGLβ, which are the enzymes responsible for the synthesis of 2-AG, show a decrease in NS cell proliferation (Goncalves et al., 2008, Gao et al., 2010). Furthermore, administration of a CB2 agonist increases the level of NS cell proliferation in the adult rodent SVZ (Goncalves et al., 2008), reinforcing the idea that an endocannabinoid tone controls cell proliferation in the SVZ.

Interestingly, both DAGL and the CB receptors are expressed in PSA-NCAM+ migrating neuroblasts, but not in GFAP+ astrocytes. Moreover, treatment with CB receptor agonists increases neuroblast migration *in vitro* (Oudin et al., 2011) and *in vivo* (Lalli lab, unpublished data), while CB receptor antagonists have the opposite effect, suggesting the existence of an endocannabinoid tone regulating RMS migration (Oudin et al., 2011). The endocannabinoid system also regulates the morphology of migrating neuroblasts *in vitro* and *in vivo*; CB receptor agonists increase the length of the neuroblast leading process, while CB receptor antagonists cause a highly branched neuroblast morphology (Oudin et al., 2011).

Table 1-1. List of factors that regulate neuroblast migration in the RMS.

Factors regulating migration in the RMS	References
Vasculature	(Snapyan et al., 2009, Whitman et al., 2009, Bozoyan et al., 2012)
CSF	(Sawamoto et al., 2006)
Astrocytes	(Lois et al., 1996, Wichterle et al., 1997, Whitman et al., 2009)
Electric current	(Cao et al., 2013)
Matrix metalloproteinases	(Bovetti et al., 2007)
Dcx	(Koizumi et al., 2006, Ocbina et al., 2006)
Fascin	(Sonego et al., 2013a)
Endocannabinoids	(Oudin et al., 2011)
PSA-NCAM	(Tomasiewicz et al., 1993, Cremer et al., 1994, Ono et al., 1994, Hu et al., 1996, Chazal et al., 2000)
Integrins	(Emsley and Hagg, 2003, Belvindrah et al., 2007, Mobley et al., 2009, Mobley and McCarty, 2011).
Galectin-3	(Comte et al., 2011)
Thrombospondin-1	(Blake et al., 2008)
Reelin	(Hack et al., 2002)
Tenascin-R	(Saghatelyan et al., 2004)
Slit/ROBO	(Hu and Rutishauser, 1996, Hu, 1999, Wu et al., 1999, Nguyen-Ba-Charvet et al., 2002, Ward et al., 2003, Nguyen-Ba-Charvet et al., 2004).
Netrin-1/Dcc	(Murase and Horwitz, 2002, Hakanen et al., 2011)
ErbB4/Neuregulin NRG1-NRG3	(Anton et al., 2004)
Ephrin/EphB2	(Conover et al., 2000)
Semaphorin/Plexin-B2	(Saha et al., 2012)

Ganglioside 9-O-acetyl GD3	(Miyakoshi et al., 2012)
ApoER2/VLDL receptor	(Andrade et al., 2007)
GDNF	(Paratcha et al., 2006)
HGF	(Garzotto et al., 2008)
BDNF	(Chiaramello et al., 2007)
VEGF	(Zhang et al., 2003, Wittko et al., 2009)
FGF-2	(Garcia-Gonzalez et al., 2010)
IGF	(Hurtado-Chong et al., 2009)
EGF	(Kim et al., 2009)
GABA	(Bolteus and Bordey, 2004)
Glutamate	(Platel et al., 2008a, Platel et al., 2008b)
MIA	(Mason et al., 2001)
ADAM2	(Murase et al., 2008)
Connexins	(Marins et al. 2009)
Meteorin and Cometin	(Jorgensen et al., 2012, Wang et al., 2012)
Nogo	(Rolando et al., 2012)
Sonic Hedgehog (Shh)	(Angot et al., 2008)
Prokineticin 2	(Ng et al., 2005, Prosser et al., 2007, Puverel et al., 2009)

1.2.3 Radial migration in the OB

The final destination of the SVZ-derived neuroblasts migrating along the RMS is the OB, where neuroblasts start to migrate radially as single cells towards the different layers of the OB (Figure 1-4) (Alvarez-Buylla, 1997). The majority migrates towards the GCL, where they will become GCs (Carleton et al. 2003), while the rest migrates towards the GL, where they will mature into PGCs (Belluzzi et al., 2003). Moreover, depending on the region of origin in the SVZ, neuroblasts populate different layers becoming specific interneuron types. For example, neural precursors from the dorsal region of the SVZ become superficial GCs and TH+ PGCs, while neural precursors from the ventral region of SVZ become deep GCs or CalB+ PGCs (Lledo et al., 2006). Interestingly, growing cells from the different SVZ regions *in vitro* or transplanting them in other SVZ areas does not change their final identity, indicating that their fate is specified intrinsically and is not influenced by the environment (Merkle et al., 2007).

The transition between tangential migration along the RMS and radial migration in the OB is regulated by different adhesion molecules, such as Reelin and Tenascin-R.

Reelin is expressed by MCs and its expression decreases in a gradient from the GCL to the RMS, where it is absent (Hack et al., 2002). Interestingly, Reelin knockout mice show an accumulation of cells at the end of the stream and a disrupted OB layer organization (Hack et al., 2002, Kim et al., 2002). Thus, Reelin acts as a switch promoting the radial migration of neuroblasts at the rostral end of the RMS (Hack et al., 2002). Reelin addition to RMS explants cultured *in vitro* disrupts neuroblast chains and promotes single cell migration, indicating that Reelin may play a role also in disassembling neuroblast chains (Hack et al., 2002).

Tenascin-R, similar to Reelin, has a role in regulating the detachment of neuroblast chains, thus promoting radial migration in the OB. Tenascin-R is expressed in the GL and in the IPL, while it is absent in the SVZ, RMS as well as the core of the OB (Saghatelyan et al., 2004). Tenascin-R knockout mice show an accumulation of neuroblasts at the end of the RMS, and *in vitro* RMS explants from the same animals show a reduction of neuroblast chain formation (Saghatelyan et al., 2004). Moreover, Tenascin-R expression is activity-dependent. Indeed, naris occlusion reduces Tenascin-R expression and decreases the number of migrating neuroblasts

reaching the OB, indicating a functional role for Tenascin-R in recruiting neuroblasts in the OB (Saghatelyan et al., 2004). Tenascin-R also acts as a chemoattractant since its ectopic expression in other areas of the brain induces neuroblasts to leave the RMS (Saghatelyan et al., 2004).

Another neuroblast chemoattractant is prokineticin 2, which plays an important role in regulating neuroblast radial migration in the OB (Ng et al., 2005). Prokineticin 2 shows specific OB expression and its knockout mice display defective neuroblast chain detachment and impaired radial migration in the OB (Ng et al., 2005).

1.2.4 Intracellular regulation of neuroblast migration

1.2.4.1 The migration cycle

A series of cytoskeletal rearrangements occur in migrating neuroblasts (Schaar and McConnell, 2005). Neuroblasts extend a leading process that ends with a growth cone-like structure rich in filopodia, as well as a trailing edge in the opposite direction (Nam et al., 2007). Filopodia are spike-like structures that contain parallel filaments of actin (Ridley et al., 2003). Leading processes are unipolar or bipolar structures established and maintained by microtubule polymerization (Schliwa et al., 1999, Nam et al., 2007).

Migration is a cyclic process during which neuronal progenitors undergo three different events (Figure 1-6; supplementary movie 1). The first step occurs in response to the integration of extracellular signals and involves cell polarization, extension of a leading edge driven by lamellipodia and filopodia, and microtubule polymerization. Actin polymerization, which results from the activity of several actin-binding proteins, creates a tension force under the cell membrane towards the direction of the migration (Schliwa et al., 1999, Lambert de Rouvroit and Goffinet, 2001, Ridley et al., 2003, Schaar and McConnell, 2005). Filopodia are capable of sampling the environment, thus orienting the leading process and choosing the direction of migration. They can stabilize the neuroblast leading process, creating adhesiveness by attaching to the surroundings, in particular to the ECM or adjacent cells, via transmembrane receptors (Ridley et al., 2003, Schaar and McConnell, 2005). The second and third steps of migration involve the translocation of the cell body into the leading process (nucleokinesis). Specifically, in the second

step there is a swelling of the leading process that contains the centrosome, which is linked to the nucleus by a cage of microtubules that encase the nucleus itself. In the third step, this dilation is separated from the nucleus by a constriction through which the nucleus is pulled by the dynein motor complex (a minus-end directed microtubule motor) and pushed by the actomyosin contraction at the cell rear. The neuroblast then retracts the trailing process, resulting in reduced adhesiveness. The leading process is now free to extend again, creating new adhesion contacts through the filopodia and initiating a new migration cycle (Figure 1-6) (Lambert de Rouvroit and Goffinet, 2001, Schaar and McConnell, 2005, Tsai and Gleeson, 2005, Marin et al., 2010).

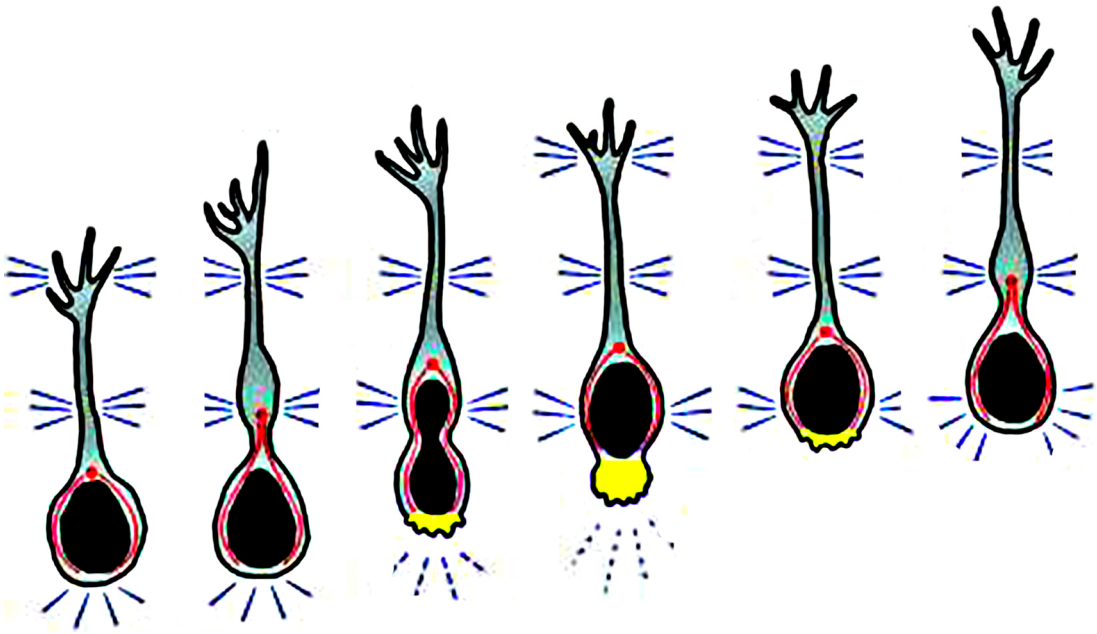


Figure 1-6. Steps of the neuroblast migration cycle.

In the first step the leading process makes adhesion contacts with the ECM (blue lines). In the second step the leading process creates a swelling that contains the centrosome (red dot). A constriction divides the leading process dilation from the nucleus, which is linked to the centrosome by a microtubule cage that surrounds the nucleus (red lines). In the third step the nucleus is pulled by the dynein motor complex and pushed by the acto-myosin contraction (yellow) and the cell rear loses adhesion contacts. This process leaves the neuroblast ready to create new adhesion contacts and start a new migration cycle (supplementary movie 1). Adapted from Schaar and McConnell, 2005.

1.2.4.2 Polarity regulation in neuroblast migration

Cell polarisation is an essential event in directed migration that involves the orientation of the leading process and the correct positioning of the centrosome in front of the nucleus. Polarisation occurs in response to an external stimulus through the activation of intracellular machinery that involves *par*titioning defective (Par) proteins, Rho family of small guanosine triphosphate (GTP)-binding proteins (GTPases), phosphoinositide 3-kinases (PI3Ks) and microtubules (Ridley et al., 2003, Goldstein and Macara, 2007).

MAP/microtubule affinity-regulating kinase 2 (MARK2 or Par1), a member of the Par family and a key regulator in cell polarity (Macara, 2004), regulates the position of the RMS neuroblast leading process and its orientation towards the OB (Figure 1-7) (Mejia-Gervacio et al., 2012). MARK2 is phosphorylated by other Par family components, but more importantly it phosphorylates proteins involved in microtubule assembly such as tau, microtubule-associated protein 2/4 (Map2/4) and Dcx, regulating axon formation and neuronal migration (Reiner and Sapir, 2009). The hypothesis that MARK2 may function through Dcx stems from the observation that Dcx is an essential regulator of neuroblast migration, controlling leading process stability as well as nucleokinesis (Gleeson et al., 1999, Koizumi et al., 2006, Belvindrah et al., 2011). Indeed, genetic removal of Dcx leads to increased branching and uncoupling of the nucleus and the centrosome (N-C) (Koizumi et al., 2006). Interestingly, MARK2 shares substrates with Cdk5, such as Dcx and nuclear distribution protein nudE-like 1 (Nudel - a protein that interacts with Lis1), suggesting that Cdk5 may also play a role in regulating neuroblast polarity through centrosome positioning (Niethammer et al., 2000, Smith et al., 2000, Mejia-Gervacio et al., 2012). Indeed, Cdk5 has been reported as a regulator of neuroblast migration, playing a role in the extension and orientation of the leading process (Figure 1-7) (Hirota et al., 2007).

The Par complex, formed by the association of Par3, Par6, and the atypical protein kinase C ζ (PKCζ), acts as a master regulator of cell polarisation by functioning as a scaffold for a variety of signalling proteins and cytoskeletal regulators (Goldstein and Macara, 2007). PKCζ and mPar6α have been reported as regulators of centrosome localisation in migrating neurons (Solecki et al., 2004). The small

GTPase cell division control protein 42 homolog (Cdc42), a crucial regulator of cell polarity, is able to bind in its GTP-bound active state to Par6, which is in a complex with PKCζ. Subsequently, PKC is capable of phosphorylating and thus inactivating glycogen synthase kinase 3 β (GSK3β). Regulation of GSK3β activity has been reported as a fundamental event in centrosome positioning during cell polarisation (Etienne-Manneville and Hall, 2003). In RMS migrating neuroblasts, where treatment with Slit leads to reorientation of the centrosome followed by repolarisation of the leading process, inhibition of either GSK3β or PKCζ leads to an impaired centrosome repositioning and leading process instability (Figure 1-7) (Higginbotham et al., 2006). This suggests that the Par complex activity has a role in establishing the correct centrosome position to ensure polarisation also in RMS migrating neuroblasts. Moreover, Par6 has recently been shown to interact with the Exo84 subunit of the exocyst (Das et al., 2013), an octameric complex involved in polarised trafficking and cell migration (Guo et al., 1999, He and Guo, 2009, Rosse et al., 2009). This interaction is promoted by active RalA (Das et al., 2013), a Ras-like GTPase known to control the morphology and polarity in embryonic cortical neurons (Lalli, 2009). Interestingly, the RalA promoted Par6-Exo84 interaction regulates RMS neuroblast morphology and polarity (Das et al., 2013).

The position of the centrosome within the neuroblast soma is dictated by the actin cytoskeleton but not by the microtubules (Higginbotham et al., 2006). Interestingly, the actin nucleator mDia (mammalian diaphanous) can regulate centrosome positioning (Shinohara et al., 2012). mDia nucleates actin monomers to create straight actin filaments, thus promoting its polymerisation (Higashida et al., 2004). Indeed mDia genetic depletion leads to a decrease in distance between the nucleus and centrosome before nuclear translocation (Shinohara et al., 2012). Moreover, mDia knockout mice neither show accumulation of filamentous actin (F-actin) at the cell rear (F-actin cup) nor in the region ahead of the nucleus, indicating that mDia dictates F-actin localisation (Shinohara et al., 2012). Importantly, in wild type animals, F-actin condensation ahead of the nucleus was concomitant to the movement of the centrosome, indicating that mDia-dependent F-actin localisation is critical for centrosome positioning during nuclear translocation (Figure 1-7) (Shinohara et al., 2012).

Therefore, while microtubule assembly seems to play a role in stabilising the leading process and promoting nucleokinesis, actin-dynamics seem to be responsible for centrosome positioning and neuroblast polarisation.

1.2.4.3 Adhesion regulation in neuroblast migration

For efficient migration, protrusion extension needs to be followed by protrusion attachment to the surrounding environment. Cell adhesion molecules, such as integrins (see above), play a fundamental role in migration by regulating interactions between the ECM and the intracellular cytoskeleton (Belvindrah et al., 2007, Elola et al., 2007) and modulating adhesion thereby creating traction forces used in forward movement. While forming adhesions stabilises cell protrusions, weakening of adhesions is necessary for cell detachment from the substrate to allow forward movement. Therefore, retraction needs to be equally balanced with protrusion and adhesion for efficient cell migration (Webb et al., 2002, Ridley et al., 2003)

Adhesion disassembly can occur either through myosin-based contractions or clathrin/dynamin-mediated endocytosis of adhesion molecules (Figure 1-7) (Schaar and McConnell, 2005, Kawauchi et al., 2010, Shieh et al., 2011). Clathrin-mediated endocytosis regulates the distribution of adhesion molecules and promotes the detachment that is needed for the cell soma to translocate into the leading process dilation (Shieh et al., 2011). Active (phosphorylated) myosin II shows a particularly high concentration at the rear of neuroblasts undergoing nucleokinesis (Schaar and McConnell, 2005). Myosin II activity is necessary for nuclear translocation and it may act by promoting contraction as well as detachment, breaking adhesions at the cell rear (Figure 1-7) (Schaar and McConnell, 2005). Thus, nuclear translocation in migrating neuroblasts is favoured by adhesion disassembly at the leading process dilation via endocytosis of adhesion molecules, and at the cell rear by myosin II-promoted contraction (Schaar and McConnell, 2005, Shieh et al., 2011).

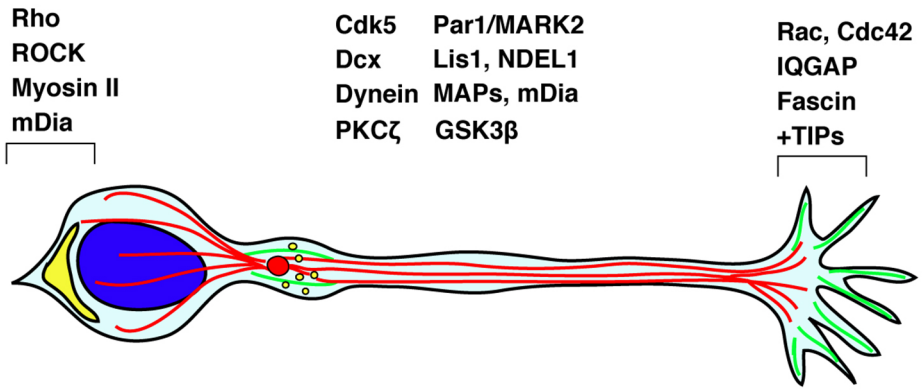


Figure 1-7. Molecular regulators of neuroblast migration.

(Top) List of the intracellular regulators involved in cytoskeletal dynamics during migration. (Bottom) Microtubules (red lines), actin (green), myosin II (yellow), nucleus (blue), Golgi apparatus and endoplasmic reticulum (yellow dots) in the swelling region in front of the nucleus together with the centrosome (red dot) are shown in the schematic representation of a migrating neuroblast. Adapted from Lalli, 2014.

1.2.5 Neuroblast migration in the injured brain

The ongoing neurogenesis in the adult brain indicates the possibility that neural stem cells could be the source of new neurons, with the potential for the regeneration of damaged tissue. In ischemic stroke and cerebral cortex injury, SVZ proliferation increases and neuroblasts are capable of leaving their native route and migrating towards the sites affected by injury (Arvidsson et al., 2002, Goings et al., 2004, Zhang et al., 2007). Interestingly, while neuroblasts express receptors such as C-X-C chemokine receptor type 4 (CXCR4), the tyrosine protein kinase receptor (Tie2) and C-C chemokine receptor type 2 (CCR2), sites of injury express their ligands such as stroma cell-derived factor 1 (SDF1), angioprotein 1 (Ang1) and monocyte chemoattractant protein 1 (MCP1), respectively (Imitola et al., 2004, Ohab et al., 2006, Robin et al., 2006, Thored et al., 2006, Yan et al., 2007). These factors, secreted by vascular endothelial cells (SDF1 and Ang1) and by activated astrocytes (MCP1) in the injured areas, act as chemoattractants for neuroblasts that form chains and migrate into the striatum, closely associated with blood vessels and astrocytic processes (Yamashita et al., 2006). It is important to note that a correlation between angiogenesis and neurogenesis also exists in damaged brains, specifically after lesion when factors such as VEGF, BDNF, FGF2, EGF and metalloproteinases are produced. This suggests that angiogenesis occurring in the ischemic area precedes neurogenesis (Hayashi et al., 2003, Shen et al., 2004, Lee et al., 2006, Grade et al., 2013).

Interestingly, increased SVZ neurogenesis followed by neuroblast migration to damaged areas of the striatum was also observed in a lesion model of Huntington's disease (Tattersfield et al., 2004, Batista et al., 2006). In a 6-hydroxydopamine (6-OHDA) rat Parkinson's model, there is reduced SVZ cell proliferation but neuroblasts are seen migrating through the striatum towards the lesion site and partially differentiate either into dopaminergic neurons or glia (Fallon et al., 2000, Baker et al., 2004, Winner et al., 2008).

SVZ neurogenesis in the injured adult human brain still needs to be properly characterized. Some reports have shown increased NS cell proliferation in the SVZ followed by migration of neuroblasts towards sites affected by injury (Jin et al., 2006, Macas et al., 2006, Ekonomou et al., 2012). Moreover, neuroblasts in the

damaged areas start to express markers of differentiated neurons (Ekonomou et al., 2011). These emerging observations have raised some hope in endogenous stem cell-based regenerative strategies. A thorough understanding of the mechanisms underlying neuroblast migration and differentiation will be essential for the development of these important therapeutic applications.

1.3 Fascin

1.3.1 History, molecular structure and expression

Fascin was first isolated in 1975 from sea urchin egg extracts as an actin-binding protein of 55 kDa (Kane, 1975). Subsequent studies revealed that fascin bundles actin filaments, forming filopodia in phagocytic coelomocytes (Otto et al., 1979). This bundling function is reflected in the Latin origin of the name "fascin" coming from "fasciculus", meaning "bundle" (Otto et al., 1979). Later, fascin was identified in *Drosophila* (Cant et al., 1994, Duh et al., 1994), Hela cells (Yamashiro-Matsumura and Matsumura, 1985), mice (Edwards and Bryan, 1995) and *Xenopus* (Holthuis et al., 1994).

There are three fascin genes: fascin-1, which is mainly expressed in the nervous system, mesenchymal tissues, dendritic cells and skeletal and smooth muscles; fascin-2, which is expressed in the retina; and fascin-3, which is expressed in the testis (Tubb et al., 2002). In this study we focused exclusively on fascin-1, which we refer to for simplicity as fascin.

Fascin is a globular protein that consists of four β-trefoil domains, which are characterized by twelve beta strands folded into three similar beta-beta-beta-loop-beta (trefoil) units (Ponting and Russell, 2000, Sedeh et al., 2010). Fascin has two actin-binding sites, one located at the N-terminus in the first β-trefoil domain between aminoacid (aa) 33 and aa47, and one located at the C-terminus in the third and fourth domains between aa277 and aa493 (Figure 1-8). These two actin-binding sites allow fascin to cross-link adjacent actin filaments, thus organizing them in parallel tight bundles in filopodial structures (Figure 1-9).

Two regulatory sites have been so far identified in fascin: serine 39 (Ser39 or S39) at the N-terminus and serine 274 (Ser274 or S274) (Ser289 in *Drosophila*) at the C-terminus (Yamakita et al., 1996, Jansen et al., 2011, Zanet et al., 2012). Ser39 is a well characterised site which is phosphorylated by PKC (Ono et al., 1997) and its phosphorylation prevents the binding of fascin to actin, inhibiting filopodia formation (Figure 1-8) (Yamakita et al., 1996). Ser274 also binds to actin: a non-phosphorylatable mutation on this site (S274A) decreases actin-bundling activity, while a phosphomimetic mutation (S274D) leads to bundle disorganization.

Interestingly, disruption of the actin-bundling activity by S274A does not interfere with the formation of filopodia since transfection of this mutant rescues filopodia formation as well as macrophage migration in fascin-depleted *Drosophila*. Moreover, S274A shows stable expression at the distal end of the filopodia (Zanet et al., 2012). This might suggest that fascin does not only stabilise preformed actin filaments with its bundling activity, but also has a role in stabilizing the tip of the growth cone, thus promoting actin polymerisation and filopodia formation.

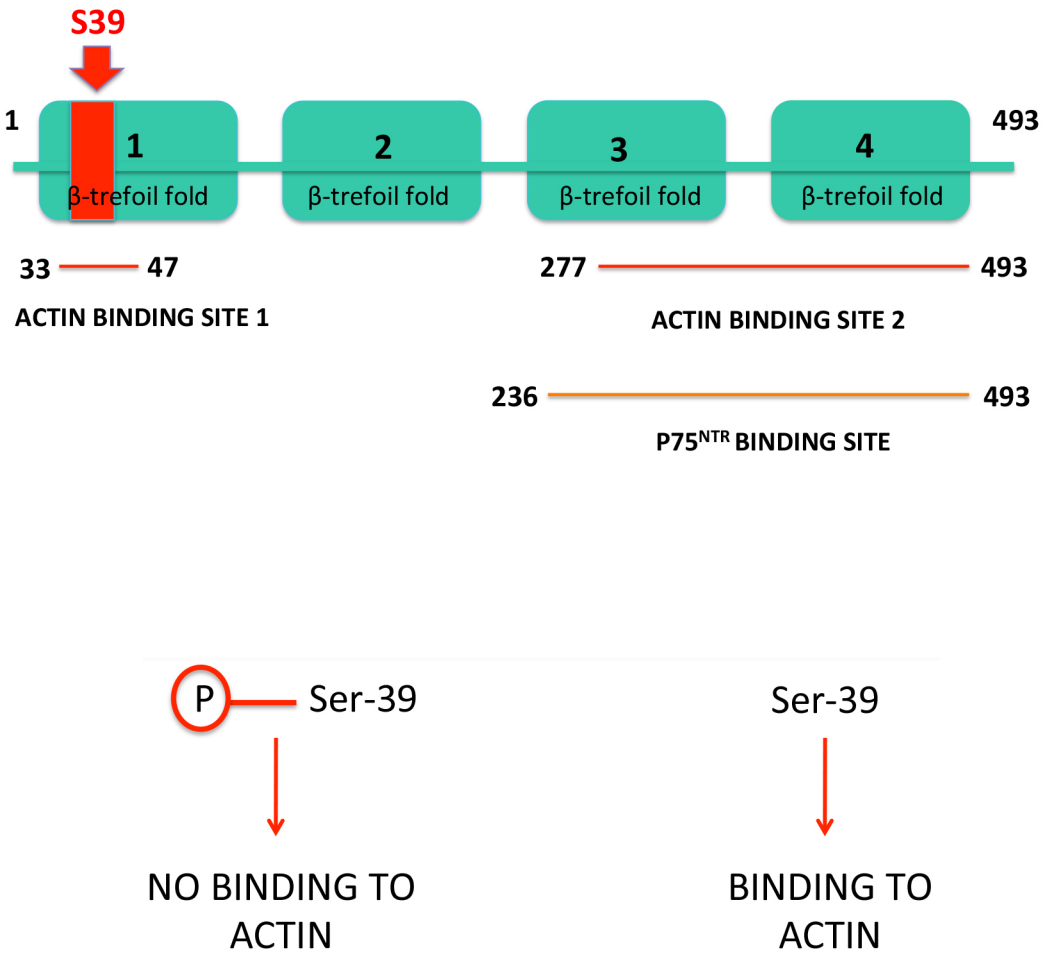


Figure 1-8. The molecular structure of fascin.

Fascin has four β-trefoil domains. The first actin-binding site is located at the N-terminus in the first β-trefoil domain. The second actin-binding site is located within the third and fourth β-trefoil domains at the C-terminus, which also contains a $p75^{NTR}$ binding site. The first β-trefoil domain contains a phosphorylation site, Ser39 (red), which regulates the ability of fascin to bind F-actin (phosphorylation of Ser39 prevents fascin from binding F-actin, while its dephosphorylation enables fascin binding to F-actin).

1.3.2 Biological functions

F-actin bundling activity and filopodia assembly

Contrary to lamellipodia, which contain a highly branched actin network, filopodia contain unbranched, parallel filaments of actin. Filopodia are thin and long finger-like structures that extend their roots into the lamellipodium, which is a thin sheet-like protrusion (Figure 1-8) (Vignjevic et al., 2003, Mattila and Lappalainen, 2008).

Filopodia can be assembled and disassembled through actin polymerisation and depolymerisation, thus promoting protrusion and retraction respectively. Filaments of actin are self-assembled by polymerisation of actin monomers, which have a 'barbed' end and a 'pointed' end. All the actin monomers are oriented in the same direction giving polarity to the actin filaments. Although polymerisation and depolymerisation can involve both ends, in most of the cases polymerisation occurs at the barbed ends, while depolymerisation occurs at the pointed ends (Chhabra and Higgs, 2007). Actin-related protein 2/3 (Arp2/3) complex can nucleate actin filaments and protect them from capping (barbed end capping proteins block F-actin extension) or bind to pre-formed actin filaments at a 70 degrees angle, creating branches of F-actin and thus the 'dendritic' actin network in the lamellipodium. To promote F-actin branching, Arp2/3 complex needs to be activated through the binding of nucleation-promoting factors such as Wiskott-Aldrich syndrome protein (WASP)/WASP-family verprolin-homologous protein (WAVE)-family proteins (Chhabra and Higgs, 2007, Mattila and Lappalainen, 2008).

Formins are a second family of actin nucleators that move along unbranched actin filaments promoting their elongation and protecting them from capping (Chhabra and Higgs, 2007, Mattila and Lappalainen, 2008).

The mechanisms underlying filopodia formation are still a matter of intense debate. An *in vitro* system using purified proteins to produce filopodia-like structures revealed that actin, fascin and the two actin nucleators WASP and Arp2/3 are sufficient to produce actin bundles (Vignjevic et al., 2003). Moreover, Svitkina and colleagues studying the mechanisms in intact melanoma cells have proposed the "convergent elongation model" (Svitkina et al., 2003). This model suggests that filopodia emerge from the Arp2/3-induced dendritic network, where a set of Arp2/3-nucleated actin filaments, protected from capping proteins by

enabled/Vasodilator-Stimulated Phosphoprotein (ENA/VASP), converge and are subsequently elongated by fascin that, by cross-linking actin filaments, creates stable bundles and thus filopodial structures (Svitkina et al., 2003, Ideses et al., 2008, Mattila and Lappalainen, 2008). Whether filopodia generate from the lamellipodial dendritic network (Svitkina et al., 2003, Ideses et al., 2008) or from the leading edge through formin activity in a lamellipodia-independent manner (Faix and Rottner, 2006, Steffen et al., 2006, Urban et al., 2010) is still a subject of intense research.

Interestingly, in neuronal cells, Arp2/3 has been shown to be important for the formation of filopodia, whose actin-bundles show expression of fascin along their entire length (Korobova and Svitkina, 2008). A subsequent study using a sophisticated filopodia assembly assay discovered that transducer of Cdc42-dependent actin assembly (Toca-1) and N-WASP recruit Arp2/3 and actin at the filopodia tip, while VASP, the diaphanous-related formin 2 (Dia2) and fascin are responsible for filopodia elongation (Figure 1-9) (Lee et al., 2010). As a consequence, fascin depletion in neurons, melanoma cells, fibroblasts and myoblasts leads to decreased filopodia assembly (Adams and Schwartz, 2000, Cohan et al., 2001, Vignjevic et al., 2007, Yamakita et al., 2009). Interestingly, myosin X, a molecular motor protein, which is a component of the tip complex (along with Dia2 and ENA/VASP) during filopodia formation (Mattila and Lappalainen, 2008), recognises and walks, using an ATP-dependent mechanism, along fascin-promoted actin-bundles, favouring filopodia extension (Ricca and Rock, 2010).

In filopodia, fascin interaction with actin is a reversible and highly dynamic process, involving cycles of F-actin association and dissociation (Vignjevic et al., 2006, Aratyn et al., 2007). Interestingly, the F-actin bundling function of fascin is destabilised by other actin-binding proteins such as skeletal muscle tropomyosin, drebrin and α-actinin, which antagonise each other in the binding to actin, and hence regulating the dynamics of filopodia by assembling and disassembling actin bundles (Yamashiro-Matsumura and Matsumura, 1985, Sasaki et al., 1996, Courson and Rock, 2010). Moreover, myosin II promotes the disassembly of fascin-promoted actin bundles, and thus of filopodia (Haviv et al., 2008). Also, the fascin-promoted

cross-linked actin bundles are disassembled by cofilin, a regulator of actin depolymerisation. Interestingly, fascin cooperates with cofilin in F-actin unbundling, reinforcing the concept that fascin-promoted actin bundling function has a highly dynamic nature (Breitsprecher et al., 2011).

Fascin attachment and detachment from actin filaments hence contributes to filopodia dynamics (filopodia extension and shrinkage) (Vignjevic et al., 2006, Aratyn et al., 2007), therefore contributing to processes where filopodia play a crucial function, like for example growth cone reorientation (Brown and Bridgman, 2009). The dynamic binding/detachment of fascin to actin filaments is regulated by PKC-mediated phosphorylation of fascin on Ser39 (Yamakita et al., 1996, Vignjevic et al., 2006, Aratyn et al., 2007). Reduced filopodia were detected in mouse melanoma cells expressing a fascin phosphomimetic variant (S39D), while the non-phosphorylatable variant, S39A, showed an increase in filopodia number and length (Vignjevic et al., 2006).

Cell adhesion and migration

Fascin has also been implicated in the regulation of cell adhesion, with the balance between phosphorylated and unphosphorylated fascin regulated by different ECM substrates as well as other extracellular cues (Adams, 2004).

Adhesion is an important function through which the cell samples the surrounding environment. Stability of adhesion is ensured by focal adhesions, which are large and stable macromolecular assemblies connecting the ECM to the actin cytoskeleton. They are constituted by clusters of integrins, which are transmembrane receptors with an extracellular domain that binds to the ECM and an intracellular domain that binds to the cytoskeleton via adapter proteins such as talin, α-actinin, filamin and vinculin. Focal adhesions are capable of responding to variations in the composition of the ECM by adapting cell adhesion to the different substrates (Geiger et al., 2009, Ross et al., 2013).

Although fascin is not considered a component of focal adhesions, it indirectly controls adhesiveness through the regulation of F-actin dynamics in the assembly/disassembly of filopodia. One of the first studies that reported a role for fascin in adhesion showed that fascin knockdown leads to a reduction in the

number of filopodia and in focal adhesion disassembly, thereby decreasing migration and metastasis in colon cancer cells (Hashimoto et al., 2007). Two other adhesive structures - podosomes and invadopodia - contain high fascin levels. Podosomes and invadopodia are finger-like membrane protrusions rich in actin, capable of invading into and degrading the surrounding ECM. While podosomes are smaller structures of normal cells such as monocytes, smooth muscle cells, endothelial cells and Src-transformed fibroblasts, invadopodia are wider structures protruding into the ECM associated with cancer cells. Moreover, podosomes and invadopodia are characterised by structural and functional differences such as interaction with ECM or composition/localisation of the actin-polymerisation machinery and of the adhesion machinery (Chhabra and Higgs, 2007, Gimona, 2008).

In the podosomes of vascular smooth muscle cells fascin increases adhesiveness and migration in response to injured blood vessels (Quintavalle et al., 2010). In the invadopodia of human melanoma cells fascin is regulated via PKC-dependent phosphorylation, and it controls adhesion stability, promoting migration (Li et al., 2010).

In *Drosophila*, fascin has a role in the assembly of F-actin rich structures such as bristles and micro-spikes of plasmatocytes (macrophages) (Zanet et al., 2009, Zhang et al., 2009). Interestingly, fascin-dependent dynamic assembly of micro-spikes of plasmatocytes is essential for the promotion of polarised lamellae, and thus for orienting the cell in the direction of migration (Zanet et al., 2009).

Fascin is localised in the stress fibres of cultured cells (Yamashiro-Matsumura and Matsumura, 1986) and its role/localisation can be regulated depending on the adhesion substrate (laminin or thrombospondin-1 versus fibronectin) (Adams, 1997). Interestingly, filopodia can entry into the lamellipodium, where fascin-containing actin bundles could constitute the seed for the formation of stress fibers (Nemethova et al., 2008).

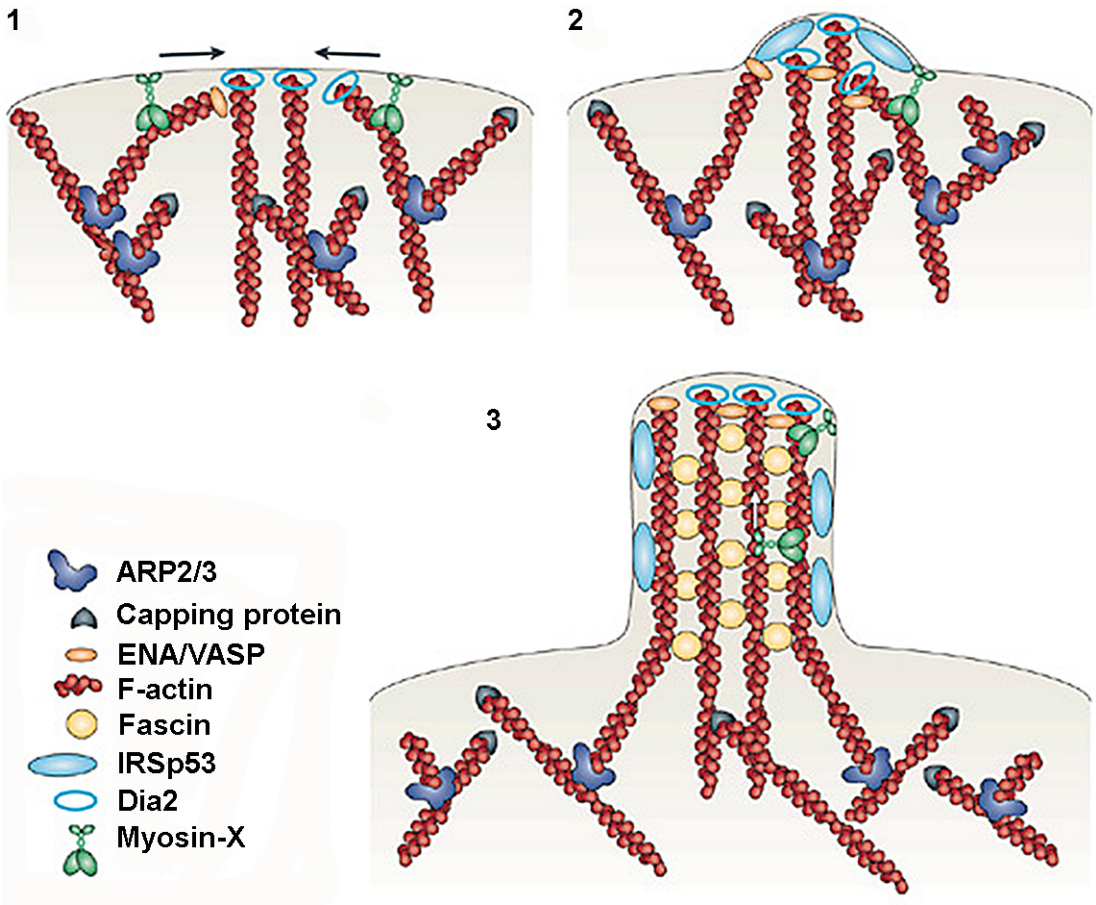


Figure 1-9. Fascin in filopodia assembly.

1) Monomers of actin elongate uncapped (no capping proteins – grey cones) actin filaments (F-actin, red). WASP family proteins (not shown) activate Arp2/3, which promotes F-actin branching and thus the lamellipodial dendritic network. A subset of uncapped filaments converges together through the activity of myosin-X at the edge of the lamellipodial membrane where they continue to elongate through Dia2 and ENA/VASP activity. 2) Insulin-receptor substrate p53 (IRSp53) deforms the membrane and facilitates the creation of a protrusion. ENA/VASP may function also as cross-linker of F-actin at the beginning of filopodia elongation. 3) Fascin is recruited at the edge of the cell with the tip complex (ENA/VASP proteins, Dia2 and myosin-X). While Dia2 controls elongation of unbranched F-actin, fascin cross-links unbranched filaments of actin organising F-actin in parallel tight bundles, forming filopodia. Adapted from Mattila and Lappalainen, 2008.

1.3.3 Fascin regulators

At the transcript level

Fascin transcript levels are up-regulated in mature dendritic cells as well as multiple malignant cancers (Mosialos et al., 1996, Hashimoto et al., 2011). Fascin transcription appears to be regulated by cAMP response element binding protein (CREB) and aryl hydrocarbon receptor (AhR) in carcinoma cells, fibroblasts and human neuronal precursors (Megiorni et al., 2005, Hashimoto et al., 2009). Moreover, micro-RNAs (miRNAs) seems to negatively regulate fascin binding to its 3'-UTR. In particular miRNA-143 and miRNA-145 decrease fascin levels and thus podosome formation in vascular smooth muscle cells (Quintavalle et al., 2010). In epithelial tissues miRNA-145 and miRNA-133 act as tumour suppressors; in bladder cancer their down-regulation leads to up-regulation of fascin transcript levels and increased cell proliferation and migration (Chiyomaru et al., 2010).

Finally, fascin is also a target of β-catenin and the T cell factor (TCF) signalling pathway. Fascin has been reported to be up-regulated in colon cancer cells and its transcription is regulated via the binding of β-catenin and TCF to the fascin promoter (Vignjevic et al., 2007). Moreover, fascin up-regulation in response to galectin-3 expression in gastric cancer cells is controlled by the direct binding of galectin-3 to GSK-3β, which leads to the formation of a complex of β–catenin and TCF-4 that binds to the fascin promoter (Kim et al., 2010).

At the protein level

Fascin is differentially regulated by the different ECM components through PKC-dependent phosphorylation on Ser39 (Adams et al., 1999). While thrombospondin-1 or tenascin-C promotes fascin dephosphorylation on Ser39, favouring actin bundling and micro-spike formation, fibronectin, vitronectin or collagen IV promotes Ser39 phosphorylation, preventing fascin-dependent actin bundling (Adams, 1995, Fischer et al., 1997). This fascin phosphorylation is driven by PKCα (Figure 1-10) (Adams and Schwartz, 2000). Moreover, regulation of fascin-actin bundles by thrombospondin-1 is mediated by the activation of the GTPases Cdc42 and Rac through their downstream effector p21 activated kinase (PAK1) (Figure 1-10) (Adams and Schwartz, 2000). The active form of Rac can also regulate the

interaction between fascin and PKC isoform γ (PKCγ) via a PAK-dependent pathway (Figure 1-10) (Parsons and Adams, 2008). Also, skeletal myoblasts adherent to thrombospondin-1 showed a loss of fascin-containing microspikes when syndecan-1, a transmembrane proteoglycan, was deleted from its cytoplasmic domain, indicating that thrombospondin-1 mediates actin-bundling of fascin through syndecan-1 (Figure 1-10) (Adams et al., 2001). Fascin may thus be seen as providing a link between the cytoskeletal dynamics in filopodia formation and different ECM substrates.

The actin-bundling function of fascin can also be regulated by another small GTPase, the intracellular trafficking protein Rab35. Active Rab35 directly binds to fascin and favours its actin-bundling function and filopodia formation by promoting its localisation at the leading edge of cells (Figure 1-10) (Zhang et al., 2009). Moreover, fascin can be positively regulated by p-Lin-11/Isl-1/Mec-3 kinases (LIMK) 1 and LIMK2 via the small GTPases Rho, which is a cell-contractility regulator. LIMK1/2-fascin complex promotes fascin actin-bundling function and filopodia stability (Figure 1-10) (Jayo et al., 2012). These studies have highlighted the importance of the small GTPases as regulators of fascin actin-bundling function.

Several other factors have been identified as fascin regulators. As mentioned above, fascin can be regulated by other actin modulators like tropomyosin, α-actinin and drebrin, which inhibit fascin binding to actin regulating filopodial dynamics (Yamashiro-Matsumura and Matsumura, 1985, Sasaki et al., 1996, Courson and Rock, 2010).

Extracellular factors regulating fascin include IGF-I and Nerve Growth Factor (NGF). In breast cancer cells, fascin actin-bundling function is dependent on IGF-I receptor tyrosine kinase activity, whose levels are altered in breast cancer, through a PI3K-dependent process (Figure 1-10) (Guvakova et al., 2002).

In addition to actin binding domains fascin has a domain that binds to $p75^{NTR}$. Interestingly, treatment with NGF, which acts through $p75^{NTR}$, leads to an increased occurrence of fascin actin-bundles and microspikes, pointing to a role for NGF as another inducer of fascin-dependent protrusions (Figure 1-10) (Shonukan et al., 2003).

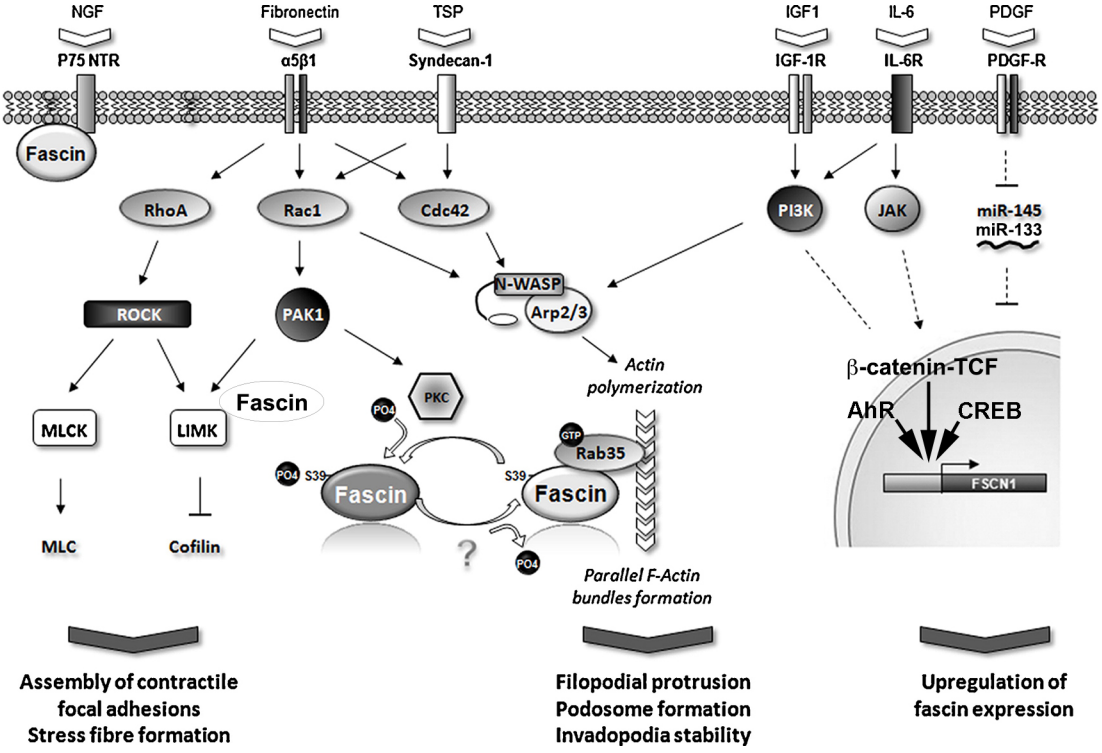


Figure 1-10. Fascin regulators.

Schematic drawing showing fascin regulators both at the expression level (dashed lines) and at the function level (solid lines). Adapted and modified from Jayo and Parsons, 2010.

1.4 Drebrin

1.4.1 History, molecular structure and expression

Drebrin (*d*evelopmentally *re*gulated *br*ain prote*in*) was first isolated from embryonic chick brain (Kojima et al., 1988, Shirao et al., 1988) and discovered to be an actin-binding protein by co-sedimentation assays and immunostaining (Shirao et al., 1994). Two drebrin isoforms are produced from a single gene by alternative splicing: an embryonic (drebrin-E) and an adult (drebrin-A) isoform, which are expressed in a development-dependent fashion (Kojima et al., 1988). In the chick brain there are two drebrin-E isoforms, E1 and E2, and they differ by an insertion of an additional residue (aa43) in E2 (Koijma et al., 1993), whereas in a mammalian brain drebrin-E has only one isoform, which is similar to E2 (Toda et al., 1993). In this study we will refer to the mammalian embryonic drebrin simply as drebrin E. Drebrin A, instead, differs from E2 because of an insertion of 46 aminoacids between the actin-domain and the proline-rich domain (see below) (Kojima et al., 1993).

The molecular structure of drebrin is highly conserved and is composed of several domains: an actin-depolymerising factor homology (ADF-H) domain, a central region of 85 aminoacids involved in actin binding containing a coiled-coil (CC) domain and a helical (Hel) domain, a proline-rich domain and a blue box domain at the C-terminus containing two Homer-binding sites, PPATF and PPPVF (Figure 1-11) (Lappalainen et al., 1998, Mammoto et al., 1998, Hayashi and Shirao, 1999, Dun and Chilton, 2010, Worth et al., 2013).

Because of its acidic nature and complex post-transcriptional modifications drebrin runs much slower on a SDS-page gel (120 kDa) than suggested by its aminoacid number (649).

As the name suggests, drebrin expression is regulated spatially and temporally. Drebrin A is expressed in dendritic spines in mature neurons and plays a role in synaptic activity (Hayashi et al., 1996, Takahashi et al., 2003, Takahashi et al., 2006, Ishikawa et al., 2007, Ivanov et al., 2009). Drebrin E, on the other hand, is expressed in the basal region of filopodia of developing neurons and regulates growth cone dynamics and neurite growth (Geraldo et al., 2008, Mizui et al., 2009).

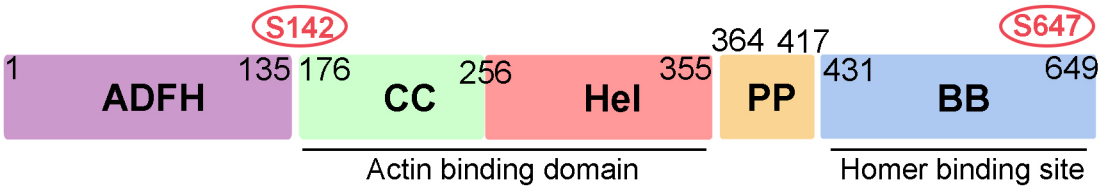


Figure 1-11. Molecular structure of drebrin.

Schematic drebrin structure showing its domains: actin-depolymerising factor homology domain (ADF-H, purple), two F-actin binding domains - coiled-coil domain (CC, green) and helical domain (Hel, pink), proline-rich domain (PP, orange), and blue box domain (BB, blue), which contains the Homer binding sites. Shown are also the two known phosphorylation sites: serine 142 (S142) and serine 647 (S647) (red ellipses).

1.4.2 Drebrin regulators

Regulators of drebrin expression

Small progress has been made in identifying the regulators of drebrin expression and its alternative splicing. In the brain the transcription factor NXF from the basic helix-loop-helix PAS-domain (bHLH-PAS) family is known to bind to the drebrin promoter, however mRNA localisation of NXF overlaps with drebrin A mRNA, and not with drebrin E, suggesting that NXF may be only the transcription factor of the adult isoform of drebrin (Ooe et al., 2004). Another member of the bHLH-PAS family, Sim2, acts as a repressor competing with NXF for binding to the drebrin promoter (Ooe et al., 2004). The homeodomain transcription factor Pax3 is also an inhibitor of drebrin expression (Mayanil et al., 2001).

Drebrin interactors

Drebrin can interact with several factors through its different domains. Drebrin competes with cofilin, an actin-binding protein involved in actin depolymerisation, for binding to F-actin through a binding site for 3-phosphoinositide-dependent protein kinase 1 (PDK1) located in the ADF-H domain (Chew et al., 2005). The proline-rich region of drebrin instead can interact with profilin, an actin polymerising factor (Mammoto et al., 1998). Through its Homer binding motifs, drebrin can also interact with the N-terminal domain of Homer2, whose C-terminal domain binds to Cdc42, forming the drebrin-Homer2-Cdc42 complex, which regulates spine morphology (Shiraishi-Yamaguchi et al., 2009).

This group of binding partners supports a role for drebrin in regulating actin dynamics. By binding to actin, drebrin inhibits the binding of other actin-binding proteins such as tropomyosin, fascin and α-actinin, thus participating in the reorganization of actin filaments (Ishikawa et al., 1994, Sasaki et al., 1996, Cheng et al., 2000). Amongst the two drebrin actin-binding domains, one is tropomyosin-sensitive while the other is tropomyosin-insensitive, since tropomyosin is not capable of entirely dissociating drebrin from actin (Ishikawa et al., 1994).

An interesting mode of regulation of drebrin function emerged from a recent study proposing that drebrin can exist in a closed conformation in which only one of the two actin-binding domains (the CC domain) is exposed and binds to actin. Cdk5-

dependent phosphorylation of drebrin on S142 causes a conformational change, exposing the second actin-binding domain (Hel domain). As such the CC domain and the Hel domain can either bind F-actin separately or bundle actin in a cooperative manner, promoting filopodia formation (Figure 1-12) (Worth et al., 2013). Moreover, the open conformation exposes another drebrin domain, which can bind the microtubule plus-tip protein EB3 (end-binding protein 3), thus allowing drebrin to act as an important link between the actin and microtubule cytoskeleton (Figure 1-12) (Geraldo et al., 2008, Worth et al., 2013).

Drebrin can also be regulated through its second phosphorylation site located at the C-terminus, S647, by phosphatase and tensin homolog (PTEN), a tumour suppressor that negatively regulates drebrin (Kreis et al., 2013).

Finally, although the molecular details are not yet fully characterised, drebrin can also bind to the C-terminal of Connexin-43, a gap junction component, acting as a gap junction stabiliser and to the Ras GTPase, thereby regulating spine morphology (Butkevich et al., 2004, Biou et al., 2008). The role of drebrin in synaptic plasticity includes its interaction with several components of the post-synaptic complex such as post-synaptic density 95 protein (PSD-95) and NMDA receptor subunits (Takahashi et al., 2003, Mizui et al., 2005, Sekino et al., 2006). Drebrin is recruited in dendritic spines by activation of AMPA (α-Amino-3-hydroxy-5-methyl-4-isoxazolepropionic acid) receptors, whereas its translocation from the spine to the dendritic shaft is promoted by activation of NMDA receptors (Sekino et al., 2006, Takahashi et al., 2006). In another study, NMDA receptor activation seems to recruit drebrin in spines, promoting microtubule “invasion” of spines (Merriam et al., 2013).

Interestingly, drebrin also appears to be required for store-operated calcium influx in T cells (Mercer et al., 2010). 3,5-bis(trifluoromethyl)pyrazole (BTP), an immuno-suppressant drug, inhibits calcium store-operated channel entry through its binding to drebrin and thus blocking drebrin-induced actin rearrangements (Mercer et al., 2010).

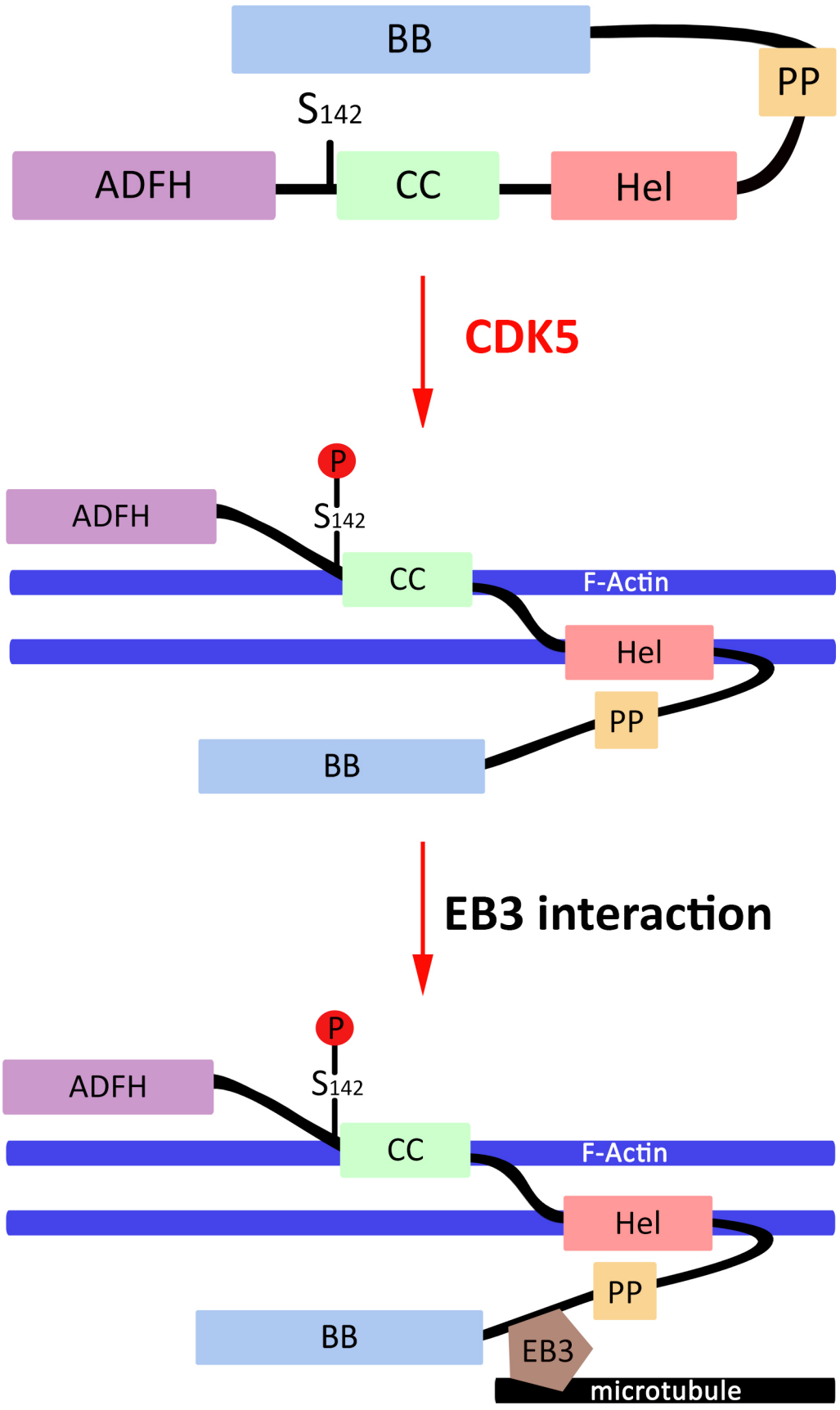

BB
PP
S142
ADFH
CC
Hel
CDK5
P
ADFH
S142
CC
F-Actin
Hel
PP
BB
EB3 interaction
P
ADFH
S142
CC
F-Actin
Hel
PP
BB
EB3
microtubule

Figure 1-12. Cdk5-dependent regulation of drebrin.

Drebrin has several domains: an actin-depolymerising factor homology (ADF-H) domain (purple), a CC domain (green), a Hel domain (pink), a prolin-rich domain (yellow) and a BB domain, which is a C-terminal Homer-binding domain (blue). Phosphorylation on S142 by Cdk5 opens the "closed" conformation of drebrin, promoting drebrin-dependent bundling of actin filaments (blue lines) and binding to microtubules (black line) through EB3 (brown pentagon). Adapted from Worth, 2013.

1.4.3 Biological function

Role in actin organisation

Drebrin plays an important role in regulating cell morphology. Its binding to actin filaments induces the formation of thick, curving actin bundles (Shirao et al., 1994). Overexpressing drebrin in both fibroblast and hippocampal neuron cultures leads to an increased number of microspikes. This effect is associated with the actin binding function of drebrin, since cells transfected with a truncated version of drebrin containing the actin-binding domain show the same phenotype (Hayashi and Shirao, 1999, Mizui et al., 2005). On the other hand, drebrin knockdown leads to a decrease in neurite outgrowth in neuroblastoma cells as well as in cortical neurons (Toda et al., 1993, Geraldo et al., 2008).

Role in cell-cell contact

Drebrin has also been found in cell processes and intercellular gap-junctions of a variety of non-neuronal cell types.

Drebrin is expressed in adherent junctions of bovine epithelial cells (Peitsch et al., 1999) as well as glioma cells (Peitsch et al., 2001). Moreover, it shows an accumulation in the adherent junctions in primary keratinocyte cultures and basal carcinoma cells, where it may have a role in inter-cell adhesion (Peitsch et al., 2005).

Interestingly, drebrin binds the C-terminal of Connexin-43, a protein involved in the formation of gap junctions as well as in the mediation of the transfer of metabolites and ions between neighbour cells (Butkevich et al., 2004). Interestingly, drebrin depletion leads to impairment of inter-cell contacts and degradation of Connexin-43, indicating that drebrin can stabilise Connexin-43 at gap-junctions (Butkevich et al., 2004).

Another recent study has shown that drebrin knockdown impairs cell-cell contacts (Rehm et al., 2013). Drebrin preserves adherent junctions of endothelial cells by stabilizing nectin, a protein forming trans-dimers between cells and thus participating in the formation of inter-cell contacts (Rehm et al., 2013).

Role in neuronal development

Drebrin has been involved in different neuronal developmental events. In cortical embryonic neurons drebrin localises to the cell soma and growth cones (Geraldo et al., 2008) where it regulates neuritogenesis through its interaction with EB3 (Geraldo et al., 2008). This interaction is important in aligning and stabilising microtubules during growth cone dynamics involved in axon extension (Geraldo et al., 2008).

In oculomotor neurons drebrin depletion inhibits the formation of the leading process as well as their migration. Indeed, overexpression of drebrin leads to defects in morphology of the axon and growth cones and to ectopic migration (Dun et al., 2012). Therefore drebrin is not only essential for the development of the leading process and the initiation of migration, but also for proper integration of the guidance cues necessary to guide neurons along the right trajectories (Dun et al., 2012).

Role in migration

Drebrin regulates migration in various contexts. Drebrin is highly expressed in adult neuroblasts migrating from the SVZ to the OB. Upon reaching the OB, drebrin appears to be downregulated, suggesting its involvement in the tangential migration of neuroblasts along the RMS (Song et al., 2008). Drebrin also regulates migration in glioblastoma, the most common and invasive brain tumour (Terakawa et al., 2013). While drebrin depletion decreases migration and invasion of the U87 glioma cell line, its overexpression increases migration and invasiveness (Terakawa et al., 2013). Interestingly, in human brain tissues from glioblastoma-positive patients, drebrin is expressed more in the peripheral tumour areas compared to the core regions (Terakawa et al., 2013).

Role in spine plasticity

Drebrin acts as a regulator of spine density and plasticity, thanks to its ability to regulate actin organisation and its high expression in dendritic spines (Shirao et al., 1994, Hayashi and Shirao, 1999). Interestingly, through its interaction with EB3, which is located at the tip of growing microtubules, drebrin appears to drive

microtubule “invasion” of active spines, where calcium influx stimulates actin polymerization (Merriam et al., 2013). Moreover, another link between drebrin and synaptic activity is provided by its interaction with PTEN, which is responsible for drebrin Ser647 dephosphorylation (Kreis et al., 2013). Indeed, neuronal activity inhibits drebrin-PTEN interaction, thereby increasing drebrin phosphorylation (Kreis et al., 2013).

Drebrin depletion leads to defective post-synaptic complex clustering in cultured neurons (Takahashi et al., 2003). Moreover, drebrin depletion in the entire mouse cortex leads to cognitive and memory formation defects (Kobayashi et al., 2004). Interestingly, drebrin levels are reduced in brains of Alzheimer’s and Down syndrome patients, implying a correlation between drebrin-dependent spine plasticity and brain functions (Harigaya et al., 1996, Shim and Lubec, 2002).

1.5 Aim: investigation of intracellular mechanisms regulating neuroblast migration in the postnatal RMS

The polarized migration of stem cell-derived neuroblasts is essential for embryonic and adult neurogenesis, ensuring the arrival and proper integration of newborn neurons into a pre-existing synaptic circuit (Belvindrah et al., 2011). Therefore, understanding how the internal signalling machinery couples with extracellular cues during neuroblast migration is critical to clarify a fundamental aspect of the neurogenic process, which could also help to fully explore the therapeutic potential of endogenous stem cell-derived neuroblasts.

Many studies have so far identified several extracellular factors regulating neuroblast migration, however still very little is known on the intracellular signalling mechanisms and the cytoskeletal dynamics controlling this process.

This thesis focused on the role of two actin-binding proteins, fascin and drebrin, in RMS neuroblast migration as well as their regulation in response to extracellular signals known to regulate neuroblast motility. This study also required the optimisation of several *in vitro* and *in vivo* assays that will continue to be used in future investigations to characterise the role of other candidate regulators of RMS neuroblast migration.

In this study the following hypotheses were pursued:

1. fascin is required for neuroblast migration
2. drebrin is required for neuroblast migration

Chapter 2 Materials and Methods

2.1 Materials

2.1.1 Animals

P2-3 mouse pups born from CD-1 mice (Charles River) and P6-7 Sprague Dawley rat pups (Harlan) of either sex were used. Sagittal brain sections for immunohistochemical analysis were obtained from P7 and adult (3 month-old) CD-1 mice.

Fascin-1 knockout mice in C57BL/6 background were a gift from Laura M. Machesky (Beatson Institute for Cancer Research, Glasgow, UK). The generation of *fascin-1* ko mice was performed by disrupting the *fascin-1* gene with a retrovirus insertion in the intron between exon 1 and exon 2 (Yamakita et al., 2009). All experiments in the *fascin-1* ko mice were performed using wild type (wt) littermates as controls. Brains were obtained from P7 and young adults (7 week-old).

All the procedures were performed in accordance with the UK Home Office Regulations (Animal Scientific Procedures Act, 1986).

2.1.2 Cell culture

Dissection media

Hank's Buffered Salt Solution (HBSS; Invitrogen) supplemented with 5 mM HEPES (Sigma) and 1% of both 100 units/ml penicillin and 100 µg/ml streptomycin (Invitrogen).

Dissociation media

HBSS containing 0.25% trypsin (Gibco) and 40 µl of DNAse I (1mg/ml; Worthington).

Neurobasal complete media

Neurobasal medium (Gibco) containing 2 mM L-glutamine (Invitrogen), B27 supplement (Invitrogen) and 0.6% glucose (Sigma) (Shieh et al., 2011).

3-dimensional Matrigel matrix

BD Matrigel™ (Basement Membrane Matrix, Growth Factor Reduced, Phenol Red-free; BD Bioscience) and Neurobasal completed media mixed in a 3:1 ratio respectively.

Phosphate Buffered Saline (PBS)

One tablet of PBS (Oxoid) containing KCl (0.2g/l), KH_2PO_4 (0.2 g/l), NaCl (8 g/l), Na_2HPO_4 (1.15 g/l) dissolved in 100 ml of water and autoclaved.

Polyhornithine

100 µl of polyornithine (50 mg/ml; Sigma) diluted in 10 ml of PBS.

Laminin

100 µl of laminin (1 mg/ml; Sigma) diluted in 10 ml of PBS.

2.1.3 Tissue culture

Brain slice collection media

Gey's Balanced Salt Solution (Invitrogen) supplemented with 0.45% glucose (Invitrogen).

Brain slice imaging media

Phenol red-free Dulbecco's Modified Eagle Medium (DMEM) supplemented with 5% foetal calf serum (FCS), 0.5% glucose, 4 mM glutamine, B27 supplement, 10 mM HEPES (pH 7.4), 100 units/ml penicillin and 100 µg/ml streptomycin.

2.1.4 Immunohistochemistry

2.1.4.1 Gelatin-embedded sections

Fixation solution

4% paraformaldehyde (PFA) in PBS.

Permeabilising and blocking solution

PBS containing 1% BSA, 0.1% Triton-X, 0.1% sodium azide.

Primary and secondary solution

PBS containing 1% BSA, 0.1% Triton-X, 0.1% sodium azide.

Permeabilising solution for bromodeoxyuridine injected animals

PBS containing 0.2% Triton-X.

Lysis solution for bromodeoxyuridine injected animals

1 N HCl and 2 N HCl.

Blocking solution for bromodeoxyuridine injected animals

PBS containing 5% BSA, 0.2% Triton-X, 1 M glycine.

Washing solution for bromodeoxyuridine injected animals

PBS containing 0.2% Triton-X.

Primary antibody solution for bromodeoxyuridine injected animals

PBS containing 5% goat serum and 0.2% Triton-X.

2.1.4.2 Paraffin-embedded sections

Blocking buffer

Tris-buffered saline (TBS) 50 mM pH 7.6 containing 1% BSA and 0.1% sodium azide.

Primary and secondary antibody solution

TBS 50 mM pH 7.6 containing 1% BSA and 0.1% sodium azide.

Dewaxing and dehydrating

Xylene and industrial methylated spirit (IMS).

Antigen Retrieval Solution

Stock solution: 20 g of citric acid in 500 ml of H_2O.

Working solution: stock solution diluted 1:100 and adjusted to pH 6 using 5 M NaOH.

StreptABComplex/HRP

Streptavidin and biotinylated HRP mixed in equal parts (DAKO).

DAB Solution

Stock solution: 5 g of diaminobenzidine tetrahydrochloride (Sigma) in 50 ml of H_2O (10% DAB stock solution).

Working solution: 10% DAB stock solution mixed with hydrogen peroxide and 0.1 M Tris buffer (pH 7.6).

2.1.5 Immunocytochemistry

Fixation Solution

4% PFA in PBS, pH 7.4.

Permeabilising and blocking solution

PBS containing 15% goat serum, 0.3% Triton-X, 0.1% bovine serum albumin (BSA).

Primary and secondary antibody solution

PBS containing 15% goat serum, 0.3% Triton-X, 0.1% BSA.

Mounting media

“Fluorescent mounting media”, from DAKO.

2.1.6 Molecular biology

pCX-EGFP

pCX-EGFP was donated from Dr Masaru Okabe (Osaka University, Japan).

Small interfering RNA (siRNA): fascin, drebrin and control

Smart pools of four pre-designed small interfering RNA (siRNA) oligos targeting rat fascin or drebrin, and control siRNA oligos (Dharmacon) were dissolved in 1X siRNA buffer (containing: 60 mM KCl, 6 mM HEPES-pH 7.5, and 0.2 mM $MgCl_2$) to a final concentration of 20 µM. The oligo sequences of each smart pool were as follows:

Fascin

5'CCGACGAGAUCGCGGUAGA3', 5'AGGCCUGCGCGGAGACUAU3',

5'UGAGAGCGUCCAACGGCAA3', and 5'GUUCAAUGAUGGCGCCUAC3'

Drebrin

5'GGUGAUUAGUAGUGGCGAC3', 5'GGUUUGAGCAGGAGCGGAU3',

5'CCUGAUAACCCACGGGAGU3', and 5'CUGAAUUCUUCCAGGGCGU3'

Short hairpin RNA (shRNA) plasmid vector

FASCIN:

Two 19 base pair (bp) sequences of mouse fascin (Chen et al., 2010):

5'-GGTGGGCAAAGATGAGCTC-3' and 5'-GTGGAGCGTGCACATCGCC-3' (Sigma) were inserted as target sequences on the AmbionOligo website for shRNA design. The resulting shRNA oligos (please see sequences below) were cloned between the ApaI and EcorV sites of the pCA-b-EGFPm5 silencer 3 expression vector (Bron et al., 2004), a gift from Matthieu Vermeren (The Babraham Institute, Cambridge). A BLAST search was performed to confirm that the shRNA oligonucleotide sequence was specifically targeting fascin.

Fascin shRNA 1:

GTGGAGCGTGCACATCGCCTTCAAGAGAGGCGATGTGCACGCTCCACTTTTTT

CCGGCACCTCGCACGTGTAGCGGAAGTTCTCTCCGCTACACGTGCGAGGTGAAAAAA -

TTAA

Fascin shRNA 2:

GGTGGGCAAAGATGAGCTCTTCAAGAGAGAGCTCATCTTTGCCCACCTTTTTT

CCGGCCACCCGTTTCTACTCGAGAAGTTCTCTCTCGAGTAGAAACGGGTGGAAAAAA - TTAA

CONTROL

The control was taken from a published sequence (Kawauchi et al., 2006).

Control sequence:

CGCGCATAAGATTAGGGAATTCAAGAGATTCCCTAATCTTATGCGCGTATTTTTT

CCGGGCGCGTATTCTAATCCCTTAAGTTCTCTAAGGGATTAGAATACGCGCATAAAAAA

Fascin and PKC plasmids

pEGFPC2 plasmids encoding different variants of *Homo sapiens* fascin-1 (wild type, fascin S39A, and fascin S39D) (Adams et al., 1999), and the monomeric RFP (mRFP)-tagged PKCα and PKCγ plasmids (Parsons and Adams, 2008), were kindly provided by Dr. Maddy Parsons (Randall Division of Cell and Molecular Biology, King's College London).

Drebrin plasmids

1) drebrin pCAG-shRNA-IRES-GFP, sequence AGAACCAGAAAGTGATGTA (Bron et al., 2004).

2) human drebrin pmCherry-N1, (all kindly donated by Britta Eickholt (Charité – Universitätsmedizin Berlin).

3) pCAG empty vector-YFP, pCAG-drebrin wild type-YFP, pCAG-drebrin 142A-YFP, and pCAG-drebrin 142D-YFP (a kind gift from Phillip Gordon-Weeks (Worth et al., 2013).

2.1.7 Western Blotting

Lysis Buffer

50 mM Tris (pH 7.5), 150 mM NaCl, 100 µM sodium beta-glycerophosphate (NaβGlyP), 0.1% sodium dodecyl sulphate (SDS), 1% $NaVO_3$, 2.5% Empigen BB™ Detergent, and 0.1% NaF.

5X Laemmli loading sample buffer (LSB)

300 mM Tris pH 6.8, 10% SDS, 25% glycerol, 0.015% bromophenol blue, 500 mM DTT.

SDS polyacrylamide gel

% Separating Gel	7%	8%	10%	12%
1.5 M Tris pH 8.8	5 ml	5 ml	5 ml	5 ml
Water	10.03 ml	9.37 ml	8.03 ml	6.7 ml
Acrylamide 30%	4.67 ml	5.33 ml	6.67 ml	8 ml
APS 10%	75 µl	75 µl	75 µl	75 µl
SDS 10%	200 µl	200 µl	200 µl	200 µl
TEMED	20 µl	20 µl	20 µl	20 µl

Stacking Gel	4%
0.5 M Tris pH 6.8	2.50 ml
Water	6 ml
Acrylamide 30%	1.4 ml
APS 10%	75 µl
SDS 10%	40 µl
TEMED	20 µl

Running Buffer 10X

0.25 M Tris, 1.92 M glycine, 1% SDS (Flowgen Bioscience).

Transfer Buffer

25 mM Tris, 0.19 M glycine, 20% methanol.

Tris Buffered Saline 10X (TBS)

1.5 M NaCl (BDH), 0.5 M Tris(hydroxymethyl)-methylamine (BDH) adjusted with HCl to pH 7.6.

Tris Buffered Saline Tween-20 (TBS-T)

1X TBS containing 0.1% Tween-20.

Blocking Solution

TBS-T containing 5% semi-skimmed milk.

Primary and secondary antibody solution

TBS-T containing 5% semi-skimmed milk.

Antibody stripping solution

Re-blot plus strong (Millipore).

2.1.8 Compounds

Name	Description	Concentration Range	Source
ACEA	CB1 receptor agonist	0.5 µM-1 µM	Sigma
AM-251	CB1 receptor antagonist	0.5 µM-1 µM	Tocris Bioscience
Bisindolylmaleimide I (BIM)	PKC inhibitor	1 µM	Calbiochem
Phorbol dibutyrate PDBu	PKC activator	10 nM	Calbiochem
BTP	Drebrin binder	1 µM	Tocris Bioscience

2.1.9 Antibodies and dyes

Primary antibodies

Antibody	Description	Dilution	Species/Conjugate	Source
Fascin	WB/IF	1:1000/1:100	Mouse	Dako
Drebrin	WB/IF	1:1000/1:100	Mouse/Rabbit	Abcam
Actin	WB	1:4000	Rabbit	Cell Signalling
βIII Tubulin	IF	1:1000	Mouse/Rabbit	Abcam
Dcx	IF/IHC	1:1000	Rabbit	Abcam
GFAP	IF	1:200	Rabbit	Dako
GFP	WB/IF	1:1000	Rabbit	Invitrogen
Cleaved caspase 3	IHC	1:1600	Rabbit	Cell signalling
PSA-NCAM	IHC	1:100	Mouse	Sigma
pS142 drebrin	WB/IF	1:1000/1:100	Rabbit	Gordon-Weeks
BrdU	IF	1:100	Mouse	Becton-Dickinson

Secondary antibodies

Antibody	Description	Dilution	Species/Conjugate	Source
Goat-Anti Mouse	WB	1:5000	HRP	Thermo Scientific
Goat-Anti Rabbit	WB	1:5000	HRP	Thermo Scientific
Goat-Anti Rat	WB	1:5000	HRP	Thermo Scientific
Goat-Anti Mouse	IF	1:1000	Alexa 488	Invitrogen
Goat-Anti Mouse	IF	1:500	Texas Red	Invitrogen
Goat-Anti Rabbit	IF	1:1000	Alexa 488	Invitrogen
Goat-Anti Rabbit	IF	1:500	Texas Red	Invitrogen
Goat-Anti Mouse	IHC	1:200	Biotinylated HRP	Dako
Goat-Anti Rabbit	IHC	1:200	Biotinylated HRP	Dako

Dyes

Dye	Description	Dilution	Source
Phalloidin A488	IF	1:200	Invitrogen
Phalloidin Texas Red	IF	1:100	Invitrogen
Hoechst	IF/IHC	1:10000/1:5000	Sigma (B-2883)

2.2 Methods

2.2.1 Cell culture

Dissection of RMS explants

Brains were dissected from Sprague Dawley P6-P7 rat pups and kept in dissection medium with the following composition: Hank's Buffered Salt Solution (HBSS; Invitrogen) containing 0.95 M HEPES (Sigma), 1 unit/ml penicillin G and 1 µg/ml streptomycin (Invitrogen). Brains were cut into 1.4 mm-thick coronal slices using a McIlwain tissue chopper. Slices were then separated under a high-magnification dissecting microscope (Leica) and the RMS was isolated from the surrounding brain tissue by its translucent appearance. RMS explants were cut in pieces of approximately 200 µm in diameter (Ward and Rao, 2005).

Culture of primary RMS neuroblasts

For cultures of dissociated neuroblasts, dissected RMS explants were triturated in HBSS containing 0.25% trypsin (Gibco) and 1 mg/ml of DNAseI (Worthington) and left at 37°C for 2 minutes. The trypsin was inactivated with 5 ml of DMEM (Gibco) containing 10% FCS, after which the cell suspension was centrifuged at 1,500 rpm for 5 minutes. Cells were then washed with 5 ml of DMEM + 10% FCS and spun at 1,500 rpm for 5 minutes. Cell counting was performed at this stage. Neuroblasts were pelleted and re-suspended in complete Neurobasal pre-equilibrated at 37°C/5% CO_2. RMS neuroblasts were plated onto glass coverslips (30,000-50,000 cells/coverslip) or 6-well plates (1,500,000 cells/well) coated with polyornithine (0.5 mg/ml; Sigma) and laminin (10 µg/ml; Sigma). Cells were maintained in Neurobasal complete medium at 37°C/5% CO_2 for 24, 48 or 72 hours.

2.2.2 Nucleofection

Dissociated neuroblasts were pelleted and re-suspended in rat neuron nucleofection solution (Lonza) at a final concentration of $3x10^6$ cells/100 µl for each nucleofection. Each sample was mixed with either 5/9 µg of siRNA or 3/5 µg of shRNA plasmid, transferred to a cuvette and nucleofected using the G-013 program on the Nucleofector 2 device (Lonza). 1 ml of DMEM + 10% FCS was immediately

added to the cuvette, and the entire sample was transferred to a 15 ml Falcon tube containing 5 ml of DMEM + 10% FCS before spinning at 1,500 rpm for 5 minutes. The resulting pellet was resuspended in 25 µl of DMEM + 10% FCS, pipetted onto the internal surface of the lid of a 35 mm dish, and suspended as a hanging drop over a dish containing 2 ml of complete culture medium pre-equilibrated at 37°C/5% CO_2. The dish was kept at 37°C/5% CO_2 for 5 hours to allow cell re-aggregation. The drop was then transferred into the medium in the dish, and cultured in suspension at 37°C/5% CO_2 for either 24 or 48 hours.

2.2.3 Electroporation

P2-3 CD1 mouse pups were anesthetized with isofluorane (0.6 L/min) for 1 minute. Using a pulled glass capillary (diameter 1.5 mm, Clark, UK), 3 µl of 1 µg/µl plasmid DNA (e.g. pCX-EGFP plasmid or control/drebrin/fascin shRNA-IRES-GFP) were injected into the right lateral ventricle of the pup, as shown in Figure 2-1. pGFPC2-fascin wt, S39A, and S39D or pCAG-drebrin-YFP wt, S142A, and S142D were co-electroporated with pCX-GFP at a 3:1 ratio to allow visualization by spinning disk confocal time-lapse microscopy. This co-electroporation ratio ensures efficient co-transfection of different plasmids with pCX-GFP as previously shown by double immunostaining (S. Gajendra, unpublished data). Animals were then subjected to five electrical pulses of 99.9 V for 50 ms with 850 ms intervals using the CUY21SC electroporator (Nepagene) and 7 mm tweezer electrodes coated with conductive gel (CEFAR, France). Animals were then reanimated under oxygen (1 L/min) and returned to their mother. Pups were sacrificed and brains were collected for analysis 5 days later.

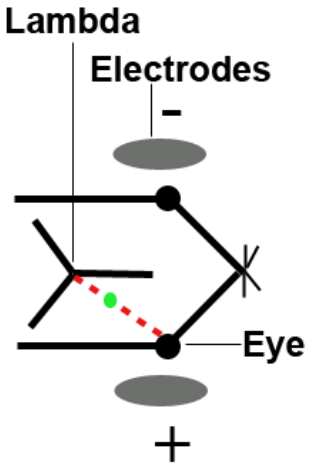


Figure 2-1. Electroporation.

Schematic picture showing the injection site in the lateral ventricle of a mouse head. The dotted red line indicates a diagonal virtual line from the bregma (lambda) to the right eye, and the green dot indicates the position of the lateral ventricle (LV), where the plasmid needs to be injected. Adopted from Sonego et al., 2013.

2.2.4 Brain slice culture

Mouse pups were killed 5 days after electroporation. Brains were hemisected and the electroporated right hemisphere was glued (midline face down) onto the Vibratome platform. Sagittal sections were cut at a thickness of 300 µm using a Vibratome (Leica). Brains slices containing the olfactory bulb (OB) were collected using a soft inoculating loop or a small paintbrush and examined for GFP expression under fluorescent light microscope. Slices containing GFP-labelled neuroblasts along the full RMS were then chosen and cultured for 1 hour on a Milli cell insert (30 mm Organotypic PTFE 0.4 µm; Millipore) placed in a p35 glass-bottom dish (MatTek) containing brain slice imaging medium.

2.2.5 3-D Matrigel migration assay using RMS explants or aggregates

Dissected RMS explants were washed twice with Neurobasal complete medium, while aggregates from hanging drops were spun down at 1,500 rpm for 5 minutes and resuspended in a small volume (16 µl) of Neurobasal complete medium. Explants/aggregates were then embedded into growth factor-reduced, phenol red-free Matrigel (Becton Dickinson, Biosciences) diluted 3:1 with Neurobasal complete medium. The explant/Matrigel mixture was spread across glass coverslips, and left to solidify for 7-10 minutes at 37°C/5% CO_2 before addition of Neurobasal complete medium. Explants were left to migrate for up to 24 hours *in vitro* at 37°C/5% CO_2. In some experiments different compounds were added to the Matrigel as well as to the culture medium and maintained in the medium for different time intervals according to the experimental plan.

2.2.6 Time-lapse imaging

Time-lapse imaging of RMS explants/aggregates using Nikon Biostation

Phase contrast movies of neuroblasts migrating out of RMS explants were taken on the Nikon Biostation (a incubator maintained at 37°C/5% CO_2 coupled with a multipoint monitoring system) 1 hour after plating onto Hi-Q4 multi experiment dishes (Nikon) for approximately 24 hours using 20x and 40x objectives. These dishes contains 4 separated chambers, therefore 4 different conditions can be

imaged at the same time. The dishes were maintained at 37°C/5% CO_2 and images were taken every 3 minutes. Frames were played at a speed of 10 frames/s.

Time-lapse imaging of brain slices using spinning disk confocal microscopy

Cultured brain slices were transferred into a pre-heated (37°C) chamber of a Perkin Elmer UltraView VoX confocal spinning disk system. Time-lapse imaging of GFP positive cells in the RMS was performed using an inverted Nikon Ti-E microscope with a Nikon CFI Super Plan Fluor ELWD 20x/0.45 objective coupled with a Hamamatsu C10600-10B (ORCA-R2) cooled digital CCD camera every 3 minutes for a total period of 3 hours. Z-stack images were taken every 4 μm over an interval of 100-150 μm inside the brain slice. Movies were acquired using the Perkin Elmer Volocity software.

2.2.7 Analysis of migration

Measuring neuroblast migration in fixed RMS explants/aggregates

Pictures of explants were taken on an Apotome microscope (Zeiss) with 10x and 20x objectives. The migration distance was measured from the edge of the explants to the nucleus of the furthest migrated cell (identified by Höechst staining) for at least 6 different positions around the explants by using ImageJ. The data generated were obtained from 3 different experiments with at least 15 explants for each condition (Falenta et al., 2013).

Tracking time-lapse imaging of RMS explants/aggregates

The dynamics of RMS neuroblasts out of explants or aggregates was quantitatively analysed using Volocity software (Perkin Elmer). Each time-lapse imaging file was drag into a new library in Volocity. Neuroblasts were tracked following the movement of the nucleus for a total period of 7 hours. Only neuroblasts exit the explant or aggregate and in focus throughout the 7 hours of tracking were considered. The following parameters were analysed: migration distance (μm), velocity (μm/h) and time spent immobile (hour).

70 cells were tracked for each condition from a total of three different experiments.

Tracking time-lapse imaging of brain slices

Brain slice movies obtained by spinning disk confocal microscopy were analysed using Volocity software. The dynamics of GFP-labelled neuroblasts was quantitatively analysed by tracking the cell body of each neuroblast present in the field of view throughout the entire duration of imaging. The following parameters were analysed: migration distance (μm), velocity (μm/h), time spent immobile (hour), displacement (μm) that is considered to be the shortest distance between start and end points, displacement rate or speed of displacement (μm/hour) that is considered to be the ratio between displacement and time, and the migratory index which is identified as the ratio between the net distance (i.e. the shorter distance from the start point to the end point) and the total distance travelled over time (Nam et al., 2007). Only cells that had a displacement of at least 50 μm were considered. Between 15 and 30 neuroblasts were tracked in each movie. At least 5 brain slices per condition were analysed.

2.2.8 Bromodeoxyuridine injections

To examine proliferation, a set of P7 mouse pups received an intraperitoneal injection of 50 mg/kg Bromodeoxyuridine (BrdU) 2 hours before killing (n=5 for both wt and *fascin-1* ko).

To examine migration, another set of P7 mouse pups received 3 intraperitoneal injections of 50 mg/kg BrdU per day for 3 consecutive days and sacrificed 12 days after the last injection (Comte et al., 2011) (n=4 for wt; n=3 for *fascin-1* ko).

2.2.9 Counting of BrdU positive cells

Proliferation analysis

All BrdU positive cells found in a 500-μm-long and 40-μm-wide area of the lateral SVZ were counted. Cell count was performed in at least 7 evenly spaced sections per animal, from co-ordinates 0.02-1.33 relative to bregma (n=5 for both wt and *fascin-1* ko).

Migration analysis

A 400-µm square outline was drawn on confocal projection images of the caudal part of the RMS and the core of the OB obtained from 35 µm-thick sagittal brain slices. Cell counting was performed in 4 slices per brain to calculate the relative percentages of BrdU-positive cells found in the two areas (n=4 for wt; n=3 for *fascin-1* ko) (Figure 3-7).

2.2.10 Immunohistochemistry

Gelatin-embedded sections

Dissected electroporated brains were kept in PBS containing 4% PFA at room temperature on a roller for 3 hours. The brains were then hemisected, and the electroporated right sides were left in 4% PFA at 4°C on a roller overnight. The following day brain hemispheres were embedded in 4% gelatin (Sigma G1890) in PBS, left in 4% PFA overnight at 4°C on a roller and then transferred in PBS with 0.1% of sodium azide. Brains were cut using a Vibratome (VT10005, Leica) into 50-µm-thick sagittal slices for immunostaining with an anti-GFP antibody. Slices were blocked for 1 hour in PBS containing 1% BSA, 0.1% Triton-X, and incubated with primary antibody (rabbit anti-GFP) overnight at 4°C on roller. After washing 3 times for 10 minutes in PBS, slices were incubated with Alexa 488 anti-rabbit IgG secondary antibody (1:1000) and Hoechst (1:5000, Sigma) for 2 hours at room temperature. After washing, slices were mounted in fluorescent mounting solution (Dako) and covered with a 22 x 50 mm coverslip. Z-stacks images were taken using a confocal microscope (Zeiss LSM 710) with 40x and 63x objectives and lasers: 405 (DAPI), and A488 (Alexa 488).

Brains of BrdU-injected animals were cut into 35-µm-thick sagittal slices. Slices were first permeabilised with 0.2% Triton-X in PBS for 30 minutes at room temperature. After 3 washes in PBS for 5 minutes, DNA denaturation was performed by incubation with 1N HCl for 10 minutes on ice. Two subsequent incubations with 2N HCl were performed: the first one at room temperature for 10 minutes and the second one at 37°C for 30 minutes. The denaturation reaction was stopped by a

quick wash with water followed by a 10-minute incubation in water. After 3 washes in PBS for 5 minutes, slices were blocked using 0.2% Triton-X, 1 M glycine, 5% BSA in PBS for 1 hour at room temperature. After 2 washes with 0.2% Triton-X in PBS for 5 minutes, slices were incubated with anti-BrdU (Becton-Dickinson) and anti-Dcx antibodies diluted in 0.2% Triton-X and 5% serum in PBS overnight at 4°C. After washing 3 times for 10 minutes in PBS, slices were incubated with Alexa 488 anti-mouse IgG secondary antibody (1:1000), Texas-Red anti rabbit secondary antibody (1:500), and anti-Hoechst (1:5000, Sigma) for 2 hours at room temperature. After washing, slices were mounted in fluorescent mounting solution (Dako) and covered with a 22 x 50 mm coverslip. Z-stacks images were taken using a confocal microscope (Zeiss LSM 710) with 40x and 63x objectives and lasers: 405 (DAPI), A488 (Alexa 488), 594 (Texas Red).

Paraffin-embedded sections

Formalin-fixed P7-8 mouse brains were embedded in paraffin and cut into 6 µm-thick sagittal sections. Brain sections were deparaffinised and rehydrated before heat-induced antigen retrieval using a sodium citrate buffer. Slices were then blocked and incubated with the primary antibody at 4°C overnight. Biotinylated secondary antibodies were incubated at room temperature and detected with StreptABComplex/HRP, and subsequently developed in DAB solution and counter stained with hematoxylin. Sections were dehydrated in 100% IMS, cleared in xyelene and mounted in DPX plastic.

For immunofluorescence sections were deparaffinised, blocked with 1% BSA for 15 min, and incubated with primary antibodies overnight at 4°C. Sections were then incubated with appropriate fluorescent secondary antibodies and Hoechst dye for 1 hour at room temperature and mounted on slides using custom made Mowiol. Z-stacks were taken using a confocal microscope (Zeiss LSM 710) equipped with 40x and 63x objectives and 405, 488 and 594 nm lasers.

2.2.11 Immunocytochemistry

Coverslips with embedded RMS explants/neuroblast aggregates were fixed in 4% PFA in PBS for 40 minutes at room temperature, washed three times for 5 minutes

with PBS, and blocked with 5% goat serum in PBS (blocking solution) for 1 hour at room temperature. After washing, coverslips were incubated with Alexa 488-conjugated phalloidin diluted in goat serum overnight at 4°C. The following day coverslips were washed with PBS and incubated with primary antibodies diluted in blocking solution overnight at 4°C. After washing, coverslips were incubated with secondary antibodies diluted in blocking solution with Hoechst for 2 hours at room temperature in the dark. After washing three times with PBS and once with sterile water, coverslips were mounted using a fluorescent mounting medium (Dako). For quantification of migration images were taken using an Apotome microscope equipped with 10x and 20x objectives. For morphological analysis images were taken using a confocal microscope (Zeiss LSM 710) using 40x and 63x objectives, and 405 488 and 594 nm lasers.

2.2.12 Fluorescence lifetime imaging microscopy (FLIM)

Rat neuroblasts were nuclefected with plasmids encoding monomeric RFP (mRFP)-tagged PKCα or PKCγ and GFP-fascin (Parsons and Adams, 2008), re-aggregated and embedded in Matrigel 24 hours after nucleofection. Neuroblasts were left to migrate for a period of 9 hours before adding a PKC activator (PDBu, 25 nM for 10 min), or a PKC inhibitor (BIM, 1 µM for 15 min), or a CB1 agonist (ACEA, 0.5 µM for 1 hour), or a CB1 antagonist (AM-251, 0.5 µM for 1 hour) (Pertwee, 2006, Parsons and Adams, 2008, Sonego et al., 2013a). Coverslips were then fixed in 4% PFA, incubated with 0.2% Triton-X in PBS for 10 min followed by quenching in 1% borohydride for 10 min, and mounted with Fluorsave (Calbiochem) for imaging. Multiphoton, time correlated single photon counting FLIM was performed by Dr. Maddy Parsons to quantify interaction between PKCα/γ-mRFP and GFP-fascin by fluorescence resonance energy transfer (FRET). In FLIM the lifetime of the donor (GFP-fascin) is measured and it decreases upon FRET with the acceptor (PKCα/γ-mRFP). To have FRET, fascin/PKC interaction must occur within 10 nm (Figure 2-2). A Nikon TE2000E inverted microscope combined with an in-house scanner and Chameleon Ti:Sapphire ultrafast pulsed multiphoton laser (Coherent) was used for the excitation of GFP (at 890 nm). All images were acquired to provide enough photon arrival times to enable accurate fitting of fluorescence decay while avoiding

detector pileup. Fluorescence lifetime imaging capability was provided by time-correlated single-photon counting electronics (SPC 700; Becker & Hickl). Widefield acceptor (mRFP) images were acquired using a CCD camera (Hamamatsu) at exposure time of <100 ms. Data were analysed by performing a single-exponential pixel fit in TRI2 time-resolved image analysis software (developed by Dr. Paul Barber, Gray Institute, Oxford, UK). All histogram data are plotted as mean FRET efficiency from >10 cells/sample. Lifetime image examples shown are presented using a pseudocolor scale, whereby blue depicts normal GFP lifetime (i.e., no FRET) and red depicts reduced GFP lifetime (areas of FRET). Each experiment was repeated at least three times, and ANOVA was used to test statistical significance between different populations of data.

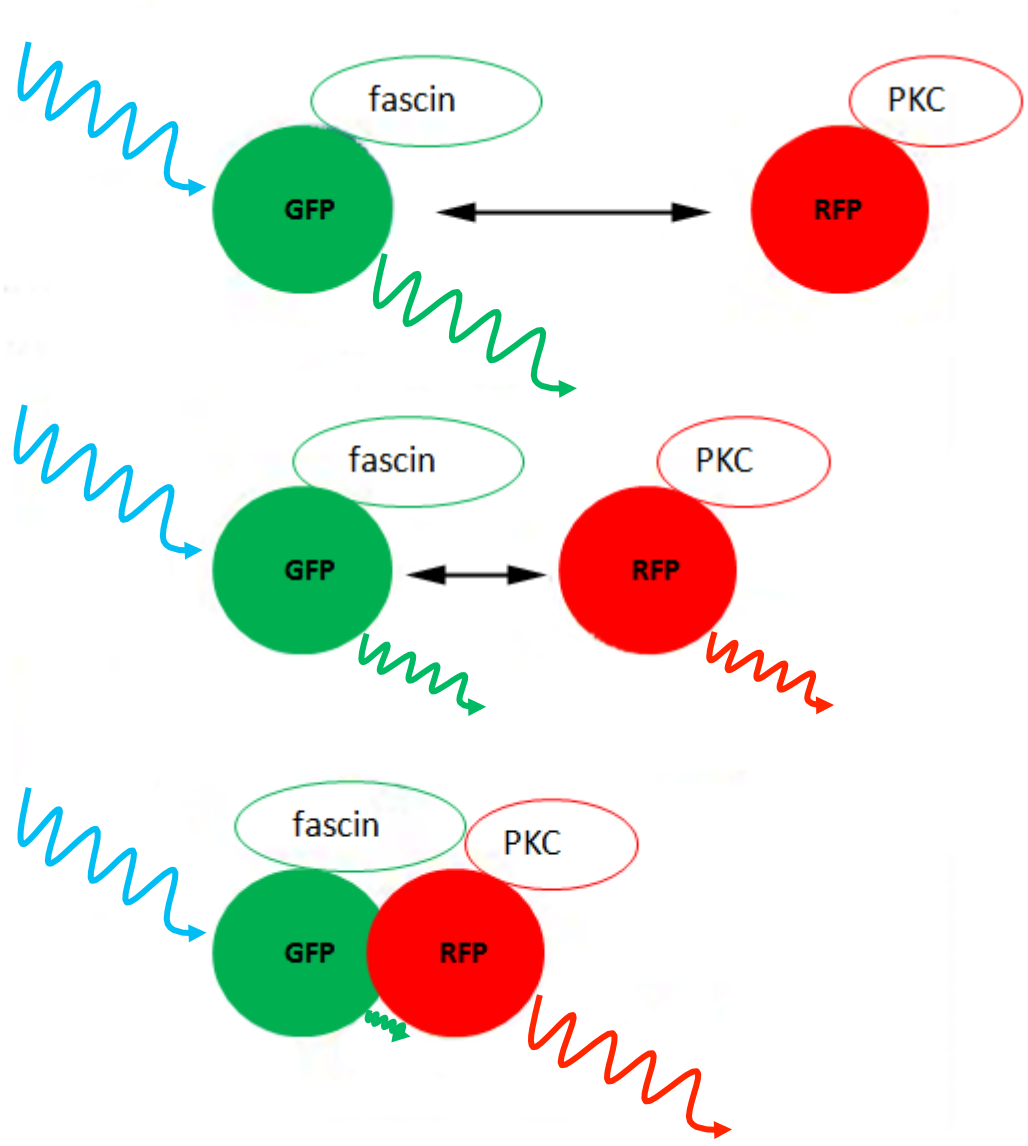


Figure 2-2. Fluorescent life-time imaging microscopy.

A schematic picture showing fluorescent life-time of the donor (GFP) decreasing upon FRET with the acceptor (RFP). The excitation of the GFP-fascin (green) produces an emission that can be absorbed by PKC-mRFP (red) only when these fluorophores are 10 nm from each other.

2.2.13 Western Blotting

Dissociated neuroblasts (nucleofected or not) were plated in 6-well plates coated with 0.5 mg/ml polyornithine (Sigma) and 10 µg/ml laminin (Sigma). After 2-3 days, cells were placed on ice, washed with cold PBS three times, and lysed in 100 µl of lysis buffer. Cell lysates were scraped from the plate surface, collected into Eppendorf tubes, and left to rotate for 30 minutes at 4°C. Lysates were then centrifuged at 12,000 rpm for 10 minutes at 4°C. Supernatants were collected, and protein concentration was measured using a BCA protein assay kit (Thermo Fisher Scientific). Loading sample buffer was added to equivalent amounts of protein made up to 60 µl with water, and loaded onto an 8%, 10% or 12% SDS-polyacrylamide gel depending on the molecular weight of the proteins to be analysed. The separated proteins were transferred to PVDF membranes (Millipore) at 70 V for 3 hours at 4°C. For detection of protein bands via enhanced chemiluminescence (ECL), membranes were blocked with 5% milk powder in TBS-T for 1 hour at room temperature, and then incubated overnight at 4°C with primary antibodies in 5% milk in TBS-T. Membranes were washed with TBS-T four times for 10 minutes each, and then incubated with horseradish peroxidase (HRP)-conjugated anti-mouse or anti-rabbit IgG secondary antibodies diluted in 5% milk-TBS-T for 1 hour at room temperature. After washing, membranes were incubated with ECL Western Blotting reagent (GE Healthcare) and exposed to hyperfilm (GE Healthcare). Membranes were stripped with Re-blot plus strong (Millipore) and re-probed for detection of additional proteins.

2.2.14 Statistical Analysis

Statistical analysis was performed using Student's t-test for dual comparison and one-way ANOVA for multiple comparisons with SigmaPlot 12.0 (Systat Software Inc). Differences were considered statistically significant if $p < 0.05$. In all figures: * $p<0.05$, ** $p<0.01$, *** $p <0.001$. The error bars in all the graphs represent the standard error of the mean (SEM).

Two-tailed comparisons were used in all the experiments. One exception was made for time-lapse imaging of brain slices electroporated with fascin shRNA where one-

tailed t-test was performed. Although two-tailed test is a much more trustable instrument in statistical analysis, one-tailed t-test can be used when previous data tell that a difference can go only towards one direction (Motulsky, 1998). For instance, based on our previous results *in vitro* we hypothesise the fascin knockdown leads to an impaired migration *in vivo*. It is also important to notice that one-tailed t-tests are used *in vivo* experiments where increasing the number of samples to have a two-tailed statistical significance leads to an unreasonable waste of animals.

Chapter 3 Fascin regulates neuroblast migration

3.1 Introduction

Fascin is an actin-bundling protein able to organise single and unstable filaments of actin in parallel tight bundles forming structures called filopodia (Kureishy et al., 2002, Vignjevic et al., 2003, Hashimoto et al., 2007). Filopodia are important structures in migration. In migrating cells, filopodia are involved in exploring the environment, responding to attractive or repulsive cues through the modulation of actin polymerization (Lambert de Rouvroit and Goffinet, 2001, Ridley et al., 2003, Schaar and McConnell, 2005). By cross-linking actin, fascin promotes filopodia stability and thereby extension of leading edge, whose adhesion to the extracellular matrix promotes cell movement (Cohan et al., 2001, Vignjevic et al., 2006, Yamakita et al., 2009). Importantly, fascin-dependent actin bundling is a dynamic process able to modulate growth cone retraction and reorientation (Cohan et al., 2001, Brown and Bridgman, 2009, Deinhardt et al., 2011). Similar events are observed in migratory neuroblasts, which can extend multiple branches from their leading process, or retract the old leading process to make a new one, thus reversing their direction (Schaar and McConnell, 2005, Ward and Rao, 2005).

Fascin binding to actin is regulated by phosphorylation on Ser39, a residue located at its N-terminus (Ono et al., 1997). In particular, Ser39 phosphorylation by Protein Kinase C (PKC, α and γ isoforms) greatly reduces actin binding and bundling activities (Yamakita et al., 1996, Adams, 2004, Jayo and Parsons, 2010). Moreover, S39-phosphorylated fascin interacts with active PKCα, a regulator of focal adhesions, to control myoblast migration on fibronectin and with active PKCγ to regulate colon cancer cell migration (Anilkumar et al., 2003, Parsons and Adams, 2008).

Consistent with an important role in cell migration, fascin is highly expressed in multiple invasive malignant cancers, like carcinomas of the breast, colon, lung, ovary and skin (Grothey et al., 2000, Hu et al., 2000, Goncharuk et al., 2002, Jawhari et al., 2003, Pelosi et al., 2003, De Arcangelis et al., 2004). Also, fascin up-regulation has been demonstrated to increase cell motility in multiple human malignancies (Hashimoto et al., 2007, Hwang et al., 2008). These observations, coupled with the

fact that fascin expression is substantially down regulated by Growth and Differentiation Factor 11 (GDF11), a cytokine that inhibits migration in neural stem cell lines (Williams et al., 2013) made us pursue the hypothesis of a functional role for fascin in RMS neuroblast migration.

In this chapter, we investigate the role of fascin in RMS neuroblast migration using *fascin-1* ko mice as well as genetic *in vitro* and *ex vivo* approaches. Furthermore we analyze the role of the PKC-dependent phosphorylation of fascin on Ser39. Finally, we identify endocannabinoid signaling as an important upstream event regulating fascin-PKC interaction in migrating neuroblasts.

In this chapter the following hypotheses were pursued:

1. Fascin is required for neuroblast migration *in vitro and in vivo*
2. Fascin phosphorylation site Serine 39 plays a role in neuroblast migration *in vitro and in vivo*
3. Fascin interaction with PKC is required for neuroblast migration
4. Factors regulating neuroblast migration in vivo can influence the interaction between Fascin and PKC
5. Fascin is a downstream mediator of endocannabinoid signalling in migrating neuroblast *in vitro*

3.2 Results

3.2.1 Fascin is expressed along the rostral migratory stream (RMS) of postnatal and adult mouse brains

We first analysed the distribution of fascin in paraffin-embedded P7 and adult mouse sagittal brain slices (Figure 3-1, top row). In both cases, fascin shows high expression along the RMS, resembling the expression pattern of PSA-NCAM and Dcx, two well-characterised RMS neuroblast markers (Doetsch, 2003) (Figure 3-1, bottom row).

3.2.2 Genetic deletion of *fascin-1* affects brain and olfactory bulb (OB) size

According to a previous report, the brain of *fascin-1* ko mice retains a gross normal morphology except for loss of the posterior region of the anterior commissure (Yamakita et al., 2009). Moreover, the ventricles are larger in comparison to those of wild type animals (Yamakita et al., 2009).

Fascin-1 ko mice are smaller in size and have a lower body weight (at P7: wt, 3.81 ± 0.22 g, n=8; heterozygous *fascin-1* ko, 3.92 ± 0.08 g, n=23; homozygous *fascin-1* ko, 2.40 ± 0.19 g, n=6) in comparison to wt and heterozygous littermates. Interestingly, these animals are not only characterized by a visibly smaller brain, but also by a significant decrease in the ratio between the length of the OB and the cerebral cortex (CC), suggesting a specific reduction in OB size (mean ± SEM; n=15 brains for wt and heterozygous *fascin-1* ko; n=6 brains for homozygous *fascin-1* ko; *$p<0.05$; **$p<0.01$) (Figure 3-2). The OB/CC length ratio was significantly lower also in *fascin-1* ko young adults (P50, wt: 0.319 ± 0.0141; n=3 brains. *Fascin-1* ko: 0.241 ± 0.00986; n=4 brains, **$p<0.01$), suggesting that fascin is essential for normal development of the OB, and that its lack cannot be compensated during the postnatal maturation of the nervous system. Although the OB in *fascin-1* ko mice is significantly smaller, hematoxylin and eosin-stained coronal slices of the OB reveal a preserved structure where all the layers (granule cell layer-GCL, internal plexiform layer-IPL, mitral cell layer-MCL, external plexiform layer-EPL, glomerular layer-GL) appear well defined (Figure 3-3), pointing out to a specific role for fascin in

regulating the size, but not the layer organization of the OB. Moreover, even though the OB was overall smaller in fascin-1 ko animals, the relative width of the internal OB layers did not appear to visibly differ compared to wt samples.

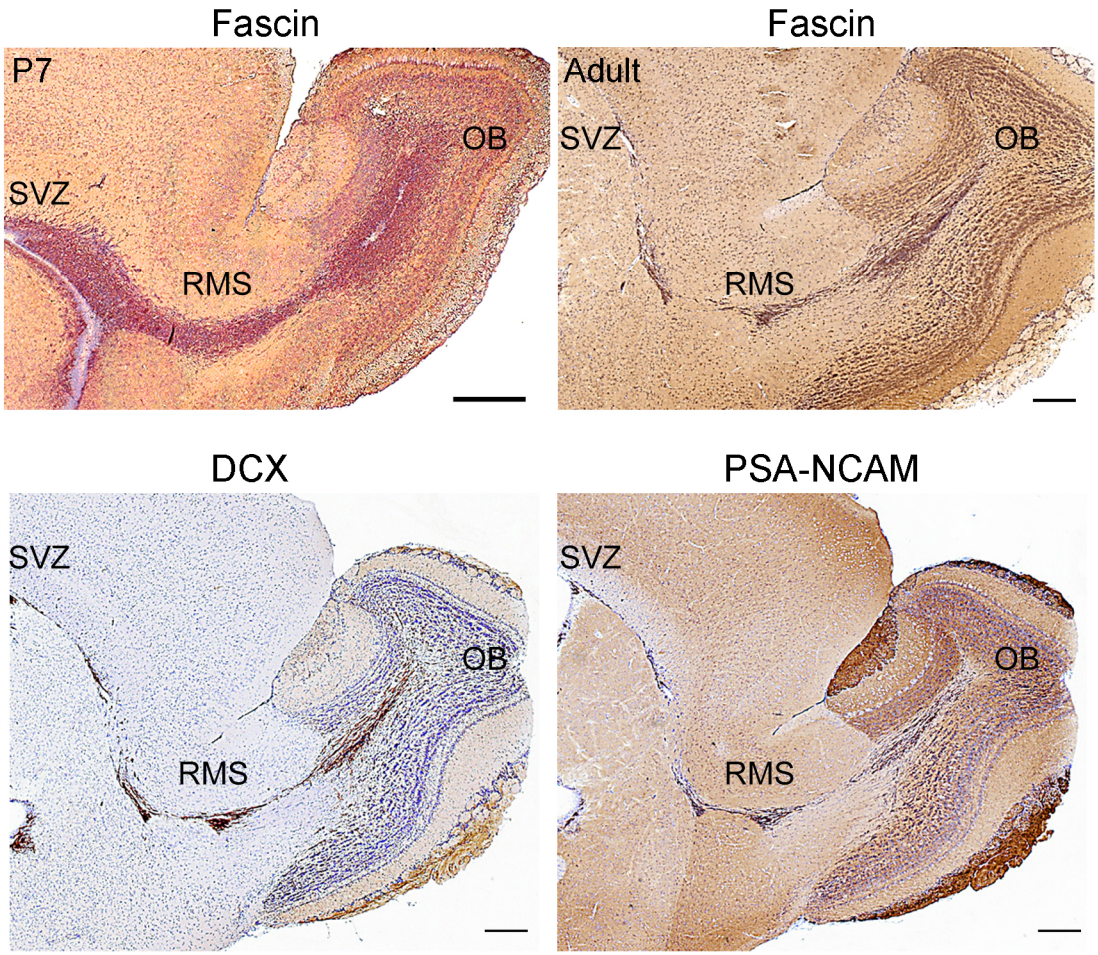
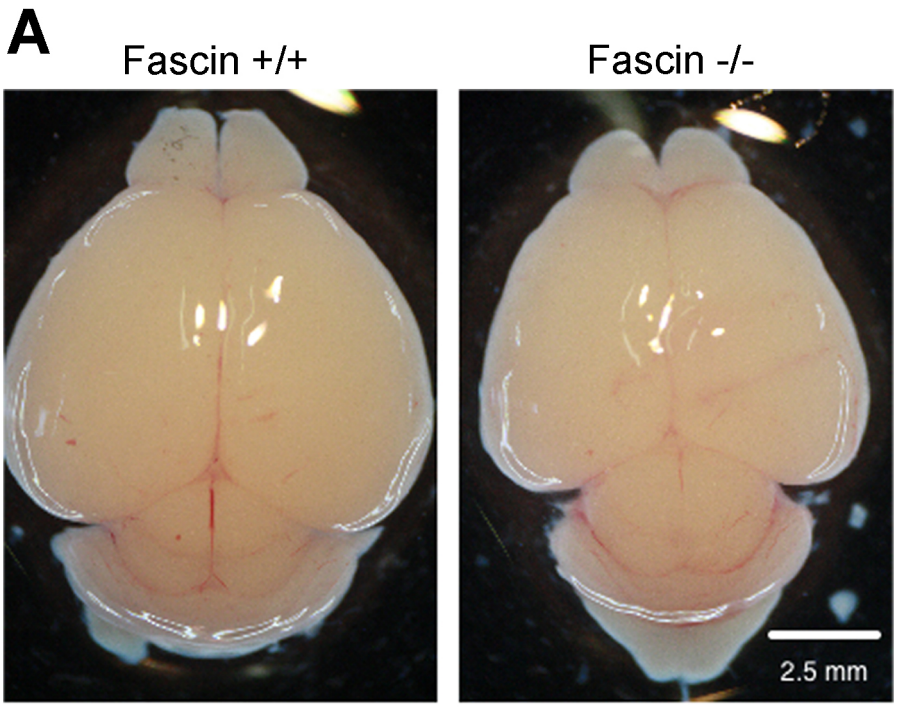


Figure 3-1. Fascin is expressed in the postnatal and adult mammalian brain.

Paraffin-embedded brain sections from P7 (top left panel) and adult (top right and bottom panels) mouse showing fascin (brown) (top pictures), doublecortin (Dcx) and PSA-NCAM immunopositivity (brown) (bottom pictures) in the SVZ, RMS and OB. Scale bars: 200 µm. Immunohistochemistry performed by Carl Hobbs.


A
Fascin +/+
Fascin -/-
2.5 mm

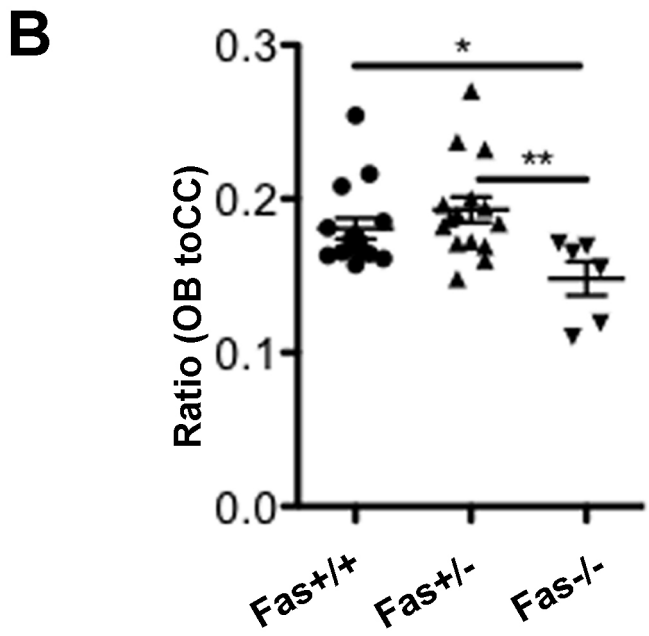

B
Ratio (OB toCC)
0.3
0.2
0.1
0.0
*
**
Fas+/+
Fas+/-
Fas-/-

Figure 3-2. *Fascin-1* ko mice show a smaller OB.

(A) Early postnatal (P7) *fascin-1* ko mice have a smaller brain and a smaller ratio between the OB and cerebral cortex (CC) length in comparison to wt littermates. (B) Graph showing differences in the ratio between OB and CC length for wt, heterozygous and *fascin-1* ko (mean ± SEM; n=15 brains for wt and heterozygous *fascin-1* ko; n=6 brains for homozygous *fascin-1* ko; *p<0.05; **p<0.01). Scale bar: 2.5 mm. Data courtesy of Dr. Laura Machesky and Yafeng Ma.

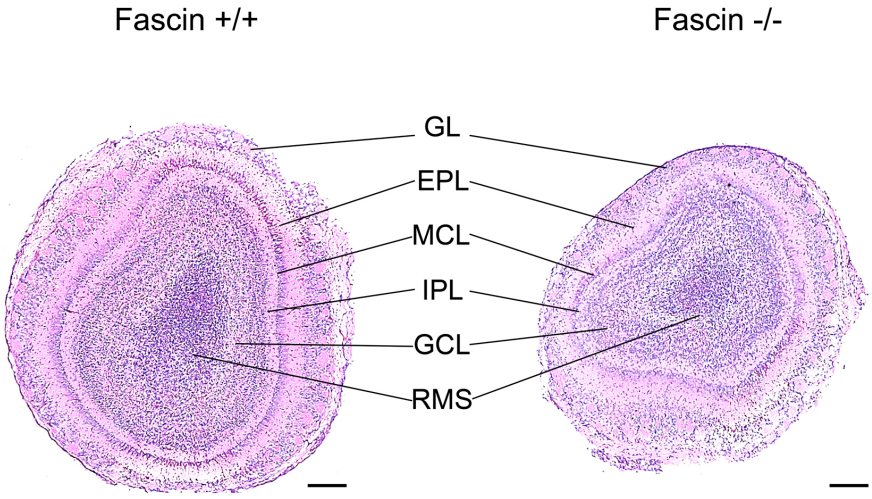


Figure 3-3. *Fascin-1* ko mice show an intact organization of the OB.

Hematoxylin and eosin-stained coronal OB sections in P7 wt and fascin-1 ko mice show a preserved general organization of the OB, where all the layers are still well defined. Tissue processing performed by Carl Hobbs. GL, Glomerular layer; EPL, external plexiform layer; MCL, mitral cell layer; IPL, internal plexiform layer; GCL, granule cell layer. Scale bars: 200 µm.

3.2.3 *Fascin-1* ko mice show a smaller and thinner RMS

The fact that the OB in *fascin-1* ko mice was smaller in size compared to wt animals and the high expression of fascin along the RMS led us to hypothesize that genetic deletion of fascin could affect RMS organization. To test this, the RMS of wt and fascin-1 ko mice was visualized in hematoxylin and eosin-stained brain sagittal sections. Close inspection of early postnatal stage (P7) slices revealed a thinner RMS compared to wt littermates and an abnormal cell accumulation in the caudal portion of the RMS (Figure 3-4, (A), top row, arrowheads). To exclude that this defect was limited to developmental stages, sagittal brain sections of adult brains (P50) were also examined. The same differences were observed in adult animals (Figure 3-4, (A), bottom row, arrowheads). Indeed, *fascin-1* ko adult mice showed a significantly decreased RMS length (wt, 2158.27 ± 45.337 µm; *fascin-1* ko, 1563.86 ± 38.866 µm; n=3 brains/genotype, **p<0.01; Figure 3-4, (B), arrows), and RMS width (elbow region) (wt, 149.673 ± 7.198 µm; *fascin-1* ko, 99.750 ± 6.396 µm; n=3 brains/genotype, p<0.01; Figure 3-4, (C), arrows). Cell accumulation in the caudal RMS was also observed in these animals, causing a significant increase in RMS width in this area (Figure 3-4, (B), arrowheads; caudal RMS width: wt, 77.670 ± 4.342 µm; *fascin-1* ko, 118.800 ± 7.557 µm; n=3 brains/genotype, **p<0.01).

In summary, genetic deletion of *fascin-1* causes defects in the RMS in both postnatal and young adult animals, indicating that fascin function is not confined to developmental stages, but extends into postnatal life. Thus, our results show that fascin is essential for proper RMS organization.

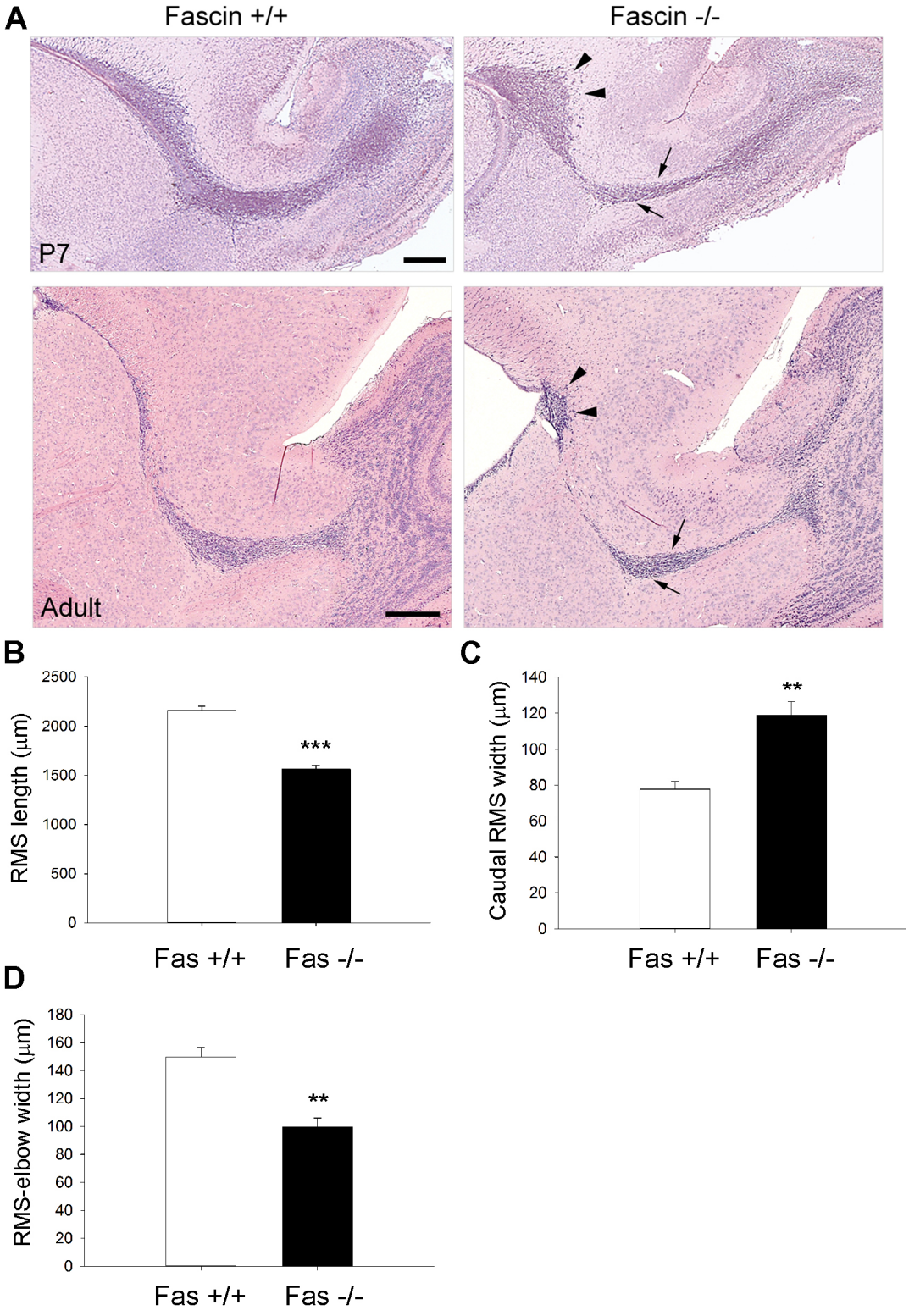

A
Fascin +/+
Fascin -/-
P7
Adult
B
RMS length (μm)
2500
2000
1500
1000
500
0
***
Fas +/+
Fas -/-
C
Caudal RMS width (μm)
140
120
100
80
60
40
20
0
**
Fas +/+
Fas -/-
D
RMS-elbow width (μm)
180
160
140
120
100
80
60
40
20
0
**
Fas +/+
Fas -/-

Figure 3-4. *Fascin-1* ko mice show an abnormal RMS.

(A) Hematoxylin and eosin-stained sagittal brain slices from P7 (top row) and P50 (bottom row) mice show an abnormal RMS organization in *fascin-1* ko animals. Note the thinner RMS rostral section (arrows) and a caudal cell accumulation (arrowheads). Tissue processing performed by Carl Hobbs. (A-C) Quantifications in P50 animals show a shorter RMS (B), a wider caudal RMS (C) and a thinner RMS elbow (D) (mean ± SEM; n=3 brains/genotype, ***p<0.001, **p<0.01). Scale bars: 200 μm.

3.2.4 *Fascin-1* ko mice show abnormal neuroblast chain organization

To further characterize the effect of fascin deletion on RMS structure, we first confirmed the absence of the protein in *fascin-1* ko mice by immunostaining (Figure 3-5, (A)). We then examined neuroblast chain organization in the RMS of *fascin-1* ko mice by immunostaining sagittal brain slices for the migrating neuroblast marker Dcx. Dcx positivity along the RMS was weaker in *fascin-1* ko animals in comparison to wt. Moreover, *fascin-1* ko mice displayed thinner neuroblast chains (Figure 3-5, (B)). In contrast, the general organization of the astrocytic scaffold surrounding the neuroblast chains appeared to be intact. Indeed, the immunostaining for GFAP-positive astrocytes appears similar to wt animals (Figure 3-5, (C)), suggesting an exclusive role for fascin in neuroblast organization along the RMS. Although the structure of the RMS is strikingly different compared to wt animals, we could not detect ectopic neuroblast migration to other brain areas in *fascin-1* ko mice.

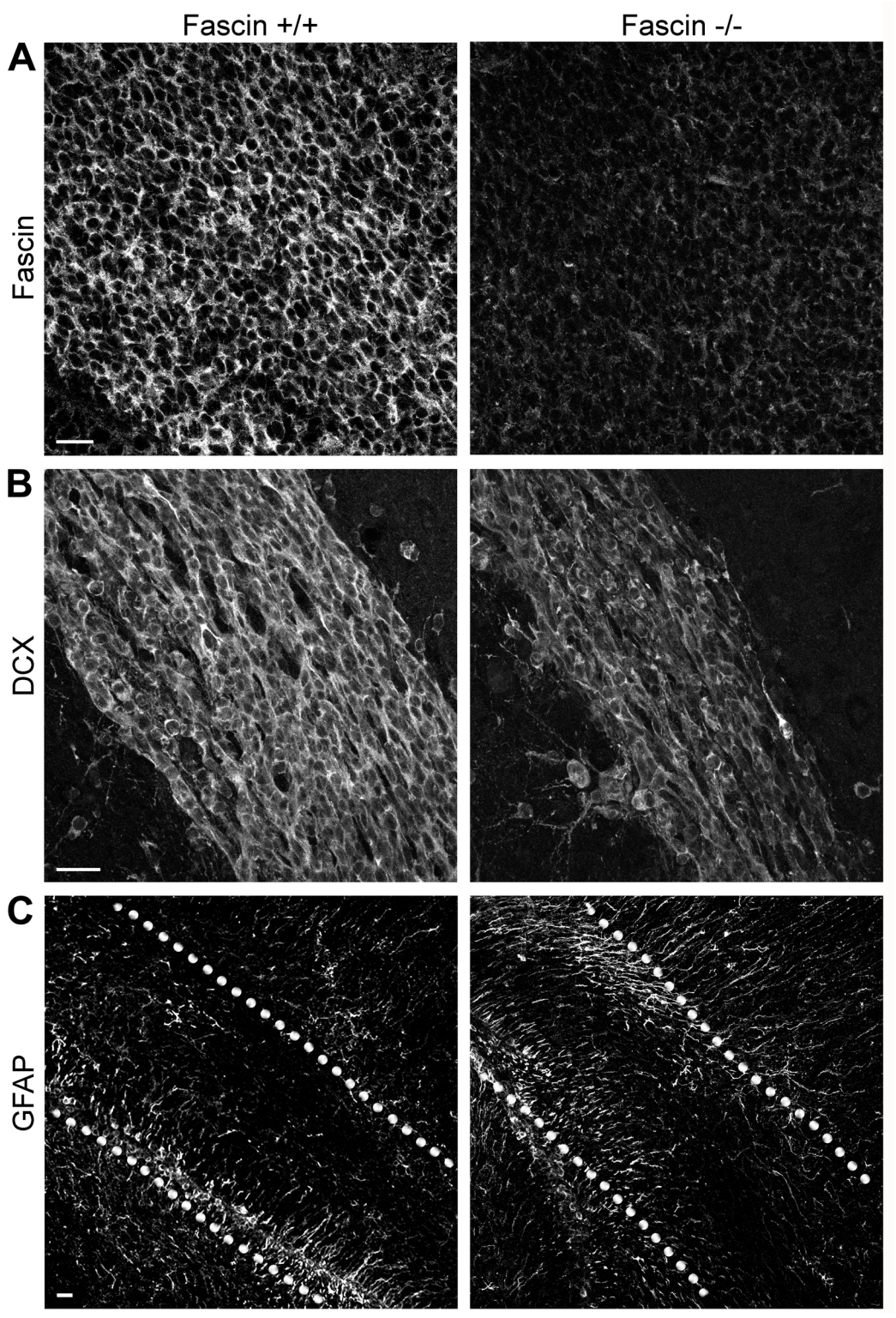

Fascin +/+
Fascin -/-
A
Fascin
B
DCX
C
GFAP

Figure 3-5. *Fascin-1* ko mice show abnormal neuroblast chain organization in the RMS.

(A) Immunostaining of the SVZ/RMS in sagittal brain slices from P7 mice shows the absence of fascin in *fascin-1* ko animals. (B) Dcx-positive neuroblast chains appear thinner in *fascin-1* ko mice compared to wt mice. (C) Lack of fascin does not appear to perturb the localization of GFAP-positive astrocytes and stem cells. The dotted lines outline the RMS borders. Scale bars: A, B, 20 µm; C, 50 µm.

3.2.5 Genetic deletion of fascin does not affect proliferation in the subventricular zone (SVZ)

To understand whether the anatomical defects in *fascin-1* ko brains were due to abnormal cell proliferation, bromodeoxyuridine (BrdU) injection experiments were carried out in early postnatal animals. BrdU is often used in proliferation studies as its similarity to the nucleoside thymidine allows its incorporation into newly synthesized DNA in replicating cells. P7 mice were injected with BrdU and sacrificed 2 hours later. This short time point allows BrdU to be incorporated only in the actively proliferating cells in the SVZ. Coronal brain sections were then stained with an anti-BrdU antibody and cells were counted along a defined section of the lateral SVZ as described in Chapter 2 (Figure 3-6, (A)). Particular attention was taken in counting histological sections at the same level. No difference in the number of BrdU positive cells was detected among wt, heterozygous, or homozygous *fascin-1* ko mice (Figure 3-6, (B); wt, 59.09 ± 3.8; heterozygous *fascin-1* ko, 53.3 ± 1.8; homozygous *fascin-1* ko, 54.2 ± 5.6; n=5 brains for each genotype).

To check apoptosis levels in *fascin-1* ko mice, immunostaining against cleaved caspase 3 was performed. We observed only few cells undergoing apoptosis, and no difference in the number of caspase 3-positive cells was seen in *fascin-1* ko mice compared to wt littermates (data not shown).

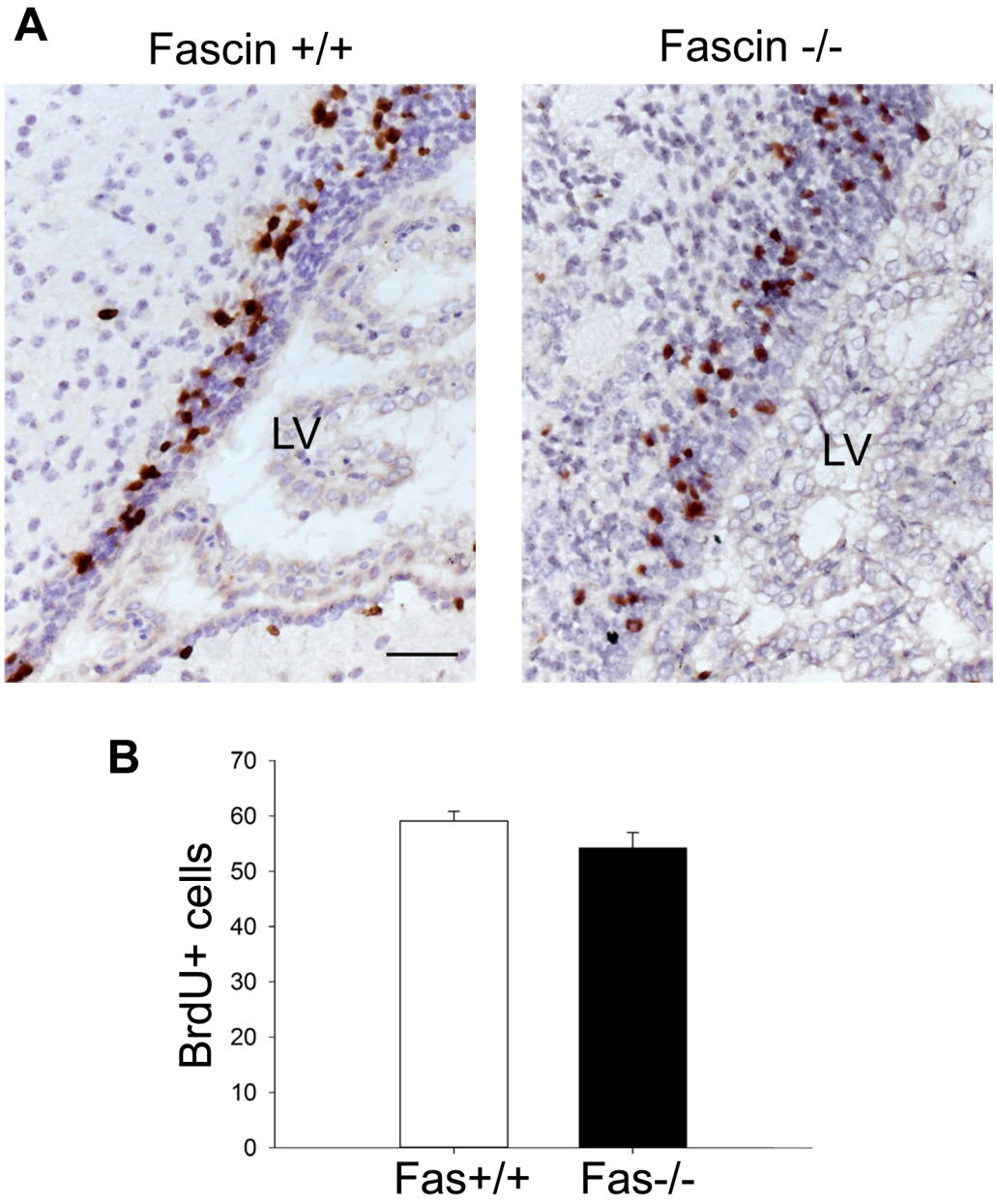


Figure 3-6. Genetic deletion of fascin does not affect SVZ cell proliferation.

(A) Coronal brain sections from wt and *fascin-1* ko mice stained with anti-BrdU antibodies show BrdU+ cells in the SVZ (brown). LV, Lateral ventricle. Tissue processing performed by Carl Hobbs. (B) Quantifications show no significant difference in the amount of BrdU+ cells between wt and *fascin-1* ko samples (mean ± SEM; n=5 brains/genotype). Scale bar: 50 µm.

3.2.6 Genetic deletion of fascin affects RMS neuroblast migration

After having excluded a defect in cell proliferation in *fascin-1* ko mice, we further examined whether the abnormal RMS observed in these animals was due to a defect in the migration of neuroblasts from the SVZ to the OB. To do so, postnatal (P7) mice were injected with BrdU over a period of 3 days and sacrificed 12 days later (Comte et al., 2011). This time period allows proliferating cells that have been incorporating BrdU to leave the SVZ and migrate along the RMS. After 2 weeks the majority of the cells should have left the SVZ, migrated along the RMS and arrived in the OB. BrdU-positive cells were counted along the descending part of the RMS and in the OB (Figure 3-7, (A), area 1 and area 2 respectively). The data are presented as a percentage of the cells found in the two areas. As expected, in the wt animals few cells were still migrating down the RMS, while most of them had already reached the OB. *Fascin-1* ko mice showed a decrease of almost 50% in the percentage of cells reaching the OB, while most of the cells (double in comparison to wt animals) remained in the descending part of the RMS (Figure 3-7, (B)).

Taken together, these data point out a role for fascin in regulating neuroblast migration from the SVZ along the RMS to the OB. Genetic deletion of fascin prevents neuroblasts to efficiently migrate and reach their final destination.

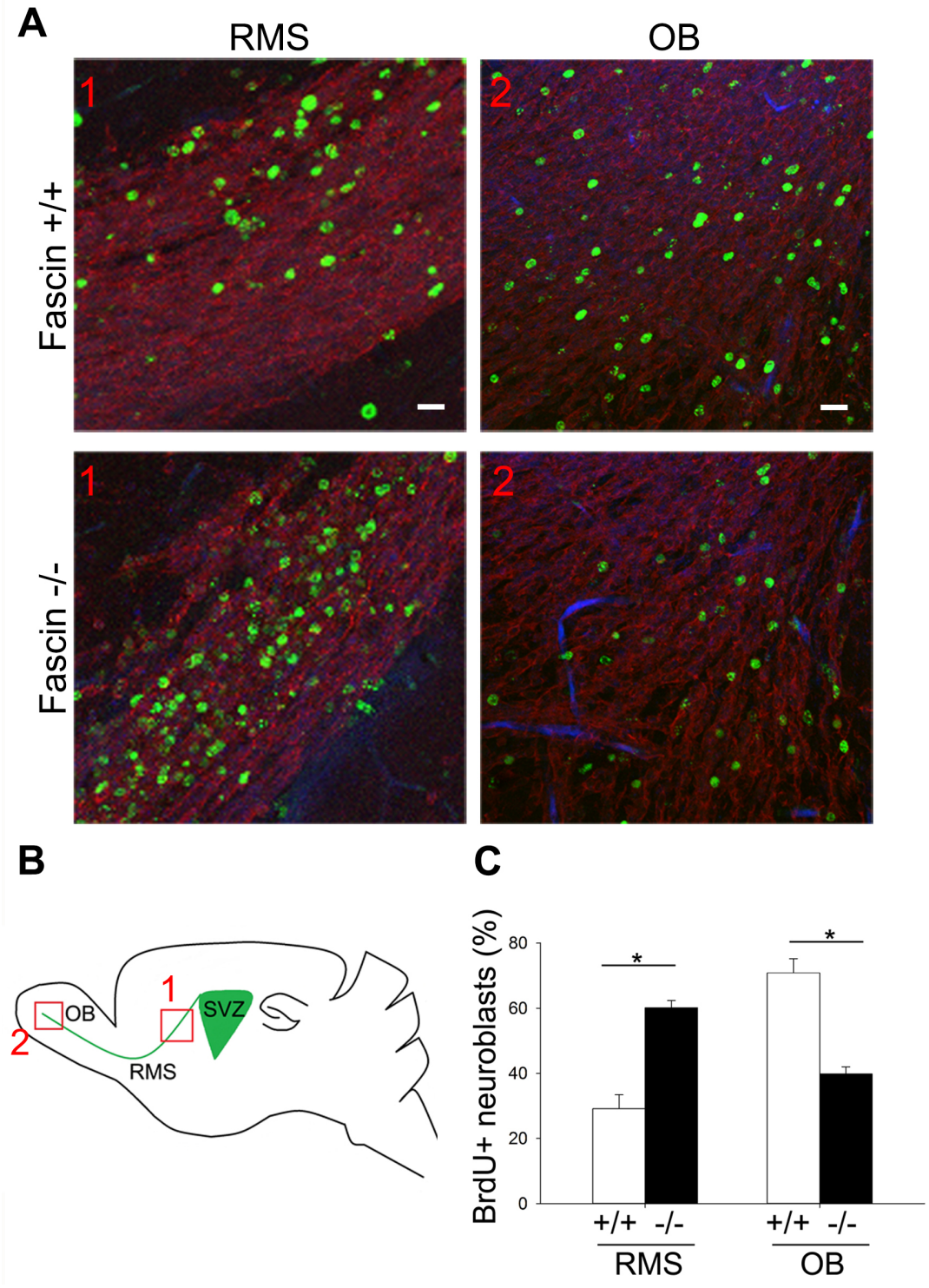

A
RMS
OB
Fascin +/+
Fascin -/-
1
2
B
OB
SVZ
RMS
C
BrdU+ neuroblasts (%)
80
60
40
20
0
*
*
+/+ -/-
+/+ -/-
RMS
OB

Figure 3-7. Genetic deletion of fascin affects neuroblast migration.

(B) Schematic diagram indicates the RMS and OB areas (areas 1 and 2) considered for quantification of BrdU+ cells. (A) Representative images show BrdU+ cells (green) in areas 1 and 2 of the RMS in wt and *fascin-1* ko mice. Sections were also stained for Dcx to visualize migrating neuroblasts (red). (C) *Fascin-1* ko animals display impaired migration, as shown by the increased percentage of BrdU+ cells in the caudal RMS and the decreased percentage of cells in the OB (mean ± SEM; n=4 brains for wt mice; and n=3 brains for *fascin-1* ko mice; *$p<0.05$). BrdU-injected wt and *fascin-1* ko mice provided by Dr. Laura Machesky ad Yafeng Ma. Scale bars: A, 1, 50 µm; A, 2, 20 µm.

3.2.7 Fascin is upregulated in migrating neuroblasts

Our previous observations showed that fascin is highly expressed in the RMS, however, its distribution in the SVZ is still uncharacterized. We therefore performed some immunohistochemical analysis with markers of different cell subtypes found in the SVZ niche. Double immunostaining of coronal SVZ sections showed a complete co-localization of fascin with the migrating neuroblast marker Dcx (Figure 3-8, (A)). In contrast, no co-localization was observed with the astrocytic stem cell marker GFAP (Figure 3-8, (B)), while very little co-localization was observed with the transit amplifying progenitor marker Mash-1 (Figure 3-8, (C)). This specific up-regulation of fascin in neuroblasts supports its exclusive role in regulating the migration of these cells.

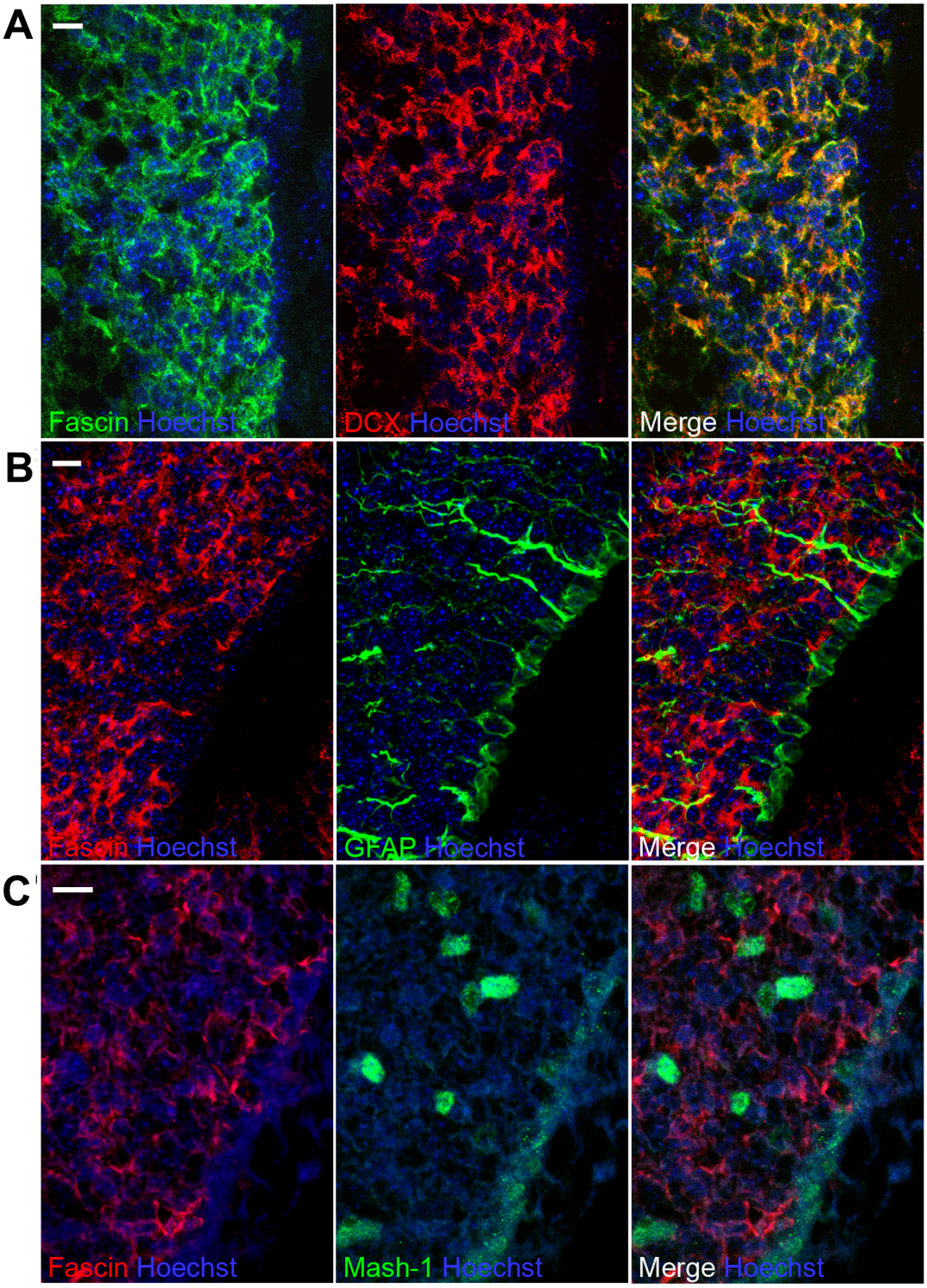


Figure 3-8. Fascin is upregulated in RMS migrating neuroblasts.

(A-C), Confocal images from P7 mouse SVZ sections showing that fascin immunostaining virtually overlaps with Dcx+ migrating neuroblasts (A), but is excluded from GFAP+ stem cells and astrocytes (B). (C), Hardly any colocalization is observed with Mash1+ transit-amplifying progenitors. Immunohistochemistry performed by Carl Hobbs. Scale bars: A-C, 10 µm.

3.2.8 Fascin is expressed in filopodia of RMS migrating neuroblasts

To further examine the spatial distribution of fascin, cultures of migrating neuroblasts were dissected from the RMS of P7 rat brains. RMS explants were then embedded in a three-dimensional Matrigel matrix, a substrate that allows neuroblasts to migrate. This migration assay has been previously shown to recapitulate *in vitro* the *in vivo* migration mode of these cells (Wichterle et al., 1997, Ward and Rao, 2005, Garzotto et al., 2008). Fascin immunostaining was performed together with fluorescent phalloidin, which visualises filamentous actin (F-actin). Fascin concentrates along F-actin-enriched filopodial structures found at the leading edge of migrating neuroblasts (Figure 3-9, top and bottom row). Interestingly, fascin-positive immunostaining was also found along the leading process, and especially ahead of the nucleus (Figure 3-9, bottom row, arrowhead), a site of F-actin condensation before nuclear translocation (Shinohara et al., 2012).

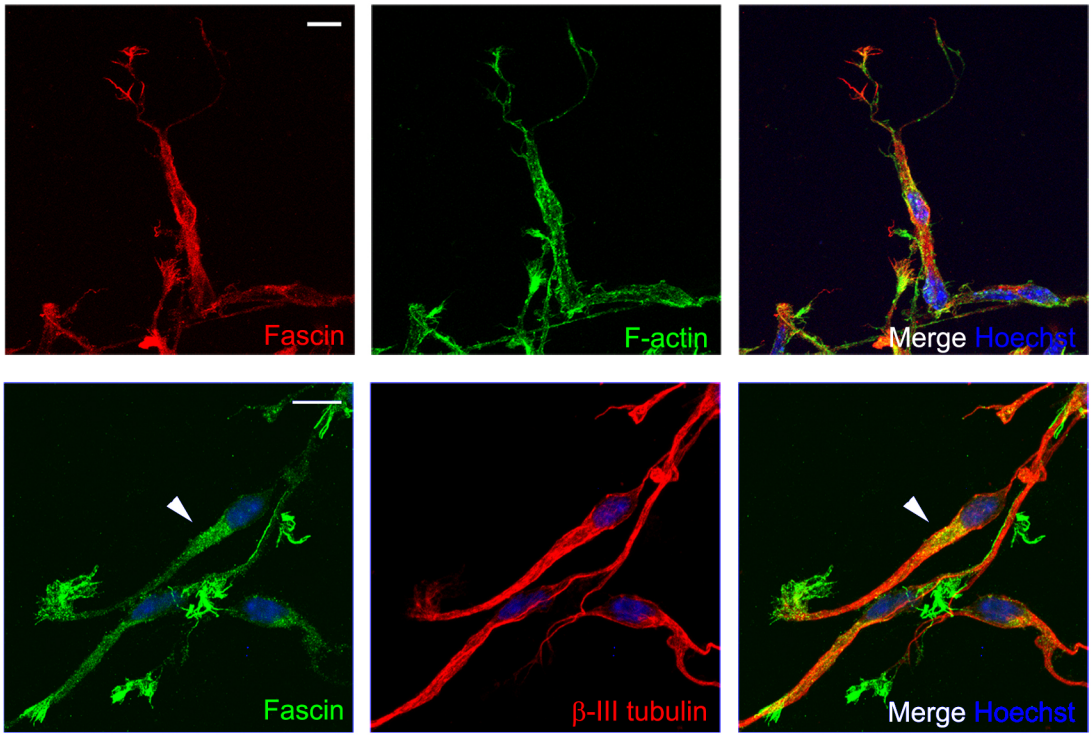


Figure 3-9. Fascin is expressed by RMS migrating neuroblasts.

Rat RMS neuroblasts migrating in Matrigel were fixed and immunostained. (Top row), Fascin (red) concentrates in peripheral filopodial structures (visualized by fluorescent phalloidin, green). Nuclei are stained with Hoechst dye (blue). (Bottom row), Fascin immunoreactivity (green) can also be detected in front of the nucleus (arrowhead). Microtubules are stained by β-III tubulin (red) and nuclei with Hoechst dye (blue). Scale bars: 10 µm.

3.2.9 Fascin knockdown impairs RMS neuroblast morphology *in vitro*

Having determined a high expression of fascin in SVZ-derived neuroblasts and given the phenotype observed in *fascin-1* ko mice, we started to investigate the functional role of fascin in neuroblast migration using RNA interference (RNAi). For initial optimization of this experimental approach, neuroblasts were nucleofected with three different amounts (5, 7, and 9 μg) of pools of four short interfering (si) RNA oligos (data not shown). Fascin levels were monitored by Western blot at two different time points (48 and 72 hours) after nucleofection. Effective fascin depletion (~60%) was observed with the highest siRNA oligo amount already 48 hours after nucleofection (Figure 3-10, (A)), as also confirmed by densitometric quantification (Figure 3-10, (B)). The greatest knockdown (~80%) was observed 72 hours after nucleofection with 9 μg of siRNA (Figure 3-10, (A-B)). We did not consider knockdown effects after 72 hours due to the fact that even neuroblasts nucleofected with control siRNA tend to display an abnormal morphology after this time point.

Upon successful knockdown of fascin by siRNA nucleofection, the effect of fascin depletion was tested on migrating neuroblasts using an *in vitro* migration assay in Matrigel. Nucleofection conditions of primary neuroblasts were optimised using a GFP-expressing plasmid and subsequently the "hanging drop" procedure was adopted to re-cluster nucleofected cells into aggregates that can be embedded in Matrigel to monitor migration (Falenta et al., 2013). According to this protocol, after nucleofection with fascin siRNA neuroblasts were cultured in suspension for 52 h, embedded in Matrigel and subsequently left to migrate for a period of 24 h before immunostaining with anti-fascin and βIII tubulin antibodies. Fascin knockdown visibly affected neuroblast morphology. While control cells displayed a single straight leading process (Figure 3-11, (A), top row, arrowheads), fascin-depleted cells showed leading processes with multiple branches (Figure 3-11, (B), bottom row, arrows). The percentage of cells with branched morphology was almost doubled in fascin-depleted cells compared to control siRNA-nucleofected neuroblasts (Figure 3-11, (B); control siRNA, 24.901 ± 2.352; fascin siRNA, 42.230 ± 3.927; **$p<0.01$, n=150 cells from four independent experiments).

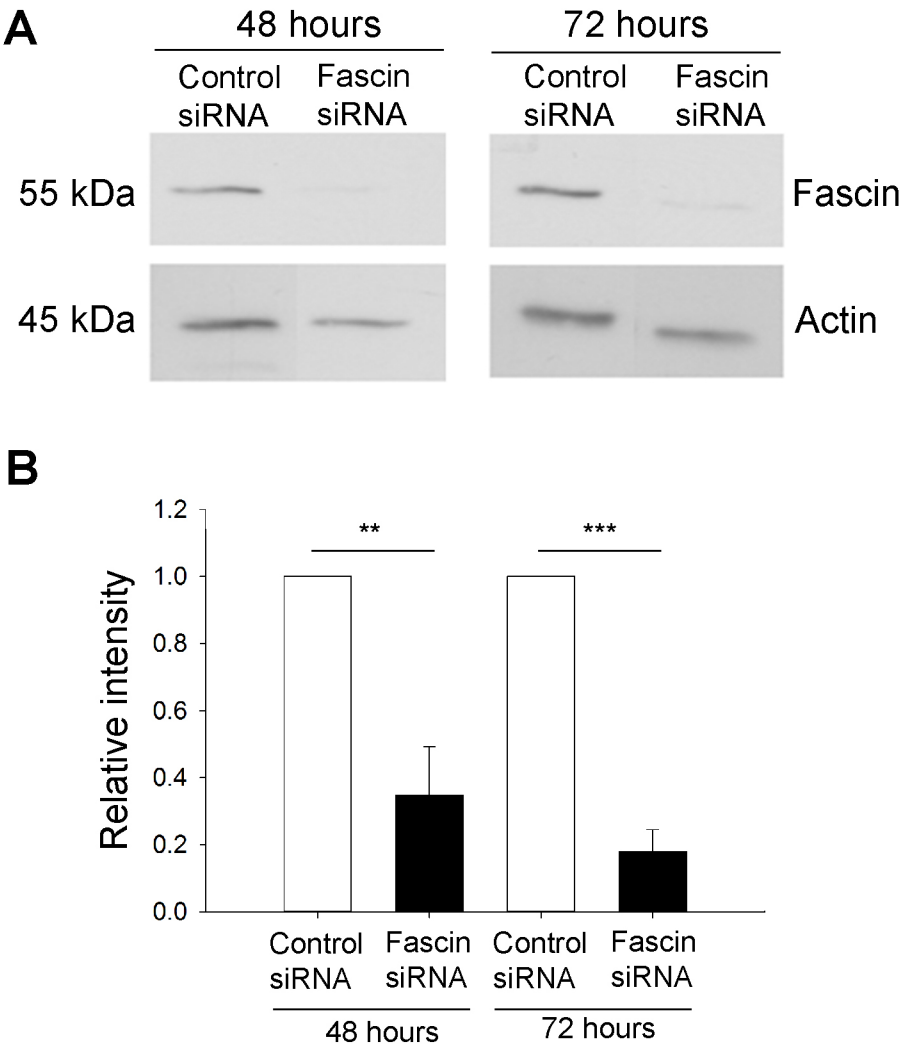


Figure 3-10. Fascin can be knocked down in RMS migrating neuroblasts using RNAi.

(A) Representative Western blots probed for fascin and actin (loading control) showing successful knockdown of fascin at 48 and 72 hours after nucleofection of RMS rat neuroblasts with either control or fascin siRNA oligos. (B) Densitometric quantitative analysis showing significant reduction of fascin levels at both time points, although the most significant reduction was seen at 72 hours (mean ± SEM; **p<0.01, ***p<0.001; n=3 independent experiments).

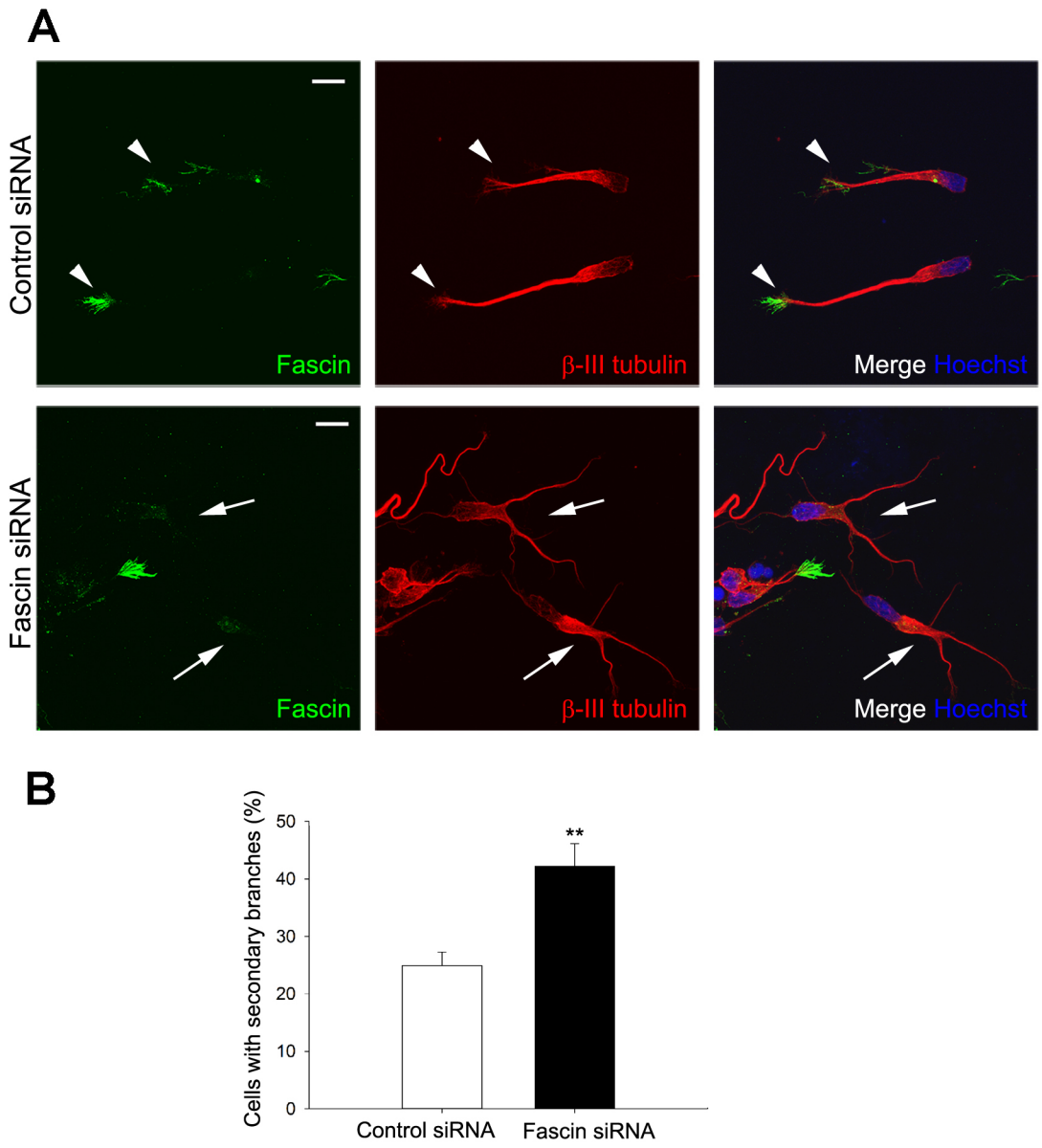


Figure 3-11. Fascin knockdown disrupts neuroblast morphology.

(A), Rat neuroblasts were nucleofected with control or fascin siRNA, embedded in Matrigel 52 h after nucleofection, and left to migrate for 24 h before immunostaining for fascin (green) and the neuroblast marker βIII tubulin (red). (Top row, arrowheads), control cells display a major leading process decorated with fascin at the leading edge. (Bottom row, arrows), fascin-depleted cells show branched protrusions. (B) Fascin depletion significantly increases the percentage of branched cells compared to control neuroblasts (mean ± SEM; **p<0.01; n=3 independent experiments). Scale bars: 10 µm.

3.2.10 siRNA-mediated fascin knockdown impairs neuroblast migration *in vitro*

Besides affecting neuroblast morphology, fascin depletion significantly impaired migration out of the reaggregated cell clusters (Figure 3-12, (A), top row). Quantitative analysis showed a ~30% decrease in migration distance for fascin-depleted cells compared to neuroblasts nucleofected with control siRNA (Figure 3-12, (B)). Moreover, to prove that defective migration was specific to lack of fascin, neuroblasts were nucleofected with fascin siRNA together with a siRNA-resistant GFP-tagged human fascin (Figure 3-12, (A), bottom row) (Hashimoto et al., 2007). Impaired migration caused by fascin siRNA was significantly rescued by co-transfecting siRNA-resistant GFP-tagged human fascin, confirming the specificity of the siRNA effect (Figure 3-12, (B)).

To further explore the impact of fascin depletion on neuroblast dynamics, cell tracking of time-lapse imaging experiments was performed over a period of 7 hours (supplementary movies 2 and 3). Quantitative analysis showed a significant decrease in migrated distance and speed for fascin-depleted cells, which also spent more time immobile (Figure 3-13, (B-D); distance: control siRNA, 117.177 ± 5.295 µm; fascin siRNA, 96.163 ± 6.003 µm; **$p<0.01$; speed: control siRNA, 16.740 ± 0.756 µm/h; fascin siRNA, 13.738 ± 0.858 µm/h; **$p<0.01$; time spent immobile: control siRNA, 3.021 ± 0.105 h; fascin siRNA, 3.813 ± 0.122 h; ***$p<0.001$, n=70 cells from three independent experiments).

Taken together, these data highlight a cell-autonomous role for fascin in regulating neuroblast migration.

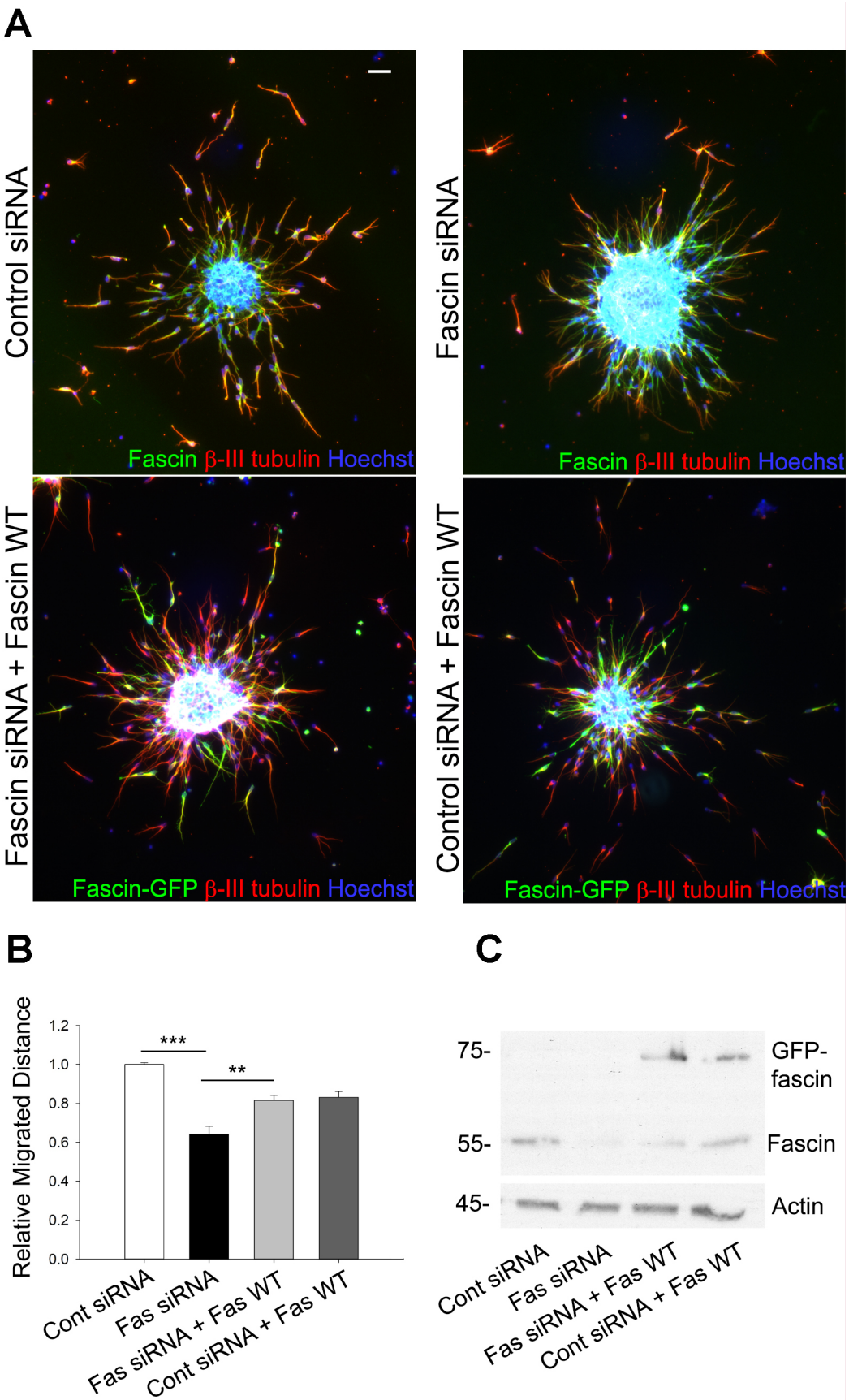

A
Control siRNA
Fascin siRNA
Fascin siRNA + Fascin WT
Control siRNA + Fascin WT
Fascin β-III tubulin Hoechst
Fascin-GFP β-III tubulin Hoechst
B
Relative Migrated Distance
1.2
1.0
0.8
0.6
0.4
0.2
0.0
***
**
Cont siRNA
Fas siRNA
Fas siRNA + Fas WT
Cont siRNA + Fas WT
C
75-
55-
45-
GFP-fascin
Fascin
Actin
Cont siRNA
Fas siRNA
Fas siRNA + Fas WT
Cont siRNA + Fas WT

Figure 3-12. Fascin regulates RMS neuroblast migration *in vitro*.

(A) Reaggregated rat neuroblasts were stained for fascin (green) and βIII-tubulin (red) after nucleofection of control or fascin siRNA oligos with or without a GFP-tagged, siRNA-resistant wt human fascin. Cell nuclei were visualized by Hoechst staining (blue). (B) Quantitative analysis shows a ~30% decrease in migration distance in fascin-depleted neuroblasts compared with cells nucleofected with control siRNA (mean ± SEM; n=3 independent experiments; **p<0.001; ***p<0.001). This effect is almost completely rescued by co-transfection with the siRNA-resistant wt fascin. (C) Western blot from nucleofected neuroblasts shows efficient fascin depletion and expression of GFP-wt fascin. Scale bar: 50 µm.

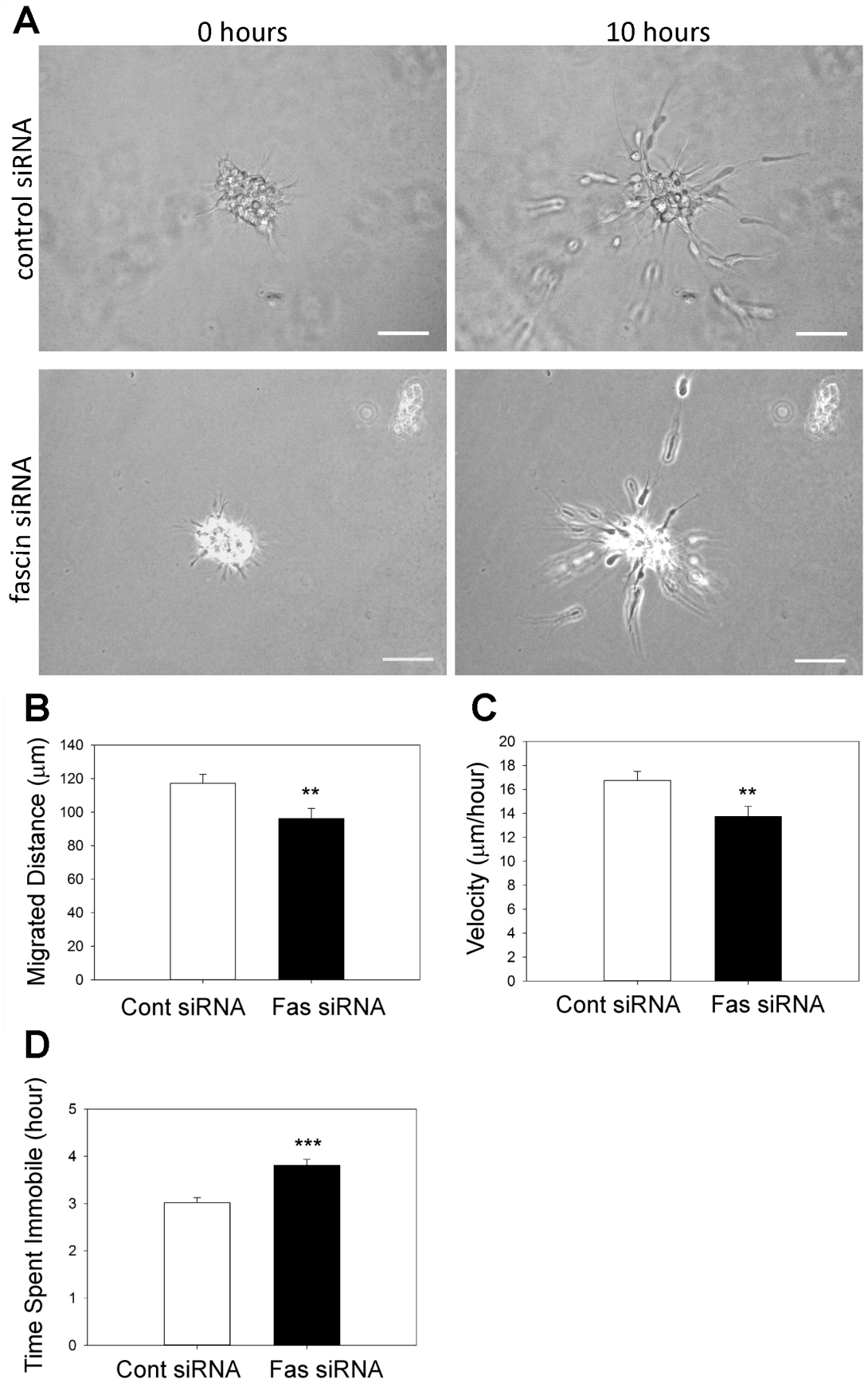

A
0 hours
10 hours
control siRNA
fascin siRNA
B
Migrated Distance (μm)
140
120
100
80
60
40
20
0
**
Cont siRNA
Fas siRNA
C
Velocity (μm/hour)
20
18
16
14
12
10
8
6
4
2
0
**
Cont siRNA
Fas siRNA
D
Time Spent Immobile (hour)
5
4
3
2
1
0
***
Cont siRNA
Fas siRNA

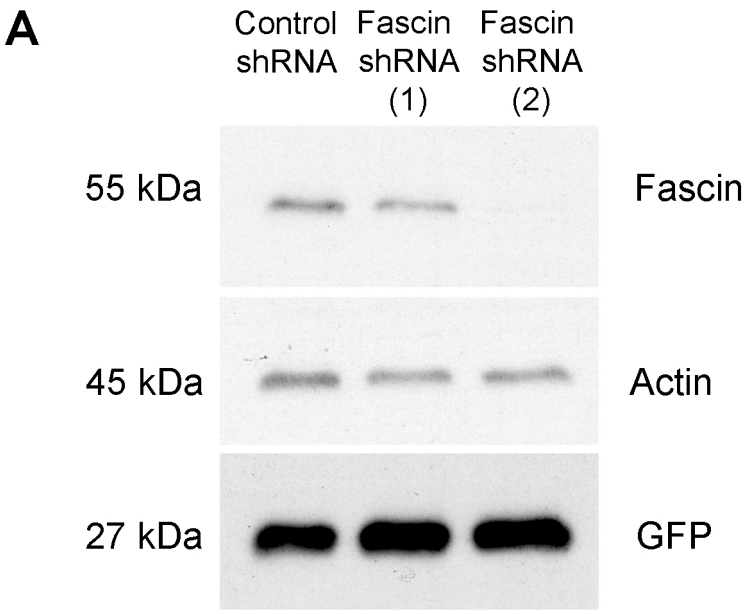
Figure 3-13. Tracking analysis of fascin-depleted cells shows impairment in RMS neuroblast migration.

(A) Snapshots of a control (top row) or a fascin-depleted (bottom) reaggregate at 0 hours and at 10 hours after embedding were taken from time-lapse imaging performed with a 20X objective in a Nikon BioStation every 3 minutes for 24 hours. See movies 1 and 2 in the attached DVD (playing speed 10 frames/s). (B-C), Based on quantitative tracking analysis over a 7 hour period, fascin-depleted cells show a shorter migrated distance (B), lower speed (C), and longer time spent immobile (D) (mean ± SEM, ***$p<0.001$, n=70 cells from 3 independent experiments). Scale bar: 50 μm. Supplementary movies 2 and 3 in the DVD (playing speed 10 frames per second).

3.2.11 shRNA-mediated fascin knockdown impairs neuroblast migration

After having successfully knocked down fascin *in vitro* using siRNA nucleofection, the role of fascin in migration was further examined using another knockdown method: short hairpin RNA (shRNA). shRNA offers a more stable and potent knockdown effect using a lower number of copies of the plasmid and so having less off-target effects in comparison to siRNA (McAnuff et al., 2007, Rao et al., 2009). This plasmid-based method to knock down genes can be used *in vivo* more effectively than siRNA (McAnuff et al., 2007). In fact, interfering with protein expression *in vivo* is generally more difficult and may require longer inhibition periods. Two fascin shRNA-sequences (fascin shRNA (1) and fascin shRNA (2)) targeting two different regions in the *fascin-1* genomic sequence and a control shRNA-sequence were cloned into pCA-b-EGFPm5 silencer 3, which also co-expresses EGFP (Bron et al., 2004). Fascin levels following nucleofection of 5 µg of fascin shRNA (1) or fascin shRNA (2) were monitored in rat RMS neuroblasts by Western blot at 48 (data not shown) and 72 hours (Figure 3-14, (A)). Only fascin shRNA (2) showed an almost complete knockdown (~90%) of fascin protein levels while fascin shRNA (1) was ineffective (Figure 3-14, (B)). The knockdown effect caused by fascin shRNA (2) was detected at 72 hours, but not at 48 hours (data not shown).

Fascin depletion using siRNA successfully impaired neuroblast migration *in vitro* (Figure 3-12). To confirm this result with an alternative RNAi strategy, we used fascin shRNA (2) in the *in vitro* migration assay. We observed a ~30% decrease in the migration of neuroblasts nucleofected with fascin shRNA (2) compared to control shRNA (Figure 3-15, (A-B)) (Falenta et al., 2013).


A
Control shRNA
Fascin shRNA (1)
Fascin shRNA (2)
55 kDa
Fascin
45 kDa
Actin
27 kDa
GFP

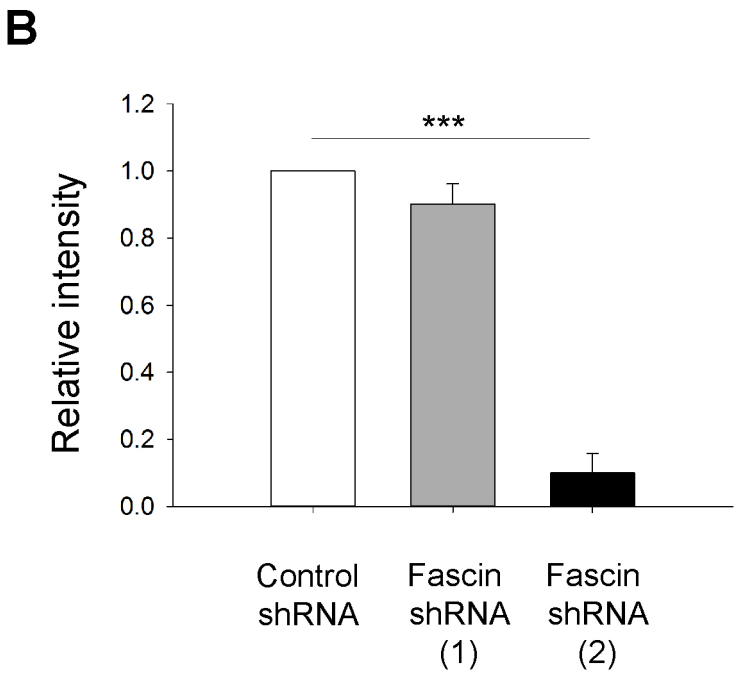
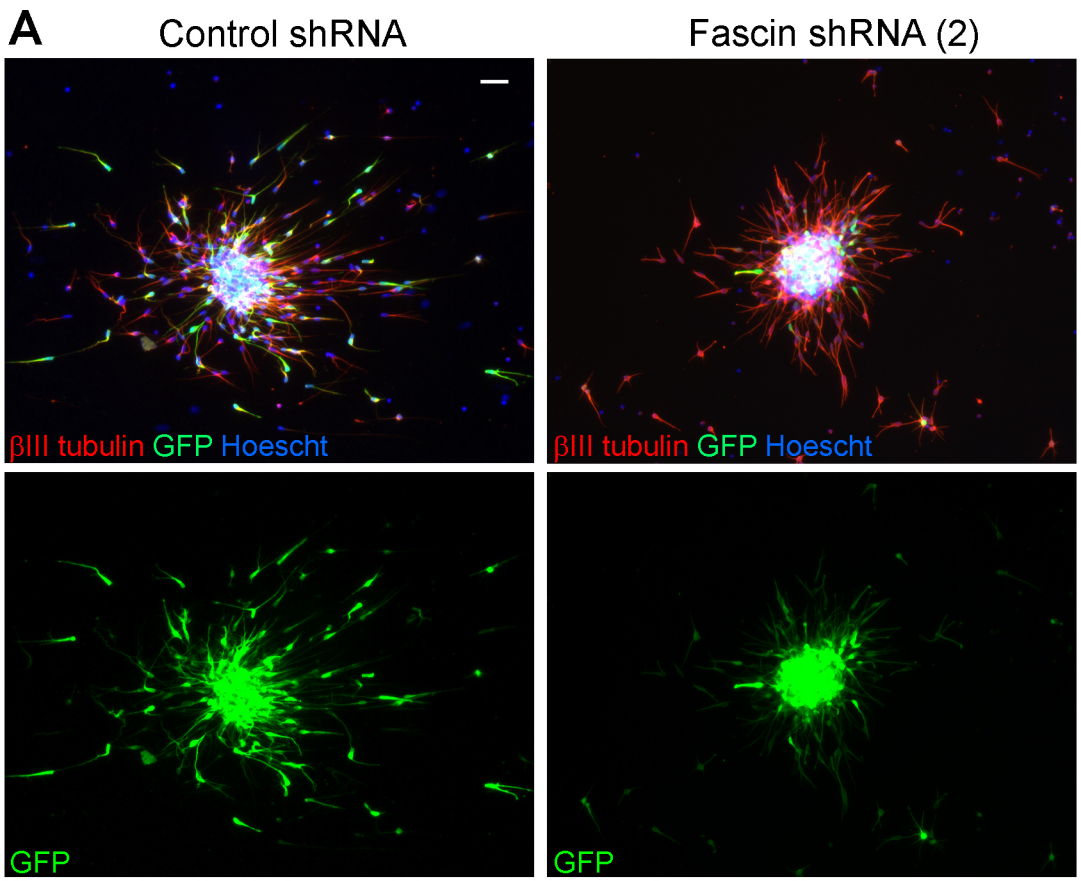

B
Relative intensity
1.2
1.0
0.8
0.6
0.4
0.2
0.0
***
Control shRNA
Fascin shRNA (1)
Fascin shRNA (2)

Figure 3-14. shRNA-mediated fascin depletion in RMS neuroblasts.

(A) Representative Western blot of lysates from dissociated rat RMS neuroblasts, nucleofected with control shRNA, fascin shRNA (1) or fascin shRNA (2), probed for fascin, actin (loading control) and GFP to confirm expression of the shRNA vector show successful knockdown only with fascin shRNA (2). (B) Densitometric quantitative analysis shows a significant reduction of fascin levels of almost 90% using fascin shRNA (2) (mean ± SEM; ***$p<0.001$; n=3 independent experiments).


A
Control shRNA
Fascin shRNA (2)
βIII tubulin GFP Hoescht
βIII tubulin GFP Hoescht
GFP
GFP

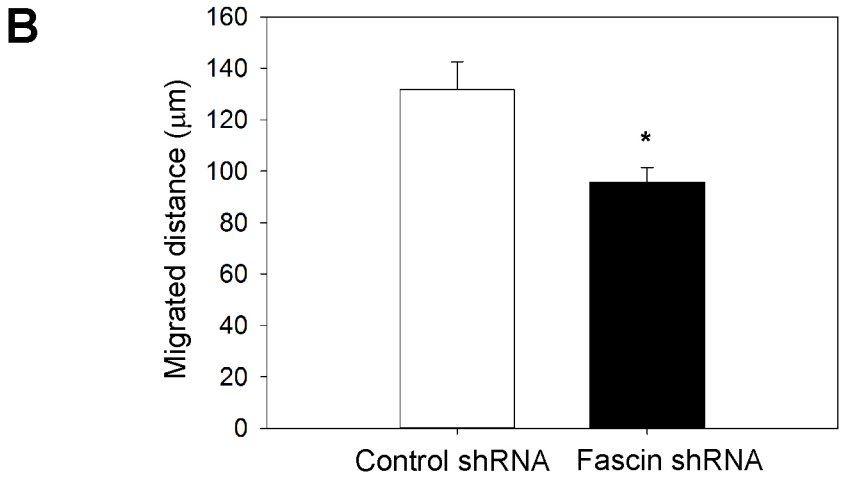

B
Migrated distance (μm)
160
140
120
100
80
60
40
20
0
*
Control shRNA
Fascin shRNA

Figure 3-15. shRNA-mediated fascin knockdown impairs neuroblast migration *in vitro*.

(A) Reaggregated rat neuroblasts were stained for GFP (green) and βIII-tubulin (red) after nucleofection of control or fascin shRNA (2) co-expressing GFP. Cell nuclei were visualized by Hoechst staining (blue). (B) Quantitative analysis shows a ~30% decrease in migration distance in fascin-depleted neuroblasts compared with control shRNA-nucleofected cells (mean ± SEM; n=3 independent experiments; *$p<0.05$). Scale bar: 50 µm.

3.2.12 Fascin knockdown impairs RMS neuroblast migration *ex vivo*

After having determined an important role for fascin in RMS neuroblast migration *in vitro* using two different RNAi approaches, we further examined the effect of fascin depletion *in vivo*. For this purpose, we performed *in vivo* postnatal electroporation in mouse pups. This technique allows transfection of a subpopulation of neuroblasts in the SVZ, achieving sparse neuroblast labelling detectable up several weeks after electroporation (Boutin et al., 2008, Sonego et al., 2013b).

We electroporated fascin shRNA (2) or control shRNA plasmids into the right ventricles of P2-3 mouse pups. Five days later the animals were sacrificed and their brains were either embedded in gelatin, sliced and stained with an anti-GFP antibody or were sliced and cultured for time-lapse imaging.

Five days after electroporation many SVZ-derived neuroblasts are found along the RMS, and some have started to reach the OB (Figure 3-16, top). Control neuroblasts generally display a single, straight leading process oriented in the direction of the migration (towards the OB) (Figure 3-16, bottom). GFP-positive cells expressing fascin shRNA (2) or control shRNA were found throughout the RMS and in the core of the OB just starting to migrate radially (our general observation, not shown). Quantitative morphological analysis of high magnification confocal images show that fascin shRNA (2)-transfected neuroblasts had a significantly shorter leading process compared to control shRNA-transfected cells (Figure 3-17, (A-B)). Moreover, a small but significantly higher percentage of fascin-depleted cells displayed a branched process compared to control cells (Figure 3-17, (A-C)).

To prove that fascin was knocked down *in vivo*, we cultured neuroblasts from dissected RMS tissue obtained from electroporated mouse brains (right side only). Significant downregulation of fascin immunoreactivity was observed in GFP-labeled cells transfected with fascin shRNA (2), although some residual fascin expression was still present.

To study whether fascin knockdown affects not only on the morphology of RMS neuroblasts but also their dynamics, we performed spinning disk confocal time-lapse imaging of brain slices obtained from shRNA-electroporated animals. Slices were imaged every 3 minutes for a total of 3 hours. As observed in previous studies (Sawamoto et al., 2006, Hirota et al., 2007, Nam et al., 2007, Bagley and Belluscio,

2010, Saha et al., 2012), although the majority of cells migrate towards the OB, some of the cells can migrate backwards (towards the SVZ) or change direction during imaging (Supplementary movie 7). Also, a previous detailed characterisation of migrating neuroblasts divided them into three sub-populations based on their migratory index, which is identified as the ratio between the net distance (i.e. the shorter distance from the start point to the end point) and the total distance travelled over time (Nam et al., 2007). In particular, cells were classified as "exploratory", "intermediate" and "migratory". "Exploratory" cells, characterised by a migratory index between 0 and 0.4, tend to move locally without a clear direction; "migratory" cells instead move in a directed fashion (migratory index 0.6-1), while "intermediate" cells display an intermediate behaviour (migratory index 0.4-0.6) (Nam et al., 2007).

The parameters analysed by tracking analysis reflect the dynamic behaviour of neuroblasts and the effects of protein knockdown/overexpression on cell motility; in particular, while migrated distance and speed offer a measurement of how long and how quickly a neuroblast can migrate within the RMS of a cultured brain slice, displacement and rate of displacement offer a measurement of the efficiency of that migration. Indeed, a neuroblast migrating along a straight line towards the OB will reach the final destination (the OB) faster than a neuroblast migrating the same distance but in a less directed fashion. Moreoever, the migratory index, which divides the neuroblast population in subpolulations of "exploratory", "intermediate" and "migratory", offers a more accurate image of the different types of migratory cells populating the RMS.

Tracking analysis of time-lapse movies showed that, compared to control shRNA cells, fascin shRNA (2) transfected neuroblasts have shorter migrated distance (Figure 3-18, (B); control shRNA: 160.3 µm ± 8.5; fascin shRNA (2): 139.3 µm ± 7.9. One-tailed t-test *$p<0.05$), reduced displacement, (the shortest distance between start and end points) (Figure 3-18, (C); control shRNA: 93.7 µm ± 4.1; fascin shRNA (2): 81.2 µm ± 4.5. One-tailed t-test *$p<0.05$), reduced velocity (Figure 3-18, (D): control shRNA: 53.4 µm/h ± 8.3; fascin shRNA (2): 46.4 µm/h ± 2.6. One-tailed t-test *$p<0.05$) and lower displacement rate, (ratio between displacement and time) (Figure 3-18, (E): control shRNA: 30.5 µm/h ± 1.46; fascin shRNA (2): 25.6 µm/h ±

1.41. Two-tailed t-test *p<0.05), while no significant difference was found in the time spent immobile (Figure 3-18, (F): control shRNA: 59.7 min ± 4.3; fascin shRNA (2): 70.9 min ± 5.3), or in the migratory index (Comte et al., 2011) (control shRNA: 0.589 ± 0.007; fascin shRNA (2): 0.574 ± 0.033). Also, the percentage of migratory, intermediate or exploratory cells was not significantly different between control and fascin shRNA neuroblasts (% of neuroblasts in control shRNA, exploratory: 18.762 ± 2.62; intermediate: 28.031 ± 4.036; migratory: 52.550 ± 2.415; % of neuroblasts in fascin shRNA, exploratory: 25.051 ± 6.052; intermediate: 29.163 ± 4.251; migratory: 52.012 ± 6.532).

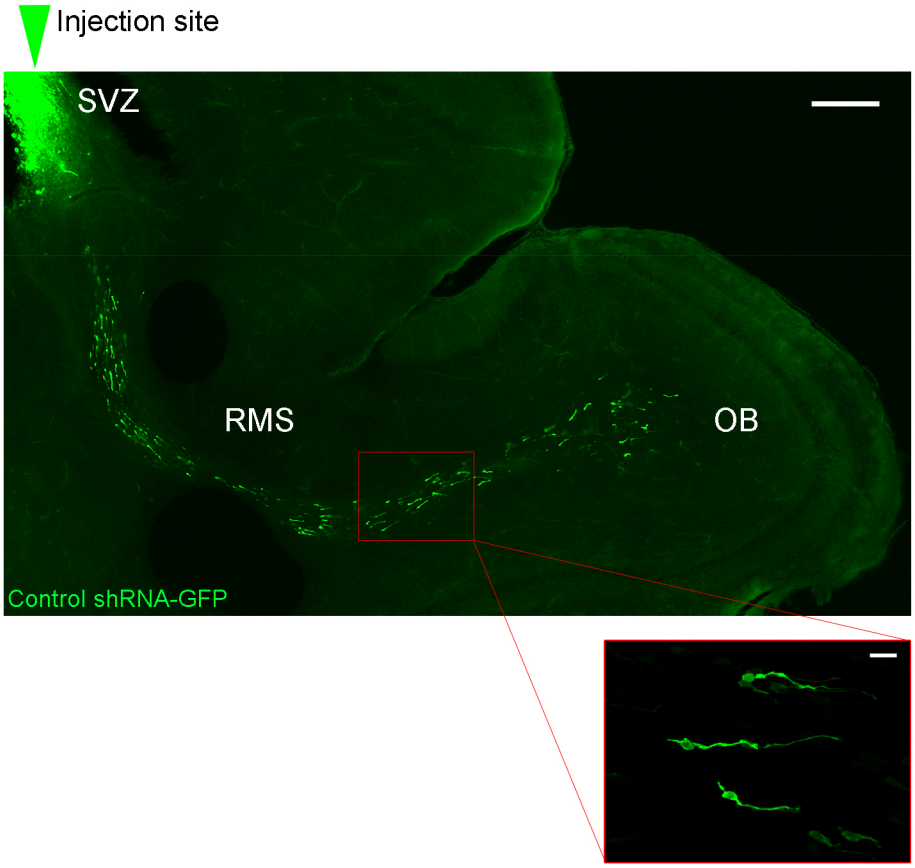


Figure 3-16. *In vivo* postnatal electroporation in mouse SVZ.

(Top) Representative confocal z-projection of a sagittal brain slice showing GFP-labelled neuroblasts migrating from the SVZ along the RMS towards the OB. (Bottom) Higher magnification picture of the RMS elbow showing neuroblasts with a single leading process pointing towards the OB. Scale bar: top, 200 µm; bottom, 10 µm. Supplemetary movie 7.

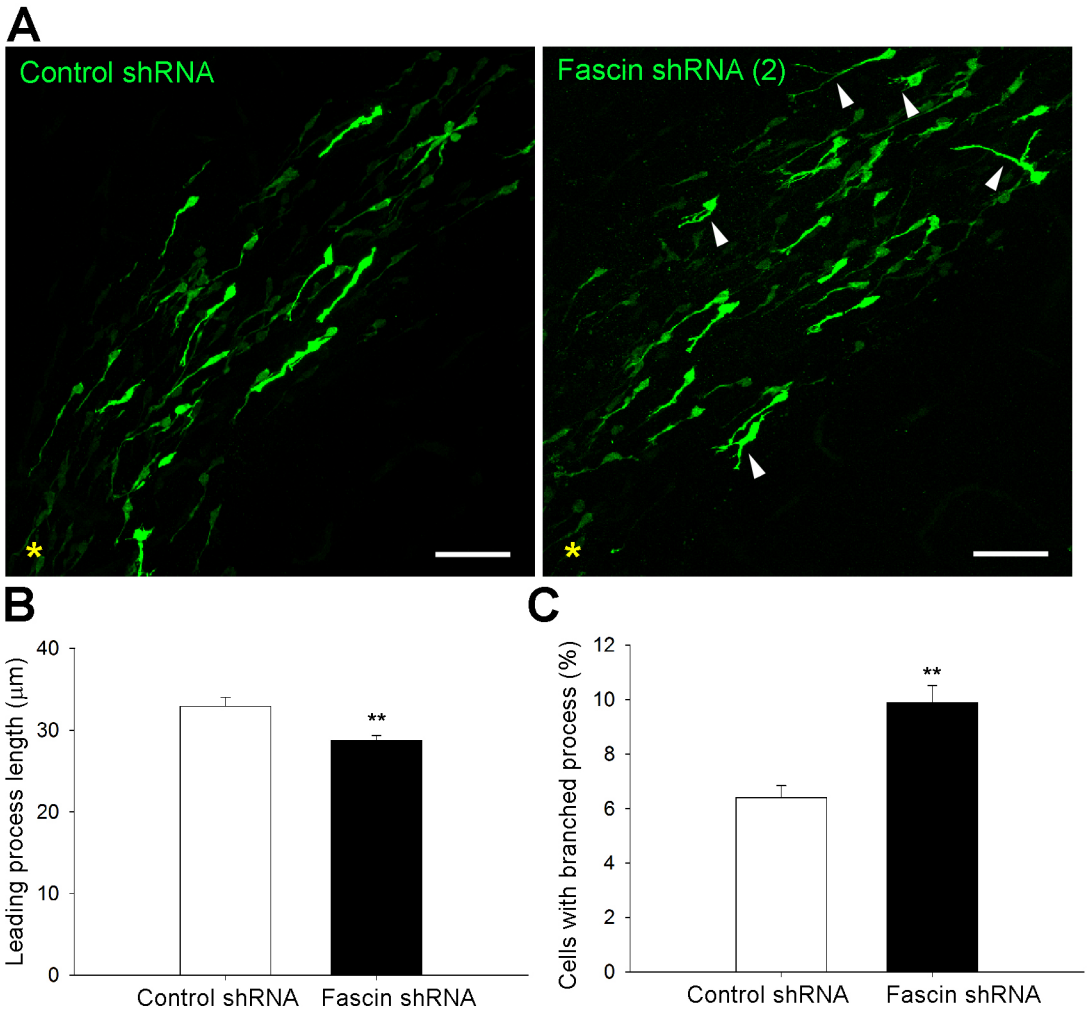


Figure 3-17. Fascin regulates neuroblast morphology *in vivo*.

(A), Confocal z-stack projections of fixed brain slices from P2-3 mice electroporated with control shRNA or fascin shRNA (2) show control cells with single processes oriented towards the OB, identified by the yellow asterisk (left), while several fascin shRNA (2) expressing cells have branched protrusions (right, arrowheads). (B) Quantifications showing that fascin shRNA in vivo electroporation causes a modest but significant decrease in leading process length (left), and a significant increase in the percentage of branched neuroblasts (mean ± SEM; **p<0.01; n=6 brains). Scale bars: A, 50 µm.

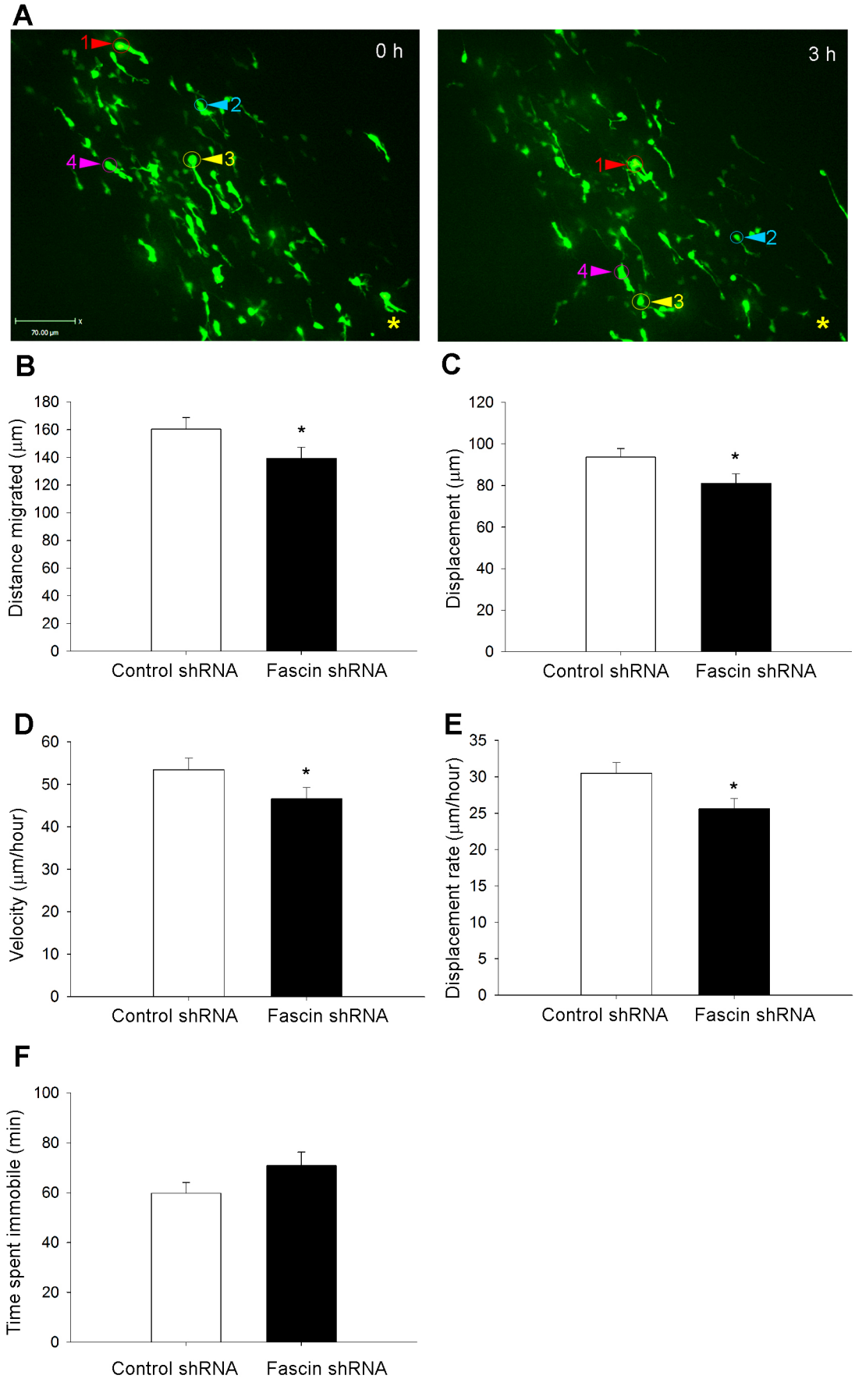

A
0 h
3 h
1
2
3
4
70.00 µm
*
B
Distance migrated (µm)
180
160
140
120
100
80
60
40
20
0
Control shRNA
Fascin shRNA
C
Displacement (µm)
120
100
80
60
40
20
0
D
Velocity (µm/hour)
60
50
40
30
20
10
0
E
Displacement rate (µm/hour)
35
30
25
20
15
10
5
0
F
Time spent immobile (min)
100
80
60
40
20
0

Figure 3-18. Fascin is necessary for efficient neuroblast migration *ex vivo*.

(A), Projections of spinning disk confocal z-stack images (taken at times 0 and 3 h) from time-lapse imaging of acute brain slice cultures showing GFP-expressing neuroblasts (coloured circle and arrowheads) migrating toward the OB (yellow asterisk). (B-G) Tracking analysis of brain slices electroporated with fascin shRNA (2) displays a shorter migrated distance (B), shorter displacement (C), and lower speed (D) (mean ± SEM; n=8 slices for control; n=7 slices for fascin shRNA (2); one tailed t-test: **p<0.01). A significant difference was found between control and fascin shRNA (2) in the displacement rate (E), while no difference was found in the time cells spent immobile (F) (mean ± SEM; n=8 slices for control; and n=7 slices for fascin shRNA (2); *p<0.05). Scale bar, 70 µm.

3.2.13 Fascin phosphorylation on Ser39 regulates neuroblast migration *in vitro*

The function of fascin is post-transcriptionally regulated by phosphorylation of a serine residue (Ser39) (Ono et al., 1997). Phosphorylation of Ser39 decreases fascin-mediated actin-bundling which is important for keeping the balance between cell adhesion and cell protrusion (Anilkumar et al., 2003, Vignjevic et al., 2003). In order to investigate the role Ser39 phosphorylation of fascin in neuroblast migration, neuroblasts were nucleofected with three different GFP-tagged fascin variants: wild-type fascin, phosphomimetic fascin (S39D), and non-phosphorylatable fascin (S39A), while GFP only was used as a control. Nucleofected cells were then re-aggregated overnight, embedded the following morning and fixed 24 hours later to analyse migration. Colour images of anti-GFP immunostained reaggregated neuroblast clusters were converted to grayscale mode to better visualize GFP+ cells migrating out of the clusters (Figure 3-19, (A)). Neuroblasts expressing GFP-tagged wild-type fascin migrated in a similar manner to control GFP-expressing neuroblasts (Figure 3-19, (B)). In contrast, a ~60% significant decrease in migration was observed for neuroblasts expressing either GFP-fascin S39D or GFP-fascin S39A (Figure 3-19, (B)). Importantly, nucleofection of GFP did not affect the ability of cells to migrate, since GFP-expressing cells migrated as well as "internal control" neuroblasts that were not expressing GFP (Figure 3-19, (B)).

Time-lapse imaging was also performed to examine how fascin phosphorylation on Ser39 affects neuroblast dynamics (supplementary movies 4, 5 and 6). Based on quantitative tracking analysis, expression of either S39A or S39D fascin significantly decreased migrated distance (Figure 3-20, (B)) and speed (Figure 3-20, (C)), while increasing pausing time compared to control (GFP expression) and wild-type fascin (Figure 3-20, (D)). As noticed before in fixed reaggregated clusters, no differences in migration were detected between neuroblasts expressing wild-type fascin and control GFP-expressing cells (Figure 3-20, (B-D)).

Taken together, these results support an important role for fascin phosphorylation on Ser39 in neuroblast migration and suggest that a tight regulation of phosphorylation on this site might be necessary for efficient neuroblast motility

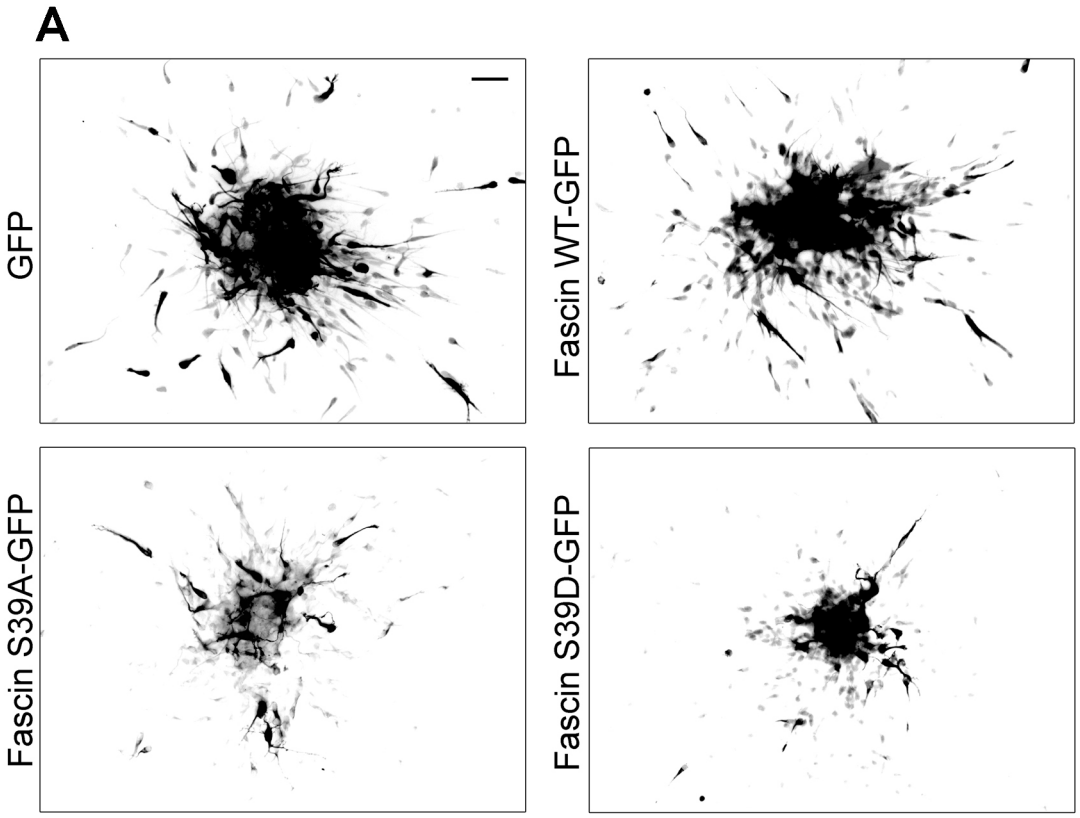

A
GFP
Fascin WT-GFP
Fascin S39A-GFP
Fascin S39D-GFP
B
Relative Migrated Distance
1.4
1.2
1.0
0.8
0.6
0.4
0.2
0.0
***
***
GFP
WT
S39A
S39D

Figure 3-19. Fascin phosphorylation site Ser39 regulates neuroblast migration *in vitro*.

(A), Representative pictures of rat reaggregated neuroblasts nucleofected with GFP, or GFP-tagged wt, S39A, or S39D fascin. The GFP channel is shown as a grayscale image. (B), Quantitative analysis from fixed samples shows a ~60% decrease in relative migration distance for neuroblasts expressing the fascin phosphomutants compared to control cells. Expression of wt fascin did not significantly affect migration. GFP-negative, untransfected cells served as an internal control (hatched columns) (mean ± SEM; n=3, ***$p<0.001$). Scale bar, 50 µm.

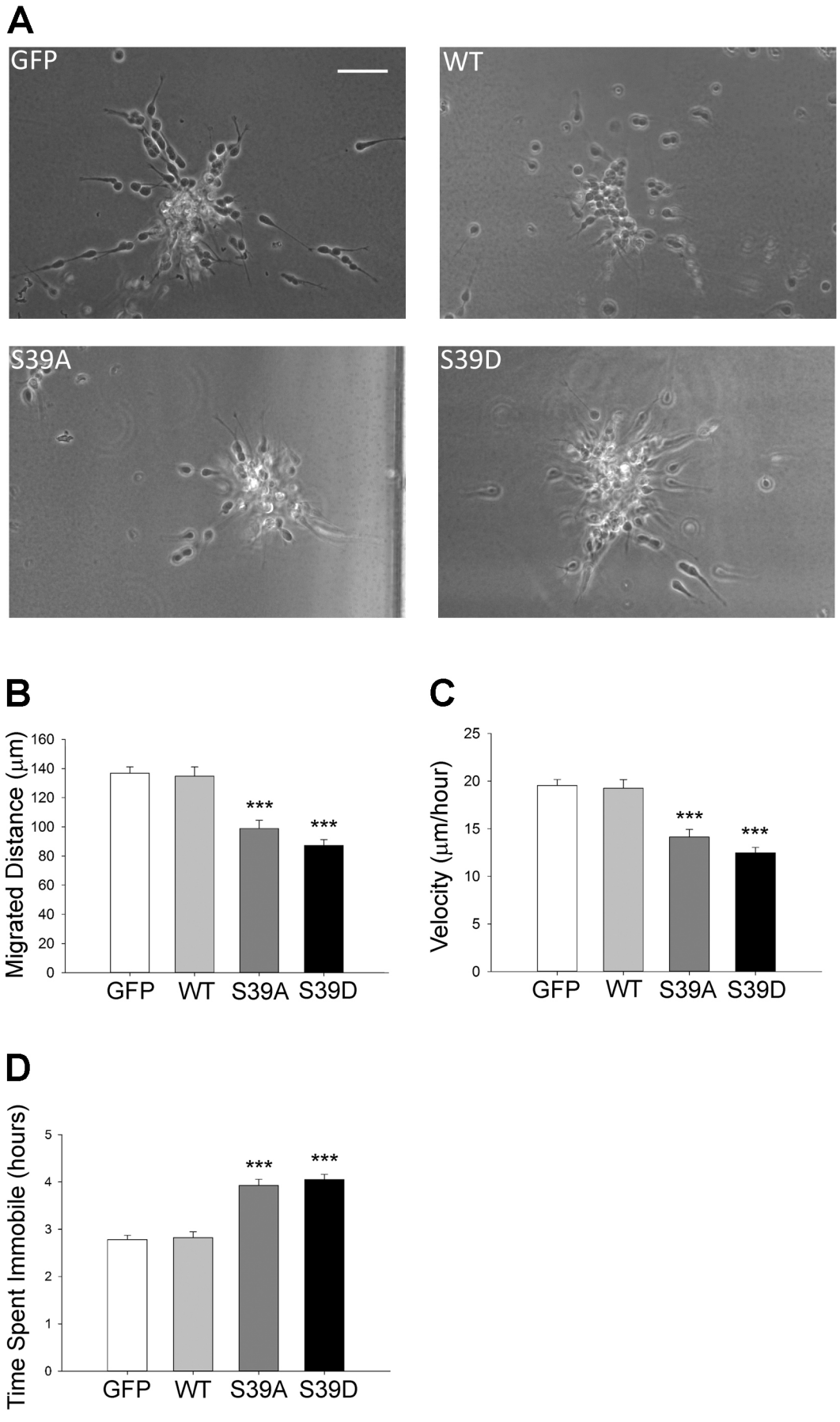
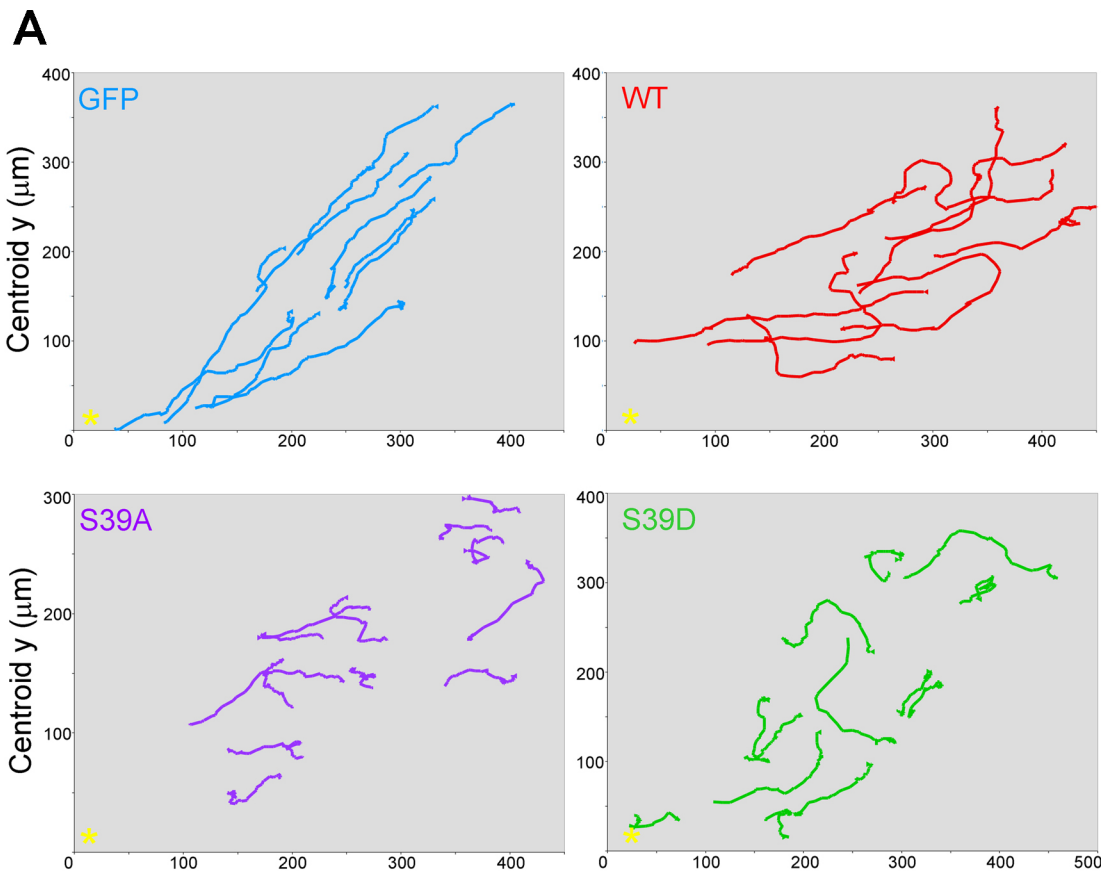

A
GFP
WT
S39A
S39D
B
Migrated Distance (μm)
160
140
120
100
80
60
40
20
0
***
***
GFP
WT
S39A
S39D
C
Velocity (μm/hour)
25
20
15
10
5
0
***
***
GFP
WT
S39A
S39D
D
Time Spent Immobile (hours)
5
4
3
2
1
0
***
***
GFP
WT
S39A
S39D

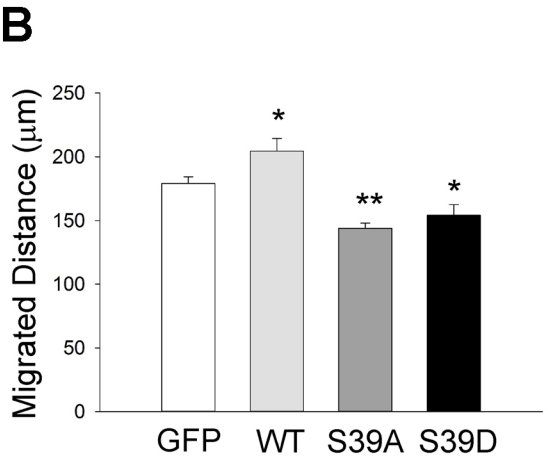
Figure 3-20. Tracking analysis shows that fascin phosphorylation site Ser39 regulates neuroblast migration *in vitro*.

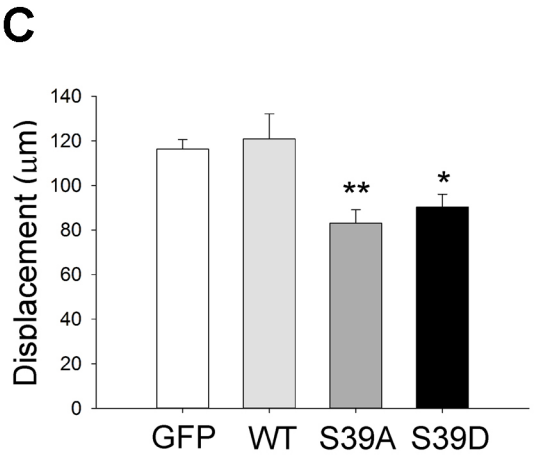
(A) Representative snapshots of rat neuroblasts nucleofected with GFP (top row, left), GFP-tagged wt fascin (top row, right) S39A fascin (bottom row, left), and S39D fascin (bottom row, right) taken 10 hours after the start of time-lapse imaging (performed with a 20X objective in a Nikon BioStation every 3 minutes for 24 hours). Please see also supplementary movies 4, 5 and 6 in the DVD (playing speed 10 frames per second). (B-D), Based on quantitative tracking analysis over a 7 hour period, neuroblasts expressing either S39A or S39D fascin migrated over shorter distances (B), were significantly slower (C), and spent more time immobile (D) compared with either GFP or wt fascin-expressing neuroblasts (mean ± SEM; n=70 cells from 3 independent experiments; ***$p<0.001$). Scale bar: 50 µm.

3.2.14 Phosphorylation of fascin on Ser39 regulates *ex vivo* RMS neuroblast migration

To examine the role for fascin phosphorylation on Ser39 in neuroblast migration in vivo, we carried out postnatal electroporations in P2-3 mouse pups (Boutin et al., 2008). Since the GFP vectors containing the different fascin variants gave low fluorescent signal for time-lapse imaging purposes, we co-electroporated either the empty vector, wt fascin, S39A fascin or S39D fascin with a GFP-expressing plasmid (pCX-GFP) in a 3:1 ratio. After 5 days, animals were sacrificed and brains were sliced in 300 µm-thick sections. Only intact brain slices displaying fluorescent signal along the entire RMS were cultured and used for time-lapse imaging. Migration was monitored every 3 minutes for a total period of 3 hours using a spinning-disk confocal microscope (supplementary movies 7, 8 and 9). Tracking analysis allowed visualization of cell trajectories and revealed that control GFP-expressing cells displayed a more directed and less exploratory motile behaviour compared to wt, S39A or S39D-expressing cells (Figure 3-21, (A)). Detailed quantitative analysis showed that wt fascin expressing cells migrated with a distance and a velocity significantly exceeding those of control cells (Figure 3-21, (B, D)). However, no difference in displacement was found between wt and control (Figure 3-21, (C)), which is likely to be due to a more exploratory behaviour in cells expressing wt fascin. In contrast, cells expressing either S39A or S39D fascin displayed shorter migrated distance and displacement, and lower speed compared to control and wt fascin (Figure 3-21, (B-D)). Moreover, further analysis of neuroblast dynamics revealed that neuroblasts expressing either fascin phosphomutants branched more frequently compared to control cells (Figure 3-22, (A-B)) and were characterised by a lower migratory index (i.e. were more “exploratory”) (Figure 3-22, (C)). On the other hand, neuroblasts expressing wt fascin display a behaviour similar to control cells (data not shown). Altogether, these data reinforce the concept that fascin expression is related to the migratory ability of neuroblasts. Moreover, the similarity of the effects produced by the two fascin phosphomutants suggests that the Ser39 residue of fascin could be controlled by a highly regulated cycle of phospho-/dephosphorylation events to achieve efficient neuroblast migration.


A
GFP
WT
S39A
S39D
Centroid y (μm)
0
100
200
300
400
500


B
Migrated Distance (μm)
0
50
100
150
200
250
*
**
*
GFP
WT
S39A
S39D


C
Displacement (μm)
0
20
40
60
80
100
120
140
**
*
GFP
WT
S39A
S39D

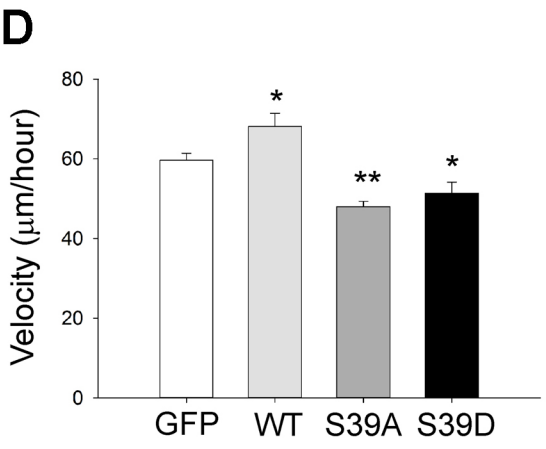

D
Velocity (μm/hour)
0
20
40
60
80
*
**
*
GFP
WT
S39A
S39D

Figure 3-21. Phosphorylation of fascin on Ser39 regulates neuroblast migration *ex vivo*.

(A), Representative migratory paths from time-lapse imaging of neuroblasts migrating within the brain slice and expressing empty vector, wt fascin, S39A fascin or S39D fascin in a 3:1 ratio with pCX-GFP over a period of 3 h. The yellow asterisk marks the location of the OB. (B-D), Based on quantitative tracking analysis, expression of S39D or S39A fascin significantly decreases migrated distance (B), speed (C), and displacement (D), while wt fascin overexpression increases migration distance and speed, but not displacement (mean ± SEM; n=8 slices for control; n=5 slices for wt; and n=6 slices for S39A and S39D; *$p<0.05$; **$p<0.01$). Scale bar: 85 µm. Please also see supplementary movies 7, 8 and 9 in the DVD (playing speed 10 frames per second).

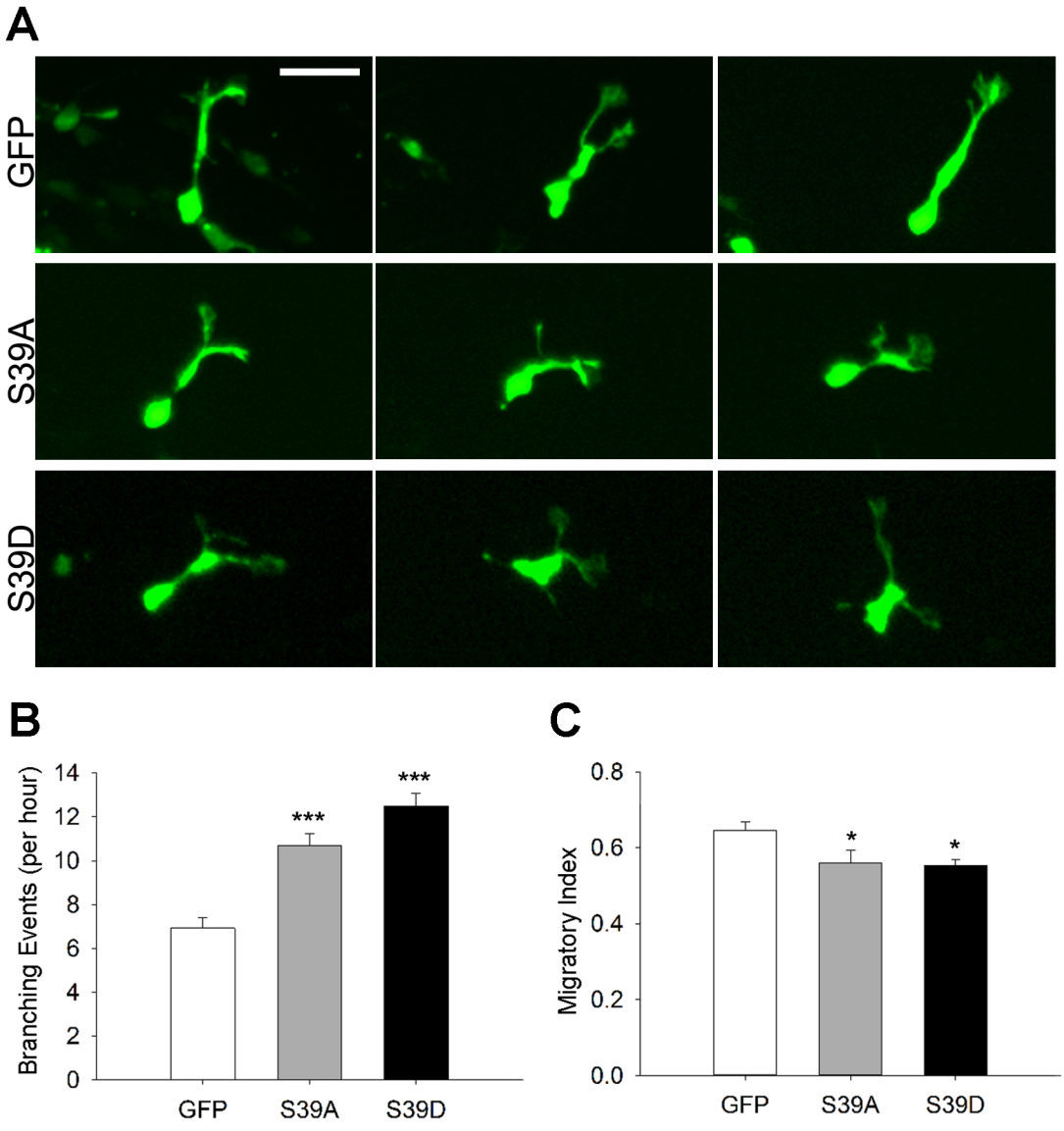

A
GFP
S39A
S39D
B
Branching Events (per hour)
0
2
4
6
8
10
12
14
***
***
GFP
S39A
S39D
C
Migratory Index
0.0
0.2
0.4
0.6
0.8
*
*
GFP
S39A
S39D

Figure 3-22. Fascin phosphorylation on Ser39 regulates neuroblast directionality *ex vivo*.

(A), Projections of spinning disk confocal z-stacks (corresponding to the same cell imaged at three different time points) showing representative migrating neuroblasts expressing pGFPC2 (empty vector) (top row), pGFPC2-S39A fascin (middle row) or -S39D (bottom row) and pCX-EGFP in a 3:1 ratio. (B), Detailed analysis of spinning disk movies shows an increase in the number of branching events per hour for neuroblasts expressing S39A or S39D fascin compared to control cells (mean ± SEM; n=80 cells from 8 brain slices for GFP; and n=60 cells from 6 brain slices for S39A and S39D; ***$p<0.001$). (C), The migratory index (net distance divided by total distance) is significantly decreased by expression of either S39A or S39D fascin (mean ± SEM; n=8 slices for control; n=6 slices each for S39A and S39D; *$p<0.05$). Scale bar: 30 µm. Please also see supplementary movies 7, 8 and 9 in the DVD (playing speed 10 frames per second).

3.2.15 Fascin overexpression and its phosphorylation at Ser39 influence neuroblast morphology and orientation

To further explore the effect of fascin overexpression and the role of its phosphorylation on Ser39 *in vivo*, we also fixed and immunostained for GFP brain slices prepared 5 days after electroporation of GFP, wt, S39A or S39D fascin. Neuroblasts expressing GFP or S39A fascin showed similar morphology, with a vast majority having a straight and long leading process oriented towards the OB (Figure 3-23, (A), top, and bottom, left). Instead, wt and S39D had a notable different morphology in comparison to GFP-expressing cells (Figure 3-23, (A), top, right, bottom, right and top, left). Leading process length was slightly but significantly longer for S39A, while for wt or S39D was shorter compared to control cells (Figure 3-23, (B)). Almost 95% of control cells expressing GFP have a leading process oriented towards the OB, with only ~5% displaying a misoriented process (Figure 3-23, (C)). Cells were considered misoriented when the leading processes were oriented at an angle of ≥180 degrees relative to the direction of migration (or to the OB location). Expression of S39A fascin did not affect neuroblast orientation, while expression of either wt or S39D fascin caused a substantial increase in the percentage of misoriented cells (Figure 3-23, (C)). Although this difference in orientation was quite noticeable, neuroblasts were still able to migrate along the RMS and reach the OB like control cells expressing GFP (data not shown). Although these data may appear contradictory to the ones shown in the previous subchapters where both phospho-mutants S39A and S39D produced similar effects, we think that this may be due to the intrinsic properties of Ser39. It is known that phosphorylation at this site reduces the binding of fascin to actin (Yamakita, Ono et al. 1996). The non-phosphorylatable variant, S39A, constitutively binding to actin may act as a stabiliser of actin filaments leading neuroblasts to have a stable growth cone, thus a straight single leading process. On the other hand the phosphomimetic variant S39D is unable to bind actin, thus portraying a dominant-negative effect that causes growth cone instability and hence shorter and a mis-oriented leading process. At this regard, we noticed that cultured RMS rat neuroblasts transfected with the S39A mutant seem to display a higher number of filopodia at the tip of

their leading process compared to cells transfected with the S39D mutant, suggesting a role for unphosphorylated fascin in binding and stabilizing actin filaments, and an actin filament destabilizing role for phosphorylated fascin (Figure 3.24, qualitative observation).

In fixed brain slices overexpression of fascin leads to a similar phenotype of S39D, showing that levels of fascin must be precisely controlled to have a correct neuroblast orientation.

In conclusion, these data suggest that fascin expression levels as well as its phosphorylation on Ser39 play a role in correctly orienting RMS neuroblasts towards the OB and in regulating their morphology.

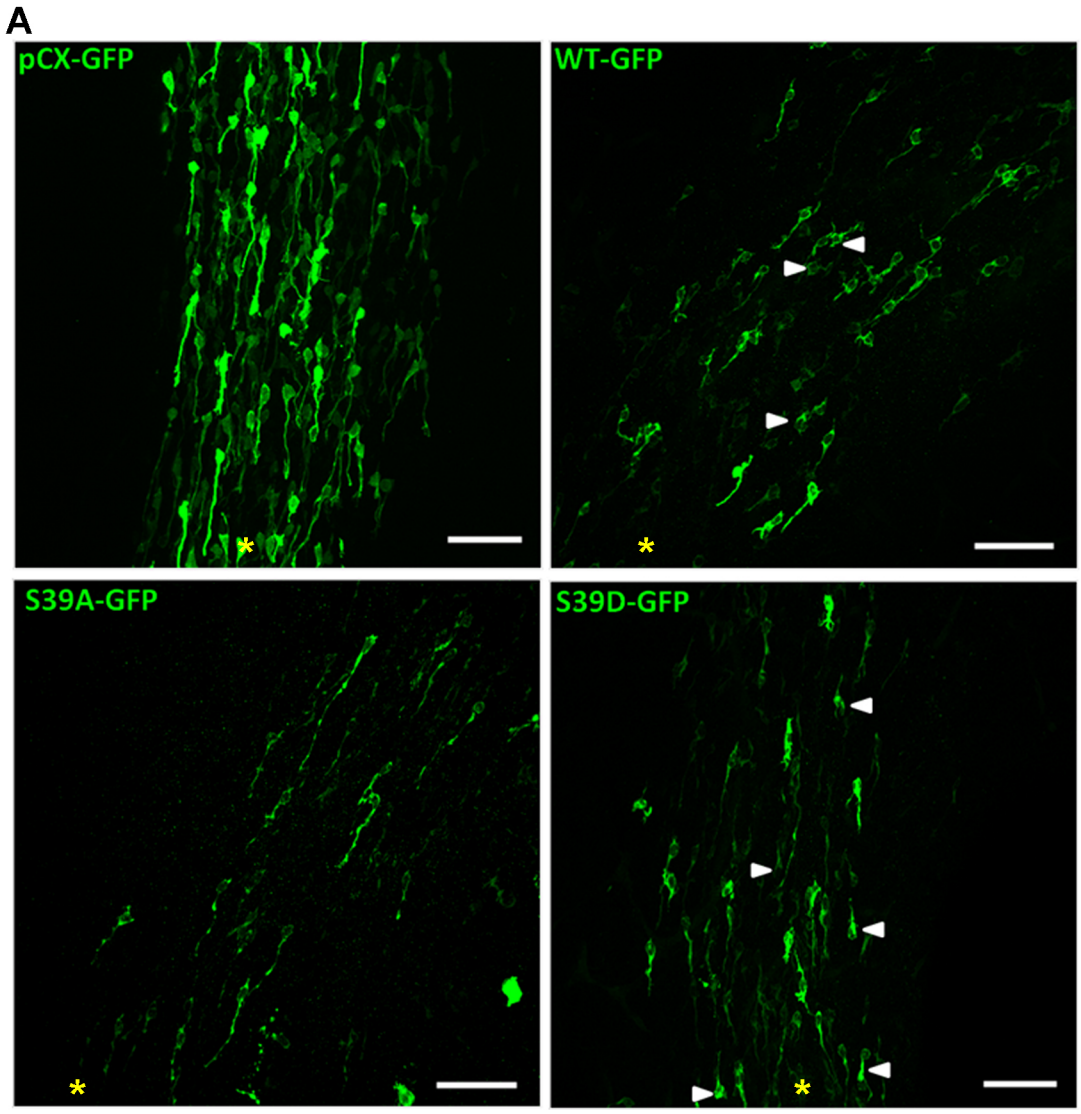

A
pCX-GFP
WT-GFP
S39A-GFP
S39D-GFP
B
Leading process length (μm)
50
40
30
20
10
0
*
*
***
GFP
WT
S39A
S39D
C
Misoriented cells (%)
20
18
16
14
12
10
8
6
4
2
0
***
***
GFP
WT
S39A
S39D

Figure 3-23. Fascin phosphorylation site Ser39 regulates neuroblast morphology and orientation *in vivo*.

(A), Confocal z-stack projections of P2-3 mice brain slices electroporated with pCX-GFP, pGFPC2-WT fascin, -S39A fascin, or -S39D fascin show control cells with a single leading process oriented towards the OB (top, left), as cells expressing S39A (bottom, left). In contrast, expression of either wt (top right) or S39D fascin (bottom right) increases the percentage of misoriented cells (arrowheads). (B) Quantitative morphological analysis showing a decrease in leading process length for wt and S39D fascin, and an increase for S39A compared to GFP expressing cells (B). Expression of either wt or S39D fascin significantly increases the percentage of misoriented cells (towards the SVZ, instead of OB) (C) (mean ± SEM; *$p<0.05$; ***$p<0.001$; n=8 brains for pCX-GFP; n=4 for pGFPC2-WT, -S39A, and -S39D). Scale bars: A, 50 μm.

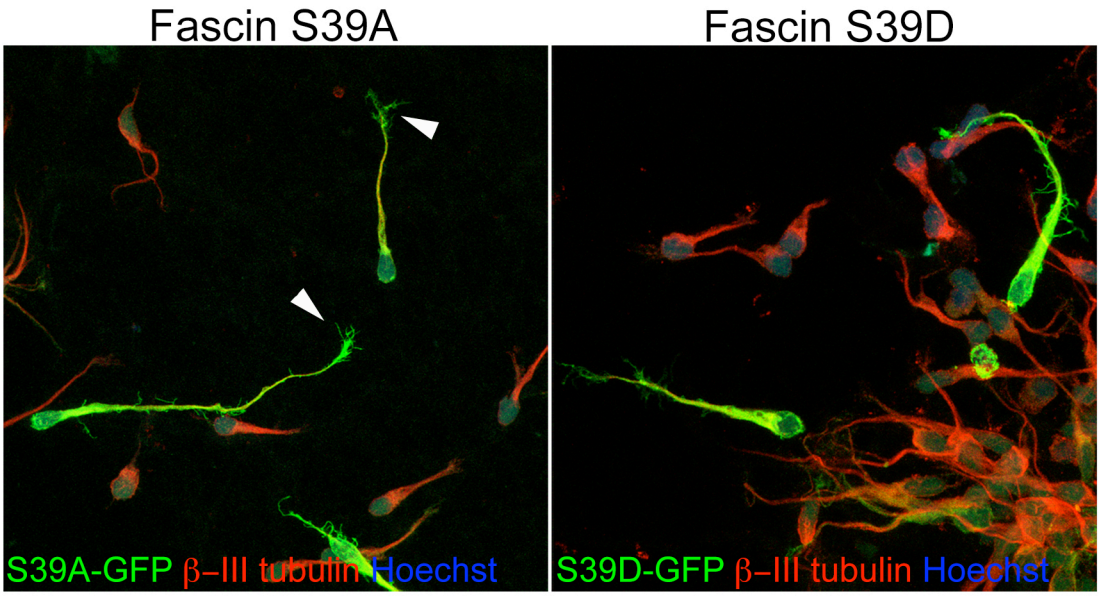


Figure 3-24. Phosphorylation of fascin at Ser39 reduces the number of filopodia in RMS migrating neuroblasts *in vitro*. Representative pictures of rat reaggregated neuroblasts nucleofected with fascin S39A-GFP (green, left), or fascin S39D-GFP (green, right) and immunostained for β-III tubulin (red). Cell nuclei were visualized by Hoechst staining (blue). Arrowheads (left panel) point to the filopodia in neuroblasts transfected with S39A.

3.2.16 Fascin and PKC interact in RMS migrating neuroblasts

Having identified fascin phosphorylation site Ser39 as a site that must be regulated for efficient neuroblast migration we next wanted to focus on the signalling mechanisms responsible for this phosphorylation.

Previous studies in other cellular systems showed that fascin can be phosphorylated on Ser39 by protein kinase C (PKC) (Ono et al., 1997, Parsons and Adams, 2008). Moreover, PKC-phosphorylated fascin interacts with PKC and this promotes migration in different cell types, like myoblasts and colon carcinoma cells (Adams and Schwartz, 2000, Hashimoto et al., 2007).

Two isoforms of PKC are known to phosphorylate fascin on Ser39: PKCα and PKCγ (Ono et al., 1997, Parsons and Adams, 2008). Both PKCα and PKCγ can be detected in SVZ and OB homogenates, and in RMS neuroblast lysates by Western blotting (Figure 3-25, (A)). The same blots were probed for PKCα first and then for PKCγ. As shown by a representative blot in Figure 3-25 (A), PKCγ appeared to be more abundant than PKCα in all the tested samples. To detect whether fascin and PKC interact in migrating neuroblasts, we used fluorescent lifetime imaging microscopy (FLIM) coupled with fluorescent resonance energy transfer (FRET) (FRET/FLIM approach) (see chapter 2). Although there are other well-established techniques that can be used to study protein-protein interaction such as Western-based pull down assay or co-localisation using fluorescently coupled antibodies, FLIM combines and implements the two, offering high sensitivity (detecting protein interaction within 10 nm) and temporal/spatial information within the intact cell (Parsons et al., 2004, Worth and Parsons, 2010). In addition, FLIM had been successfully used in previous studies to monitor fascin-PKC interaction in non-neuronal cells (Anilkumar et al., 2003, Parsons and Adams, 2008). Neuroblasts were co-nucleofected with GFP-tagged fascin and PKCα or PKCγ tagged with mRFP (PKCα/PKCγ-mRFP). The GFP and RFP fluorophores were chosen as donor and acceptor, respectively, since the emission spectrum of GFP overlaps with the absorbance spectrum of RFP. FLIM allows the measurement of the lifetime of GFP that decreases upon FRET with RFP (FRET is possible only when these two fluorophores are 10 nm apart).

Nucleofected neuroblasts were left in suspension for 24 hours before embedding in

Matrigel. Cells were left to migrate for 9 hours, fixed, mounted on a slide and visualised using FLIM. The interaction between the two molecules is reported as FRET efficiency. Both isoforms of PKC interacted with fascin in migrating neuroblasts (Figure 3-25, (B) red dots), although fascin and PKCγ interaction showed a higher FRET efficiency compared to fascin-PKCα (Figure 3-25, (C); fascin/PKCγ, 9.5000 ± 1.1851%; fascin/PKCα, 6.0667 ± 0.6391%; n=12 cells for each condition). For this reason the following studies focused on the interaction between fascin and PKCγ.

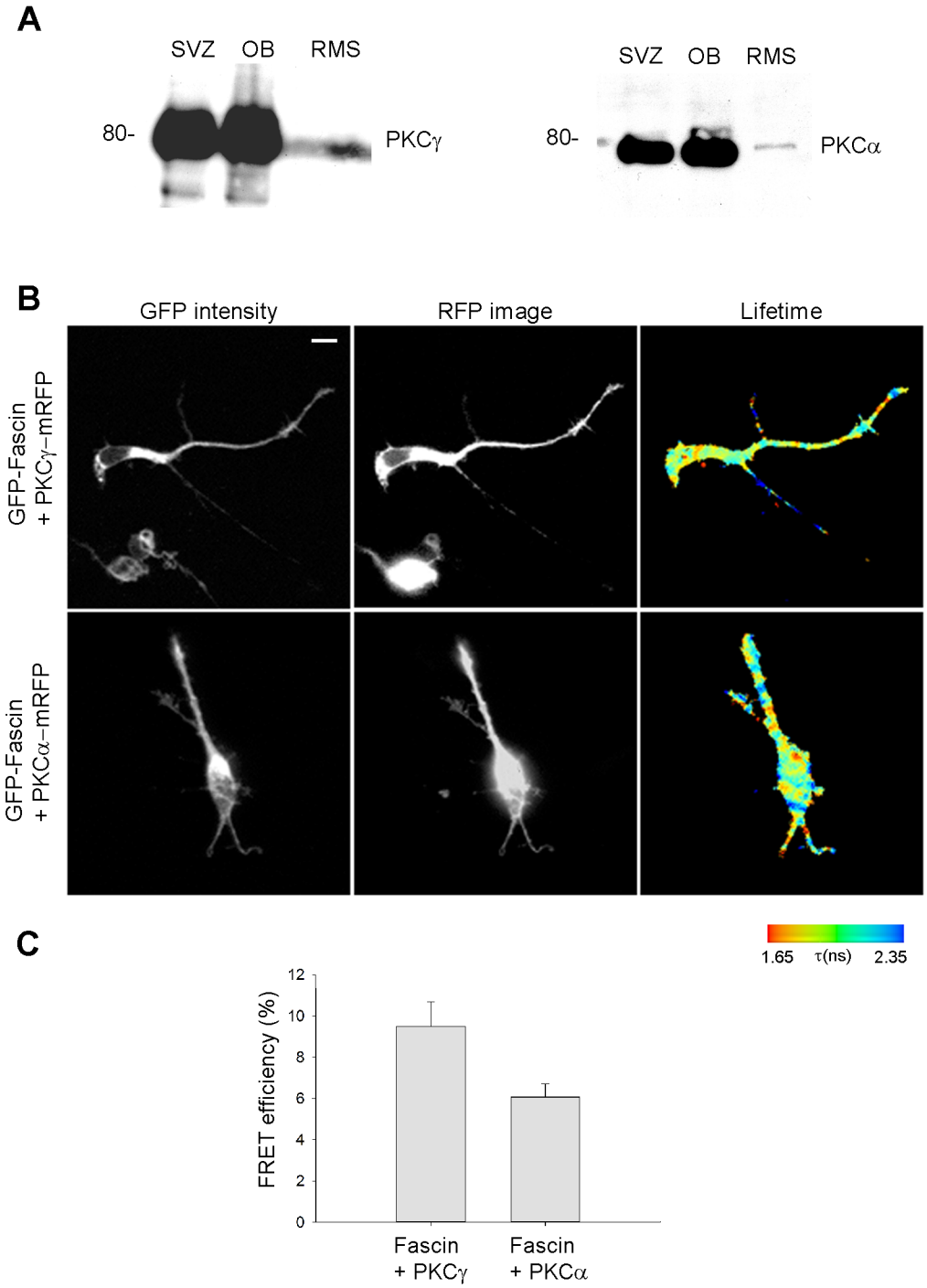

A
SVZ
OB
RMS
80-
PKCγ
SVZ
OB
RMS
80-
PKCα
B
GFP intensity
RFP image
Lifetime
GFP-Fascin
+ PKCγ–mRFP
GFP-Fascin
+ PKCα–mRFP
C
1.65
τ(ns)
2.35
FRET efficiency (%)
12
10
8
6
4
2
0
Fascin
+ PKCγ
Fascin
+ PKCα

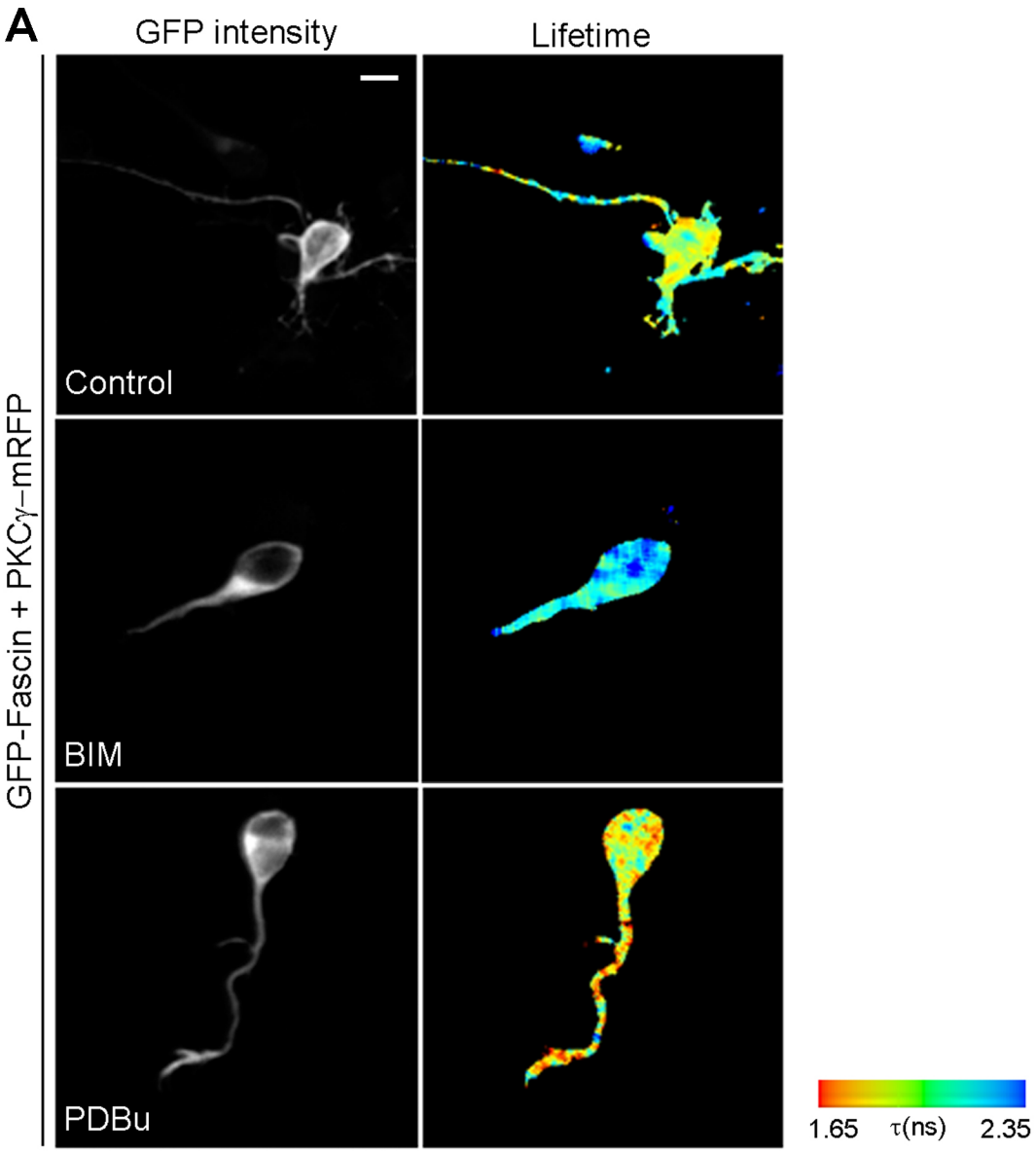
Figure 3-25. The interaction between fascin and PKCγ or PKCα can be detected by FLIM analysis in migrating neuroblasts.

(A), PKCγ and PKCα are detected in the same Western blot of lysates from P7 rat SVZ, OB, and cultured RMS neuroblasts. (B) Images in the GFP channel (donor) and RFP channel (acceptor) of rat neuroblasts expressing GFP-fascin and mRFP-tagged PKCγ (top row) or PKCα (bottom row). Lifetime images are depicted using a pseudocolor scale where red is a low GFP lifetime (high FRET) and blue is a high GFP lifetime (no FRET). (C) Quantifications of FRET efficiency show higher FRET efficiency levels for PKCγ compared to PKCα (FRET analysis carried out by Dr. Maddy Parsons). Scale bar: 5 μm.

3.2.17 Fascin/PKC interaction depends on PKC activity

Having established that fascin and PKC interact in migrating neuroblasts, we wanted to confirm that this interaction was dependent on PKC activity. In order to do so, migrating neuroblasts nucleofected with GFP-fascin and PKCγ-mRFP were treated with a PKC activator, 10 nM phorbol dibutyrate (PDBu) or a PKC inhibitor 1 µM bisindolylmaleimide I (BIM) (Kazanietz et al., 1993, Wilkinson et al., 1993, Parsons and Adams, 2008) (Figure 3-26, (A)).

Incubation with PDBu significantly increased FRET efficiency between GFP-fascin and PKCγ-mRFP, while treatment with BIM drastically decreased it (Figure 3-26, (B)). These results indicate that fascin/PKC interaction directly depends on PKC activity, suggesting that PKC-dependent phosphorylation of fascin on Ser39 is involved in this interaction.


A
GFP intensity
Lifetime
GFP-Fascin + PKCγ–mRFP
Control
BIM
PDBu
1.65
τ(ns)
2.35

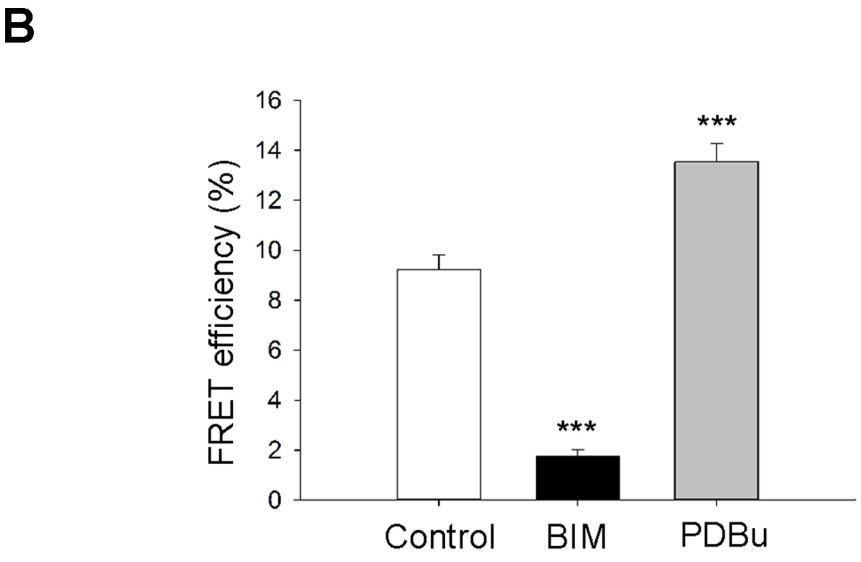

B
FRET efficiency (%)
16
14
12
10
8
6
4
2
0
***
***
Control
BIM
PDBu

Figure 3-26. The interaction between fascin and PKCγ detected by FLIM in migrating neuroblasts depends on PKC activity.

(A), Images in the GFP channel (donor, left) and pseudocolored lifetime images (right) showing rat neuroblasts expressing GFP-fascin and PKCγ-mRFP after treatment with the vehicle control (top row), the PKC activator PDBu (middle row), or the PKC inhibitor BIM (bottom row). (B), Activating PKC with PDBu enhances the fascin/PKCγ interaction as shown by the significant increase in FRET efficiency levels for the fascin/PKCγ pair, while inhibiting PKC with BIM severely reduces FRET efficiency (mean ± SEM; n=27 cells for control; n=19 cells for PDBu; and n=22 cells for BIM from 3 independent experiments; ***$p<0.001$). FRET analysis carried out by Dr. Maddy Parsons. Scale bar: 5 µm.

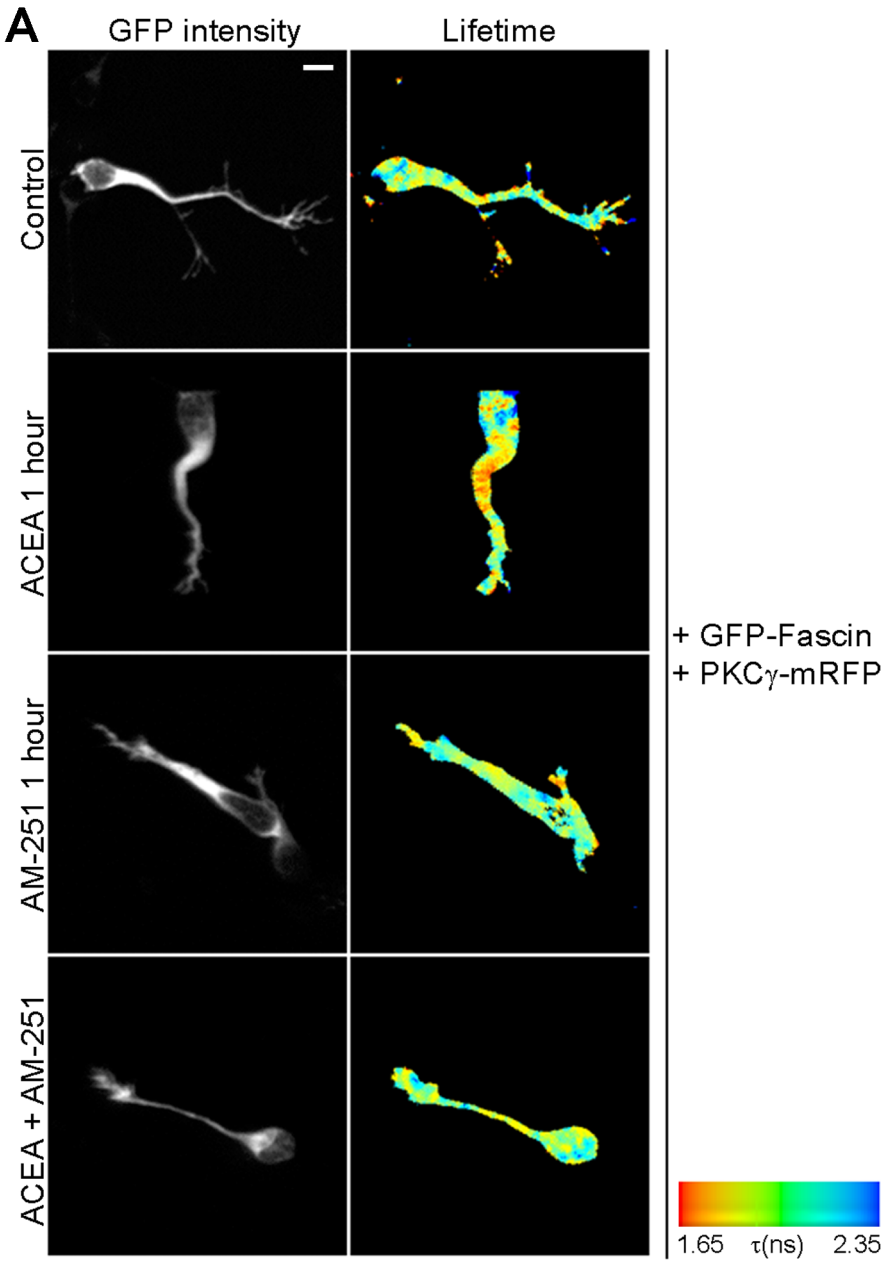
3.2.18 Cannabinoid signalling regulates fascin/PKC interaction in RMS migrating neuroblasts

The previous *in vitro* and *in vivo* data we obtained using the fascin phosphomutants strongly suggest that phosphorylation of fascin on Ser39 needs to be tightly regulated to promote efficient neuroblast migration. Our FLIM results show that PKC interacts with fascin in migrating neuroblasts and that this interaction depends on PKC activity. When this interaction occurs fascin is displaced from actin filaments (Anilkumar et al., 2003). We therefore asked whether the fascin/PKC interaction is necessary for neuroblast motility and whether it can be modulated downstream of signals promoting neuroblast migration. We have recently demonstrated that endocannabinoid signaling contributes to the regulation of neuroblast migration *in vitro* and *in vivo* (Oudin et al., 2011). Thus, we asked whether cannabinoid receptor signaling can regulate the fascin/PKC interaction using the FLIM approach described earlier. After co-nucleofecting neuroblasts with GFP-fascin and PKC-mRFP, cells were embedded in Matrigel and left to migrate for 9 hours. Treatment was performed at this time point with either the CB1 receptor selective agonist arachidonyl-2'-chloroethylamide (ACEA) (Pertwee, 2006), 2006), which significantly enhances neuroblast migration (Oudin et al., 2011) or with the CB1 receptor antagonist AM-251 (Pertwee, 2006), which inhibits neuroblast migration (Oudin et al., 2011) (Figure 3-27, (A)).

ACEA treatment enhanced FRET efficiency for GFP-fascin/PKCγ-mRFP compared to vehicle-treated cells, indicating that fascin/PKC interaction is promoted by CB1 activation (Figure 3-27, (B)). In contrast, treatment with AM-251 significantly decreased fascin/PKC FRET efficiency levels, suggesting that an endogenous cannabinoid tone promotes fascin/PKC interaction in migrating neuroblasts (Figure 3-27, (B)). Finally, the fascin/PKC interaction promoted by ACEA was abolished by incubation with AM-251, confirming its specific dependence on CB1 activation (Figure 3-27, (B)).

Taken together, these data show that the interaction between fascin and PKC can be modulated by endogenous stimuli controlling neuroblast migration. In particular,

these experiments show that endocannabinoid signaling regulates the interaction between fascin and PKC, ultimately promoting efficient neuroblast migration.


A
GFP intensity
Lifetime
Control
ACEA 1 hour
AM-251 1 hour
ACEA + AM-251
+ GFP-Fascin
+ PKCγ-mRFP
1.65 τ(ns) 2.35

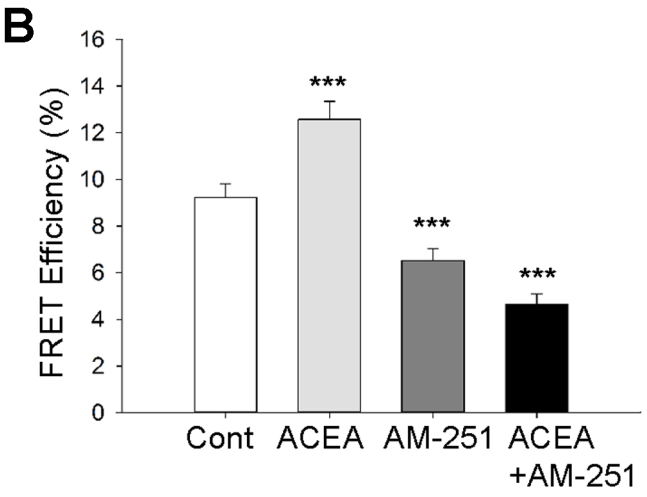

B
FRET Efficiency (%)
16
14
12
10
8
6
4
2
0
***
***
***
Cont
ACEA
AM-251
ACEA
+AM-251

Figure 3-27. Cannabinoid signalling regulates the interaction between PKC and fascin.

(A), Intensity multiphoton GFP images (donor) and pseudocolored lifetime images showing rat neuroblasts expressing GFP-fascin and PKCγ-mRFP treated with control (Cont) vehicle (first row), the CB1 agonist ACEA (second row), or the CB1 antagonist AM-251 (third row) or preincubated for 1 h with AM-251 before adding ACEA for 1 h to the medium (fourth row). (B), Quantitative analysis of FRET efficiency shows that CB1 receptor activation by ACEA stimulates PKC/fascin interaction, while preincubation with the CB1 receptor antagonist AM-251 prevents this effect. AM-251 on its own also significantly inhibits the PKC/fascin interaction, consistent with the presence of an endogenous cannabinoid tone in the neuroblast culture (mean ± SEM; n=27 cells for control; n=17 cells for ACEA; n=19 cells for AM-251; n=16 cells for ACEA + AM-251, from three independent experiments; ***$p<0.001$). Scale bar, 5 µm.

3.2.19 Fascin may act as a downstream mediator of CB-promoted neuroblast migration.

Our data strongly suggest that endocannabinoid signalling regulates fascin/PKC interaction. We therefore asked whether fascin is itself necessary for CB-promoted neuroblast migration. RMS neuroblasts were nucleofected with fascin siRNA, re-aggregated into clusters and embedded in a Matrigel matrix containing ACEA 52 hours after nucleofection. Cells were left to migrate for 24 hours in the presence of 0.5 μM ACEA and then stained for βIII tubulin (Figure 3-28, (A)). As shown previously (Oudin et al., 2011), incubation with ACEA enhanced neuroblast migration in control siRNA nucleofected cells compared to vehicle-treated control siRNA nucleofected cells (Figure 3-28, (B)). This increase in migration was not observed in fascin-depleted cells (Figure 3-28, (B)). These results suggest that fascin could be a downstream mediator of cannabinoid-stimulated migration in SVZ-derived neuroblasts. It will be important to complete these experiments by including a non-transfected, wild type control with/without ACEA to assess any off-target effects of siRNA transfection.

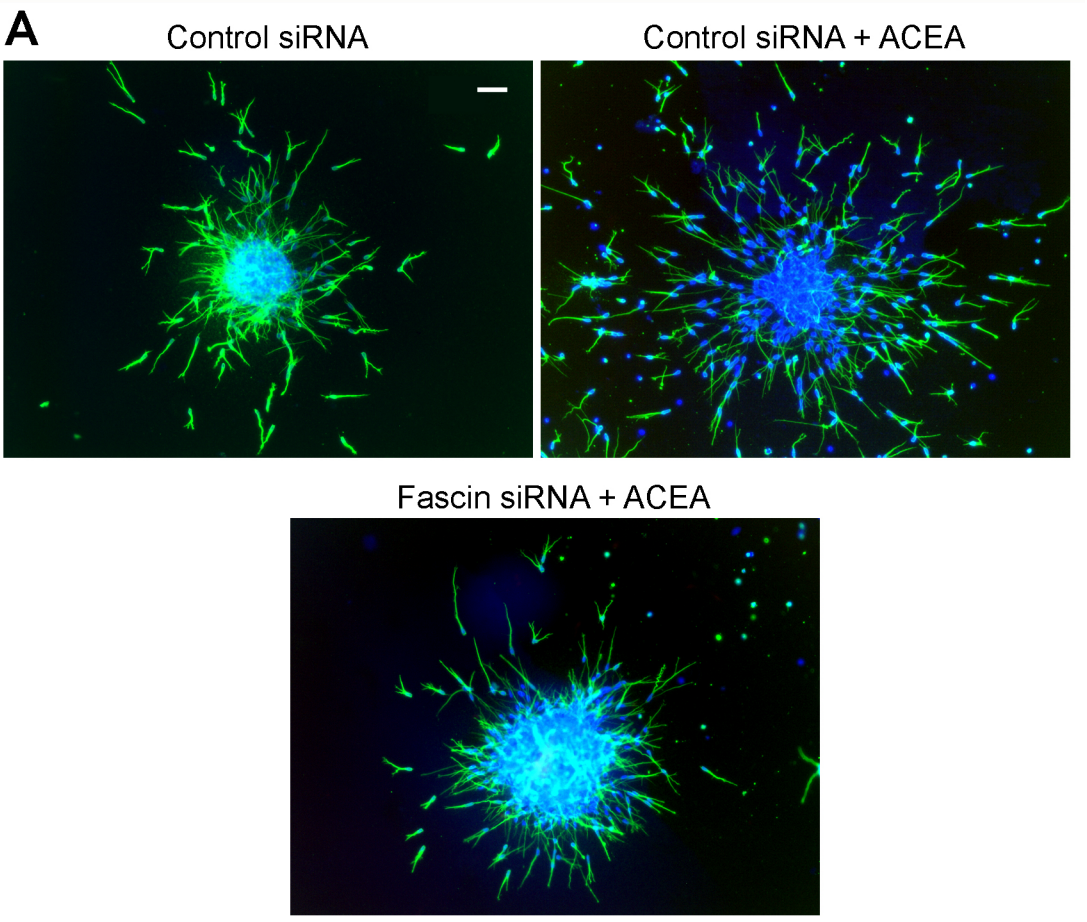

A
Control siRNA
Control siRNA + ACEA
Fascin siRNA + ACEA
B
Migrated Distance (μm)
300
250
200
150
100
50
0
***
***
Control siRNA
Control siRNA +ACEA
Fascin siRNA +ACEA

Figure 3-28. Fascin is a downstream mediator of CB-promoted migration *in vitro*.
(A) Representative pictures of RMS neuroblasts nucleofected with either control or fascin siRNA oligos, reaggregated, allowed to migrate for 24 hours in the presence of the CB1 agonist ACEA or vehicle medium and stained for β-III tubulin (green) and Hoechst (blue). (B), Quantification showing an increase of migrated distance in control siRNA-nucleofected neuroblasts incubated with the CB1 agonist ACEA compared to control vehicle-treated cells. ACEA-promoted migration was inhibited in fascin siRNA-nucleofected cells (mean ± SEM; **p<0.001; n=3 independent experiments. Between 15 and 20 explants were considered for quantifications in each experiment). Scale bar, 50 µm.

3.3 Discussion

In this chapter we uncover a novel role for the actin-bundling protein fascin in postnatal neurogenesis. We show that fascin is upregulated in RMS migrating neuroblasts and is required for their polarised morphology and migration *in vitro* and *in vivo*. Moreover, a tightly regulated cycle between the phospho- and dephospho-form of fascin at Ser39 is needed to ensure an efficient RMS neuroblast migration. Finally, our results strongly suggest that the interaction of fascin with PKC observed during neuroblast migration can be regulated downstream of endocannabinoid signalling.

3.3.1 Fascin: a novel marker for RMS migrating neuroblasts

Fascin-1 is highly expressed in the central nervous system of adult mice (Edwards and Bryan, 1995) and in the developing nervous system during embryogenesis (De Arcangelis et al., 2004). Fascin has a role in growth cone morphogenesis, controlling filopodia formation and dynamics (Cohan et al., 2001, Yamakita et al., 2009, Nagel et al., 2012).

Here we have discovered that fascin is highly expressed in the SVZ, along the RMS and in the OB in both postnatal and adult mammalian brain. Importantly, in the SVZ fascin staining overlaps with the migrating neuroblast marker, Dcx, but not with GFAP+ stem cells/astrocytes or the transit amplifying marker Mash-1, leading to the conclusion that fascin can be considered a new marker for migrating neuroblasts along the RMS.

As expression suggests function, the hypothesis that fascin could have a role in regulating neuroblast migration is proven by the 2-week BrdU experiments in *fascin-1* ko animals as well as by the RNAi approach *in vitro* in neuroblast primary cultures and *ex vivo* in brain slices. Based on our results from the 2-week BrdU experiments, only few BrdU+ cells are observed in the OB of *fascin-1* ko mice, with a parallel doubled amount of neuroblasts found along the stream compared to control animals, indicating a much slower and ineffective migration. Moreover, the fact that fascin is not expressed by the highly proliferative population in the SVZ (almost no co-localisation with Mash-1) together with the negative results from 2-

hour pulse BrdU injections suggest that fascin does not have a role in cell proliferation. Interestingly, *fascin-1* ko mice display a cell accumulation in the caudal RMS (Figure 3-4), suggesting that genetic deletion of fascin impairs neuroblast exit from the SVZ.

Our discovery that fascin is required for neuroblast migration is in line with several reports showing a role for fascin in cell motility in other contexts, such as metastatic and invasive type of cancers (Hashimoto et al., 2011). In the past decade several genes have been linked to the regulation of neuroblast migration (Comte et al., 2011, Zhou et al., 2011, Feliciano et al., 2012). Particularly interesting is the role of fascin in relation to some of these other genes. For instance, fascin is upregulated in the Tuberous Sclerosis Complex component (TSC1) knockout mice, where its knockdown prevents hematopoietic stem cell mobilization (Gan et al., 2008). Interestingly, genetic deletion of TSC1 impairs SVZ-derived stem cell migration creating an abnormal accumulation in the lateral ventricle (Zhou et al., 2011, Feliciano et al., 2012); a similar phenotype was detected in *fascin-1* ko mice, suggesting the possibility of a link between TSC1 and fascin in regulating neuroblast migration. Interestingly, TSC1-null cells were re-routed and found in cortical and subcortical regions indicating an increased migratory heterotopia (Feliciano et al., 2012). Although we have not detected much ectopic migration in *fascin-1* ko animals, it would be interesting to see whether TSC1 ko cells, which have lost directionality, have increased fascin levels.

Upregulation of fascin was also observed in connection with overexpression of galectin-3, leading to an increase in gastric cancer cell motility (Kim et al., 2010). Interestingly, galectin-3 has been reported to play a role also in neuroblast migration. Similarly to *fascin-1* ko mice, BrdU pulse-chase experiments in *Gal-3* ko animals show fewer BrdU+ cells in the OB compared to wt mice, indicating a defect in migration but not in cell proliferation (Comte et al., 2011). It is tempting to speculate a link between galectin-3 and fascin in neuroblast migration. Whether galectin-3 is required for fascin-promoted migration modulating neuroblast adhesiveness through the astrocytic tunnel remains to be investigated. Future experiments would need to investigate galectin-3 expression in *fascin-1* ko animals and *fascin-1* expression in *Gal-3* ko.

Our *in vitro* and *in vivo* results have also uncovered a function for fascin in regulating the polarised morphology of neuroblasts. While control cells generally exhibit a single straight leading process oriented towards the direction of the migration, fascin-depleted cells show a doubled percentage of cells with multiple branches. Fascin has been previously involved in neuronal morphogenesis in *Drosophila*, where its deficiency leads to abnormal neurite shape and trajectory (Kraft et al., 2006). Since fascin is highly localised in filopodia present at the leading edge of migrating neuroblasts, its absence may lead to instability of the growth cone-like structure observed at the tip of these cells, thus resulting in the inability of neuroblasts to form a stable straight leading process. We therefore speculate that the branched neuroblast morphology in fascin-depleted cells may be due to lack of adhesion with the substrate. Indeed, efficient neuroblast migration relies on proper adhesion contacts between filopodia and the surrounding matrix (Schaar and McConnell, 2005).

Adhesions between cells or between cells and the ECM enable traction forces (Hashimoto et al., 2007) that may be important to create a stable polarised leading process, which is in turn required for the subsequent nucleokinesis step (Schaar and McConnell, 2005, Marin et al., 2010). In migrating neuroblasts this adhesion may be integrin-based, since several integrin subunits such as β1 are in fact expressed throughout the RMS (Belvindrah et al., 2007). β1-integrin is expressed on the surface of the leading process of migrating neuroblast (Belvindrah et al., 2007, Shieh et al., 2011) and on the growth cone of fibroblasts (Galbraith et al., 2007). Although β1-integrin is dispensable for neuroblast migration, its presence is necessary to form compact neuroblast chains in the RMS (Belvindrah et al., 2007). Interestingly, genetic deletion of β1-integrin results in similar effects caused by *fascin-1* deletion, namely random neuroblast movement, and loss of polarised morphology (Belvindrah et al., 2007). The speculation that fascin may have a role in adhesiveness through β1-integrin arises from a previous report in colon epithelial cells where fascin overexpression leads to reorganization of cell-matrix contacts by altering the localisation of β1-integrin (Jawhari et al., 2003). It would be interesting to investigate whether the potential link between fascin and β1-integrin activation

at peripheral filopodia ensures neuroblast adhesiveness and therefore creates the traction necessary for forward cell movement.

3.3.2 The role of Ser39 phosphorylation in regulating neuroblast migration

Our experiments show that altering the phosphorylation state of Ser39 on fascin impairs neuroblast migration *in vitro*, significantly decreasing migration distance and speed, and increasing the time that these cells spend immobile. Moreover, *ex vivo* experiments, using time-lapse imaging of electroporated brain slices, show that cells expressing either the phosphomimetic variant or the non-phosphorylatable variant show not only a shorter migrated distance and lower speed, but also a shorter displacement and an overall defect in directionality. On the other hand, overexpression of fascin increases migration distance and velocity compared to control. Although this increase should have also been reflected on the cell displacement, quantifications show a similar displacement for the wt and the control indicating a more random type of migration when fascin levels are altered. While it has been reported that overexpression of wt fascin increases cell motility and metastatic capacity (Hashimoto et al., 2007), the role of fascin phosphorylation on Ser39 in cell migration is controversial. Expression of fascin S39D decreases migration in colon cancer cells (Hashimoto et al., 2007), while fascin phosphorylation on this site is not required for blood cell motility (Zanet et al., 2009). In another report, instead, Ser39 phospho/unphosphorylation appears to have a dual effect; indeed, NGF-induced melanoma cell migration is impaired by expression of S39D fascin, but increased by S39A fascin (Shonukan et al., 2003). Our findings demonstrate for the first time a role for Ser39 phosphorylation of fascin in cell migration *in vivo*. In particular, a cycle between phosphorylation and dephosphorylation on Ser39 of fascin is required for efficient neuroblast migration. A possible explanation for this can be found in the dynamic nature of neuroblast migration (Schaar and McConnell, 2005), in which fascin-dependent actin remodelling and filopodia stability (Vignjevic et al., 2006, Hashimoto et al., 2007) are required for protrusion/retraction of the leading process that needs to probe

the environment before moving towards a specific direction (Schaar and McConnell, 2005). This role may be very important, especially considering the fact that neuroblasts migrate by sliding along each other in chains surrounded by a scaffold of astrocytic processes and blood vessels offering physical support and molecular cue guidance (Peretto et al., 2005, Bovetti et al., 2007, Snapyan et al., 2009, Whitman et al., 2009, Bozoyan et al., 2012). To move through this complex environment, neuroblasts need to dynamically reorganise their cytoskeleton and adhesiveness and fascin may be an important player in this process. At this regard it is interesting to mention the interaction between fascin and $p75^{NTR}$, a membrane glycoprotein (Shonukan et al., 2003, Deinhardt et al., 2011). The $p75^{NTR}$ is expressed by neuroblasts in postnatal and adult mice (Gascon et al., 2007, Snapyan et al., 2009) and appears to be involved in their migration via its ligand BDNF, which is secreted by the blood vessels (Snapyan et al., 2009). Interestingly, $p75^{NTR}$ interacts with the C-terminus of fascin in melanoma cells (Shonukan et al., 2003) and in brain during embryonic development (Deinhardt et al., 2011). Moreover, $p75^{NTR}$/fascin interaction is driven by NGF which leads to fascin dephosphorylation at Ser39, promoting its binding to actin and cell migration in melanoma (Shonukan et al., 2003). Interestingly, the precursor of NGF, proNGF induces growth cone collapse, and this requires $p75^{NTR}$ and fascin phosphorylation (Deinhardt et al., 2011). It would be interesting to investigate whether neuroblast adhesiveness to the substrate requires neurotrophin-induced fascin dephosphorylation.

Differently from what was shown by our previous experiments in isolated neuroblasts, in fixed electroporated brain slices S39A and S39D appear to have opposite effects. Cells expressing S39D have a shorter leading process and are misoriented (this is also observed when fascin is overexpressed), while S39A expressing cells show a longer leading process oriented towards the OB. Previous reports have described opposite effects for the fascin phosphomutants; for example, in cancer cell lines the phosphomimetic fascin variant S39D reduces the number of filopodia, whereas the non-phosphorylatable variant S39A has an enhanced actin-bundling capacity, and increases filopodia frequency (Ono et al., 1997, Vignjevic et al., 2006, Hashimoto et al., 2007). We have also noticed that in primary cultures neuroblasts nucleofected with the S39A mutant seem to show

more filopodia compared to neuroblasts nucleofected with the S39D mutant (Figure 3-24). These two fascin phosphomutants similarly impair neuroblast migration in acute brain slice cultures whereas they have opposite effects in controlling neuroblast morphology in fixed brain slices. Differences can be detected in fixed brain slices versus cultured brain slices (Gajendra S, PhD thesis 2012). In particular, we have found that in fixed brain slices S39D, but not S39A, causes misorientation of neuroblasts, whereas in cultured brain slices both mutants S39D and S39A show an increased branching and loss of directionality compared to control. Although cultured brain slices show the advantage of having neuroblasts migrating within the cellular and matrix structures of the RMS *ex vivo* (Snapyan et al., 2009, Khlghatyan and Saghatelyan, 2012), loss of the intact brain architecture as well as dilution of guidance cues may explain the differences observed with the fixed brain slices. Although these effects may appear contradictory, they lead again to the conclusion that altering the phosphorylation state of fascin on Ser39 may affect filopodia remodeling required for an efficient and directed migration.

3.3.3 Signals regulating fascin in neuroblast migration

Due to the importance of Ser39 in regulating neuroblast migration, we have used FLIM to investigate whether fascin co-localises with PKC, a previously reported regulator of fascin phosphorylation on Ser39 (Hashimoto et al., 2007, Parsons and Adams, 2008). Using this approach, PKCγ/fascin interaction appears to be particularly concentrated along the leading process and is specifically regulated by PKC activity. In order to understand whether the PKCγ/fascin interaction needs to be regulated during neuroblast migration, we explored signalling pathways working upstream fascin and fascin/PKC interaction. Several extracellular matrix components such as thrombospondin-1 (TSP-1), fibronectin, laminin and tenascin-C as well as cell adhesion molecules like syndecan-1 and integrins can regulate the fascin/PKC interaction (Adams et al., 1999, Jayo and Parsons, 2010, Hashimoto et al., 2011). While TSP-1/syndecan, tenascin-C and laminin promote the actin-bundling function of fascin and spike formation in epithelial cells and skeletal myoblasts, integrin-mediated adhesion to fibronectin inhibit fascin bundling by promoting fascin/PKC interaction (Adams et al., 1999, Kureishy et al., 2002, Adams,

2004, Hashimoto et al., 2011). Interestingly, many of these factors are highly expressed in the RMS and have a function in regulating neuroblast migration. For instance, syndecan-1 is highly expressed by migrating neuroblasts along the RMS (Kazanis et al., 2010) and in the SVZ, and its genetic depletion disrupts RMS morphology and reduces the number of neuroblasts reaching the OB (Blake et al., 2008). Moreover, several integrin subunits and laminins are expressed along the RMS. In particular, β1-integrins and their laminin ligands play a role in forming neuroblast chains in the RMS (Belvindrah et al., 2007).

Neuroblast migration can also be regulated by growth factors such as IGF-1 (Hurtado-Chong et al., 2009), VEGF (Bozoyan et al., 2012), BDNF (Chiaramello et al., 2007), HGF (Garzotto et al., 2008), GDNF (Paratcha et al., 2006), EGF (Kim et al., 2009), and FGF (Garcia-Gonzalez et al., 2010). Absence of IGF-1 leads to a decrease in neuroblast exit out of the SVZ and to an impairment in the radial migration in the OB (Hurtado-Chong et al., 2009). Interestingly, a link between IGF-1 and fascin has been reported in breast cancer cells, where fascin upregulation occurs upon activation of IGF-1 receptor, increasing the number of protrusions containing fascin and thus cell motility (Guvakova et al., 2002).

FGF-2 also has been reported as an important “motogenic” factor used by SVZ-neuronal precursors in their migration towards the OB (Garcia-Gonzalez et al., 2010). The FGF-2 activation response couples with CB1 receptor in developmental axon growth (Williams et al., 2003). Importantly, eCB signalling plays a fundamental role in CNS development (Williams et al., 2003, Harkany et al., 2008) and recently we have shown that it also controls RMS neuroblast migration and morphology *in vitro* and *in vivo* (Oudin et al., 2011).

Treatment with CB1 agonist promotes fascin/PKC interaction monitored by FLIM and this effect was abolished by pre-incubation with CB1 antagonist, indicating a specific dependence on CB1 receptor activation. On the other hand, CB1 antagonist decreases fascin/PKC interaction, proving the existence of an endocannabinoid tone able to modulate interaction between fascin and PKC. While FLIM allowed the spatial identification of fascin/PKC interaction in intact migrating neuroblasts, it needed to relie on overexpressed donor/acceptor proteins. We therefore also investigated whether phosphorylation of either endogenous PKC or fascin could be

detected in primary neuroblasts. Cells were either plated on polyornithine and laminin-coated glass coverslips, (where neuroblasts cannot migrate), or embedded into the 3-D Matrigel matrix (where neuroblasts migrate). This was done to avoid potential discrepancies that may arise from activation of different signalling cascades in migratory versus non-migratory contexts.

Unfortunately, the fascin phospho-Ser39 antibody tested in this study appeared to be non-specific and therefore we were unable to monitor changes in endogenous fascin phosphorylation. On the other hand, we could use an anti-phospho Thr655 antibody previously shown to be a reporter of PKCγ activation (Parsons and Adams, 2008). Although we detected endogenous PKCγ phosphorylation on this site in control conditions by Western blot, no changes in phosphorylation were detected following treatment with PKC activators, inhibitors or CB agonists/antagonists. We may have failed to detect changes in endogenous PKCγ phosphorylation due to the very transient nature of this process, as phosphorylation is a reversible post-translational modification regulated by kinase-phosphatase activity. Another potential explanation is that these treatments did not affect PKCγ phosphorylation at Thr655 but instead impacted the sub-cellular localisation of this kinase relative to fascin.

It remains unclear how eCB signalling acts on fascin and fascin/PKC interaction leading to efficient migration. Further investigations should aim on identifying intermediate signalling molecules involved in this process, for instance rises of intracellular calcium (Williams et al., 2003) or activation of small GTPases (Parsons and Adams, 2008).

In conclusion, we have shown that fascin is upregulated in SVZ-derived migrating neuroblasts and is required for polarised neuroblast morphology and efficient neuroblast migration towards the OB. We have highlighted the importance of fascin phosphorylation on Ser39; in particular its dynamic regulation which is required for efficient neuroblast migration. Finally, our results have led us to propose the existence of an eCB tone regulating the interaction between active PKC and Ser39-phosphorylated fascin to control actin remodelling/PKC localization during polarized neuroblast migration along the RMS.

Chapter 4 Drebrin regulates RMS neuroblast migration

4.1 Introduction

Drebrin is one of the major actin-binding proteins in the brain where it has been reported to play several regulatory functions (Shirao, 1995). In developing neurons drebrin localizes throughout the neuron but preferentially in the growth cone and it is involved in neuritogenesis (Geraldo et al., 2008). Interestingly, its role in neurite outgrowth is regulated by Cdk5-phosphorylation at Ser142. Phosphorylation at this site leads to drebrin actin-bundling function and drebrin binding to microtubules enhancing neuritogenesis (Worth et al., 2013).

During neurite outgrowth drebrin can regulate interactions between F-actin and several binding partners (Ishikawa et al., 1994, Shirao, 1995, Ishikawa et al., 2007, Sekino et al., 2007). Of particular interest is the evidence of a link between drebrin and fascin. Indeed, drebrin can inhibit the actin binding as well as the actin bundling function of fascin (Sasaki et al., 1996). Moreover, while fascin is expressed in peripheral filopodia of growth cones, drebrin localizes at the basal side of the growth cones (Sasaki et al., 1996). Interestingly drebrin and fascin colocalise at the roots of filopodia (Sasaki et al., 1996).

Among the other roles, drebrin plays a role in migration in neuronal contexts during development. In the cerebellum during embryonic development there is a strong correlation between expression levels of drebrin mRNA and cell migration (Shirao et al., 1990). Drebrin is also necessary for the migration of oculomotor neurons. Here, it is involved in forming the leading process and, subsequently, in orienting the leading process and cell body towards the direction of the migration (Dun et al., 2012). Similarly, in glioma cells drebrin localizes at the leading edge of lamellipodia and regulates cell morphology as well as cell motility (Terakawa et al., 2013).

Drebrin-E is expressed by migrating neuroblasts in the SVZ and RMS of the adult rat brain (Song et al., 2008). Interestingly, cessation of migration of these cells in the OB coincides with the disappearance of the protein (Song et al., 2008).

In this chapter, we investigate the role of drebrin in RMS neuroblast morphology and migration *in vitro* and *in vivo*.

In this chapter the following hypotheses were pursued:

1. Drebrin is required for neuroblast migration *in vitro and in vivo*
2. Drebrin phosphorylation site Serine 142 plays a role in neuroblast migration *in vitro and in vivo*
3. Endocannabinoids and/or FGF-2 can regulate phosphorylation of drebrin at Serine 142 in migrating neuroblasts

4.2 Results

4.2.1 Drebrin is expressed in the RMS

We first analysed the distribution of drebrin in paraffin-embedded P7 and adult sagittal brain slices from CD-1 mice (Figure 4-1). In both cases drebrin shows high expression along the RMS, resembling the expression pattern of PSA-NCAM and Dcx, two well-characterised RMS neuroblast markers (Doetsch, 2003) and fascin (Chapter 3, Figure 3-1).

4.2.2 Drebrin is upregulated in migrating neuroblasts

A previous study reported that drebrin is present in the SVZ-RMS (Song et al., 2008) and that drebrin-positive cells also express the migrating neuroblast marker PSA-NCAM, with some co-localization with the proliferating cell marker Ki-67 (Scholzen and Gerdes, 2000, Kee et al., 2002). However, no co-expression was detected with the astrocytic stem cell marker GFAP (Song et al., 2008). Consistent with these observations, double immunostaining of coronal SVZ sections shows a complete co-localization of drebrin with the migrating neuroblast marker Dcx (Figure 4-2, top row), while no co-localization was observed with GFAP (Figure 4-2, middle row). A partial co-localization was observed between drebrin and the transit amplifying progenitor marker Mash-1 (Figure 4-2, bottom row). This specific up-regulation of drebrin in neuroblasts led us to pursue the hypothesis of a role for drebrin in regulating the migration of SVZ-derived neuroblasts.

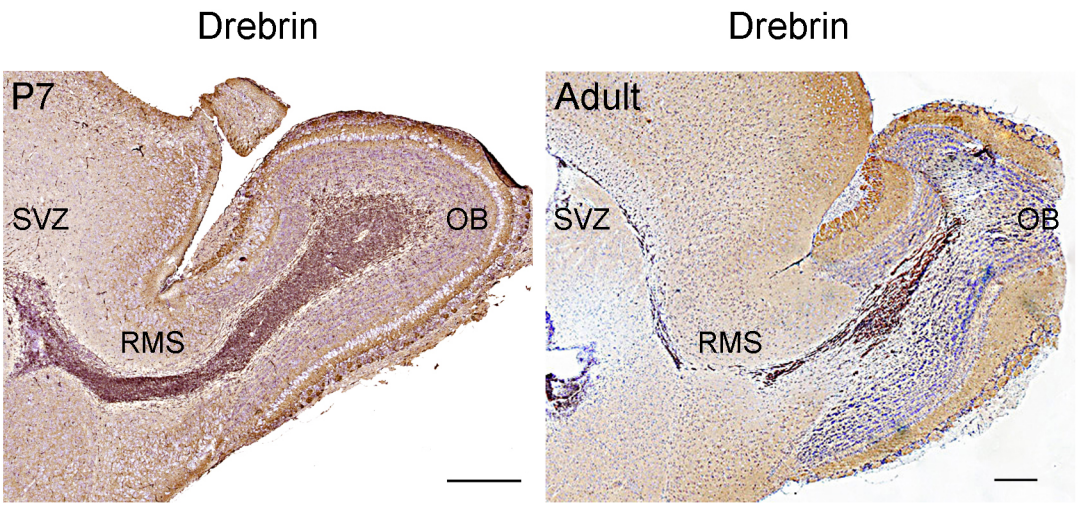


Figure 4-1. Drebrin is expressed in the postnatal and adult mammalian brain. Paraffin-embedded brain sections from P7 (top left panel) and adult (top right panel) mouse showing drebrin positive immunostaining (brown) in the SVZ, RMS and OB. Scale bars: 200 µm. Immunohistochemistry performed by Carl Hobbs.

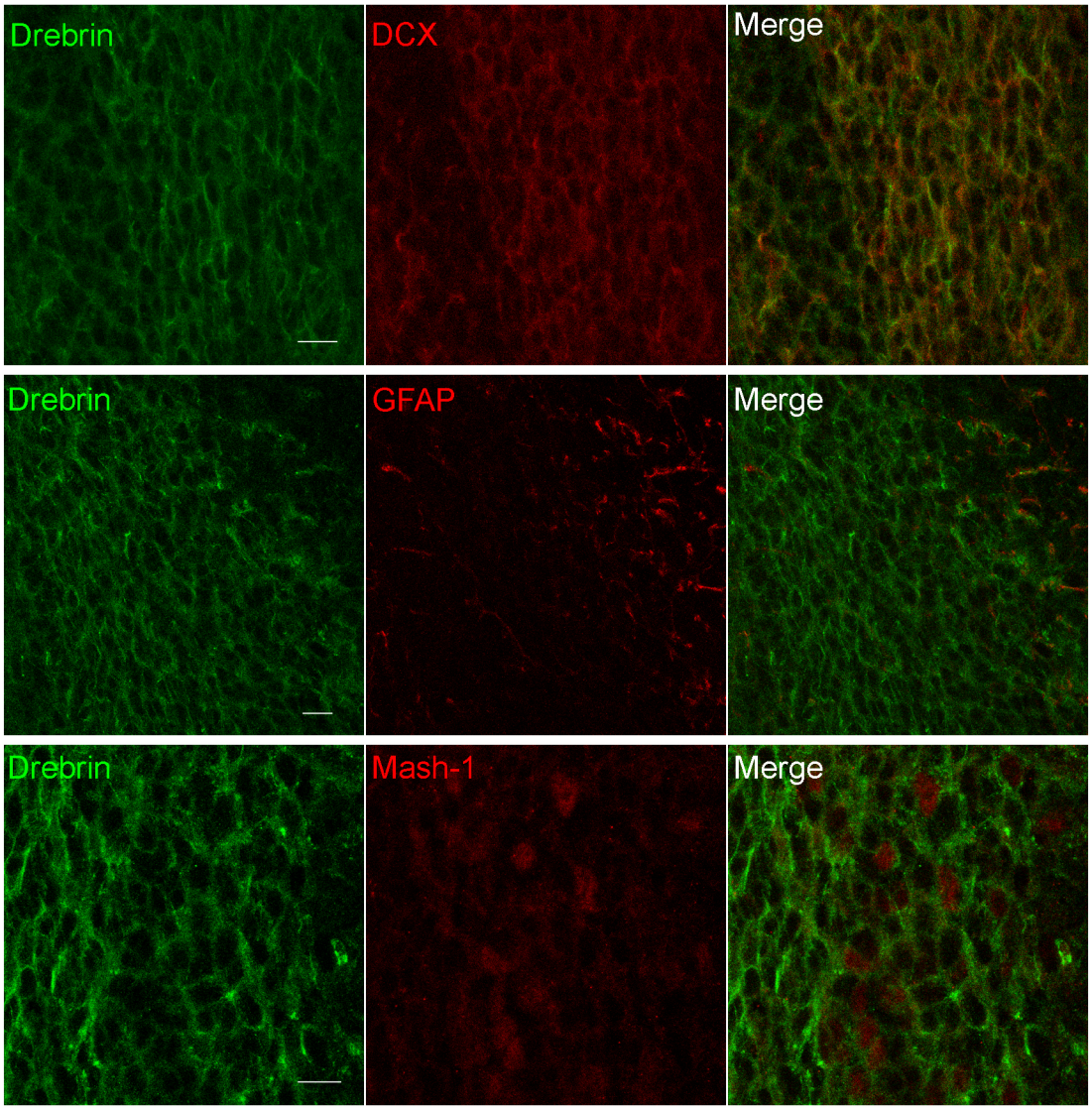


Figure 4-2. Drebrin is upregulated in RMS migrating neuroblasts.

Confocal images from P7 mouse SVZ sections showing that drebrin immunostaining virtually overlaps with Dcx+ migrating neuroblasts (top row), but is excluded from GFAP+ stem cells and astrocytes (middle row). (Bottom row), Hardly any co-localization is observed with Mash-1+ transit-amplifying progenitors. Scale bars: 10 µm. Immunohistochemistry performed by Carl Hobbs.

4.2.3 Drebrin is expressed in RMS migrating neuroblasts in primary cultures

To further examine the spatial distribution of drebrin in isolated neuroblasts, P7 rat RMS explants were dissected and embedded in a three-dimensional Matrigel matrix, a substrate allowing neuroblast migration. Like fascin, drebrin is highly expressed in neuroblasts, but its localisation appears to be different. Indeed, while fascin mainly localises to peripheral filopodia, drebrin is detected along the leading process, particularly concentrates in an area of the terminal growth cone preceding the filopodia and in the thin area behind the nucleus (Figure 4-3, middle row). These observations were confirmed when F-actin was visualised by transfection of Life-Act GFP, a GFP-fused 17-amino-acid peptide (Riedl et al., 2008) (Figure 4-3, top row), even though in this case we observed some partial colocalisation with drebrin at the basal region of filopodia (Figure 4-3, top row). Drebrin appeared to concentrate at the tip of the βIII–positive microtubules present in the leading process of neuroblasts (Figure 4-3, bottom row).

In summary, drebrin is expressed along the leading process of migrating neuroblasts, with a particular high expression at the membrane, at the back of the nucleus and at the tip of the leading process preceding the terminal filopodia.

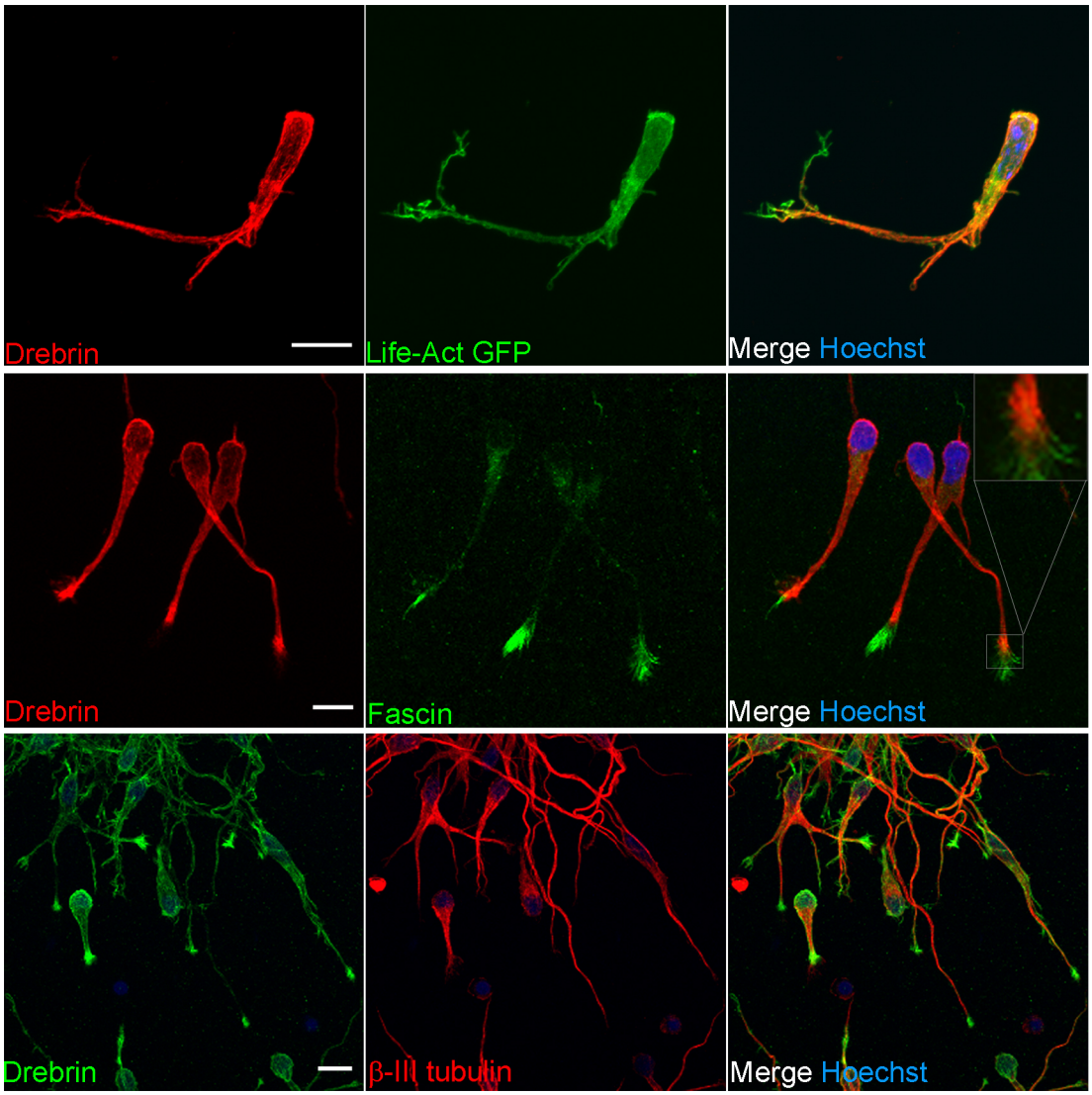


Figure 4-3. Drebrin is highly expressed by RMS migrating neuroblasts.

(Top row), RMS neuroblasts embedded in a 3-D Matrigel matrix and immunostained for drebrin (red) is concentrated along the leading process and it is mostly excluded from peripheral filopodia visualized by Life-Act GFP (green). Nuclei are stained with Hoechst dye (blue). (Middle row), Drebrin (red) does not colocalize with fascin (green) in migrating neuroblasts. Insert shows higher magnification of the leading process tip in a migrating neuroblast where fascin and drebrin seem to colocalise only at the root of the filopodia. (Bottom row), Drebrin (green) is found along the membrane, behind the nucleus and at the tip of leading processes containing microtubules positive for β–III tubulin (red). Nuclei are stained with Hoechst dye (blue). Scale bars: top row, 10 µm; middle and bottom rows, 20 µm.

4.2.4 Pharmacological inhibition of drebrin impairs neuroblast migration *in vitro*

We asked whether the high expression of drebrin in neuroblasts dictates a functional role for this protein in these highly migratory cells. To initially assess whether drebrin is involved in neuroblast migration, we treated RMS explants with 3,5-bis(trifluoromethyl)pyrazole (BTP), an immuno-suppressant drug able to bind drebrin (Mercer et al., 2010). BTP blocks store-operated calcium entry as well as actin rearrangements induced by drebrin (Zitt et al., 2004, Mercer et al., 2010). Mercer and colleagues (2010) showed that the BTP effect on store-operated calcium channel influx requires drebrin in T cells (Mercer et al., 2010).

To test whether pharmacological inhibition of drebrin had an effect on neuroblast migration, P7 rat RMS explants were embedded in Matrigel and left to migrate for 18 hours in presence of vehicle or BTP (1 μM) (Figure 4-4, (A)). Incubation with BTP substantially impaired migration of neuroblasts out of RMS explants compared to control cells (Figure 4-4, (B)). These results suggest that drebrin may have a role in neuroblast migration *in vitro*.

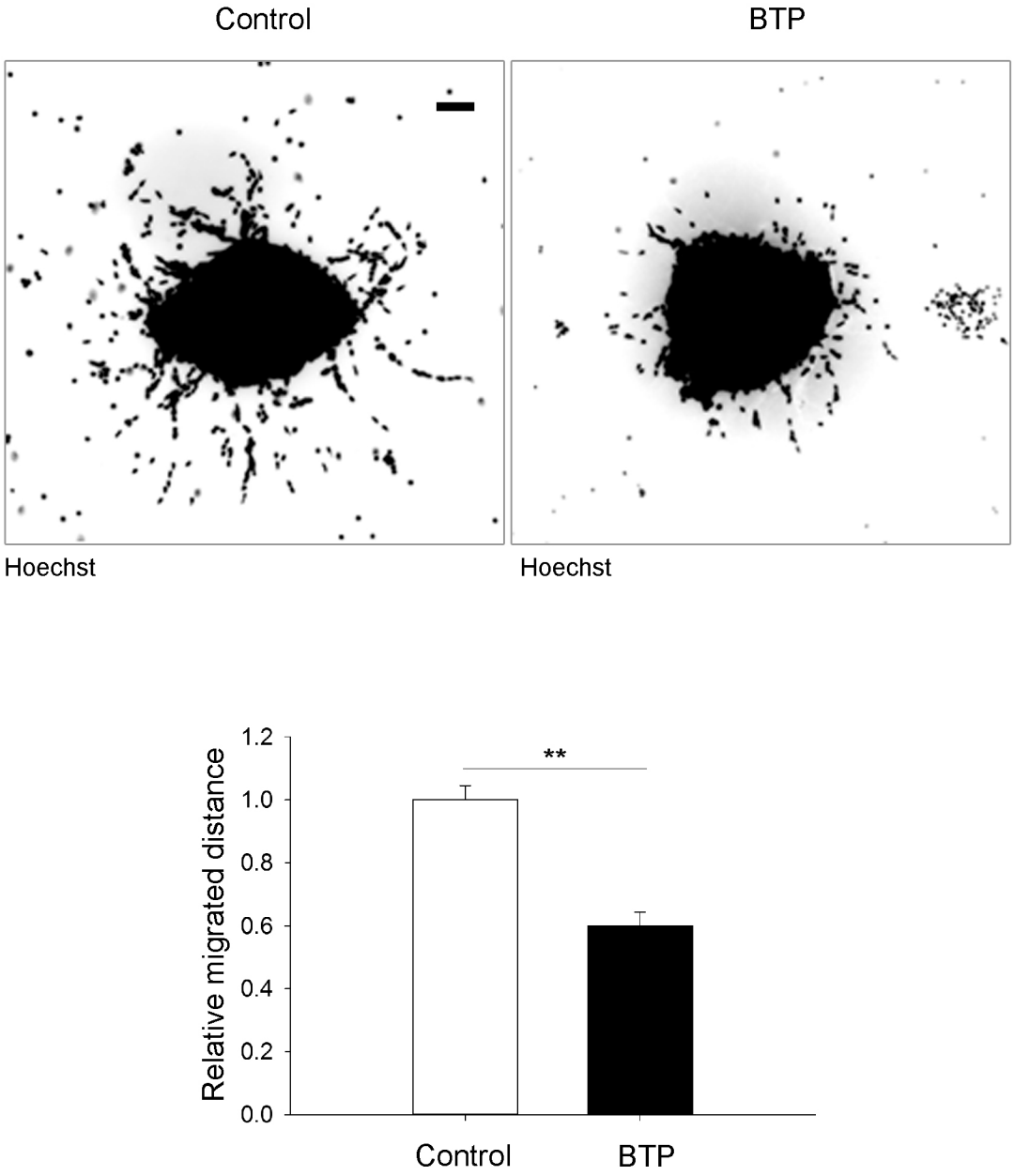


Figure 4-4. BTP treatment impairs neuroblast migration *in vitro*.

(A) Inverted contrast grayscale pictures of rat RMS explants embedded in Matrigel, incubated with normal culture medium as control or medium with 1 µM BTP for 18 hours and stained with the nuclear dye Hoechst for better nuclei visualisation. (B) Quantitative analysis shows a ~50% decrease of the migration distance in BTP-treated cells (mean ± SEM; n=3 independent experiments; 15-20 explants were counted for each condition; **p<0.01). Scale bar: 50 µm.

4.2.5 Pharmacological inhibition of drebrin impairs neuroblast migration *ex vivo*

We subsequently examined the effect of a pharmacological drebrin inhibition on neuroblast migration *ex vivo* (Figure 4-5). P2-3 mice were electroporated with pCX-GFP to label a subpopulation of RMS neuroblasts with GFP. 5 days later animals were sacrificed and brain slices were cultured for 1 hour in movie medium with vehicle or BTP. Two different concentrations of BTP were used (1 µM and 2 µM). Time-lapse imaging was performed every 3 minutes for 3 hours. At both concentrations of BTP, neuroblasts migrating in the brain slice show significant decrease in migrated distance (A), displacement (B), and velocity (C). Interestingly, at the higher BTP concentration, brain slices also show a significantly lower percentage of migratory neuroblasts compared to the control (D).

These data show that pharmacological inhibition of drebrin using BTP impairs RMS neuroblast migration *ex vivo*.

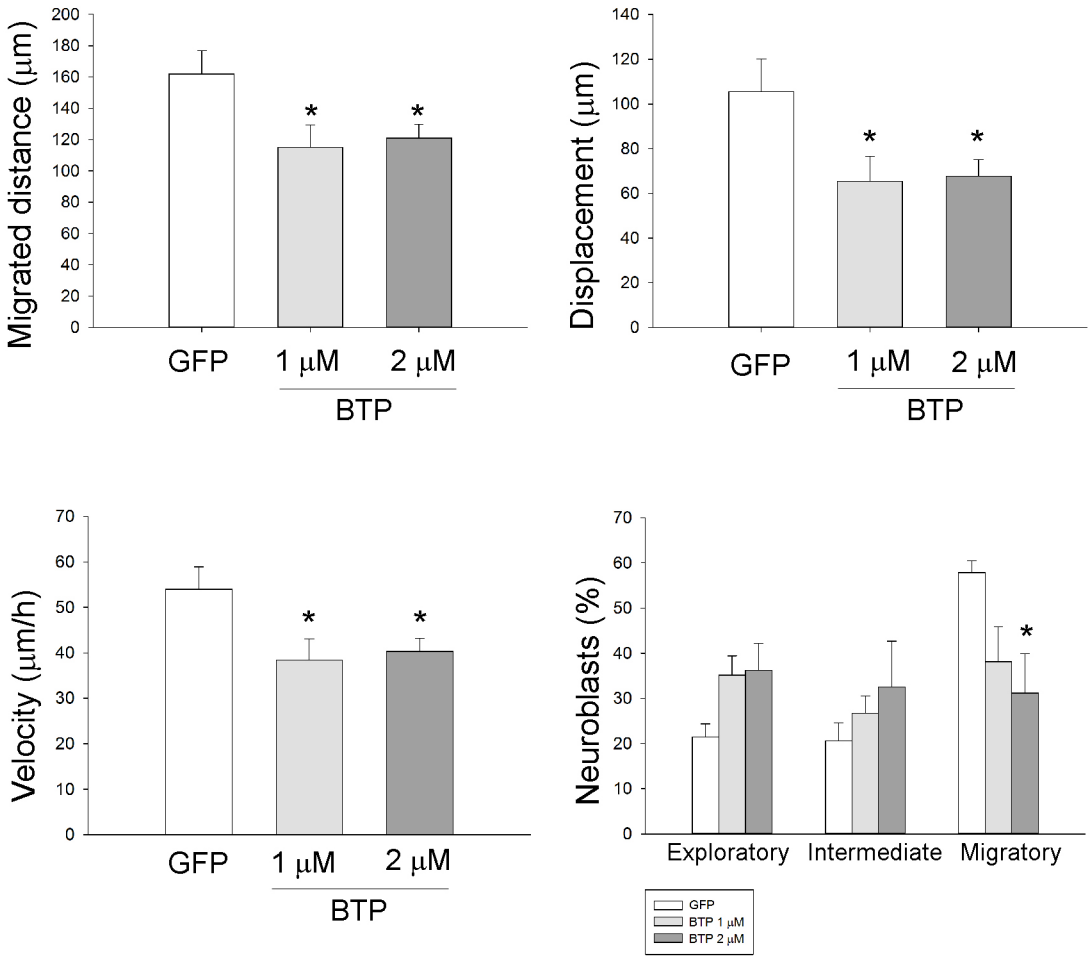


Figure 4-5. BTP decreases migration of neuroblasts *ex vivo*.

pCX-EGFP electroporated brain slices were incubated with or without BTP at 1 µM or 2 µM for 1 hour prior to imaging and were imaged in the RMS elbow every 3 minutes for 3 hours. Drugs were present throughout the imaging period. Both concentrations of BTP decrease the distance migrated (A), the displacement (B) and the velocity (C). Incubation with BTP (2 µM) causes a reduction in the percentage of migratory cells (D) (each bar represents the mean ± SEM; n=5 brains for control, n=3 for BTP 1 µM and n=7 for BTP 2 µM; *$p<0.05$).

4.2.6 Drebrin knockdown impairs RMS neuroblast migration *in vitro*

Since the specificity of the BTP compound could be questionable, we further investigated the role of drebrin in migration using RNAi in RMS neuroblasts. For initial tests, neuroblasts were nucleofected with three different amounts (5, 7, and 9 µg) of a siRNA pool containing four short interfering (si) RNA oligos. Drebrin levels were monitored by Western blot at two different time points (48 and 72 hours) after nucleofection (data not shown). Partial drebrin depletion (~40%) was observed with the higher siRNA oligo amounts already 48 hours after nucleofection (Figure 4-6, (A-B) while the greatest knockdown (~80%) was observed 72 hours after nucleofection of 9 µg of siRNA (Figure 4-6, (A-B)).

The effect of drebrin depletion was tested on migrating neuroblasts using a 3-D Matrigel matrix *in vitro* migration assay. Following this protocol (see Methods, Chapter 2), after nucleofection with drebrin siRNA neuroblasts were reaggregated in hanging drops and cultured in suspension for 52 h, subsequently embedded in Matrigel and left to migrate for a period of 24 h before immunostaining with drebrin and βIII tubulin.

Drebrin depletion significantly impaired migration of cells out of the re-aggregated clusters (Figure 4-7). Quantitative analysis showed a ~30% decrease in migration distance for the drebrin-depleted cells compared to neuroblasts nucleofected with control siRNA.

Taken together, these data indicate that drebrin regulates neuroblast migration *in vitro*.

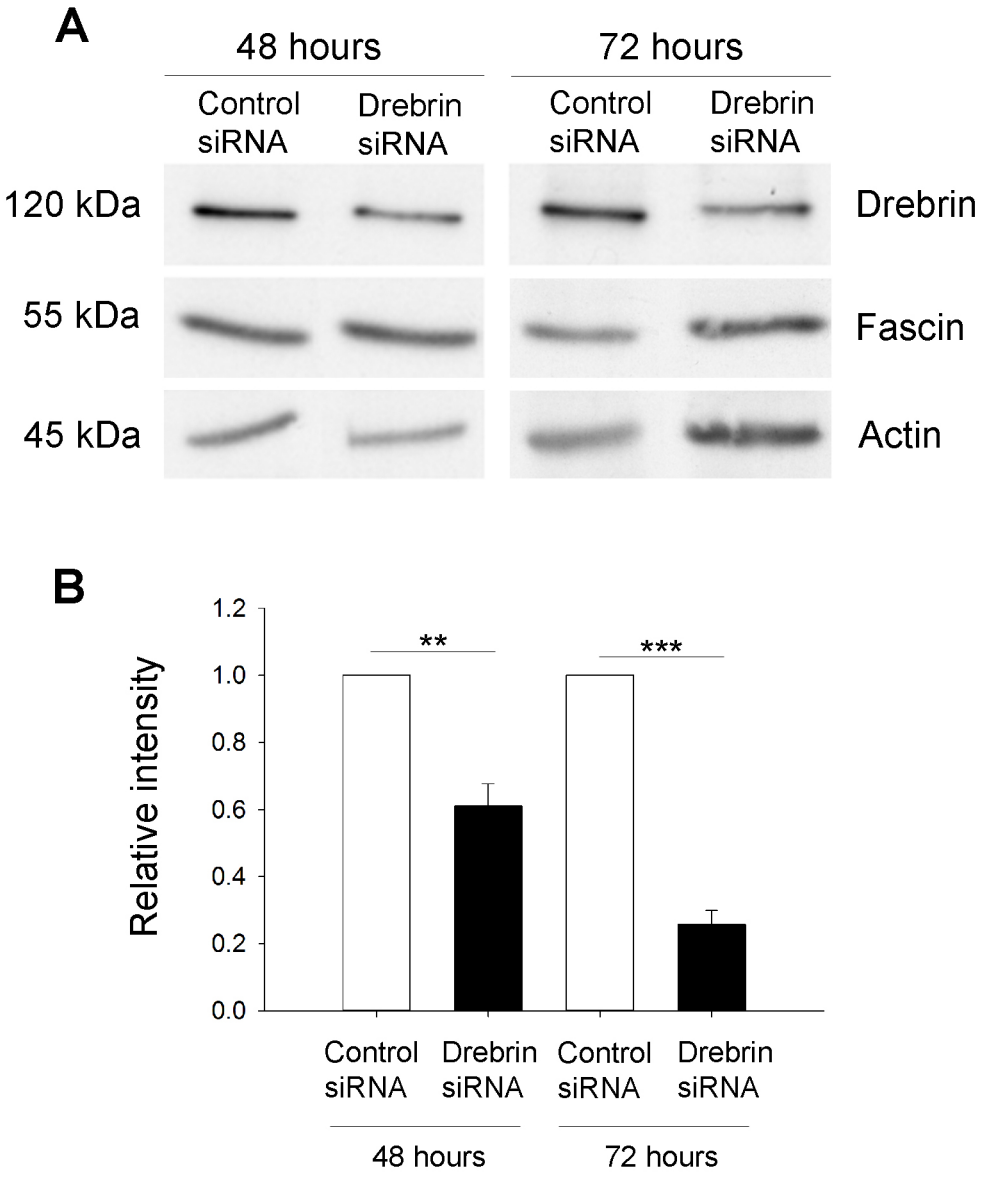


Figure 4-6. Drebrin can be knocked down in RMS migrating neuroblasts using siRNA.

(A) Representative blots from lysates of rat RMS neuroblasts nucleofected with control siRNA or siRNA oligos against drebrin and cultured for 48 or 72 hours were probed for drebrin, fascin and actin (loading control). (B) Densitometric quantitative analysis shows a significant reduction of drebrin levels at both time points, although the most significant reduction was seen at 72 hours (mean ± SEM; **p<0.01, ***p<0.001; n=3 independent experiments).

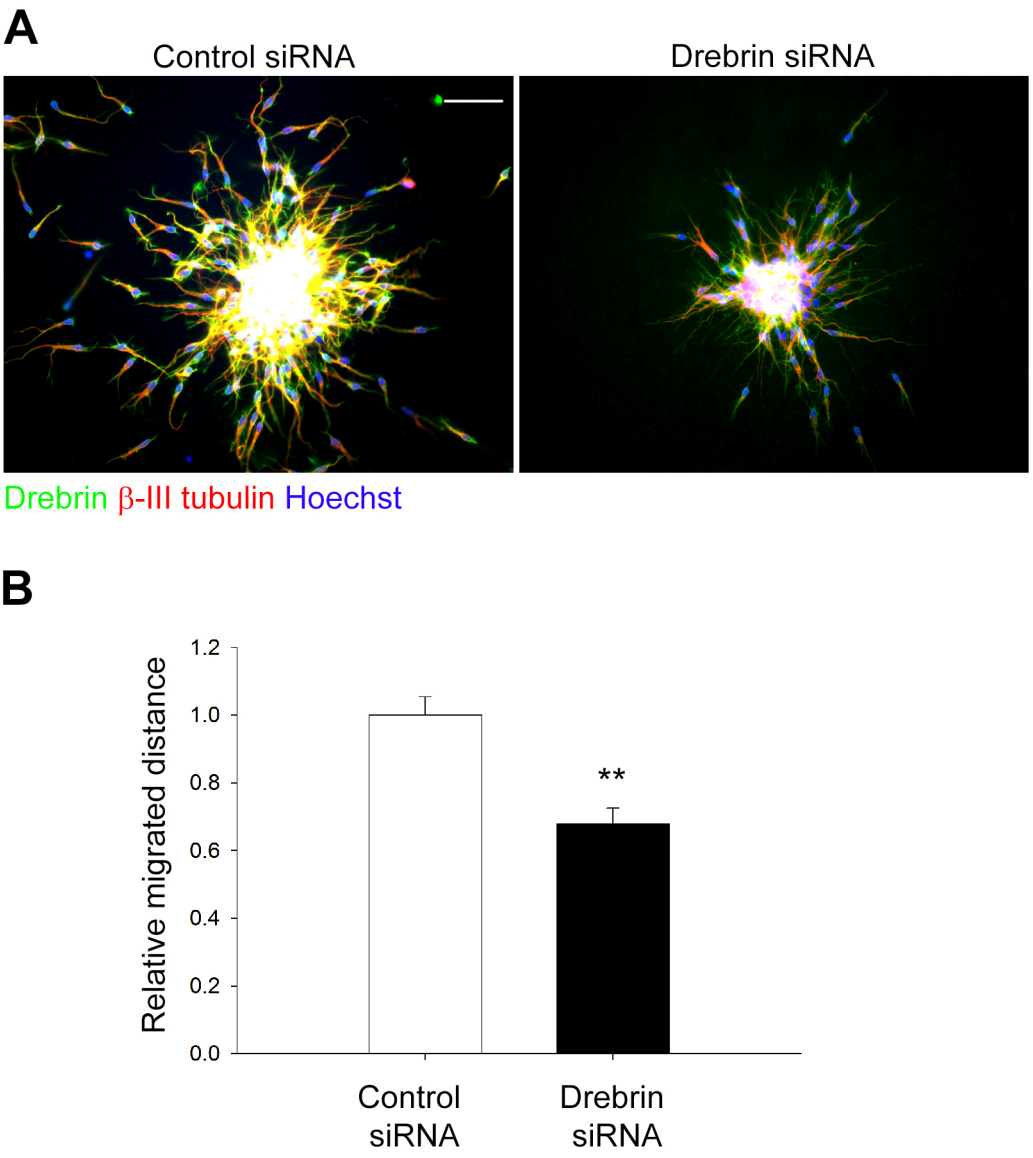


Figure 4-7. Drebrin regulates RMS neuroblast migration *in vitro*.

(A) Reaggregated rat neuroblasts were embedded in Matrigel 52 h after nucleofection of control or drebrin siRNA oligos and allowed to migrate for 24 h before immunostaining for drebrin (green) and βIII tubulin (red). Cell nuclei were visualized by Hoechst staining (blue). (B) Quantitative analysis shows a ~30% decrease in migration distance in drebrin-depleted neuroblasts compared with cells nucleofected with control siRNA (mean ± SEM; n=3 independent experiments; 15 to 20 explants were counted per experiment; **p<0.01). Scale bar: 50 µm.

4.2.7 shRNA-mediated drebrin knockdown impairs neuroblast migration

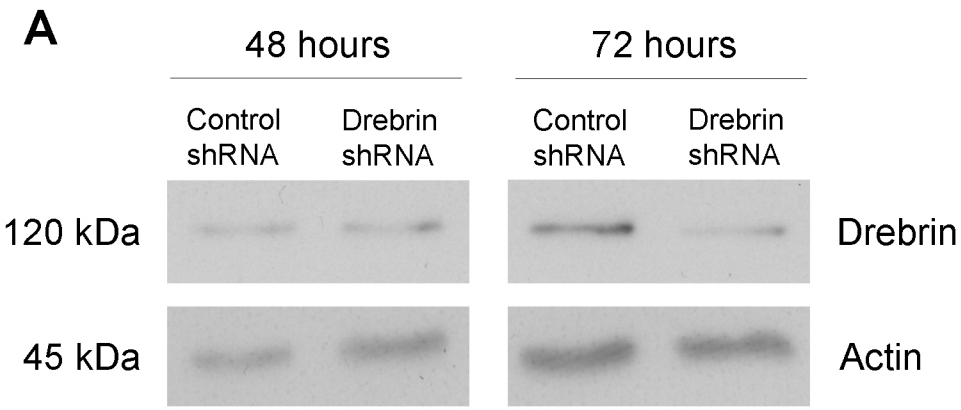
After having successfully knocked down drebrin *in vitro* using siRNA nucleofection, the role of drebrin in migration was further examined using another knockdown method: short hairpin RNA (shRNA). As mentioned in chapter 3, shRNA produces a stronger and more stable knockdown using lower amount of plasmid, therefore limiting the off-target effects (McAnuff et al., 2007, Rao et al., 2009), and is a preferred tool to achieve protein depletion *in vivo*.

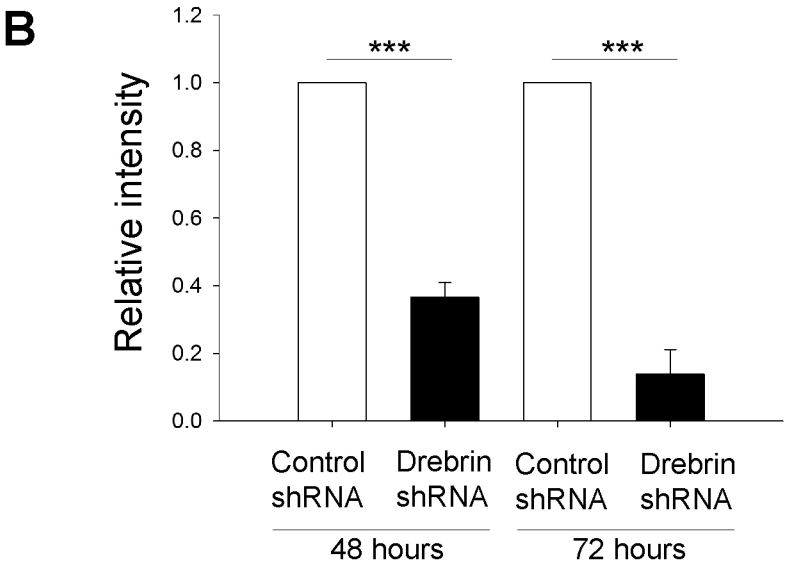
Drebrin knockdown in rat neuroblasts was tested by Western blot and immunostaining 48 and 72 hours after nucleofection of 5 µg of a drebrin shRNA plasmid expressing GFP (see Materials in Chapter 2). Drebrin levels were successfully reduced as shown by Western blot at both time points, 48 and 72 hours (Figure 4-8, (A)). Densitometric quantifications show reduction in drebrin expression of ~60% at 48 hours and of ~80% at 72 hours (Figure 4-8, (A)). Immunostaining to confirm drebrin knockdown in cells expressing drebrin shRNA was also performed. As shown in Figure 4-8, (C) neuroblasts nuclefected with drebrin shRNA show a high reduction in drebrin expression (Figure 4-8, (C), arrowheads), compared to non-tranfected neuroblasts (Figure 4-8, (C), arrows).

We have shown above that drebrin depletion using siRNA successfully impaired neuroblast migration *in vitro* (Figure 4-7). To confirm this result with an alternative RNAi strategy, we used drebrin shRNA in the *in vitro* migration assay. We observed a ~20% decrease in migration of neuroblasts nucleofected with drebrin shRNA compared to control shRNA (Figure 4-9).

To prove that defective migration was specifically caused by the lack of drebrin, neuroblasts were nucleofected with drebrin shRNA together with a siRNA-resistant m-cherry-tagged human drebrin (Figure 4-10, (A)). Impaired migration by drebrin shRNA was significantly rescued by co-transfecting siRNA-resistant human drebrin, confirming the specificity of the shRNA effect (Figure 4-10, (B)).

Taken together, these results show that drebrin is required for neuroblast migration *in vitro*.


A
48 hours
72 hours
Control shRNA
Drebrin shRNA
Control shRNA
Drebrin shRNA
120 kDa
Drebrin
45 kDa
Actin


B
Relative intensity
1.2
1.0
0.8
0.6
0.4
0.2
0.0
***
***
Control shRNA
Drebrin shRNA
Control shRNA
Drebrin shRNA
48 hours
72 hours

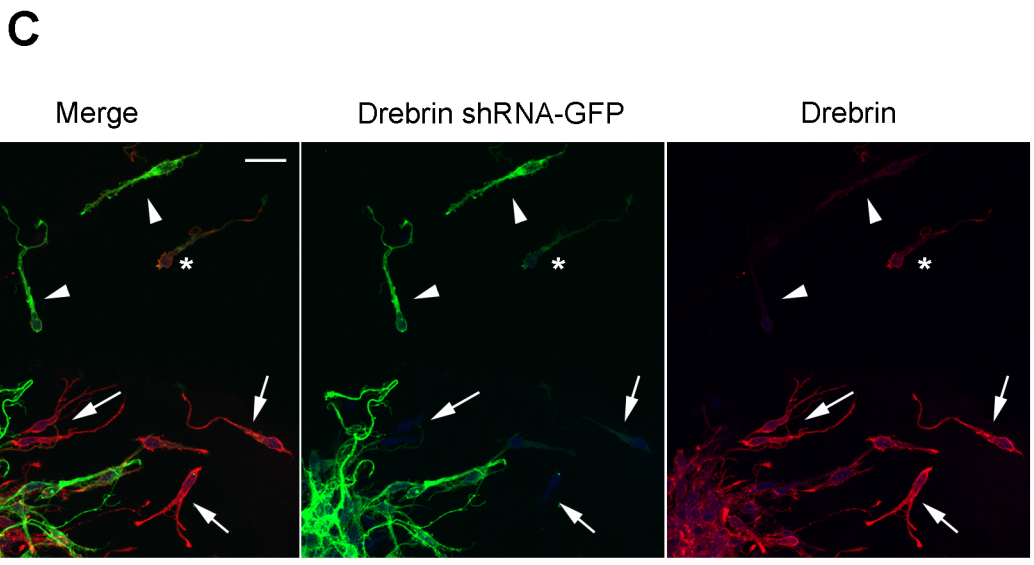

C
Merge
Drebrin shRNA-GFP
Drebrin

Figure 4-8. shRNA-mediated drebrin depletion in RMS neuroblasts.

(A) Representative Western blots from lysates of rat RMS neuroblasts nucleofected with control shRNA or drebrin shRNA and cultured for 48 or 72 hours were probed for drebrin and actin (loading control). (B) Densitometric quantitative analysis shows a significant reduction of drebrin levels of ~60% at 48 hours and ~80% at 72 hours (mean ± SEM; ***$p<0.001$; n=3 independent experiments). (C) Confocal image showing drebrin knockdown in migrating neuroblasts expressing drebrin shRNA-GFP (green) (arrowheads). Neuroblasts that are not GFP-labelled have high drebrin expression (red) (arrows). The asterisk shows a cell with low GFP expression (low drebrin knockdown) as well as a lower amount of drebrin (red) compared to control, GFP-negative cells. Scale bar: 20 μm.

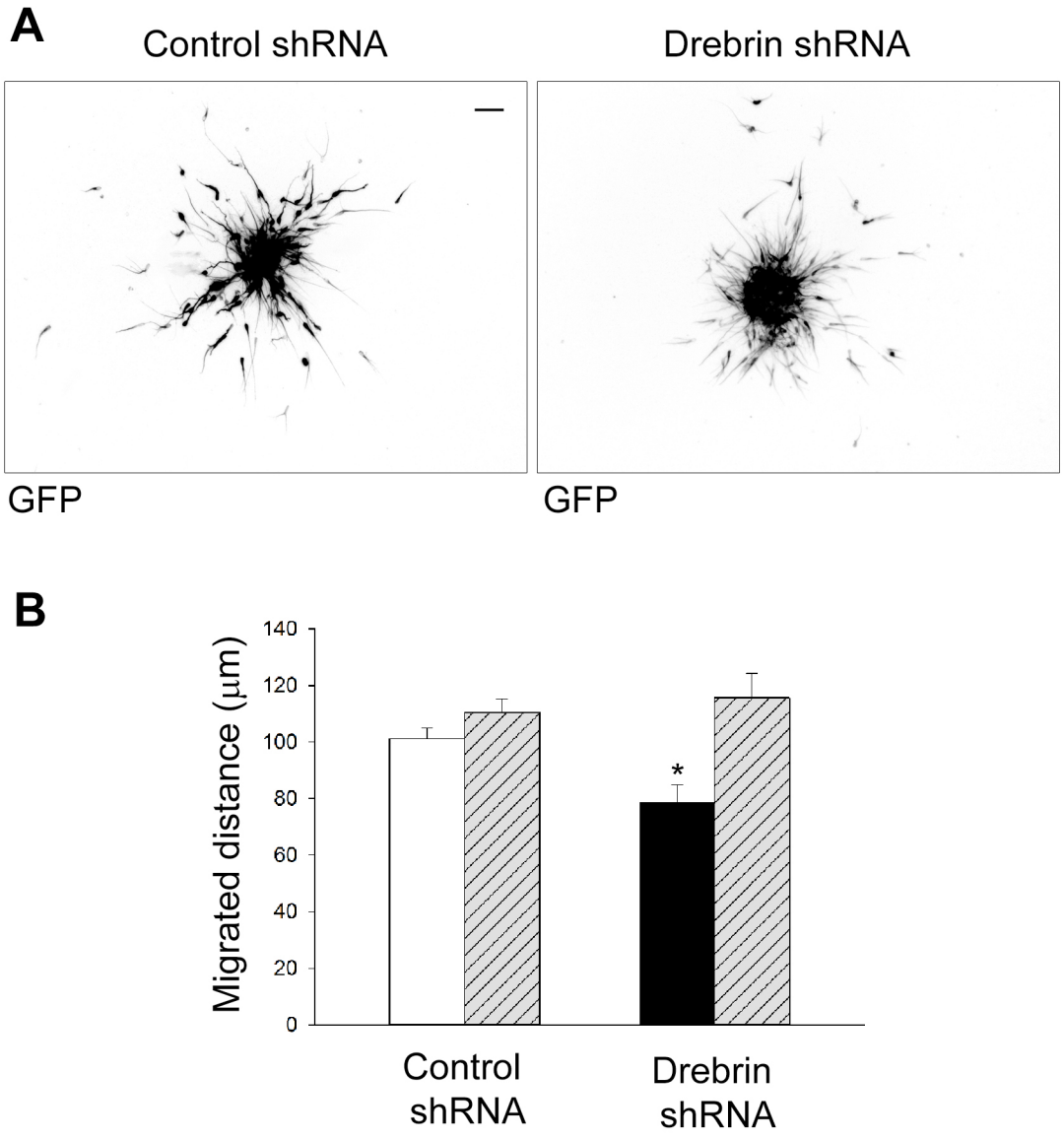


Figure 4-9. Drebrin regulates RMS neuroblast migration *in vitro*.

(A) Reaggregated rat neuroblasts were embedded in Matrigel 52 h after nucleofection of control or drebrin shRNA-GFP and allowed to migrate for 24 h. The GFP channel is shown as a grayscale image. (B) Quantitative analysis shows a ~20% decrease in migration distance in drebrin-depleted neuroblasts compared with cells nucleofected with control shRNA. GFP-negative, untransfected cells served as an internal control (hatched columns) (mean ± SEM; n=3 independent experiments; 15 to 20 explants were counted per experiment; *p<0.05). Scale bar: 50 µm.

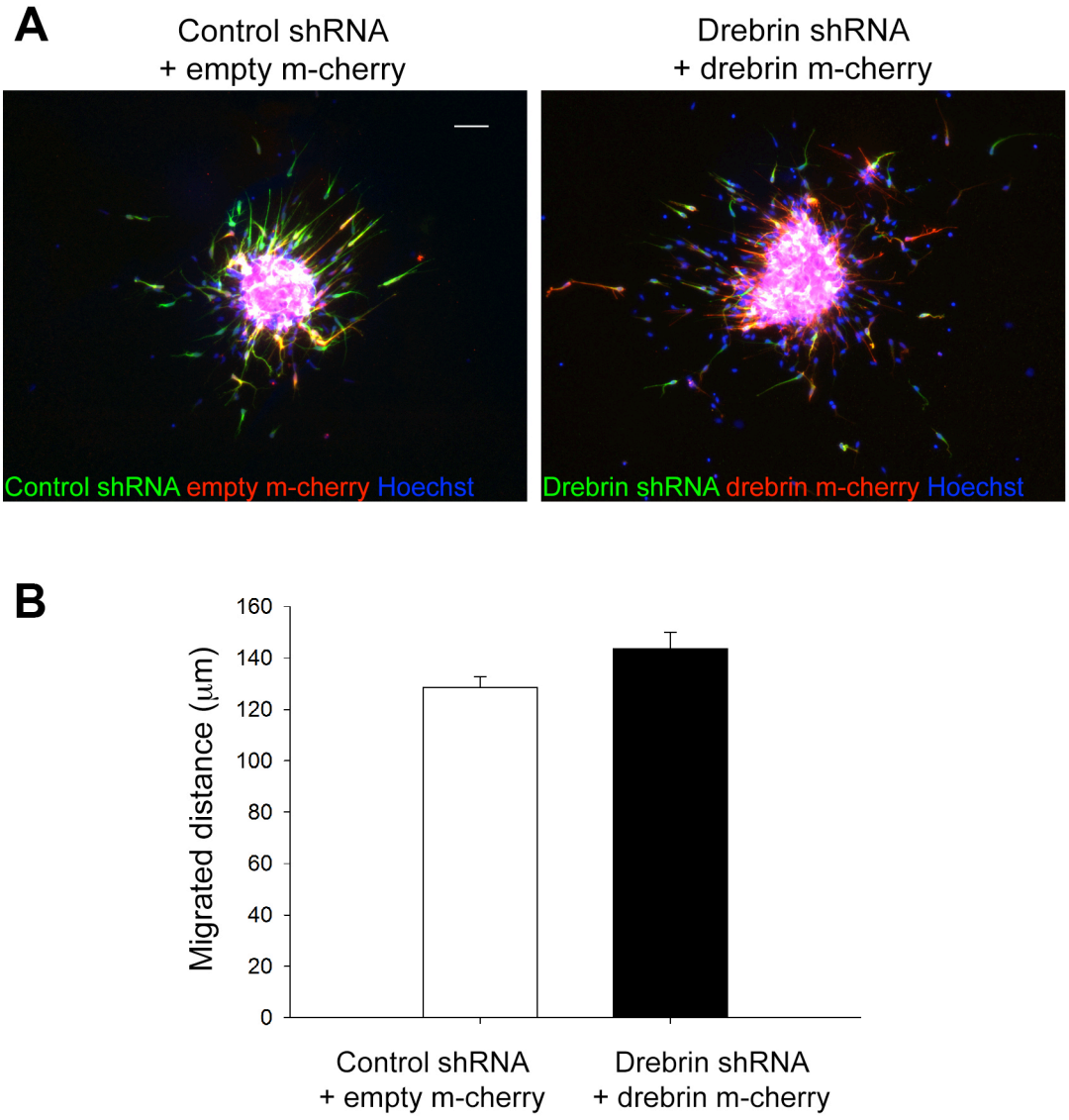


Figure 4-10. Drebrin shRNA has a specific effect in impairing neuroblast migration. (A) Reaggregated rat neuroblasts were embedded in Matrigel 52 h after nucleofection with control shRNA-GFP and m-cherry-empty vector or drebrin shRNA-GFP and m-cherry-tagged human drebrin and allowed to migrate for 24 h before immunostaining for GFP (green) and m-cherry (red). Cell nuclei were visualized by Hoechst staining (blue). (B) Quantitative analysis shows that the impaired migration caused by drebrin knockdown was completely rescued by co-transfection with the siRNA-resistant wt drebrin (mean ± SEM; n=3 independent experiments; 15 to 20 explants were counted per experiments). Scale bar: 50 µm.

4.2.8 Drebrin regulates neuroblast morphology

After establishing a role for drebrin in neuroblast migration, we examined neuroblast morphology in drebrin-depleted cells. It has been previously reported that defects in migration can be accompanied by a higher percentage of secondary branches (Koizumi et al., 2006, Oudin et al., 2011, Sonego et al., 2013a). RMS neuroblasts were nucleofected with control shRNA or drebrin shRNA, cultured in suspension for 52 h, embedded in Matrigel and subsequently left to migrate for a period of 24 h, before immunostaining with GFP and βIII tubulin. Drebrin knockdown visibly affected neuroblast morphology (Figure 4-11, (A)). Some drebrin-depleted cells showed a longer leading process compared to control cells (Figure 4-11, (B)). Moreover, while control cells displayed a single straight leading process (Figure 4-11, (A), top left), many drebrin-depleted cells showed leading processes with multiple branches (Figure 4-11, (A), top right). The percentage of cells with a branched morphology was almost double in drebrin-depleted samples compared to control shRNA-nucleofected neuroblasts (Figure 4-11, (C)).

We confirmed the effects of drebrin-depletion in neuroblast morphology using siRNA oligos against drebrin. This drebrin knockdown method was shown before to have an effect on neuroblast migration. A doubled increase in the percentage of secondary branches was detected also in cells nucleofected with drebrin siRNA in comparison to control cells (Figure 4-11, (D)) indicating drebrin's role as a regulator of both neuroblast morphology and neuroblast migration.

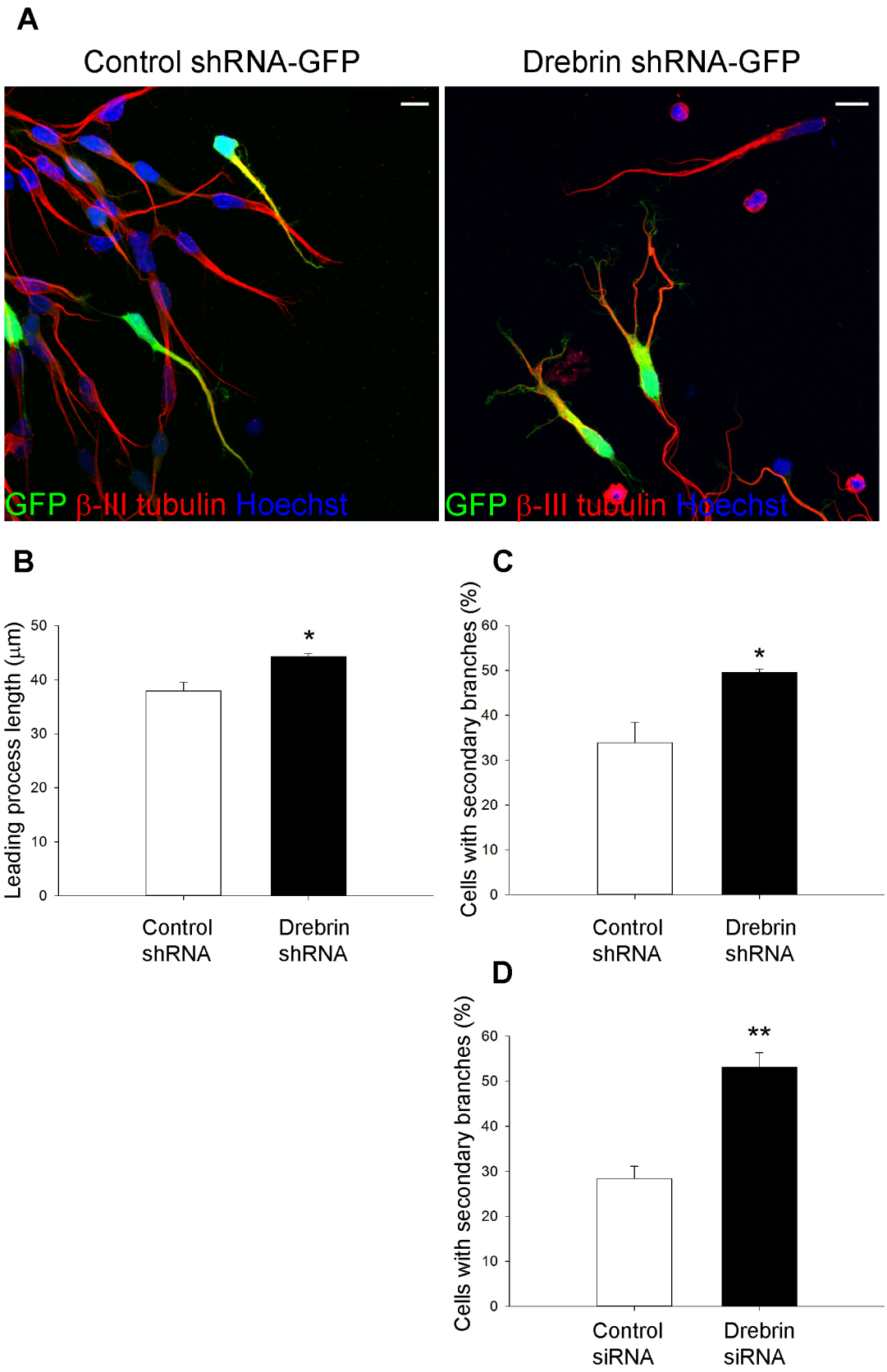

A
Control shRNA-GFP
Drebrin shRNA-GFP
GFP β-III tubulin Hoechst
GFP β-III tubulin Hoechst
B
Leading process length (μm)
0
10
20
30
40
50
*
Control shRNA
Drebrin shRNA
C
Cells with secondary branches (%)
0
10
20
30
40
50
60
*
Control shRNA
Drebrin shRNA
D
Cells with secondary branches (%)
0
10
20
30
40
50
60
**
Control siRNA
Drebrin siRNA

Figure 4-11. **Drebrin knockdown disrupts neuroblast morphology.**

(A) Representative images of rat RMS neuroblasts nucleofected with control (left) or drebrin (right) shRNA showing cells with a major single straight leading process (left) or cells with branched protrusions (right) respectively. (B, C), shRNA-mediated drebrin depletion causes a significant increase in leading process length (B) and in the percentage of cells with branched morphology (C) (mean ± SEM; n=3 independent experiments; 191 cells counted for control shRNA, 192 cells counted for drebrin shRNA; *$p<0.05$). (D), siRNA-mediated drebrin depletion causes a significant increase in the percentage of branched cells (mean ± SEM; n=3 independent experiments; 202 cells counted for control siRNA, 207 cells counted for drebrin siRNA; **$p<0.01$). Scale bars: 10 µm.

4.2.9 Drebrin knockdown impairs RMS neuroblast migration *ex vivo*

After having determined an important role for drebrin in RMS neuroblast migration *in vitro* using two different RNAi approaches, we further examined the effect of drebrin depletion *in vivo*. For this purpose, we performed *in vivo* postnatal electroporation in mouse pups, as described in the previous chapters (Boutin et al., 2008, Sonego et al., 2013b).

We electroporated drebrin shRNA-GFP or control shRNA-GFP plasmids into the right ventricles of P2-3 mouse pups. Five days later the animals were sacrificed and their brains were sliced for immunostaining or cultured for time-lapse imaging. To prove that drebrin was knocked down *in vivo*, neuroblast cultures were obtained by dissociating the RMS of the electroporated mouse right brain hemispheres. GFP-labelled cells had lower levels of drebrin immunostaining compared to control shRNA-transfected neuroblasts (data not shown).

To study the dynamics of drebrin-depleted cells, we performed spinning disk confocal time-lapse imaging of brain slices from control and drebrin shRNA-electroporated mice every 3 minutes for a total of 3 hours. In these movies, although the majority of the cells migrate forward towards the OB, some migrate backwards (towards the SVZ) or change direction multiple times during imaging (see also Chapter 3 and supplementary movies 7 and 10).

Tracking analysis of time-lapse movies showed that, compared to control shRNA cells, drebrin shRNA-transfected neuroblasts have a reduced migrated distance (Figure 4-12, (A) *$p<0.05$), reduced displacement, (the shortest distance between start and end points) (Figure 4-12, (B); *$p<0.05$), reduced velocity (Figure 4-12, (C): *$p<0.05$) and lower displacement rate, (ratio between displacement and time) (Figure 4-12, (D) *$p<0.05$), while no significant difference was found in the migratory index that (ratio between net distance and total distance covered) (Comte et al., 2011) (Figure 4-12, (E)).

Altogether, these data show that drebrin plays a cell-autonomous role in controlling RMS neuroblast migration *ex vivo*.

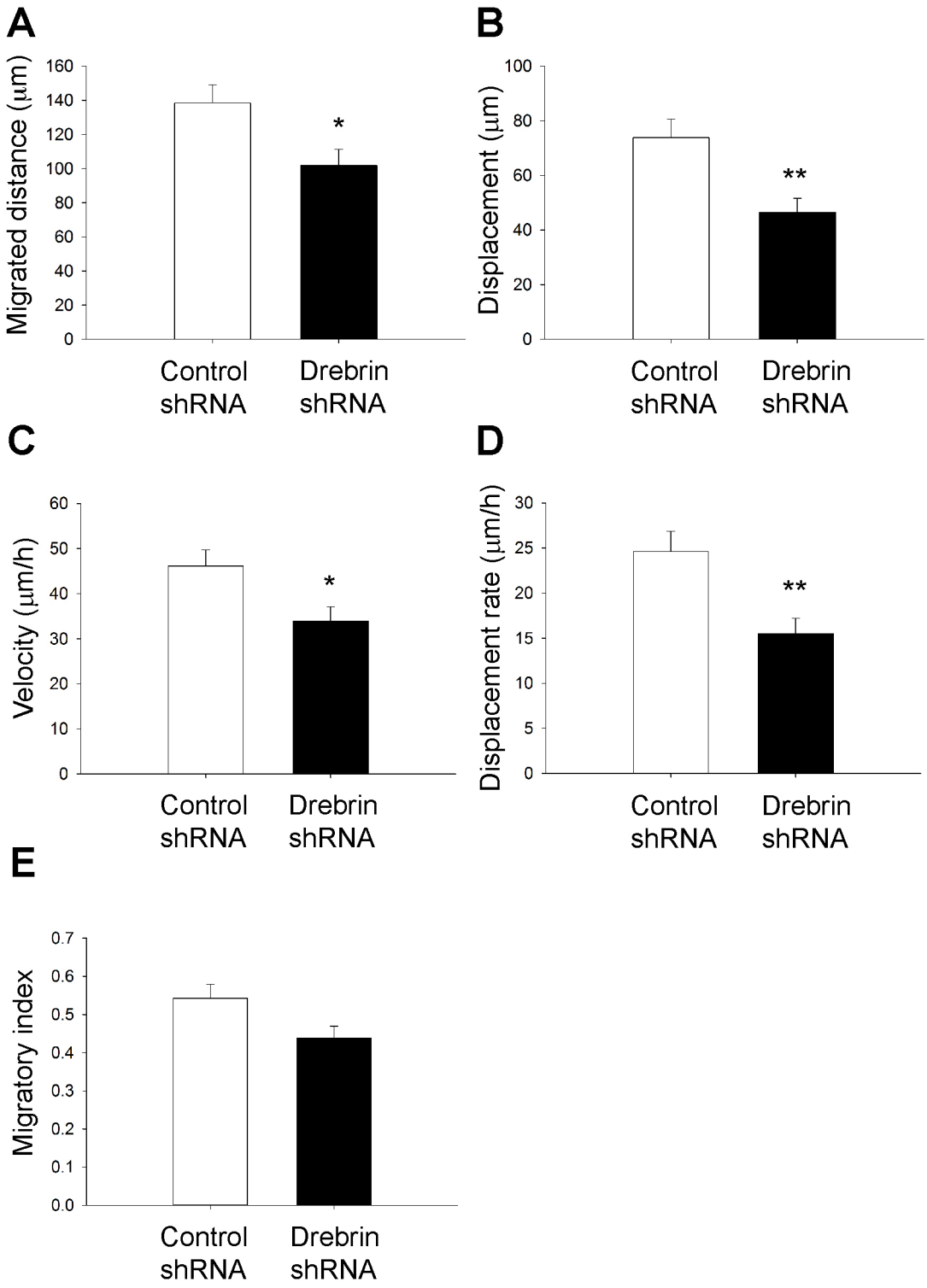

A
Migrated distance (μm)
160
140
120
100
80
60
40
20
0
*
Control shRNA
Drebrin shRNA
B
Displacement (μm)
100
80
60
40
20
0
**
Control shRNA
Drebrin shRNA
C
Velocity (μm/h)
60
50
40
30
20
10
0
*
Control shRNA
Drebrin shRNA
D
Displacement rate (μm/h)
30
25
20
15
10
5
0
**
Control shRNA
Drebrin shRNA
E
Migratory index
0.7
0.6
0.5
0.4
0.3
0.2
0.1
0.0
Control shRNA
Drebrin shRNA

Figure 4-12. Drebrin is necessary for efficient neuroblast migration *ex vivo*.

(A-E) Tracking analysis of RMS neuroblasts after *in vivo* electroporation with drebrin shRNA displays a shorter migrated distance (A), shorter displacement (B), and lower speed (C) (mean ± SEM; n=8 slices for control; n=7 slices for drebrin shRNA; **p<0.01). A significant difference was found between control and drebrin shRNA in the displacement rate (D), while no significant difference was found in the migratory index (E) (mean ± SEM; n=7 slices for control; and n=6 slices drebrin shRNA; *p<0.05).

4.2.10 Drebrin knockdown affects neuroblast morphology *ex vivo*

After showing that drebrin has a role in regulating neuroblast migration *ex vivo*, we wanted to investigate whether drebrin knockdown also affects morphology of RMS neuroblasts.

Electroporation was performed as previously described using control or drebrin shRNA-GFP. Five days later the animals were sacrificed and their brains were fixed, embedded in gelatin, sliced and stained with an anti-GFP antibody.

In both cases GFP-positive cells were found throughout the RMS and in the core of the OB, just starting to migrate radially (general observation, not shown). Quantitative morphological analysis of high magnification confocal images (Figure 4-13, (A)) shows that electroporation of drebrin shRNA increased leading process length compared to control shRNA-transfected cells (Figure 4-13, (B)) – process length was quantified in both branched (where the longest process was considered) and non-branched neuroblasts – and also led to a significant higher amount of neuroblasts with secondary branches (Figure 4-13, (C)). About 50% of drebrin-depleted neuroblasts displayed increased branching, while >30% of drebrin-depleted neuroblasts had a leading process longer than 40 µm (which is the average leading process length in control cells). Although we have not qualitatively detected a correlation between the brightness of GFP signal (indicative of efficiency of expression of the shRNA plasmid) in neuroblasts and different phenotypes, we cannot exclude that these differences might be correlated with different drebrin knockdown levels. Further investigations are required to understand why and how drebrin depletion leads to these different phenotypes.

These data indicate that drebrin controls the length and the branching of the leading process in migratory neuroblasts.

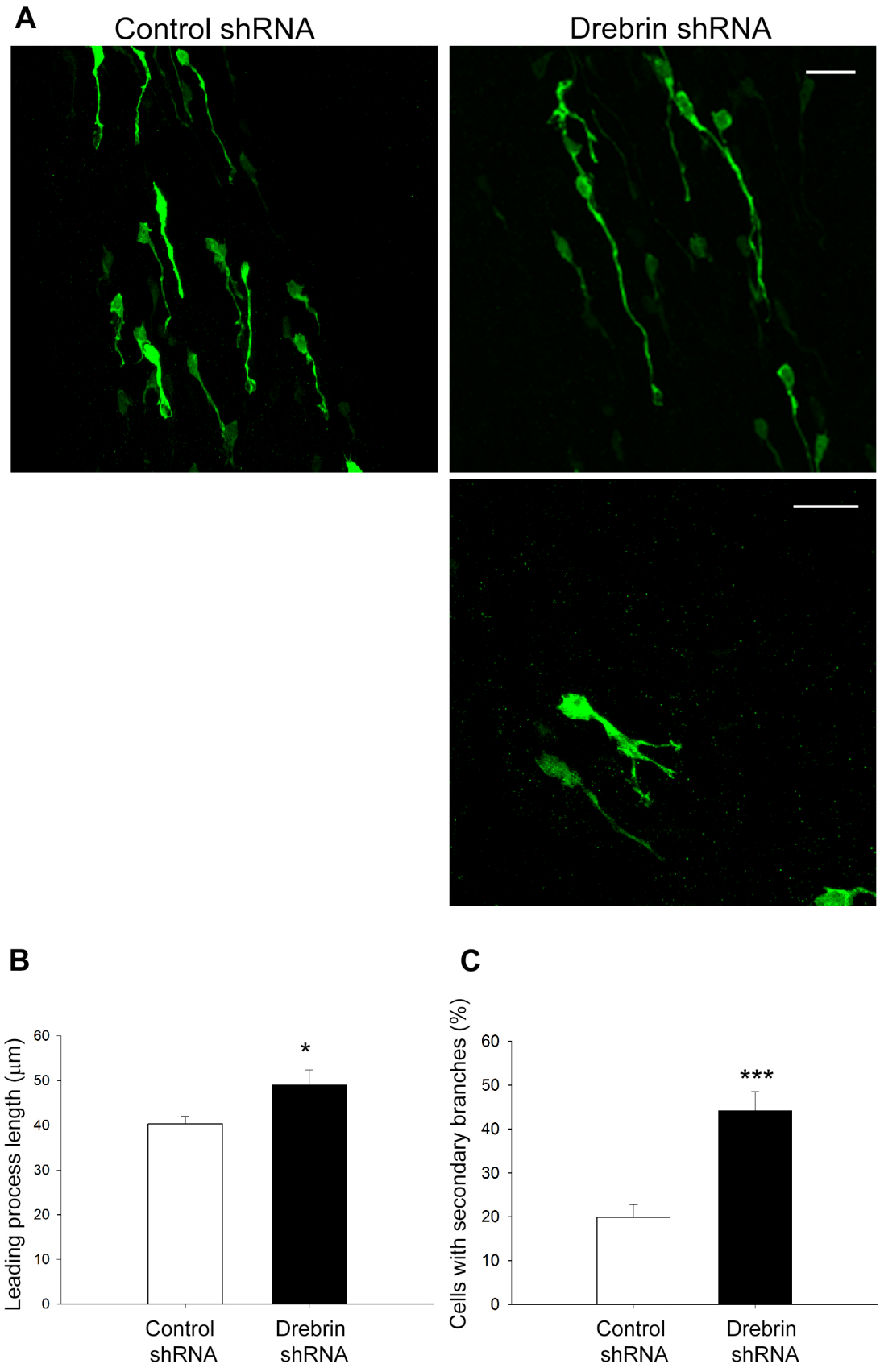

A
Control shRNA
Drebrin shRNA
B
Leading process length (μm)
60
50
40
30
20
10
0
*
Control shRNA
Drebrin shRNA
C
Cells with secondary branches (%)
60
50
40
30
20
10
0
***
Control shRNA
Drebrin shRNA

Figure 4-13. Drebrin regulates neuroblast morphology *in vivo*.

(A), Confocal z-stack projections of P2-3 mouse brain slices electroporated with control or drebrin shRNA show control cells with single processes oriented towards the OB, identified by the yellow asterisk (top left), while drebrin shRNA expressing cells have longer leading processes (top right) and branched protrusions (bottom right). (B-C) Quantifications showing that drebrin shRNA in vivo electroporation causes a modest but significant increase in leading process length (B), and a significant increase in the percentage of branched neuroblasts (C) (mean ± SEM; n=6 brains per condition, 400 cells analysed for control shRNA and 303 cells analysed for drebrin shRNA; **p<0.01). Scale bars: 50 μm.

4.2.11 Regulation of drebrin by phosphorylation

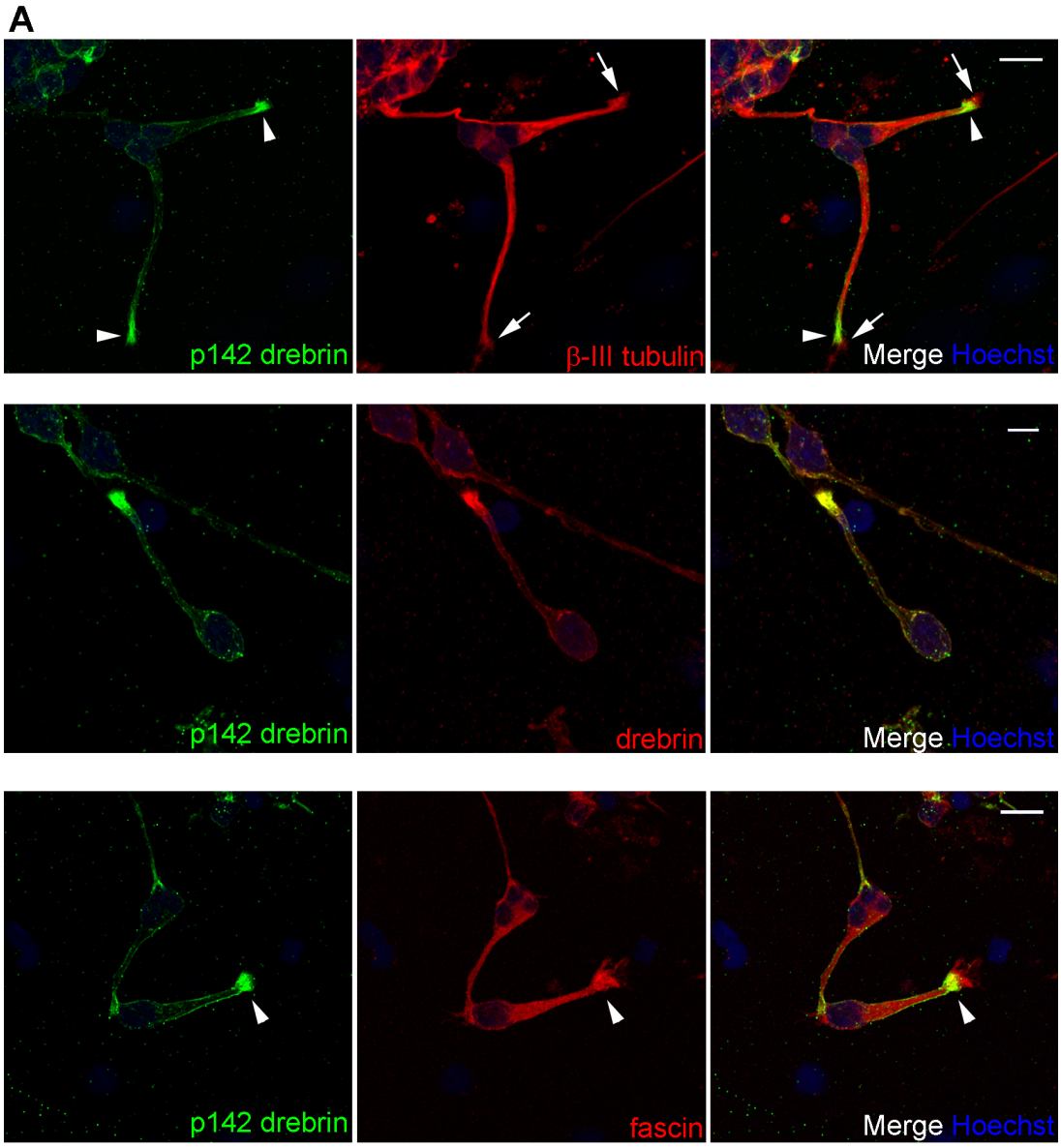
After establishing that drebrin expression is necessary for efficient RMS neuroblast migration, we started to explore the molecular mechanisms through which drebrin controls neuroblast migration. For this purpose we have initially examined drebrin phosphorylation on Ser142, a crucial site regulating the actin bundling function and microtubule-binding ability of this protein (Worth et al., 2013). More precisely, when this site is covered by the BB domain (see Chapter 1), drebrin cannot bind actin through its CC domain. Phosphorylation by Cdk5 on this site opens the "close" conformation, enabling drebrin to bundle actin filaments and bind to microtubules via its interaction with EB3 (Worth et al., 2013). Phosphorylation on Ser142 is therefore necessary for the ability of drebrin to bundle actin and is functionally important in stimulating neuritogenesis (Worth et al., 2013).

In order to investigate whether drebrin is phosphorylated on S142 in migrating neuroblasts, P7 rat RMS explants were embedded in Matrigel and immunostained for pSer142-drebrin and βIII tubulin (Figure 4-14, (A), top, row). Although we cannot completely rule out the possibility that pS142 antibody recognizes other phospho-sites in other proteins, the specificity of the pS142 drebrin has been previously characterised by Worth and colleagues (2013).

Drebrin pSer142 is highly concentrated at the tip of the leading process in a restricted region that does not seem to coincide with microtubule ends, since microtubule staining extends beyond drebrin pSer142 immunostaining (Figure 4-14, (A), top, row; arrowheads and arrows). Moreover, as also clearly shown in the co-staining with fascin (Figure 4-14, (A), bottom, row), drebrin pS142 is also confined to the membrane of the leading process (Figure 4-14, (A)). Neuroblasts were co-stained for drebrin pS142 and drebrin; colocalisation was detected especially at the tip (Figure 4-14, (A), middle, row). Interestingly, the drebrin pS142 and fascin co-staining showed strong localization of pS142 at the tip of the leading process preceeding the actual fascin-positive filopodia structures (Figure 4-14, (A) bottom, row). Colocalisation of drebrin pS142 with fascin was observed only at the base of filopodia (Figure 4-14, (A), bottom, row; arrowhead).

Both drebrin and pS142 drebrin could also be detected by Western blot analysis in RMS as well as OB homogenates from P7 rat pups (Figure 4-14, (B)).

In summary, high levels of pS142 drebrin are found in migrating neuroblasts along the membrane of their extending protrusions and in a confined region at the tip of the leading process overlapping with the basal region of peripheral filopodia.


A
p142 drebrin
β-III tubulin
Merge Hoechst
p142 drebrin
drebrin
Merge Hoechst
p142 drebrin
fascin
Merge Hoechst

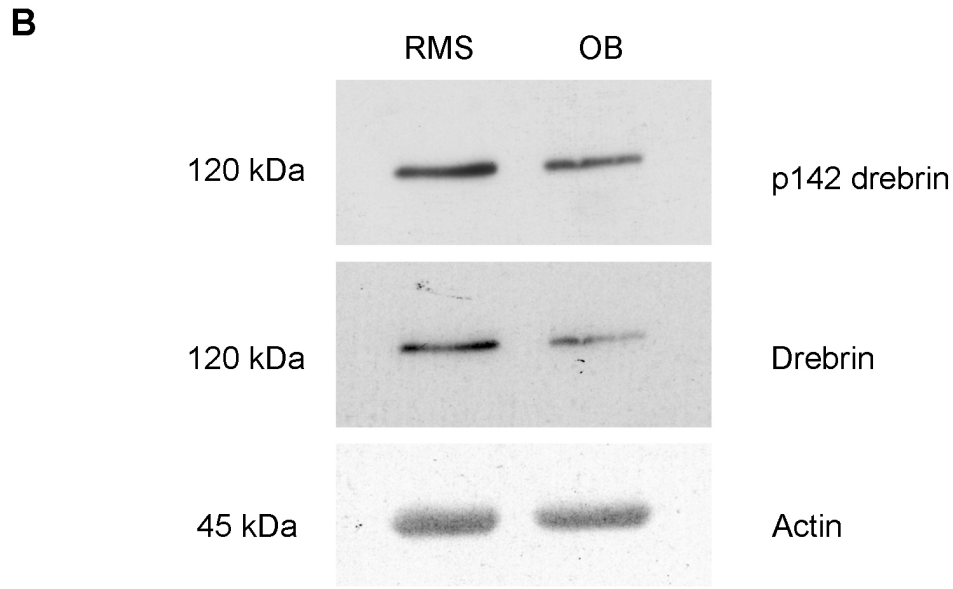

B
RMS
OB
120 kDa
p142 drebrin
120 kDa
Drebrin
45 kDa
Actin

Figure 4-14. Drebrin is phosphorylated on S142 in RMS migrating neuroblasts.

(A), (top, row), Rat RMS neuroblasts were immunostained for drebrin pS142 (green, arrowheads) and βIII tubulin (red, arrows). Drebrin pS142 is concentrated along the membrane of the leading process and in a specific region at the tip of the leading process. Nuclei are stained with Hoechst (blue). (A), (middle, row), Rat RMS neuroblasts were immunostained for drebrin pS142 (green) and drebrin (red). Nuclei are stained in blue with Hoechst. (A), (bottom, row), Rat RMS neuroblasts were immunostained for drebrin pS142 (green, arrowheads) and fascin (red). Fascin and drebrin show colocalisation at the basal side of the filopodia. pS142 drebrin is excluded from most of the filopodial structures and is also evident along the membrane of the leading process. Nuclei are stained with Hoechst (blue). (B), Western blots of RMS and OB homogenates from P7 rat pups probed for drebrin, pS142 and actin (as loading control) show detectable levels of drebrin and pS142 drebrin in both RMS and OB. Scale bars: (A) top row, 10 μm; middle row, 5 μm; bottom row, 10 μm.

4.2.12 Drebrin phosphorylation on S142 regulates neuroblast morphology *in vitro*

The high levels of pS142 drebrin observed in neuroblasts suggest a functional role for drebrin phosphorylation on this site in these highly migratory cells. We therefore nucleofected RMS neuroblasts with a YFP-tagged phosphomimetic drebrin variant, S142D (where S has been mutated to D), or a non-phosphorylatable variant, S142A (where S has been mutated to A) (Worth et al., 2013). Neuroblasts were also nucleofected with a plasmid encoding a human wild type drebrin (drebrin wt), to examine the effects of drebrin overexpression, and the empty vector as a control. Nucleofected cells were then re-aggregated overnight, embedded the following morning and fixed 24 hours later to analyse migration. Colour images of anti-GFP immunostained re-aggregated neuroblast clusters were converted to grayscale mode to better visualize GFP+ cells migrating out of the clusters (Figure 4-15, (A)). We did not detect significant differences in neuroblast migration *in vitro* since cells expressing YFP-tagged wild-type drebrin, S142A or S142D migrated in a similar manner to control YFP-expressing neuroblasts (Figure 4-15, (B)).

Interestingly, although we could not detect a difference in the migration of neuroblasts nucleofected with wt or drebrin phosphomutants, we noticed a difference in leading process length (Figure 4-16, (A)). In particular, although both phosphomutants and drebrin wt had a significantly shorter leading process compared to control cells (Figure 4-16, (B)), there were differences between the phosphomutants. Indeed, both S142A and drebrin wt-expressing neuroblasts displayed an even shorter process compared to S142D-expressing cells (Figure 4-16, (B)).

In summary, neither drebrin overexpression nor drebrin S142 appeared to have a role in controlling neuroblast migration *in vitro*, but they both controlled neuroblast morphology *in vitro*. In particular, similarly to control cells, the S142D transfected cells have a longer leading process compared to S142A or wt drebrin. These data suggest that the actin-bundling and microtubule binding ability regulated by phosphorylation of drebrin on S142 actin-bundling function could be involved in

controlling leading process length. Moreover, our data suggest that drebrin expression levels need to be tightly regulated to control neuroblast morphology.

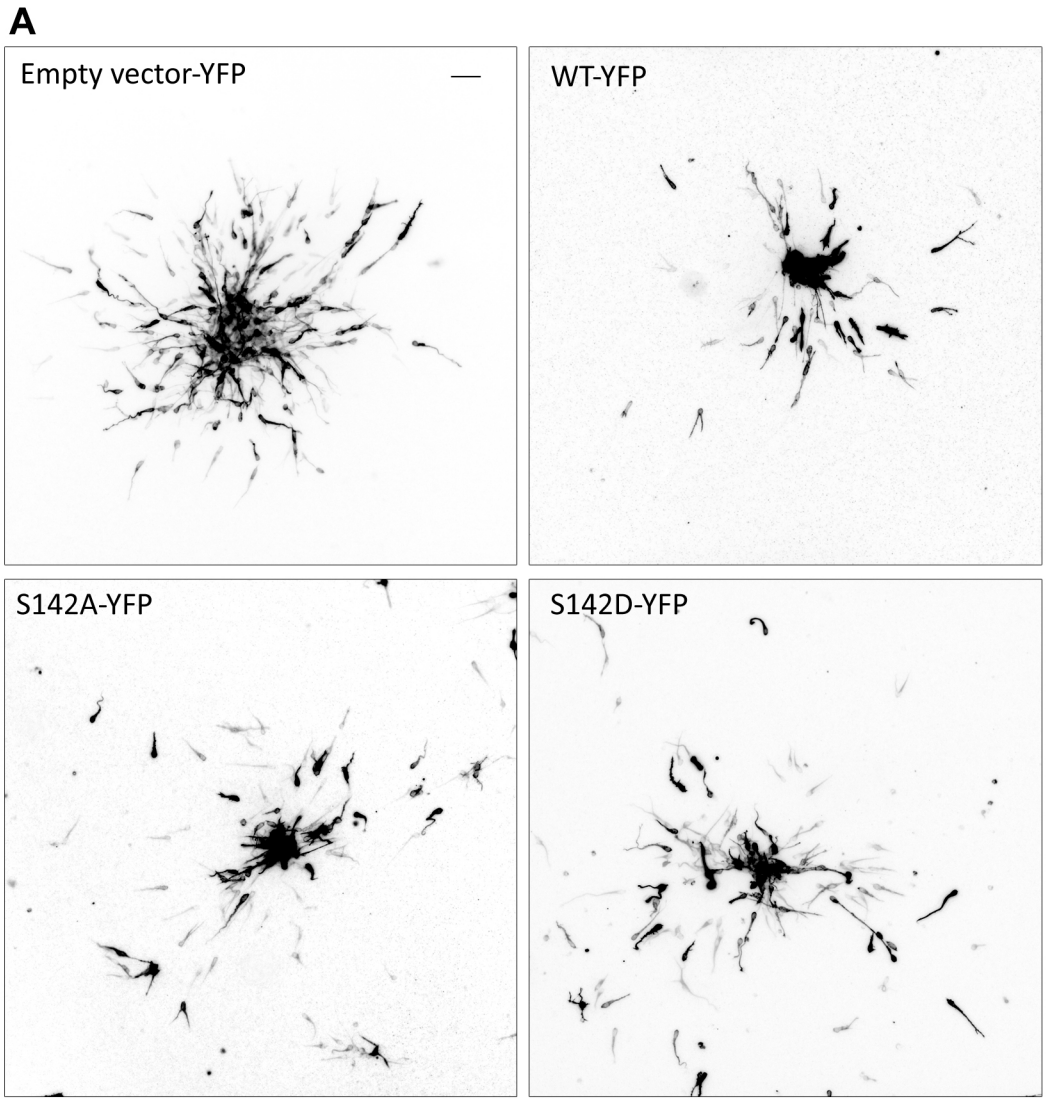
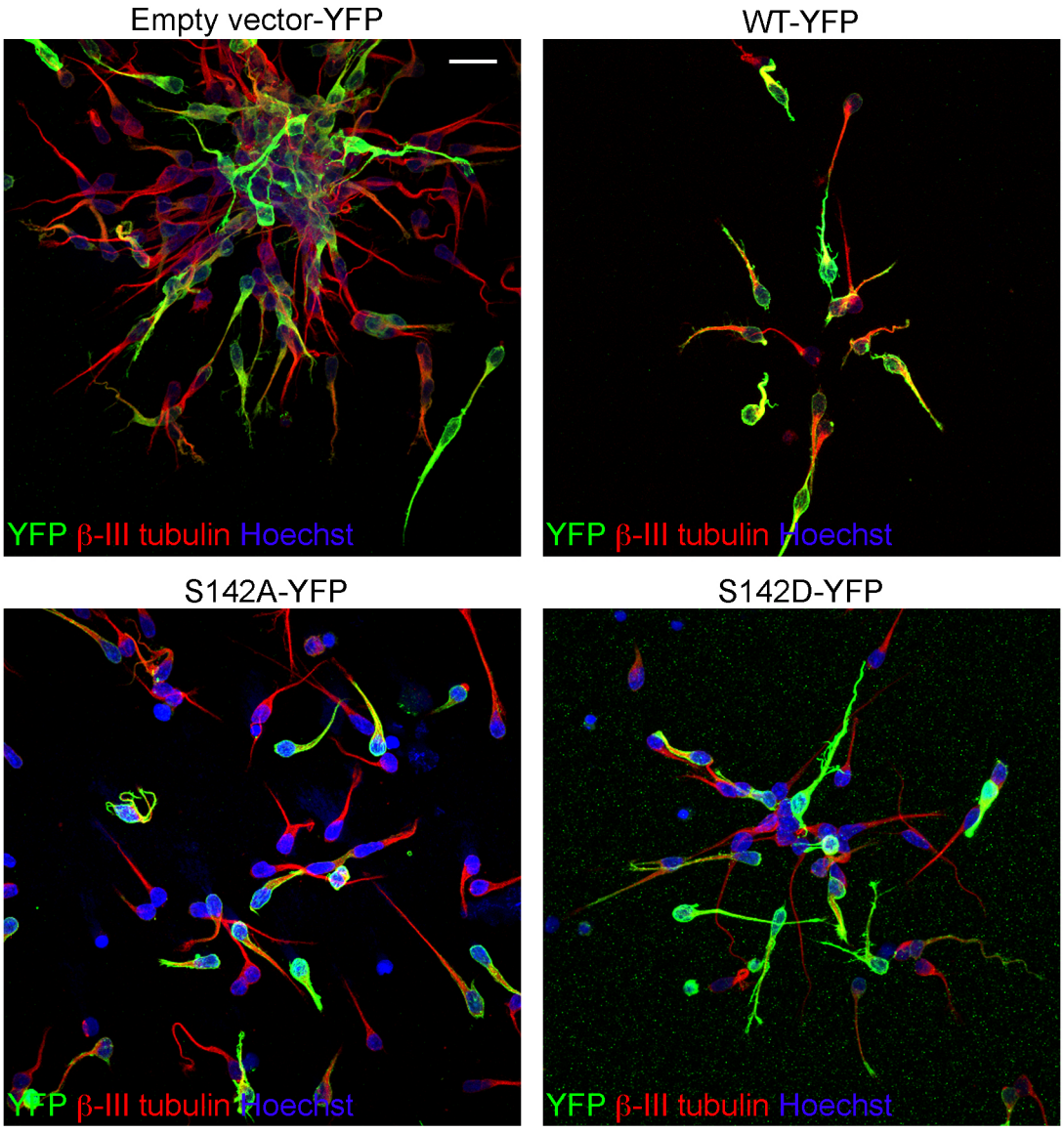

A
Empty vector-YFP
WT-YFP
S142A-YFP
S142D-YFP
B
Relative migrated distance
1.2
1.0
0.8
0.6
0.4
0.2
0.0
YFP
WT
S142A
S142D

Figure 4-15. Altering the phosphorylation state of drebrin on S142 does not affect RMS neuroblast migration *in vitro*.

(A), Representative pictures of rat neuroblasts nucleofected with empty vector, or YFP-tagged wt, S142A, or S142D drebrin. The GFP channel is shown as a grayscale image. (B), Quantitative analysis from fixed samples shows no significant effect on migration distance for neuroblasts expressing the wt or drebrin phosphomutants compared to control cells (mean ± SEM; n=4, between 15 and 20 reaggregates were counted in each experiment). Scale bar, 50 μm.


Empty vector-YFP
WT-YFP
S142A-YFP
S142D-YFP
YFP β-III tubulin Hoechst
YFP β-III tubulin Hoechst
YFP β-III tubulin Hoechst
YFP β-III tubulin Hoechst

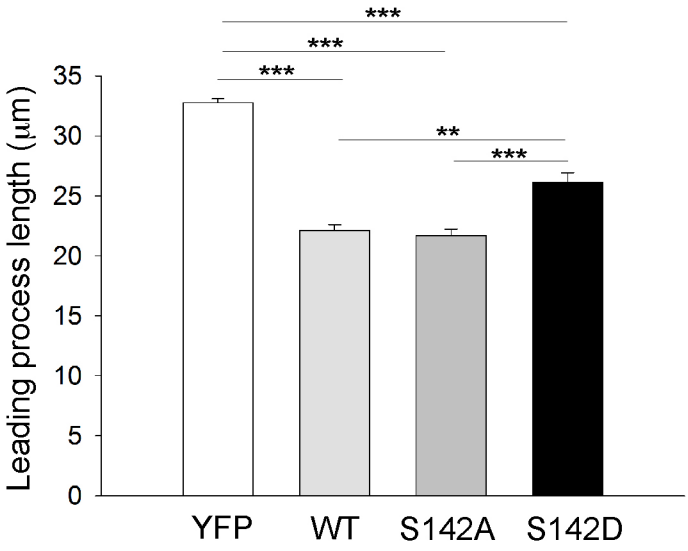

***
***
***
**
***
Leading process length (μm)
35
30
25
20
15
10
5
0
YFP
WT
S142A
S142D

Figure 4-16. Drebrin pS142 regulates RMS neuroblast morphology *in vitro*.

(A) Confocal images show rat RMS reaggregated neuroblasts nucleofected with empty vector, drebrin wt, S142A or S142D and immunostained for YFP (green) and βIII tubulin (red). Nuclei are stained with Hoechst (blue). (B) Control neuroblasts have a longer leading process compared to cells overexpressing wt, S142A or S142D drebrin. Wt and S142A drebrin-expressing cells have significantly shorter processes compared to S142D and the empty vector (mean ± SEM; n=4 independent experiments. 251 cells analysed for empty vector, 262 for wt and S142A drebrin and 400 for S142D; *p<0.05). Scale bar: 20 μm.

4.2.13 Drebrin phosphorylation on S142 regulates neuroblast migration *ex vivo*

To examine the role for drebrin phosphorylation on Ser142 in neuroblast migration *ex vivo*, we carried out postnatal electroporations of either empty vector, wt, S142A or S142D drebrin in P2-3 mouse pups as previously described (Boutin et al., 2008, Sonego et al., 2013b). Animals were sacrificed 5 days later and brains were sliced in 300 µm-thick sections. Only intact brain slices displaying fluorescent signal along the entire RMS were cultured and used for time-lapse imaging. Migration was monitored every 3 minutes for a total period of 3 hours using a spinning-disk confocal microscope (supplementary movies 10, 11, 12 and 13). Tracking analysis allowed visualization of cell trajectories and revealed that control YFP-expressing cells displayed a more directed and less exploratory motile behaviour compared to wt-, S142A- or S142D-expressing cells (Figure 4-17, (A)). Differences between drebrin wt and both phospho-mutants reveal a specific role for S142 in regulating neuroblast migration *ex vivo*. In particular, S142D and drebrin wt show a decrease in migration distance (Figure 4-17, (B)), displacement (Figure 4-17, (C)), and velocity (Figure 4-17, (D)) in comparison to S142A. Instead no significant differences were detected in the migratory index (Figure 4-17, (D)).

Altogether, these data show that drebrin expression levels must be tightly regulated for proper neuroblast migration, but they also suggest a role for drebrin S142 phosphorylation in neuroblast migration *ex vivo*. The actin-bundling and microtubule-binding activity regulated by drebrin phosphorylation is likely to be controlled in a dynamic cycle during neuroblast migration.

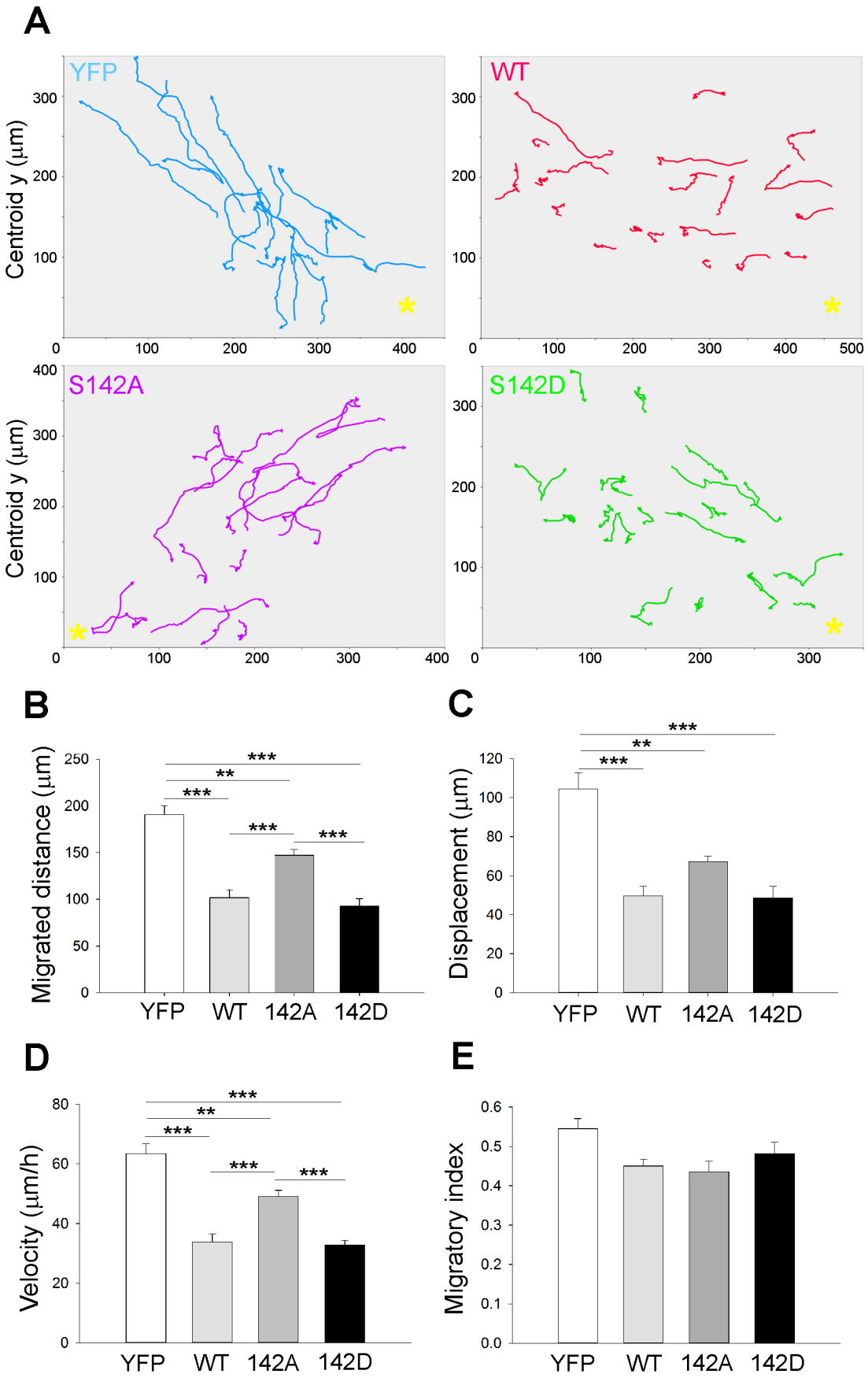

A
YFP
WT
S142A
S142D
Centroid y (μm)
B
Migrated distance (μm)
C
Displacement (μm)
D
Velocity (μm/h)
E
Migratory index
YFP
WT
142A
142D

Figure 4-17. Drebrin phosphorylation on Ser142 regulates neuroblast migration *ex vivo*.

(A), Representative migratory paths from time-lapse imaging of neuroblasts migrating within the brain slice and expressing YFP-tagged empty vector, wt, S142A, or S142D drebrin over a period of 3 h. Yellow asterisks mark the location of the OB. Please see also supplementary movies 10, 11, 12 and 13. (B-E), Quantitative tracking analysis shows that although control neuroblasts display a longer migration distance (B), displacement (C) and greater velocity (D) compared to cells expressing wt and phospho-mutant drebrin, S142D and wt-expressing cells migrate over a shorter distance (B) and have lower speed (D) compared to S142A. No significant difference was detected in the migratory index (E) (mean ± SEM; n=6 brains for control; n=5 brains for wt; and n=4 brains for S142A and n=5 for S142D; **p<0.01; ***p<0.001).

4.2.14 Drebrin phosphorylation on S142 regulates neuroblast orientation *in vivo*

To further explore the effect of drebrin overexpression and its phosphorylation on S142 on neuroblast morphology and directionality *in vivo*, brains from animals electroporated with the empty vector or with plasmids encoding YFP-tagged wt, S142A or S142D drebrin were fixed and immunostained for YFP 5 days after electroporation. Neuroblasts transfected with the empty vector encoding only YFP showed a similar morphology to neuroblasts transfected with pCX-EGFP or control shRNA (see Chapter 3, Figure 3-16 and Figure 3-21) with a vast majority having a straight and long leading process oriented towards the OB (Figure 4-18, (A), top left). Instead, neuroblasts expressing wt, S142A and S142D drebrin had a visibly different morphology compared to control cells (Figure 4-18, (A), arrowheads). Leading process lengths were shorter for wt, S142A and S142D compared to control cells (Figure 4-18, (B)). More than 95% of control cells expressing only YFP have a leading process oriented towards the OB (Figure 4-18, (C)). Expression of S142A and S142D drebrin significantly affected neuroblast orientation (Figure 4-18, (C)), while expression of wt caused a substantial increase in the percentage of cells having two protrusions extending from the cell body (one oriented towards the OB and the other perfectly opposite oriented towards the SVZ) (Figure 4-18, (D)). Although this difference in orientation was quite noticeable, neuroblasts appeared still able to migrate along the RMS and reach the OB (data not shown).

In conclusion, these data suggest that drebrin S142 phosphorylation could play a role in orienting the leading process towards the OB and that a tight regulation of phospho/dephospho drebrin may be required for the correct neuroblast orientation. Moreover, drebrin seems to regulate the unipolar morphology of these cells, as its expression levels need to be controlled for the maintenance of a single leading process oriented towards the OB.

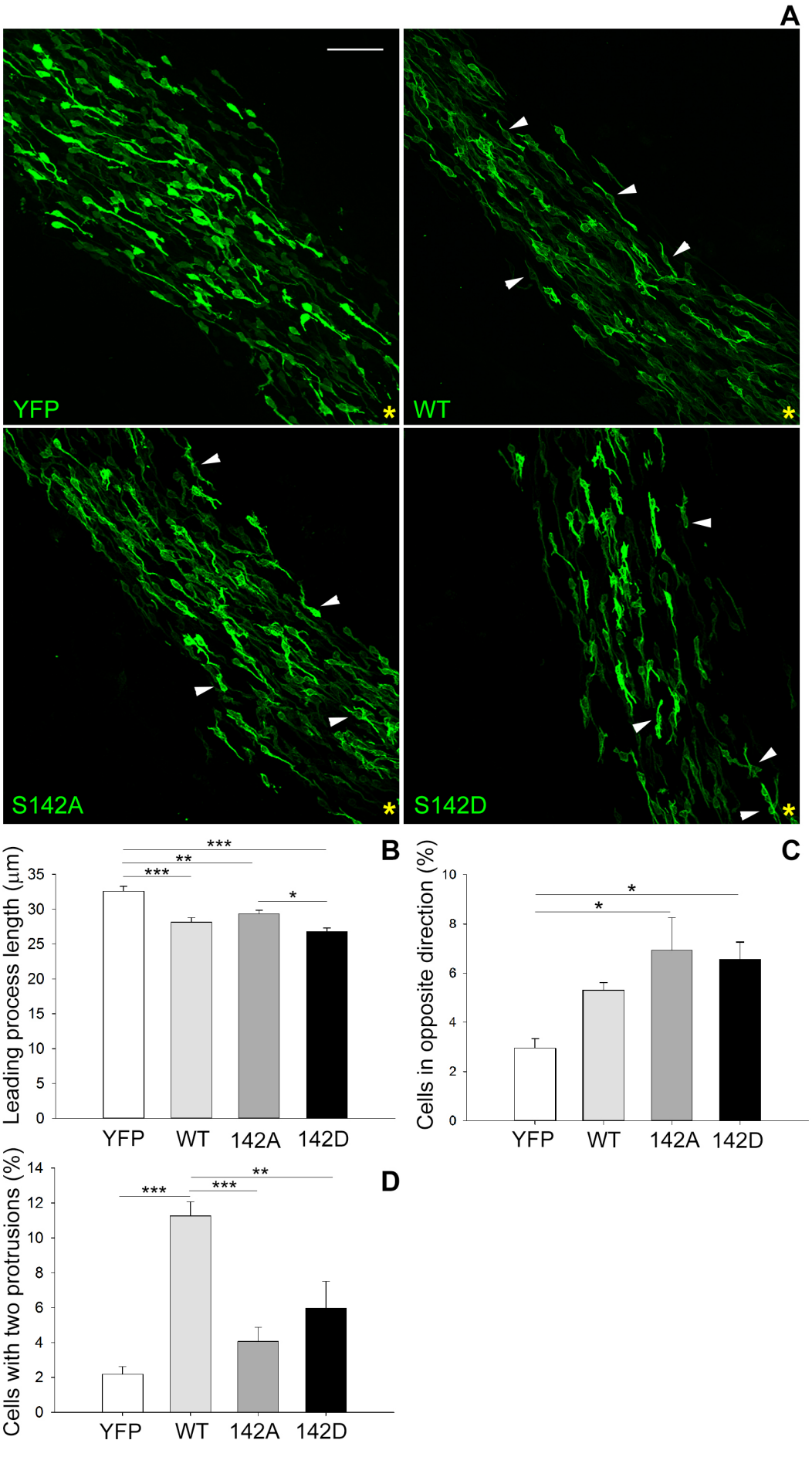

A
YFP
WT
S142A
S142D
B
Leading process length (μm)
C
Cells in opposite direction (%)
D
Cells with two protrusions (%)
YFP
WT
142A
142D

Figure 4-18. Drebrin phosphorylation on S142 regulates neuroblast morphology and orientation *in vivo*.

(A), Confocal z-stack projections of P2-3 mouse brain slices electroporated with empty vector (top left), or vectors expressing wt (top right), S142A (bottom left), or S14D (bottom, right) drebrin show control cells with a single leading process oriented towards the OB (top left) in contrast to neuroblasts expressing wt (top right, arrowheads), S142A (bottom left, arrowheads) or S142D drebrin (bottom, right; arrowheads) that displayed misoriented processes. The yellow asterisk marks the location of the OB. (B), Quantitative morphological analysis shows a decrease in leading process length for wt, S142A and S142D compared to the control, and a slight decrease for S142D compared to S142A-expressing cells. (C) Expression of either S142A or S142D drebrin significantly increases the percentage of misoriented cells (pointing towards the SVZ instead of the OB). (D) Overexpression of drebrin increases the number of cells with two protrusions (one towards the OB and towards the SVZ) compared to control, S142A and S142D (mean ± SEM; *p<0.05; **p<0.01; ***p<0.001; n=8 brains for empty vector; n=5 brains for drebrin wt, S142A, and S142D). Scale bars: (A), 50 μm.

4.2.15 Investigating the regulation of drebrin phosphorylation on S142

Having identified S142 as a site that may potentially be regulated for the efficient directed migration of neuroblasts, we next focussed on the signalling mechanisms regulating the phosphorylation of this drebrin residue during neuroblast migration. Neuroblast motility is modulated by several factors (Introduction chapter). We have recently showed that endocannabinoid signaling regulates neuroblast migration *in vitro* and *ex vivo* (Oudin et al., 2011). The modulation of the fascin/PKC interaction may be one event acting downstream CB receptor activation (Sonego et al., 2013a). In this study we also decided to examine the effects of FGF-2 signaling, which can be modulated by CB1 receptor in neurite outgrowth (Williams et al., 2003). Moreover, FGF-2 appears to regulate neuroblast migration in a caudo-rostral gradient manner as well as increasing neuroblast migration in RMS explants *in vitro* ((Garcia-Gonzalez et al., 2010), Oudin, unpublished data).

We therefore tested whether CB1 receptor or FGF-2 signaling could modulate S142 drebrin phosphorylation in neuroblasts. RMS neuroblasts were either plated on p35 plastic dishes coated with polyornithine and laminin or embedded in Matrigel. Cells were then incubated with the CB1 agonist ACEA (0.5 µM) or with the CB1 antagonist AM-251 (0.5 µM) for 30 or 60 minutes. Incubation with FGF-2 (20 ng/µl) lasted 60 minutes.

Western blots were performed to measure levels of pS142 and total drebrin (Figure 4-19, (A)). While it was possible to detect drebrin phosphorylation on S142 in control conditions, no significant change in phosphorylation levels was detected after treatment with ACEA or FGF-2 (Figure 4-19, (B)). Similarly, incubation with AM-251 did not show any reproducible change (Figure 4-19, (B)).

To examine whether treatment with ACEA or AM-251 caused relocalisation of pS142, co-immunostaining for pS142 and βIII tubulin was also performed. No difference in localization was found in any of the treatments and pS142 was still able to concentrate at the tip of the leading process even in cells displaying multiple secondary branches (data not shown).

In summary, in our experimental conditions neither FGF-2 nor modulation of cannabinoid signalling affected the phosphorylation levels of drebrin on S142 in neuroblasts. Further studies will be required not only to completely exclude a role

for endocannabinoids or FGF-2 in the regulation of drebrin phosphorylation, but also to identify other upstream signals potentially controlling this event in migratory neuroblasts.

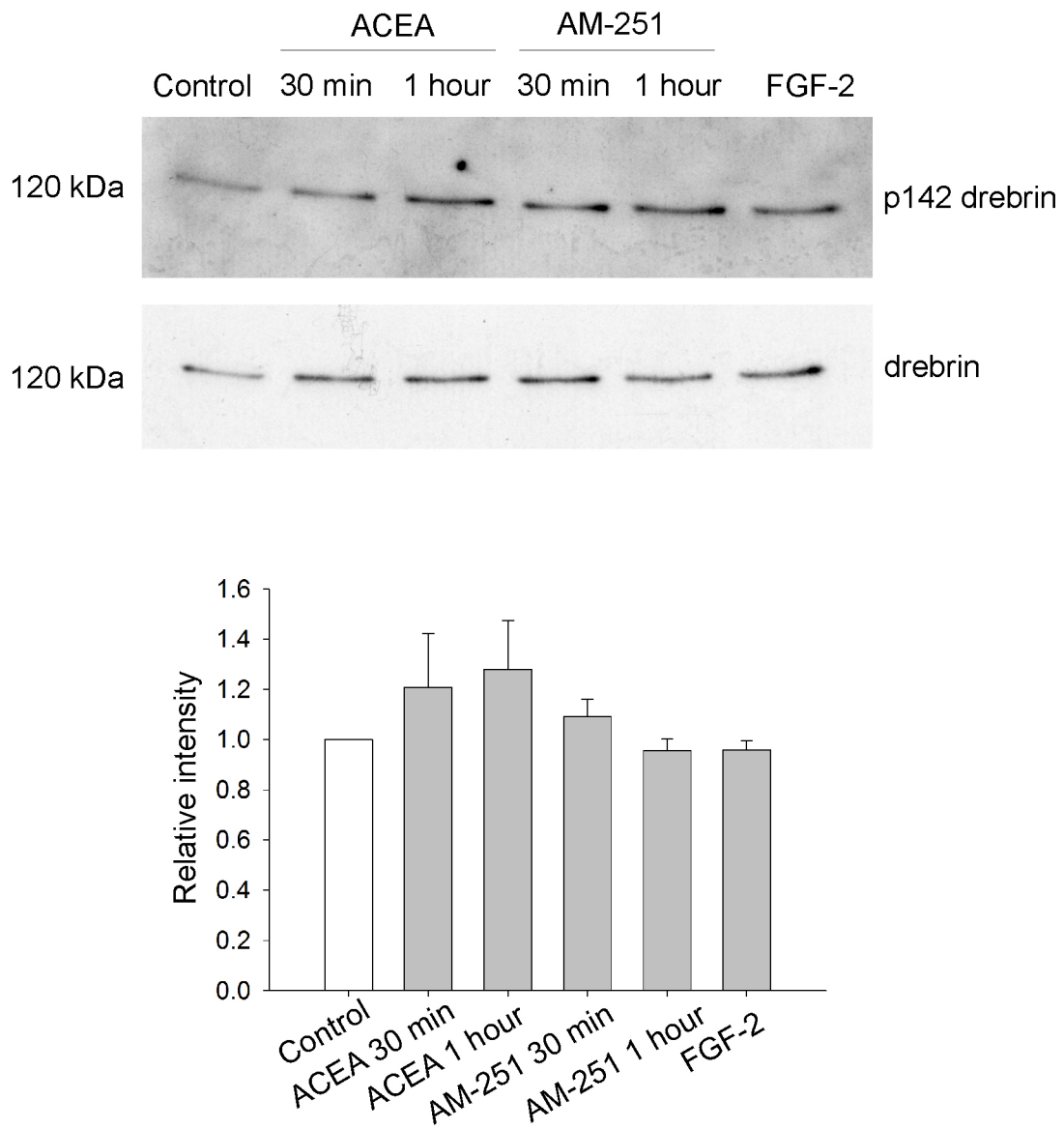


Figure 4-19. Endocannabinoid signalling and FGF-2 do not appear to regulate phosphorylation of drebrin on S142 in migrating neuroblasts.

(A) WBs of cell lysates from rat RMS neuroblasts treated with ACEA (0.5 µM), AM-251 (0.5 µM), or FGF-2 (20 ng/µl) were probed for pS142 and total drebrin. (B) Densitometric analysis shows that ACEA, AM-251 and FGF-2 treatments do not significantly change the levels of drebrin phosphorylation on S142.

4.3 Discussion

In the previous chapter we explored the role of cytoskeletal rearrangements in migrating neuroblasts, focusing on the function of the actin-bundling protein fascin. We discovered the importance of actin-bundling activity at the process tip in RMS neuroblast migration.

In this chapter we uncovered a role for another major actin-binding protein in the brain, drebrin. We found that drebrin regulates neuroblast migration *in vitro* and *in vivo* through its actin-bundling function, which was recently shown to be regulated by phosphorylation on S142 (Worth et al., 2013).

4.3.1 Drebrin expression in migrating neuroblasts

Drebrin is one of the major actin binding protein in the brain, and is highly expressed in the RMS of adult mice (Song et al., 2008). We extended these initial observations by confirming that drebrin is upregulated in migrating neuroblasts also in early postnatal stages. Drebrin co-localises with the migrating neuroblast marker, Dcx, but not with the astrocytic/stem cell marker GFAP and only partially with Mash1-positive proliferative progenitors. We have, moreover, examined the sub-cellular distribution of drebrin in RMS neuroblasts, and found that this protein is expressed throughout the leading process, but is especially concentrated along the membrane and in a particular region of the process tip before peripheral filopodia (Figure 4-14). A recent study has reported that drebrin is essential for the entry of microtubules in dendritic spines of embryonic hippocampal neurons (Merriam et al., 2013). Whether drebrin is needed for entry of the microtubules in the distal region of the leading process during neuroblast migration remains unknown.

pS142 drebrin is also found along the leading process membrane and in a limited area at the tip of the leading process preceding the peripheral filopodia. This area is very reminiscent of the “transition zone (T-zone)” located between the central and peripheral domains found in growth cones of developing neurons (Geraldo et al., 2008, Mizui et al., 2009). Interestingly, while F-actin localises in the peripheral zone as well as the T-zone and microtubules localise mainly in the central domain and in

the proximal part of the T-zone, drebrin localise in the T-zone, interfacing F-actin and microtubules (Mizui et al., 2009).

Drebrin co-localises with F-actin and fascin at the roots of filopodia in growth cones of cortical neurons and PC12 cells, respectively (Sasaki et al., 1996, Geraldo et al., 2008). Interestingly, while drebrin is expressed in the transition zone of the growth cone in neurons, pS142 does not show expression in that zone, but instead appears to localise more peripherally in proximity to the filopodia (Worth et al., 2013). In line with these previous discoveries, we have also found that both drebrin and pS142 drebrin co-localise with F-actin and fascin at the tip of the leading process in the basal side of the filopodia. Although it is evident that drebrin and pS142 drebrin co-localise in migrating neuroblasts, it seems that there is a greater co-localisation with fascin and pS142 drebrin. This observation, however, needs to be clarified with more detailed investigations. Further studies are needed to understand whether the actin-bundling function of pS142 drebrin can stabilise of F-actin bundles at the base of growing filopodia, allowing, for instance, fascin actin-bundling function to take place.

4.3.2 Drebrin function in migrating neuroblasts

We have reported a new role for drebrin in regulating neuroblast migration in a cell-autonomous manner *in vitro* and *ex vivo*, using two different genetic methods and a pharmacological approach. Drebrin has been seen to regulate migration of oculomotor neurons (Dun et al., 2012) and glioma cells (Terakawa et al., 2013) through formation and maintenance of cell morphology. This seems to be the case also in migrating neuroblasts. It has been previously reported that the polarised neuroblast morphology is necessary for efficient neuroblast migration (Koizumi et al., 2006, Oudin et al., 2011, Sonego et al., 2013a). Along this line, we have seen that drebrin regulates polarised neuroblast morphology and migration *in vitro* and *ex vivo*. Indeed, lack of drebrin leads to an increase in the percentage of cells with secondary branches as well as cells with longer leading processes. Moreover, drebrin-depleted cells are impaired in their migration distance, displacement and speed. Interestingly, also drebrin overexpression leads to impairment in neuroblast migration and to an unpolarised morphology. This leads us to the conclusion that

drebrin has a specific and cell-autonomous role in controlling morphology and migration of RMS neuroblasts and, in particular, its levels must be tightly regulated in order to achieve an efficient coordination of these events.

4.3.3 Ser142 function in migrating neuroblasts

We have uncovered a new role for drebrin phosphorylation on Ser142. We show that pS142 plays a role in controlling neuroblast migration; in particular, the phosphomimetic variant decreases neuroblast migration compared to the non-phosphorylatable variant. Interestingly, the fact that S142D and S142A act in an opposite manner is in line to what has been previously shown by Worth et al. (2013), where phosphorylation on S142 increases actin-bundling and thus neuritogenesis in cortical neurons. In our model, S142D may impair neuroblast migration by having a dominant negative effect on filopodia disassembly.

Our current hypothesis is that drebrin in its unphophorylated form could act as a destabiliser. Indeed, it has been previously shown that drebrin inhibits tropomyosin, fascin and actinin binding to actin, thus destabilising actin filaments (Ishikawa et al., 1994, Sasaki et al., 1996). In contrast, S142-phosphorylated drebrin may act as a stabiliser, bundling F-actin and thus giving support for adhesiveness. Moreover phosphorylation of drebrin on S142 opens the drebrin structure exposing a site that can be bound by EB3 (Worth et al., 2013). As EB3 is a microtubule-binding protein we are tempted to speculate that S142-phosphorylated drebrin could act as an intermediate between actin filaments and EB3, perhaps promoting the invasion of the microtubules in the advancing leading edge. Lifetime microscopy as well as time-lapse imaging in migrating neuroblasts expressing drebrin and EB3 could help clarify the dynamics of drebrin-EB3 interaction and its role during neuroblast migration.

Since migration is a dynamic process that requires adhesion and retraction (Schaar and McConnell, 2005), a dynamic regulation of drebrin, switching between the phosphorylated and unphosphorylated form may give the leading process and its growth cone the plasticity required for sensing the environment before the movement of the cell body.

Interestingly, phosphorylation of drebrin on S142 is regulated by Cdk5, a well-known kinase controlling neuronal migration in the neocortex (Ohshima et al., 1996, Chae et al., 1997). Importantly, Cdk5 also regulates neuroblast migration in the postnatal brain (Hirota et al., 2007). In parallel with our findings on drebrin, Cdk5 is required for proper extension of the leading process (Hirota et al., 2007). Moreover, Cdk5 is regulated downstream of GDNF, a chemoattractant factor promoting migration along the RMS (Paratcha et al., 2006). It would be important to investigate whether this kinase has a role in regulating drebrin phosphorylation on S142 also in neuroblasts and to characterize the factors regulating this signaling event in the RMS.

It is interesting to point out that drebrin, and in particular pS142 drebrin, is also localised on the membrane of the leading process of migrating neuroblasts. This localisation, together with our discovery that drebrin is required for neuroblast polarisation leads us to think that drebrin may also regulate intercellular contacts in the chains of migrating neuroblasts. At this regard, drebrin has been involved in regulating adhesion in different contexts. For example in epithelial cells, keratinocytes and basal cell carcinomas, drebrin is highly expressed in adherent junctions (Peitsch et al., 1999, Peitsch et al., 2005). Drebrin also plays a role in stabilising nectin at adherent junctions, thus regulating intercellular contacts in endothelial cells (Rehm et al., 2013). In non-neuronal cells drebrin can also stabilise connexin 43-containing gap junctions (Butkevich et al., 2004). Moreover, it is worth to point out that Cdk5, which can phosphorylate drebrin on S142 (Worth et al., 2013), is required for the formation of chains during neuroblast migration (Hirota et al., 2007). Interestingly, we noticed that treating RMS explants with the drebrin-binding drug BTP (Mercer et al., 2010) reduces the migration of these cells out of the explants, while treating RMS re-aggregates with BTP does not interfere with their migration. This effect has prevented us from understanding whether BTP impairs migration specifically through drebrin using mutant forms of drebrin that bind or do not bind BTP (Mercer et al., 2010). The failure of BTP to stop RMS migration in the re-aggregates (data not shown) might be explained by the loss of specific contacts caused by the dissociation of neuroblasts, a necessary step before their nucleofection. Indeed, rat nucleofected neuroblasts have a lower tendency to

form chains during their migration in Matrigel compared to RMS tissue explants (data not shown). Surely a full understanding of whether drebrin is involved in neuroblast chain formation through gap junction stabilisation needs further investigations that would ideally include three-dimensional migration assay of RMS explants dissected from drebrin knockout animals.

An extra clue for a potential function for drebrin in regulating intercellular contacts comes from its ability to interact with the C-terminal domain of connexin-43 (Butkevich et al., 2004). Importantly, deletion of connexin-43 C-terminal domain decreases neuronal migration in the neocortex (Cina et al., 2009). Connexin-43 is also highly expressed along the RMS (Hobbs C., unpublished data) and in specific areas along the membrane of the neuroblast leading process, with a particularly high concentration between cells migrating in chains (Sonego M., unpublished data). The possibility that drebrin may be a key player for the dynamic coordination between cytoskeletal rearrangements and intercellular contacts for the efficient chain migration of neuroblasts will need to be further investigated.

In conclusion, we have shown that drebrin, and in particular pS142, is found along the membrane and in a restricted area at the tip of the leading process in migrating neuroblasts. Drebrin has a cell-autonomous role in regulating polarised neuroblast morphology and efficient neuroblast migration, which is also influenced by drebrin phosphorylation on S142. We propose the existence of a cycle between the phosphorylated (required for adhesiveness/process elongation) and unphosphorylated (required for retraction) form of drebrin during polarised neuroblast migration along the RMS.

Chapter 5 General Discussion

5.1 The importance of studying migration in neurogenesis

The SVZ/RMS/OB system is a powerful model for the study of the different processes involved in postnatal neurogenesis: proliferation of NS cells in the SVZ, migration of neuroblasts along the RMS and differentiation of these cells into neurons in the OB. In this project we focused on one aspect of SVZ neurogenesis: the migration of neuroblasts along the RMS. The importance of studying this process is twofold: in physiological conditions, migration is an essential event for the correct integration of newborn neurons into the synaptic circuit (Belvindrah et al., 2011) and in pathological conditions, neuroblasts have the ability to leave their natural route and migrate towards sites affected by injury and/or neurodegeneration (Arvidsson et al., 2002, Tattersfield et al., 2004, Zhang et al., 2007). Interestingly, in the human brain RMS migration is very prominent in early infancy, an important time for postnatal brain development (Sanai et al., 2011). Moreover, in the adult human brain neuroblasts and new neurons are found in the striatum adjacent to the SVZ whereas they are almost absent in the OB, suggesting that newborn neurons may change direction of migration once the olfactory system is fully developed (Spalding et al., 2013, Ernst et al., 2014).

In the past decade many studies have investigated extracellular factors such as chemoattractants or chemorepellents involved in modulating neuroblast migration. However, few reports have focused on the intracellular mechanisms underlying this type of cell motility, an important aspect for the exploitation of the therapeutic potential of these cells. We have discovered that two actin modulators, fascin and drebrin, are required for polarised neuroblast migration.

5.2 RMS migration *in vitro* and *ex vivo*

To investigate the role of fascin and drebrin in neuroblast migration we have used a wide range of techniques *in vitro* as well as *ex vivo*, that allowed us to validate our results in a more physiological experimental system.

To recreate RMS neuroblast migration *in vitro* we have adopted a 3-dimensional migration assay using a Matrigel matrix. This widely used technique allows to recapitulate *in vitro* the neuroblast "chain migration" observed in the intact brain (Wichterle et al., 1997, Ward and Rao, 2005). We combined this assay with DNA/siRNA nucleofection (Falenta et al., 2013) to study the effect of protein knockdown or overexpression on neuroblast morphology and motility *in vitro*.

While the Matrigel migration assay is a powerful method that led us to preliminary discoveries of proteins involved in migration (i.e. fascin and drebrin), it obviously has the limitations of an *in vitro* system. The RMS in the intact brain is a complex environment where chains of neuroblasts interact with the surroundings, including astrocytes and blood vessels (Bovetti et al., 2007, Snapyan et al., 2009, Bozoyan et al., 2012). For this reason we have also optimised an *ex vivo* approach, which combines *in vivo* electroporation of young postnatal mice to transfect neural progenitors in the SVZ (Boutin et al., 2008) with time-lapse imaging of their movement in acute brain slices (Nam et al., 2007, Sonego et al., 2013b). *In vivo* postnatal electroporation is a robust and reliable method that offers efficient but sparse neuroblast labelling, enabling detailed analysis of cell morphology and migration dynamics (Sonego et al., 2013).

Our findings have shown that fascin and drebrin are each essential for polarised neuroblast morphology and migration. Moreover, a tighly-regulated phospho-dephosphorylation cycle for fascin at Ser39 or for drebrin at Ser142 may be required to ensure efficient neuroblast migration. Interestingly, for both fascin and drebrin we observed a correlation between *in vitro* and *ex vivo* results. For example, fascin knockdown leads to a branched neuroblast morphology in the "fixed" context of the *in vitro* migration assay as well as in the dynamic context of the time-lapse imaging of brain slices. Moreover, altering fascin phosphorylation on Ser39 impairs neuroblast migration to a similar extent *in vitro* and *ex vivo*. Similarly, drebrin

knockdown affects neuroblast morphology and decreases neuroblast migration in RMS reaggregates as well as in brain slices. However, differences between *in vitro* and *ex vivo* experiments were observed between drebrin phospho-mutants. While altering drebrin phosphorylation does not cause any significant effect *in vitro*, *ex vivo* cells expressing S142A migrate significantly more than cells expressing S142D. Moreover, while *in vitro* S142D transfected cells have a longer leading process compared to S142A transfected cells, the opposite effect has been seen *ex vivo* in fixed brain slices (S142A slightly longer than S142D). Since discrepancies of results between the two model systems were seen only in drebrin phospho-mutants, it is plausible that they might be related to the role of drebrin phosphorylation in different migration contexts. It is in fact possible that, due to the specific localisation of S142 phospho-drebrin along the leading process membrane, S142 may also have a role in cell-cell adhesion. The fact that nucleofection *per se* tends to decrease cell-cell adhesion could mask some potential effects on migration *in vitro*. Further studies, including re-expression of drebrin phosphomutants in drebrin-depleted neuroblasts, should help clarify the role of drebrin phosphorylation in neuroblast migration.

Coupling postnatal electroporation with time-lapse imaging has provided a powerful tool to study neuroblast migration within intact brain slices and has yielded important and reliable results (Sonego et al., 2013b). However, analysis of fixed electroporated brain slices has often shown differences compared to time-lapse imaging data. Indeed, time-lapse imaging allows detection of migration defects in neuroblasts knocked down for fascin or drebrin compared to the control. These results were not detected in fixed brain slices, where electroporated cells in fascin or drebrin knockdown reach the OB as they do in the control. One possible explanation of this could be the fact that electroporated cells migrating in the intact brain may have been carried on to the OB by the flow of the surrounding chains of neuroblasts. This speculation is reinforced by experimental evidence carried out by Hu et al. (1996), where PSA-NCAM knockout cells are shown to be capable of migration if transplanted in wild-type animals, while wild-type cells cannot migrate in PSA-NCAM ko mice, indicating that the environment plays a role in guiding neuroblast migration. The authors speculated that actively migrating wild-type cells

might be associating with PSA-NCAM knockout cells, towing them along towards the OB (Hu et al., 1996). Examining whether neuroblast migration is impaired in *drebrin* ko mice and whether wild type neuroblasts have impaired motility when transplanted in a drebrin ko mouse would help address this possibility.

Therefore, while the time-lapse imaging of acute brain slice cultures may be a more reliable method to study whether a protein affects the intrinsic ability of neuroblasts to migrate, the fixed electroporated brain slices offer a snapshot of what happens in the intact architecture of the brain, and thus a powerful tool to investigate cell shape and polarity.

It is important to clarify that while the *in vitro* experiments were performed using rats, the *in vivo* experiments were performed using mice. The reason of using different species for different procedures finds explanations in the limitations of the animal models. For example, dissection of P7 rat RMS yields a higher number of neuroblasts (1 x 10^6 cells/brain) compared to dissection of P7 mouse RMS (5 x 10^5 cells/brain) (Falenta et al., 2013). Since each nucleofection experiment requires about 3 x 10^6 neuroblasts, rats were preferred over mice for the *in vitro* migration assay (Falenta et al., 2013). Moreover, rat neuroblasts show more resistance to the nucleofection procedure compared to mouse neuroblasts (Falenta et al., 2013).

For the opposite reasons, which include size of the animals and the possibility of using transgenics, mouse is a better model to perform *in vivo* electroporation.

Importantly, rats and mice have no differences in the anatomical organization of the RMS and their RMS neuroblasts migrate to a similar extent *in vitro* (Peretto et al., 2005, Falenta et al., 2013). Moreover, using sequence alignments tools an overall 99% homology was identified between *Mus musculus* and *Rattus norvegicus* for both fascin and drebrin, including conservation of the actin binding sites, Ser39 and Ser142 respectively and the aminoacids sourrounding these sites.

While our *in vitro* and *in vivo* techniques are powerful and reliable methods to investigate neuroblast migration defects, we recognise the limitations of the *in vitro*/*ex vivo* approaches. For instance, before embedding in the 3-D Matrigel matrix, nucleofected neuroblasts are reaggregated in a hanging drop for 5 hours and then cultured in suspension for 24 to 52 hours. This time interval has been optimized in our laboratory, since increasing the time in suspension leads to

abnormal changes in cell shape and motility. However, the migration of RMS reaggregates is shorter and slower than the migration of RMS explants (Falenta et al., 2013, Oudin et al., 2011). In addition, it is important to mention that the 3-D Matrigel matrix used to embed neuroblasts derives from the Engelbroth-Holm-Swarm mouse sarcoma and is composed by laminins, collagen, fibronectin and proteoglycans. The heterogeneous composition of this matrix may change depending on the source, however, we found that different batches showed high reproducibility of results.

The fact that the complex architecture of blood vessels and astrocytes that characterise the RMS is absent in the *in vitro* assay is the major limiting factor of this technique. While using *in vivo* electroporation has partially addressed this issue, further optimisation of co-cultures systems could help recapitulate *in vitro* much more closely the cell-cell interactions present the intact RMS.

Coupling *in vivo* electroporation with spinning-disk confocal time-lapse imaging is a powerful system, which enables to preserve at least some of the physiological RMS architecture and monitor neuroblast soma and leading process movement at high resolution. On the other hand, in our hands filming time is limited to no more than 4 hours per brain slice with an imaging rate not exceeding 3 minutes to avoid phototoxicity. However, in this relatively short time interval the majority of the neuroblasts appear to be alive and migratory. Further development of imaging technologies (*e.g.* employing multiphoton imaging through a cranial window of a living mouse) will allow analysis of neuroblast migration in a truly “in vivo” context compared to the use of brain slices.

5.3 Fascin and drebrin in neuroblast migration

Fascin and drebrin are major actin binding proteins in the brain. Fascin is capable of organizing F-actin in parallel tight bundles, forming filopodia (Vignjevic et al., 2003). Drebrin can also bundle actin (Worth et al., 2013), but its expression is confined at the basal side of filopodia (Sasaki et al., 1996, Worth et al., 2013).

Using primary cultures of RMS migrating neuroblasts we have discovered that, while fascin concentrates in two specific areas, in front of the nucleus and along peripheral filopodia, drebrin is enriched along the cell membrane and on a particular region at the tip of the leading process preceding the peripheral filopodia. Fascin and drebrin seem to co-localise at the roots of filopodia. Interestingly, both proteins appear to control leading process branching, which can originate from both proximal and distal areas of the leading process (Figure 3-11; Figure 4-11).

Although it has been demonstrated before that fascin and drebrin inhibit each other in binding to actin (Sasaki et al., 1996), we have not observed down-regulation of drebrin when fascin was overexpressed or up-regulation of drebrin after fascin knockdown (or vice versa), using either immunostaining or Western blot. Therefore our primary focus was on understanding the intrinsic role of these two proteins, which we studied separately, in neuroblast migration.

Based on our preliminary immunohistochemistry results we could speculate that drebrin phosphorylation at Ser142 might stabilise F-actin at the basal side of growing filopodia, allowing drebrin to bundle actin filaments. This stability at the root of the filopodia might lead to dephosphorylation of fascin, which would in turn bundle F-actin, elongating and stabilizing filopodia. On the other hand, unphosphorylated drebrin might act as a destabiliser of actin bundles and thus interfere with fascin actin-bundling activity and formation of filopodia by promoting fascin phosphorylation. The use of a specific anti-phosphofascin antibody (currently unavailable) would help address these hypotheses.

It remains, however, unclear whether fascin and drebrin play an antagonistic or a cooperative role in regulating neuroblast migration. It would be interesting to pursue the hypothesis of a link between fascin and drebrin in future research using

biochemistry assays, such as pull-down and Western blots as well as imaging techniques, such as FLIM, to spatially identify their potential interaction.

5.3.1 Fascin in neuroblast migration

Fascin is highly expressed in the brain of rodents and humans, in particular in microglia, neurons and astrocytes (Edwards and Bryan, 1995, Roma and Prayson, 2005). In neuronal cells fascin localises in the filopodial structures of the growth cones (Mosialos et al., 1994) and has a role in neurite extension and growth cone dynamics (Cohan et al., 2001, Yamakita et al., 2009, Nagel et al., 2012). Moreover, fascin is associated with increased cell migration as well as invasion in glioblastomas (Hwang et al., 2008) and astrocytomas (Peraud et al., 2003). Consistent with these studies highlighting an important function for fascin in regulating cell motility, we found that fascin also regulates RMS neuroblast migration. Interestingly, fascin has been identified as a highly up-regulated protein in neural progenitors derived from human embryonic stem cells, indicating that cytoskeleton rearrangements are playing an important role in differentiation towards the neuronal lineage (Chae et al., 2009). At this regard, it is interesting to mention that fascin is also up-regulated during neuronal differentiation of NTera2/cloneD1 (NT2) neuronal precursor cells (Megiorni et al., 2005). Moreover, fascin is strongly down-regulated after treatment with GDF11, a cytokine member of the TGFβ family able to inhibit neural stem cell migration (Williams et al., 2003). Fascin is also up-regulated in Tuberous Sclerosis Complex component (TSC1) knockout mice, where it promotes hematopoietic stem cell mobilization (Gan et al., 2008). Interestingly, in the SVZ, fascin is not expressed by GFAP+ NS cells or astrocytes and is barely detectable in Mash-1+ transit amplifying cells, whereas it is up-regulated in Dcx+ neuroblasts. This specificity of expression makes fascin a novel marker for migrating neuroblasts.

Fascin is highly expressed in filopodia and also in a specific area in front of the nucleus. Interestingly, a previous study has reported localisation of fascin in the perinuclear cytoplasmic area of neuronal cells (Mosialos et al., 1994). In migrating neuroblasts the area in front of the nucleus contains a high concentration of F-actin and the centrosome (Solecki et al., 2004, Shinohara et al., 2012). The F-actin condensation may be involved in positioning the centrosome before the movement

of the nucleus. Since fascin accumulates in the same area, it would be interesting to investigate whether fascin controls neuroblast migration through centrosome positioning. Investigating the localisation of the centrosome by immunostaining as well as nucleofection of a fluorescently-tagged centrosomal marker to monitor dynamic centrosome movement using time-lapse imaging (Solecki et al., 2004) are interesting points to be addressed in future experiments, ideally using *fascin-1* ko mice.

Using several approaches (ko mice, siRNA, shRNA) we have demonstrated that fascin is required for neuroblast migration. Interestingly, analysis of *fascin-1* ko mice shows an accumulation of cells at the caudal part of the RMS. A similar phenotype was detected in TSC1 ko animals (Zhou et al., 2011), which also display brain lesions such as subependymal nodules and subependymal giant cell astrocytomas in the lateral ventricle (Zhou et al., 2011, Feliciano et al., 2012). Moreover, TSC1 ko NS cells differentiate into neurons, astrocytes and oligodendrocytes within the lateral ventricle (Zhou et al., 2011). In future research it would be interesting to investigate whether *fascin-1* ko neuroblasts accumulating in the SVZ can also differentiate into proper neurons. Interestingly, fascin upregulation during neuronal differentiation of NT2 is prevented in cAMP response element binding protein (CREB)-depleted NT2 cells (Megiorni et al., 2005). It is important to note that CREB is one of the two major regulators for fascin transcriptional function in fibroblasts, dendritic and cancer cells (Bros et al., 2003, Hashimoto et al., 2009). CREB has been reported to be in its active and phosphorylated form during neuroblast tangential migration as well as in the early stages of neuronal differentiation in the OB (Giachino et al., 2005, Herold et al., 2011). Whether fascin has a role in neuronal differentiation, and thus in the integration of newborn neurons in the synaptic circuit of the olfactory system, remains to be investigated.

Fascin actin-binding function is regulated by phosphorylation on Ser39 (Ono et al., 1997). Although we cannot exclude potential conformational change(s) caused by the Ser39 mutants, our *in vitro* and *in vivo* experiments using phosphomimetic and unphosphorylatable forms of fascin suggest that dynamic phosphorylation of Ser39 is important for polarised neuroblast migration. Phosphorylation and dephosphorylation of fascin on Ser39 would create a dynamic cycle, in which fascin

is either located on or displaced from actin filaments at the leading edge of the neuroblast process. This dynamic event would control fascin actin-bundling function, thus modulating adhesion and retraction of filopodia during migration. Similar mechanisms were observed in cancer cells, where blocking the actin-bundling function of fascin by expression of phosphomimetic fascin (Hashimoto et al., 2007) or by treatment with migrastatin (a compound interacting with the fascin actin-binding site) (Chen et al., 2010) inhibited cell migration. Therefore, while de-phosphorylation of fascin is required for actin-bundling function and thus for filopodia formation, fascin phosphorylation may be required for down-regulating the actin-bundling function and promote the formation of a phospho-fascin/PKC complex, which would allow proper localisation of active PKC (e.g. in integrin signalling) to control adhesions. This model could explain why nucleofection of either S39A or S39D in migrating neuroblasts would perturb the controlled cycle of phospho-dephospho fascin, thus leading to polarity and migration defects.

Recently a new phosphorylation site located at the C-terminus of fascin (Ser274) has been shown to play an important role in regulating filopodia extension independently of fascin actin-bundling function (Zanet et al., 2012). The authors speculate that fascin may be part of an adhesion-dependent complex that could promote the subsequent formation of actin bundles (Zanet et al., 2012). Whether also phosphorylation on Ser274 needs to be regulated to ensure neuroblast migration is unknown, and it would be interesting to explore its role to better understand the function of fascin in this process.

Finally, we discovered that CB signaling, which regulates neuroblast migration (Oudin et al., 2011), modulates the fascin-PKC interaction. While a CB1 agonist, which promotes neuroblast migration, increases the fascin-PKC interaction, a CB1 antagonist, (which inhibits neuroblast migration), decreases this interaction. CB signaling could modulate fascin phosphorylation through PKC activation, ultimately promoting migration. Moreover, while FLIM experiments in fixed migrating neuroblasts indicate that CB receptor activation increases the fascin-PKC interaction, in a living migrating neuroblast the dynamics of this process may be quite complex. We speculate that activation of CB receptor increases the efficiency of the fascin phospho-dephosphorylation cycle by recruiting at the right subcellular

location PKC, which would become available for rapid fascin phosphorylation, leading to faster and more efficient migration (Figure 5-1). Instead, CB receptor inhibition would decrease migration by keeping fascin in an unphosphorylated state, leading to inefficient neuroblast migration. The molecular mechanisms by which CB signaling regulates fascin/PKC interaction will need to be further investigated spatially and temporally in migrating neuroblasts.

5.3.2 Drebrin in neuroblast migration

In developing neurons, drebrin is concentrated in the transitional domain of growth cones, favouring axonal growth and neuritogenesis through Cdk5-dependent phosphorylation on Ser142 (Geraldo et al., 2008, Mizui et al., 2009, Worth et al., 2013). During development, drebrin is involved in cerebellar and oculomotor neuron migration, besides controlling the motility of glioma cells (Shirao et al., 1990, Dun et al., 2012, Terakawa et al., 2013). In adult mice, drebrin appears to be strongly down-regulated at the rostral end of the RMS, where tangential migration terminates (Song et al., 2008). Building on these previous findings we have shown that in the postnatal mouse and rat brain drebrin is upregulated in the migratory neuroblast population (Dcx+ cells) compared to GFAP+ cells and Mash1+ cells.

We have also investigated the cellular localization of drebrin and pS142 drebrin as well as their function in neuroblast morphology and migration *in vitro* and *in vivo*. Drebrin immunostaining appears to be more diffuse along the leading process compared to pS142 drebrin immunostaining, which is confined to two locations: the membrane of the leading process and a region at the tip resembling the transitional domain of a growth cone. A previous study described a more peripheral localisation of pS142 drebrin compared to drebrin in the growth cones of embryonic cortical neurons (Worth et al., 2013). Consistent with these observations, in our RMS neuroblast cultures pS142 also appears localised in more peripheral regions (close to the base of the filopodia) compared to drebrin, however this result needs to be further characterized. Nevertheless, it is tempting to speculate that while unphosphorylated drebrin acts as a destabilizer of actin bundles, inhibiting fascin binding to actin (Sasaki et al., 1996), pS142 drebrin may be able to bundle actin more efficiently by the “opening” of a second actin binding site, thus creating a

stable base at the root of filopodia for fascin-mediated actin bundling (Figure 5-1). Moreover, following the model proposed by Worth and colleagues (2013) pS142 drebrin, exposing a domain that binds to EB3, could also facilitate the invasion of dynamic microtubules in the peripheral area of the tip of the leading process, growing along the existing filopodia and enhancing their stability.

Interestingly, in *in vivo* postnatal electroporation experiments phosphomimetic S142 drebrin decreases neuroblast migration compared to unphosphorylatable S142 drebrin. A possible explanation of this could be that the phosphomimetic variant acts as a dominant negative, promoting actin bundling and stability, thus decreasing actin and filopodia dynamics. Although neuroblasts transfected with the unphosphorylatable variant migrate significantly more compared to the phosphomimetic variant, they still migrate less than the control cells. Moreover, analysis in fixed brain slices after electroporation reveals that altering the phosphorylation state of the S142 site leads to defects in neuroblast orientation. These data suggest that both phospho-drebrin and unphospho-drebrin are required for efficient neuroblast migration and orientation. It is likely that the actin-bundling function promoted by drebrin phosphorylation on S142 needs to be dynamically controlled during the neuroblast migration cycle.

Drebrin has been implicated in controlling cell morphology in different contexts, where its overexpression leads to an increased number of neurite-like processes and to the formation of long protrusions (Shirao et al., 1994, Hayashi and Shirao, 1999, Keon et al., 2000). In oculomotor neurons drebrin depletion leads to a lack of leading process formation, while its overexpression affects axon and growth cone morphology (Dun et al., 2012). Overexpression of drebrin in glioma cells alters cell morphology, leading to stellate cells with more projections (Peitsch et al., 2006). Moreover, in both oculomotor neurons and glioma cells drebrin also regulates cell migration (Dun et al., 2012). Consistent with these findings, we have now discovered that drebrin regulates neuroblast morphology as well as migration. Analysis of fixed brain slices shows that drebrin depletion leads to a highly branched morphology and drebrin overexpression leads to the development of two protrusions from the cell body, oriented in opposite directions (one towards the OB and one towards the SVZ), suggesting that drebrin induces remodeling of the

actin/microtubule cytoskeleton. Using time-lapse imaging in cultured brain slices we discovered that both drebrin depletion and overexpression impairs neuroblast migration. Overall these observations lead us to conclude that drebrin is not only required for the development of a proper polarized leading process and efficient migration, but also that its expression must be highly regulated.

The striking unpolarised morphology observed in drebrin-depleted neuroblasts may be linked to the alteration in the activation state of the small GTPase Cdc42, a master regulator of cell polarity and filopodia formation (Etienne-Manneville and Hall, 2002). Interestingly, drebrin can interact with the Cdc42 scaffold protein Homer2 through its Homer binding domain, and the Drebrin-Homer-Cdc42 complex has been involved in the regulation of spine morphology and synaptic function (Shiraishi-Yamaguchi et al., 2009, Dun and Chilton, 2010). Pull-down assays to understand whether drebrin depletion and/or overexpression can alter Cdc42 activation in RMS neuroblasts could help clarify the role of drebrin in the control of neuroblast polarity.

Drebrin has been involved in spine morphogenesis and synaptic plasticity (Hayashi and Shirao, 1999, Takahashi et al., 2003, Takahashi et al., 2006) and its dysregulation has been linked to synaptic dysfunction and cognitive defects (Kojima and Shirao, 2007). Interestingly, while drebrin is highly expressed in the cell body of migrating neuroblasts along the RMS, drebrin expression becomes confined to dendritic spines of integrated neurons in the OB (Song et al., 2008). Whether drebrin has a role in neuroblast differentiation or in synaptic function in the OB remains unknown. Future experiments would need to explore the role of drebrin depletion/knockdown in spine morphogenesis in the OB and its functional implications, for example in odor discrimination as well as olfactory memory using patch-clamp recordings and behavioral studies (Alonso et al., 2012).

Finally, drebrin appears to be important for the correct functioning of store-operated calcium channels, since its depletion reduces channel-mediated calcium influx in T cells (Mercer et al., 2010). Changes in intracellular calcium are known to play a role in neuronal migration in embryonic and early postnatal stages as well as growth cone motility and neurite extension in developing neurons (Darcy and Isaacson, 2009). Interestingly, a calcium-dependent increase of F-actin in dendritic

spines in neurons promotes a drebrin-mediated interaction between F-actin and microtubules (Merriam et al., 2013). In non-neuronal cells, a link between cytoskeletal rearrangements and store-operated channel regulation or calcium influx has been reported (Nolz et al., 2006) and inhibition of store-operated calcium channel function or knockdown of channel components can prevent Platelet-Derived Growth Factor (PDGF)-induced smooth muscle cell migration (Bisaillon et al., 2010). While calcium release from IP3-sensitive intracellular stores after GABA exposure reduces neuroblast speed (Bolteus and Bordey, 2004), the role of store-operated calcium channels in neuroblast migration remains to be understood. Future studies investigating a potential link between drebrin and store-operated calcium channels in controlling neuroblast motility could be informative.

In conclusion, our studies have highlighted the important role of cytoskeletal rearrangements in RMS migrating neuroblasts by focusing on the functions of the actin-binding proteins fascin and drebrin. We have identified fascin and drebrin as two novel markers for migrating neuroblasts. Fascin and drebrin are both required for polarised neuroblast morphology and efficient neuroblast migration. Our data suggest that phosphorylation of fascin and drebrin on specific sites, (Ser39 for fascin and Ser142 for drebrin) could play a role in neuroblast migration and that a tightly regulated phospho-dephosphorylation cycle for both proteins may be required for their efficient polarised movement. While CB signalling, an endogenous regulator of neuroblast migration (Oudin et al., 2011), modulates the interaction between fascin and PKCγ, the extracellular stimuli and signalling mechanisms promoting drebrin phosphorylation on Ser142 remain to be identified. Given that neuroblast migration is essential for the proper maturation of neuroblasts into neurons in the OB (Belvindrah et al., 2011), future studies will be required to clarify the contribution of fascin and drebrin to the differentiation and integration of newborn neurons into the pre-existing synaptic network.

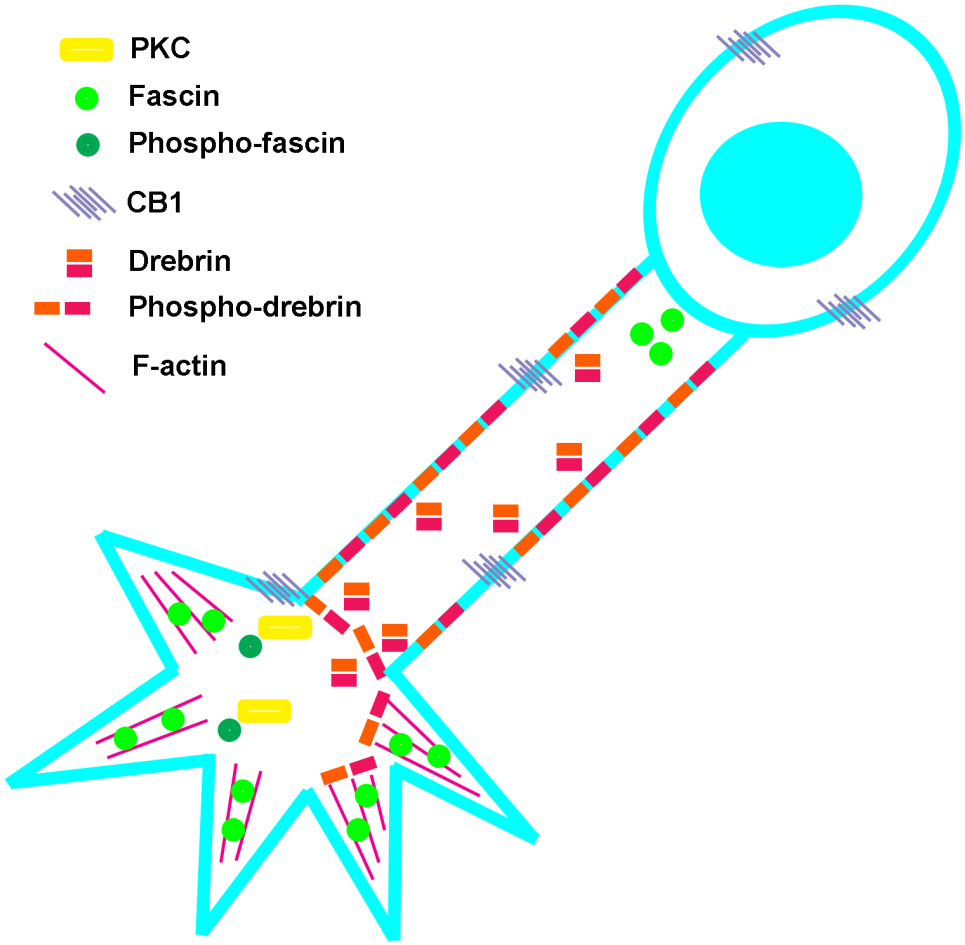


Figure 5-1. The role of fascin and drebrin in RMS migrating neuroblasts.

Schematic drawing showing the distribution of fascin (light green) bundling F-actin (pink lines); phospho-fascin (dark green) interacting with PKC (yellow) after activation of the CB1 receptor (purple lines); drebrin (pink and orange parallel lines); and phospho-drebrin bundling F-actin at the root of filopodia (pink and orange juxtaposed lines).

Bibliography

Adams JC (1995) Formation of stable microspikes containing actin and the 55 kDa actin bundling protein, fascin, is a consequence of cell adhesion to thrombospondin-1: implications for the anti-adhesive activities of thrombospondin-1. Journal of cell science 108 (Pt 5):1977-1990.

Adams JC (1997) Characterization of cell-matrix adhesion requirements for the formation of fascin microspikes. Molecular biology of the cell 8:2345-2363.

Adams JC (2004) Roles of fascin in cell adhesion and motility. Current opinion in cell biology 16:590-596.

Adams JC, Clelland JD, Collett GD, Matsumura F, Yamashiro S, Zhang L (1999) Cell-matrix adhesions differentially regulate fascin phosphorylation. Molecular biology of the cell 10:4177-4190.

Adams JC, Kureishy N, Taylor AL (2001) A role for syndecan-1 in coupling fascin spike formation by thrombospondin-1. The Journal of cell biology 152:1169-1182.

Adams JC, Schwartz MA (2000) Stimulation of fascin spikes by thrombospondin-1 is mediated by the GTPases Rac and Cdc42. The Journal of cell biology 150:807-822.

Aguado T, Palazuelos J, Monory K, Stella N, Cravatt B, Lutz B, Marsicano G, Kokaia Z, Guzman M, Galve-Roperh I (2006) The endocannabinoid system promotes astroglial differentiation by acting on neural progenitor cells. The Journal of neuroscience : the official journal of the Society for Neuroscience 26:1551-1561.

Alonso M, Lepousez G, Sebastien W, Bardy C, Gabellec MM, Torquet N, Lledo PM (2012) Activation of adult-born neurons facilitates learning and memory. Nature neuroscience 15:897-904.

Altman J (1962) Are new neurons formed in the brains of adult mammals? Science 135:1127-1128.

Altman J (1963) Autoradiographic investigation of cell proliferation in the brains of rats and cats. The Anatomical record 145:573-591.

Altman J (1969) Autoradiographic and histological studies of postnatal neurogenesis. IV. Cell proliferation and migration in the anterior forebrain, with special reference to persisting neurogenesis in the olfactory bulb. The Journal of comparative neurology 137:433-457.

Altman J, Das GD (1965) Autoradiographic and histological evidence of postnatal hippocampal neurogenesis in rats. The Journal of comparative neurology 124:319-335.

Alvarez-Buylla A, Buskirk DR, Nottebohm F (1987) Monoclonal antibody reveals radial glia in adult avian brain. The Journal of comparative neurology 264:159-170.

Alvarez-Buylla A, Garcia-Verdugo JM, Tramontin AD (2001) A unified hypothesis on the lineage of neural stem cells. Nature reviews Neuroscience 2:287-293.

Alvarez-Buylla A, Lim DA (2004) For the long run: maintaining germinal niches in the adult brain. Neuron 41:683-686.

Alvarez-Buylla A, Nottebohm F (1988) Migration of young neurons in adult avian brain. Nature 335:353-354.

Andrade N, Komnenovic V, Blake SM, Jossin Y, Howell B, Goffinet A, Schneider WJ, Nimpf J (2007) ApoER2/VLDL receptor and Dab1 in the rostral migratory stream function in postnatal neuronal migration independently of Reelin. Proceedings of the National Academy of Sciences of the United States of America 104:8508-8513.

Angot E, Loulier K, Nguyen-Ba-Charvet KT, Gadeau AP, Ruat M, Traiffort E (2008) Chemoattractive activity of sonic hedgehog in the adult subventricular zone modulates the number of neural precursors reaching the olfactory bulb. Stem cells 26:2311-2320.

Anilkumar N, Parsons M, Monk R, Ng T, Adams JC (2003) Interaction of fascin and protein kinase Calpha: a novel intersection in cell adhesion and motility. The EMBO journal 22:5390-5402.

Anton ES, Ghashghaei HT, Weber JL, McCann C, Fischer TM, Cheung ID, Gassmann M, Messing A, Klein R, Schwab MH, Lloyd KC, Lai C (2004) Receptor tyrosine kinase ErbB4 modulates neuroblast migration and placement in the adult forebrain. Nature neuroscience 7:1319-1328.

Aratyn YS, Schaus TE, Taylor EW, Borisy GG (2007) Intrinsic dynamic behavior of fascin in filopodia. Molecular biology of the cell 18:3928-3940.

Arvidsson A, Collin T, Kirik D, Kokaia Z, Lindvall O (2002) Neuronal replacement from endogenous precursors in the adult brain after stroke. Nature medicine 8:963-970.

Bagley JA, Belluscio L (2010) Dynamic imaging reveals that brain-derived neurotrophic factor can independently regulate motility and direction of neuroblasts within the rostral migratory stream. Neuroscience 169:1449-1461.

Baker SA, Baker KA, Hagg T (2004) Dopaminergic nigrostriatal projections regulate neural precursor proliferation in the adult mouse subventricular zone. The European journal of neuroscience 20:575-579.

Bath KG, Mandairon N, Jing D, Rajagopal R, Kapoor R, Chen ZY, Khan T, Proenca CC, Kraemer R, Cleland TA, Hempstead BL, Chao MV, Lee FS (2008) Variant brain-derived neurotrophic factor (Val66Met) alters adult olfactory bulb neurogenesis and

spontaneous olfactory discrimination. The Journal of neuroscience : the official journal of the Society for Neuroscience 28:2383-2393.

Batista CM, Kippin TE, Willaime-Morawek S, Shimabukuro MK, Akamatsu W, van der Kooy D (2006) A progressive and cell non-autonomous increase in striatal neural stem cells in the Huntington's disease R6/2 mouse. The Journal of neuroscience : the official journal of the Society for Neuroscience 26:10452-10460.

Batista-Brito R, Close J, Machold R, Fishell G (2008) The distinct temporal origins of olfactory bulb interneuron subtypes. The Journal of neuroscience : the official journal of the Society for Neuroscience 28:3966-3975.

Bedard A, Parent A (2004) Evidence of newly generated neurons in the human olfactory bulb. Brain research Developmental brain research 151:159-168.

Belluzzi O, Benedusi M, Ackman J, LoTurco JJ (2003) Electrophysiological differentiation of new neurons in the olfactory bulb. The Journal of neuroscience : the official journal of the Society for Neuroscience 23:10411-10418.

Belvindrah R, Hankel S, Walker J, Patton BL, Muller U (2007) Beta1 integrins control the formation of cell chains in the adult rostral migratory stream. The Journal of neuroscience : the official journal of the Society for Neuroscience 27:2704-2717.

Belvindrah R, Nissant A, Lledo PM (2011) Abnormal neuronal migration changes the fate of developing neurons in the postnatal olfactory bulb. The Journal of neuroscience : the official journal of the Society for Neuroscience 31:7551-7562.

Bergmann O, Liebl J, Bernard S, Alkass K, Yeung MS, Steier P, Kutschera W, Johnson L, Landen M, Druid H, Spalding KL, Frisen J (2012) The age of olfactory bulb neurons in humans. Neuron 74:634-639.

Bignami A, Dahl D (1974) Astrocyte-specific protein and neuroglial differentiation. An immunofluorescence study with antibodies to the glial fibrillary acidic protein. The Journal of comparative neurology 153:27-38.

Biou V, Brinkhaus H, Malenka RC, Matus A (2008) Interactions between drebrin and Ras regulate dendritic spine plasticity. The European journal of neuroscience 27:2847-2859.

Birchmeier C, Gherardi E (1998) Developmental roles of HGF/SF and its receptor, the c-Met tyrosine kinase. Trends in cell biology 8:404-410.

Bisaillon JM, Motiani RK, Gonzalez-Cobos JC, Potier M, Halligan KE, Alzawahra WF, Barroso M, Singer HA, Jourd'heuil D, Trebak M (2010) Essential role for STIM1/Orai1-mediated calcium influx in PDGF-induced smooth muscle migration. American journal of physiology Cell physiology 298:C993-1005.

Blake SM, Strasser V, Andrade N, Duit S, Hofbauer R, Schneider WJ, Nimpf J (2008) Thrombospondin-1 binds to ApoER2 and VLDL receptor and functions in postnatal neuronal migration. The EMBO journal 27:3069-3080.

Bolteus AJ, Bordey A (2004) GABA release and uptake regulate neuronal precursor migration in the postnatal subventricular zone. The Journal of neuroscience : the official journal of the Society for Neuroscience 24:7623-7631.

Boutin C, Diestel S, Desoeuvre A, Tiveron MC, Cremer H (2008) Efficient in vivo electroporation of the postnatal rodent forebrain. PloS one 3:e1883.

Bovetti S, Hsieh YC, Bovolin P, Perroteau I, Kazunori T, Puche AC (2007) Blood vessels form a scaffold for neuroblast migration in the adult olfactory bulb. The Journal of neuroscience : the official journal of the Society for Neuroscience 27:5976-5980.

Bozoyan L, Khlghatyan J, Saghatelyan A (2012) Astrocytes control the development of the migration-promoting vasculature scaffold in the postnatal brain via VEGF signaling. The Journal of neuroscience : the official journal of the Society for Neuroscience 32:1687-1704.

Breitsprecher D, Koestler SA, Chizhov I, Nemethova M, Mueller J, Goode BL, Small JV, Rottner K, Faix J (2011) Cofilin cooperates with fascin to disassemble filopodial actin filaments. Journal of cell science 124:3305-3318.

Breton-Provencher V, Lemasson M, Peralta MR, 3rd, Saghatelyan A (2009) Interneurons produced in adulthood are required for the normal functioning of the olfactory bulb network and for the execution of selected olfactory behaviors. The Journal of neuroscience : the official journal of the Society for Neuroscience 29:15245-15257.

Brill MS, Ninkovic J, Winpenny E, Hodge RD, Ozen I, Yang R, Lepier A, Gascon S, Erdelyi F, Szabo G, Parras C, Guillemot F, Frotscher M, Berninger B, Hevner RF, Raineteau O, Gotz M (2009) Adult generation of glutamatergic olfactory bulb interneurons. Nature neuroscience 12:1524-1533.

Bron R, Eickholt BJ, Vermeren M, Fragale N, Cohen J (2004) Functional knockdown of neuropilin-1 in the developing chick nervous system by siRNA hairpins phenocopies genetic ablation in the mouse. Developmental dynamics : an official publication of the American Association of Anatomists 230:299-308.

Bros M, Ross XL, Pautz A, Reske-Kunz AB, Ross R (2003) The human fascin gene promoter is highly active in mature dendritic cells due to a stage-specific enhancer. Journal of immunology 171:1825-1834.

Brose K, Bland KS, Wang KH, Arnott D, Henzel W, Goodman CS, Tessier-Lavigne M, Kidd T (1999) Slit proteins bind Robo receptors and have an evolutionarily conserved role in repulsive axon guidance. Cell 96:795-806.

Brown JA, Bridgman PC (2009) Disruption of the cytoskeleton during Semaphorin 3A induced growth cone collapse correlates with differences in actin organization and associated binding proteins. Developmental neurobiology 69:633-646.

Butkevich E, Hulsmann S, Wenzel D, Shirao T, Duden R, Majoul I (2004) Drebrin is a novel connexin-43 binding partner that links gap junctions to the submembrane cytoskeleton. Current biology : CB 14:650-658.

Cant K, Knowles BA, Mooseker MS, Cooley L (1994) Drosophila singed, a fascin homolog, is required for actin bundle formation during oogenesis and bristle extension. The Journal of cell biology 125:369-380.

Cao L, Jiao X, Zuzga DS, Liu Y, Fong DM, Young D, During MJ (2004) VEGF links hippocampal activity with neurogenesis, learning and memory. Nature genetics 36:827-835.

Cao L, Wei D, Reid B, Zhao S, Pu J, Pan T, Yamoah E, Zhao M (2013) Endogenous electric currents might guide rostral migration of neuroblasts. EMBO reports 14:184-190.

Carleton A, Petreanu LT, Lansford R, Alvarez-Buylla A, Lledo PM (2003) Becoming a new neuron in the adult olfactory bulb. Nature neuroscience 6:507-518.

Casarosa S, Fode C, Guillemot F (1999) Mash1 regulates neurogenesis in the ventral telencephalon. Development 126:525-534.

Cayre M, Canoll P, Goldman JE (2009) Cell migration in the normal and pathological postnatal mammalian brain. Progress in neurobiology 88:41-63.

Chae JI, Kim J, Woo SM, Han HW, Cho YK, Oh KB, Nam KH, Kang YK (2009) Cytoskeleton-associated proteins are enriched in human embryonic-stem cell-derived neuroectodermal spheres. Proteomics 9:1128-1141.

Chae T, Kwon YT, Bronson R, Dikkes P, Li E, Tsai LH (1997) Mice lacking p35, a neuronal specific activator of Cdk5, display cortical lamination defects, seizures, and adult lethality. Neuron 18:29-42.

Chazal G, Durbec P, Jankovski A, Rougon G, Cremer H (2000) Consequences of neural cell adhesion molecule deficiency on cell migration in the rostral migratory stream of the mouse. The Journal of neuroscience : the official journal of the Society for Neuroscience 20:1446-1457.

Chen L, Yang S, Jakoncic J, Zhang JJ, Huang XY (2010) Migrastatin analogues target fascin to block tumour metastasis. Nature 464:1062-1066.

Cheng MF (2013) Hypothalamic neurogenesis in the adult brain. Frontiers in neuroendocrinology 34:167-178.

Cheng XT, Hayashi K, Shirao T (2000) Non-muscle myosin IIB-like immunoreactivity is present at the drebrin-binding cytoskeleton in neurons. Neuroscience research 36:167-173.

Chew CS, Okamoto CT, Chen X, Thomas R (2005) Drebrin E2 is differentially expressed and phosphorylated in parietal cells in the gastric mucosa. American journal of physiology Gastrointestinal and liver physiology 289:G320-331.

Chhabra ES, Higgs HN (2007) The many faces of actin: matching assembly factors with cellular structures. Nature cell biology 9:1110-1121.

Chiaramello S, Dalmasso G, Bezin L, Marcel D, Jourdan F, Peretto P, Fasolo A, De Marchis S (2007) BDNF/ TrkB interaction regulates migration of SVZ precursor cells via PI3-K and MAP-K signalling pathways. The European journal of neuroscience 26:1780-1790.

Chiyomaru T, Enokida H, Tatarano S, Kawahara K, Uchida Y, Nishiyama K, Fujimura L, Kikkawa N, Seki N, Nakagawa M (2010) miR-145 and miR-133a function as tumour suppressors and directly regulate FSCN1 expression in bladder cancer. British journal of cancer 102:883-891.

Cina C, Maass K, Theis M, Willecke K, Bechberger JF, Naus CC (2009) Involvement of the cytoplasmic C-terminal domain of connexin43 in neuronal migration. The Journal of neuroscience : the official journal of the Society for Neuroscience 29:2009-2021.

Cochard P, Paulin D (1984) Initial expression of neurofilaments and vimentin in the central and peripheral nervous system of the mouse embryo in vivo. The Journal of neuroscience : the official journal of the Society for Neuroscience 4:2080-2094.

Cohan CS, Welnhofer EA, Zhao L, Matsumura F, Yamashiro S (2001) Role of the actin bundling protein fascin in growth cone morphogenesis: localization in filopodia and lamellipodia. Cell motility and the cytoskeleton 48:109-120.

Comte I, Kim Y, Young CC, van der Harg JM, Hockberger P, Bolam PJ, Poirier F, Szele FG (2011) Galectin-3 maintains cell motility from the subventricular zone to the olfactory bulb. Journal of cell science 124:2438-2447.

Conover JC, Doetsch F, Garcia-Verdugo JM, Gale NW, Yancopoulos GD, Alvarez-Buylla A (2000) Disruption of Eph/ephrin signaling affects migration and proliferation in the adult subventricular zone. Nature neuroscience 3:1091-1097.

Courson DS, Rock RS (2010) Actin cross-link assembly and disassembly mechanics for alpha-Actinin and fascin. The Journal of biological chemistry 285:26350-26357.

Craig CG, Tropepe V, Morshead CM, Reynolds BA, Weiss S, van der Kooy D (1996) In vivo growth factor expansion of endogenous subependymal neural precursor cell populations in the adult mouse brain. The Journal of neuroscience : the official journal of the Society for Neuroscience 16:2649-2658.

Cremer H, Lange R, Christoph A, Plomann M, Vopper G, Roes J, Brown R, Baldwin S, Kraemer P, Scheff S, et al. (1994) Inactivation of the N-CAM gene in mice results in size reduction of the olfactory bulb and deficits in spatial learning. Nature 367:455-459.

Curtis MA, Kam M, Nannmark U, Anderson MF, Axell MZ, Wikkelso C, Holtas S, van Roon-Mom WM, Bjork-Eriksson T, Nordborg C, Frisen J, Dragunow M, Faull RL, Eriksson PS (2007) Human neuroblasts migrate to the olfactory bulb via a lateral ventricular extension. Science 315:1243-1249.

Darcy DP, Isaacson JS (2009) L-type calcium channels govern calcium signaling in migrating newborn neurons in the postnatal olfactory bulb. The Journal of neuroscience : the official journal of the Society for Neuroscience 29:2510-2518.

Das A, Gajendra S, Falenta K, Oudin MJ, Peschard P, Feng S, Wu B, Marshall CJ, Doherty P, Guo W, Lalli G (2013) RalA promotes a direct exocyst-Par6 interaction to regulate polarity in neuronal development. Journal of cell science.

De Arcangelis A, Georges-Labouesse E, Adams JC (2004) Expression of fascin-1, the gene encoding the actin-bundling protein fascin-1, during mouse embryogenesis. Gene expression patterns : GEP 4:637-643.

Deinhardt K, Kim T, Spellman DS, Mains RE, Eipper BA, Neubert TA, Chao MV, Hempstead BL (2011) Neuronal growth cone retraction relies on proneurotrophin receptor signaling through Rac. Science signaling 4:ra82.

Devane WA, Hanus L, Breuer A, Pertwee RG, Stevenson LA, Griffin G, Gibson D, Mandelbaum A, Etinger A, Mechoulam R (1992) Isolation and structure of a brain constituent that binds to the cannabinoid receptor. Science 258:1946-1949.

Doetsch F (2003) A niche for adult neural stem cells. Current opinion in genetics & development 13:543-550.

Doetsch F, Alvarez-Buylla A (1996) Network of tangential pathways for neuronal migration in adult mammalian brain. Proceedings of the National Academy of Sciences of the United States of America 93:14895-14900.

Doetsch F, Caille I, Lim DA, Garcia-Verdugo JM, Alvarez-Buylla A (1999) Subventricular zone astrocytes are neural stem cells in the adult mammalian brain. Cell 97:703-716.

Doetsch F, Garcia-Verdugo JM, Alvarez-Buylla A (1997) Cellular composition and three-dimensional organization of the subventricular germinal zone in the adult mammalian brain. The Journal of neuroscience : the official journal of the Society for Neuroscience 17:5046-5061.

Doetsch F, Petreanu L, Caille I, Garcia-Verdugo JM, Alvarez-Buylla A (2002) EGF converts transit-amplifying neurogenic precursors in the adult brain into multipotent stem cells. Neuron 36:1021-1034.

Doherty P, Cohen J, Walsh FS (1990) Neurite outgrowth in response to transfected N-CAM changes during development and is modulated by polysialic acid. Neuron 5:209-219.

Duh FM, Latif F, Weng Y, Geil L, Modi W, Stackhouse T, Matsumura F, Duan DR, Linehan WM, Lerman MI, et al. (1994) cDNA cloning and expression of the human homolog of the sea urchin fascin and Drosophila singed genes which encodes an actin-bundling protein. DNA and cell biology 13:821-827.

Dun XP, Bandeira de Lima T, Allen J, Geraldo S, Gordon-Weeks P, Chilton JK (2012) Drebrin controls neuronal migration through the formation and alignment of the leading process. Molecular and cellular neurosciences 49:341-350.

Dun XP, Chilton JK (2010) Control of cell shape and plasticity during development and disease by the actin-binding protein Drebrin. Histology and histopathology 25:533-540.

Easter SS, Jr., Ross LS, Frankfurter A (1993) Initial tract formation in the mouse brain. The Journal of neuroscience : the official journal of the Society for Neuroscience 13:285-299.

Edwards RA, Bryan J (1995) Fascins, a family of actin bundling proteins. Cell motility and the cytoskeleton 32:1-9.

Ekonomou A, Ballard CG, Pathmanaban ON, Perry RH, Perry EK, Kalaria RN, Minger SL (2011) Increased neural progenitors in vascular dementia. Neurobiology of aging 32:2152-2161.

Ekonomou A, Johnson M, Perry RH, Perry EK, Kalaria RN, Minger SL, Ballard CG (2012) Increased neural progenitors in individuals with cerebral small vessel disease. Neuropathology and applied neurobiology 38:344-353.

Elola MT, Wolfenstein-Todel C, Troncoso MF, Vasta GR, Rabinovich GA (2007) Galectins: matricellular glycan-binding proteins linking cell adhesion, migration, and survival. Cellular and molecular life sciences : CMLS 64:1679-1700.

Emsley JG, Hagg T (2003) alpha6beta1 integrin directs migration of neuronal precursors in adult mouse forebrain. Experimental neurology 183:273-285.

Eriksson PS, Perfilieva E, Bjork-Eriksson T, Alborn AM, Nordborg C, Peterson DA, Gage FH (1998) Neurogenesis in the adult human hippocampus. Nature medicine 4:1313-1317.

Ernst A, Alkass K, Bernard S, Salehpour M, Perl S, Tisdale J, Possnert G, Druid H, Frisen J (2014) Neurogenesis in the striatum of the adult human brain. Cell 156:1072-1083.

Etienne-Manneville S, Hall A (2002) Rho GTPases in cell biology. Nature 420:629-635.

Etienne-Manneville S, Hall A (2003) Cell polarity: Par6, aPKC and cytoskeletal crosstalk. Current opinion in cell biology 15:67-72.

Faix J, Rottner K (2006) The making of filopodia. Current opinion in cell biology 18:18-25.

Falenta K, Gajendra S, Sonego M, Doherty P, Lalli G (2013) Nucleofection of Rodent Neuroblasts to Study Neuroblast Migration In vitro. Journal of visualized experiments : JoVE.

Fallon J, Reid S, Kinyamu R, Opole I, Opole R, Baratta J, Korc M, Endo TL, Duong A, Nguyen G, Karkehabadhi M, Twardzik D, Patel S, Loughlin S (2000) In vivo induction of massive proliferation, directed migration, and differentiation of neural cells in the adult mammalian brain. Proceedings of the National Academy of Sciences of the United States of America 97:14686-14691.

Feliciano DM, Quon JL, Su T, Taylor MM, Bordey A (2012) Postnatal neurogenesis generates heterotopias, olfactory micronodules and cortical infiltration following single-cell Tsc1 deletion. Human molecular genetics 21:799-810.

Fischer D, Tucker RP, Chiquet-Ehrismann R, Adams JC (1997) Cell-adhesive responses to tenascin-C splice variants involve formation of fascin microspikes. Molecular biology of the cell 8:2055-2075.

Frazier-Cierpial L, Brunjes PC (1989) Early postnatal cellular proliferation and survival in the olfactory bulb and rostral migratory stream of normal and unilaterally odor-deprived rats. The Journal of comparative neurology 289:481-492.

Gage FH (2002) Neurogenesis in the adult brain. The Journal of neuroscience : the official journal of the Society for Neuroscience 22:612-613.

Gage FH, Coates PW, Palmer TD, Kuhn HG, Fisher LJ, Suhonen JO, Peterson DA, Suhr ST, Ray J (1995) Survival and differentiation of adult neuronal progenitor cells transplanted to the adult brain. Proceedings of the National Academy of Sciences of the United States of America 92:11879-11883.

Galbraith CG, Yamada KM, Galbraith JA (2007) Polymerizing actin fibers position integrins primed to probe for adhesion sites. Science 315:992-995.

Gan B, Sahin E, Jiang S, Sanchez-Aguilera A, Scott KL, Chin L, Williams DA, Kwiatkowski DJ, DePinho RA (2008) mTORC1-dependent and -independent regulation of stem cell renewal, differentiation, and mobilization. Proceedings of the National Academy of Sciences of the United States of America 105:19384-19389.

Gao Y, Vasilyev DV, Goncalves MB, Howell FV, Hobbs C, Reisenberg M, Shen R, Zhang MY, Strassle BW, Lu P, Mark L, Piesla MJ, Deng K, Kouranova EV, Ring RH, Whiteside GT, Bates B, Walsh FS, Williams G, Pangalos MN, Samad TA, Doherty P (2010) Loss of retrograde endocannabinoid signaling and reduced adult

neurogenesis in diacylglycerol lipase knock-out mice. The Journal of neuroscience : the official journal of the Society for Neuroscience 30:2017-2024.

Garcia AD, Doan NB, Imura T, Bush TG, Sofroniew MV (2004) GFAP-expressing progenitors are the principal source of constitutive neurogenesis in adult mouse forebrain. Nature neuroscience 7:1233-1241.

Garcia-Gonzalez D, Clemente D, Coelho M, Esteban PF, Soussi-Yanicostas N, de Castro F (2010) Dynamic roles of FGF-2 and Anosmin-1 in the migration of neuronal precursors from the subventricular zone during pre- and postnatal development. Experimental neurology 222:285-295.

Garzotto D, Giacobini P, Crepaldi T, Fasolo A, De Marchis S (2008) Hepatocyte growth factor regulates migration of olfactory interneuron precursors in the rostral migratory stream through Met-Grb2 coupling. The Journal of neuroscience : the official journal of the Society for Neuroscience 28:5901-5909.

Gascon E, Vutskits L, Jenny B, Durbec P, Kiss JZ (2007) PSA-NCAM in postnatally generated immature neurons of the olfactory bulb: a crucial role in regulating p75 expression and cell survival. Development 134:1181-1190.

Geiger B, Spatz JP, Bershadsky AD (2009) Environmental sensing through focal adhesions. Nature reviews Molecular cell biology 10:21-33.

Geraldo S, Khanzada UK, Parsons M, Chilton JK, Gordon-Weeks PR (2008) Targeting of the F-actin-binding protein drebrin by the microtubule plus-tip protein EB3 is required for neuritogenesis. Nature cell biology 10:1181-1189.

Gheusi G, Cremer H, McLean H, Chazal G, Vincent JD, Lledo PM (2000) Importance of newly generated neurons in the adult olfactory bulb for odor discrimination. Proceedings of the National Academy of Sciences of the United States of America 97:1823-1828.

Giachino C, De Marchis S, Giampietro C, Parlato R, Perroteau I, Schutz G, Fasolo A, Peretto P (2005) cAMP response element-binding protein regulates differentiation and survival of newborn neurons in the olfactory bulb. The Journal of neuroscience : the official journal of the Society for Neuroscience 25:10105-10118.

Gimona M (2008) The microfilament system in the formation of invasive adhesions. Seminars in cancer biology 18:23-34.

Gleeson JG, Lin PT, Flanagan LA, Walsh CA (1999) Doublecortin is a microtubule-associated protein and is expressed widely by migrating neurons. Neuron 23:257-271.

Goings GE, Sahni V, Szele FG (2004) Migration patterns of subventricular zone cells in adult mice change after cerebral cortex injury. Brain research 996:213-226.

Goldman SA, Nottebohm F (1983) Neuronal production, migration, and differentiation in a vocal control nucleus of the adult female canary brain. Proceedings of the National Academy of Sciences of the United States of America 80:2390-2394.

Goldstein B, Macara IG (2007) The PAR proteins: fundamental players in animal cell polarization. Developmental cell 13:609-622.

Goncalves MB, Suetterlin P, Yip P, Molina-Holgado F, Walker DJ, Oudin MJ, Zentar MP, Pollard S, Yanez-Munoz RJ, Williams G, Walsh FS, Pangalos MN, Doherty P (2008) A diacylglycerol lipase-CB2 cannabinoid pathway regulates adult subventricular zone neurogenesis in an age-dependent manner. Molecular and cellular neurosciences 38:526-536.

Goncharuk VN, Ross JS, Carlson JA (2002) Actin-binding protein fascin expression in skin neoplasia. Journal of cutaneous pathology 29:430-438.

Grade S, Weng YC, Snapyan M, Kriz J, Malva JO, Saghatelyan A (2013) Brain-derived neurotrophic factor promotes vasculature-associated migration of neuronal precursors toward the ischemic striatum. PloS one 8:e55039.

Grothey A, Hashizume R, Sahin AA, McCrea PD (2000) Fascin, an actin-bundling protein associated with cell motility, is upregulated in hormone receptor negative breast cancer. British journal of cancer 83:870-873.

Guo W, Grant A, Novick P (1999) Exo84p is an exocyst protein essential for secretion. The Journal of biological chemistry 274:23558-23564.

Guvakova MA, Boettiger D, Adams JC (2002) Induction of fascin spikes in breast cancer cells by activation of the insulin-like growth factor-I receptor. The international journal of biochemistry & cell biology 34:685-698.

Hack I, Bancila M, Loulier K, Carroll P, Cremer H (2002) Reelin is a detachment signal in tangential chain-migration during postnatal neurogenesis. Nature neuroscience 5:939-945.

Hakanen J, Duprat S, Salminen M (2011) Netrin1 is required for neural and glial precursor migrations into the olfactory bulb. Developmental biology 355:101-114.

Halfter W, Dong S, Schurer B, Cole GJ (1998) Collagen XVIII is a basement membrane heparan sulfate proteoglycan. The Journal of biological chemistry 273:25404-25412.

Harigaya Y, Shoji M, Shirao T, Hirai S (1996) Disappearance of actin-binding protein, drebrin, from hippocampal synapses in Alzheimer's disease. Journal of neuroscience research 43:87-92.

Harkany T, Guzman M, Galve-Roperh I, Berghuis P, Devi LA, Mackie K (2007) The emerging functions of endocannabinoid signaling during CNS development. Trends in pharmacological sciences 28:83-92.

Harkany T, Mackie K, Doherty P (2008) Wiring and firing neuronal networks: endocannabinoids take center stage. Current opinion in neurobiology 18:338-345.

Hashimoto Y, Kim DJ, Adams JC (2011) The roles of fascins in health and disease. The Journal of pathology 224:289-300.

Hashimoto Y, Loftis DW, Adams JC (2009) Fascin-1 promoter activity is regulated by CREB and the aryl hydrocarbon receptor in human carcinoma cells. PloS one 4:e5130.

Hashimoto Y, Parsons M, Adams JC (2007) Dual actin-bundling and protein kinase C-binding activities of fascin regulate carcinoma cell migration downstream of Rac and contribute to metastasis. Molecular biology of the cell 18:4591-4602.

Haviv L, Gillo D, Backouche F, Bernheim-Groswasser A (2008) A cytoskeletal demolition worker: myosin II acts as an actin depolymerization agent. Journal of molecular biology 375:325-330.

Hayashi K, Ishikawa R, Ye LH, He XL, Takata K, Kohama K, Shirao T (1996) Modulatory role of drebrin on the cytoskeleton within dendritic spines in the rat cerebral cortex. The Journal of neuroscience : the official journal of the Society for Neuroscience 16:7161-7170.

Hayashi K, Shirao T (1999) Change in the shape of dendritic spines caused by overexpression of drebrin in cultured cortical neurons. The Journal of neuroscience : the official journal of the Society for Neuroscience 19:3918-3925.

Hayashi T, Noshita N, Sugawara T, Chan PH (2003) Temporal profile of angiogenesis and expression of related genes in the brain after ischemia. Journal of cerebral blood flow and metabolism : official journal of the International Society of Cerebral Blood Flow and Metabolism 23:166-180.

He B, Guo W (2009) The exocyst complex in polarized exocytosis. Current opinion in cell biology 21:537-542.

Hebb O D (1949) The Organisation of Behavior. New York: Wiley & Sons.

Herold S, Jagasia R, Merz K, Wassmer K, Lie DC (2011) CREB signalling regulates early survival, neuronal gene expression and morphological development in adult subventricular zone neurogenesis. Molecular and cellular neurosciences 46:79-88.

Higashida C, Miyoshi T, Fujita A, Oceguera-Yanez F, Monypenny J, Andou Y, Narumiya S, Watanabe N (2004) Actin polymerization-driven molecular movement of mDia1 in living cells. Science 303:2007-2010.

Higginbotham H, Tanaka T, Brinkman BC, Gleeson JG (2006) GSK3beta and PKCzeta function in centrosome localization and process stabilization during Slit-mediated neuronal repolarization. Molecular and cellular neurosciences 32:118-132.

Hirota Y, Ohshima T, Kaneko N, Ikeda M, Iwasato T, Kulkarni AB, Mikoshiba K, Okano H, Sawamoto K (2007) Cyclin-dependent kinase 5 is required for control of neuroblast migration in the postnatal subventricular zone. The Journal of neuroscience : the official journal of the Society for Neuroscience 27:12829-12838.

Holthuis JC, Schoonderwoert VT, Martens GJ (1994) A vertebrate homolog of the actin-bundling protein fascin. Biochimica et biophysica acta 1219:184-188.

Hu H (1999) Chemorepulsion of neuronal migration by Slit2 in the developing mammalian forebrain. Neuron 23:703-711.

Hu H, Rutishauser U (1996) A septum-derived chemorepulsive factor for migrating olfactory interneuron precursors. Neuron 16:933-940.

Hu H, Tomasiewicz H, Magnuson T, Rutishauser U (1996) The role of polysialic acid in migration of olfactory bulb interneuron precursors in the subventricular zone. Neuron 16:735-743.

Hu W, McCrea PD, Deavers M, Kavanagh JJ, Kudelka AP, Verschraegen CF (2000) Increased expression of fascin, motility associated protein, in cell cultures derived from ovarian cancer and in borderline and carcinomatous ovarian tumors. Clinical & experimental metastasis 18:83-88.

Hurtado-Chong A, Yusta-Boyo MJ, Vergano-Vera E, Bulfone A, de Pablo F, Vicario-Abejon C (2009) IGF-I promotes neuronal migration and positioning in the olfactory bulb and the exit of neuroblasts from the subventricular zone. The European journal of neuroscience 30:742-755.

Hwang JH, Smith CA, Salhia B, Rutka JT (2008) The role of fascin in the migration and invasiveness of malignant glioma cells. Neoplasia 10:149-159.

Hynes RO (2002) Integrins: bidirectional, allosteric signaling machines. Cell 110:673-687.

Ideses Y, Brill-Karniely Y, Haviv L, Ben-Shaul A, Bernheim-Groswasser A (2008) Arp2/3 branched actin network mediates filopodia-like bundles formation in vitro. PloS one 3:e3297.

Imayoshi I, Sakamoto M, Ohtsuka T, Takao K, Miyakawa T, Yamaguchi M, Mori K, Ikeda T, Itohara S, Kageyama R (2008) Roles of continuous neurogenesis in the structural and functional integrity of the adult forebrain. Nature neuroscience 11:1153-1161.

Imitola J, Raddassi K, Park KI, Mueller FJ, Nieto M, Teng YD, Frenkel D, Li J, Sidman RL, Walsh CA, Snyder EY, Khoury SJ (2004) Directed migration of neural stem cells to sites of CNS injury by the stromal cell-derived factor 1alpha/CXC chemokine receptor 4 pathway. Proceedings of the National Academy of Sciences of the United States of America 101:18117-18122.

Imura T, Kornblum HI, Sofroniew MV (2003) The predominant neural stem cell isolated from postnatal and adult forebrain but not early embryonic forebrain expresses GFAP. The Journal of neuroscience : the official journal of the Society for Neuroscience 23:2824-2832.

Iozzo RV (2005) Basement membrane proteoglycans: from cellar to ceiling. Nature reviews Molecular cell biology 6:646-656.

Ishikawa R, Hayashi K, Shirao T, Xue Y, Takagi T, Sasaki Y, Kohama K (1994) Drebrin, a development-associated brain protein from rat embryo, causes the dissociation of tropomyosin from actin filaments. The Journal of biological chemistry 269:29928-29933.

Ishikawa R, Katoh K, Takahashi A, Xie C, Oseki K, Watanabe M, Igarashi M, Nakamura A, Kohama K (2007) Drebrin attenuates the interaction between actin and myosin-V. Biochemical and biophysical research communications 359:398-401.

Ivanov A, Esclapez M, Pellegrino C, Shirao T, Ferhat L (2009) Drebrin A regulates dendritic spine plasticity and synaptic function in mature cultured hippocampal neurons. Journal of cell science 122:524-534.

Jansen S, Collins A, Yang C, Rebowski G, Svitkina T, Dominguez R (2011) Mechanism of actin filament bundling by fascin. The Journal of biological chemistry 286:30087-30096.

Jawhari AU, Buda A, Jenkins M, Shehzad K, Sarraf C, Noda M, Farthing MJ, Pignatelli M, Adams JC (2003) Fascin, an actin-bundling protein, modulates colonic epithelial cell invasiveness and differentiation in vitro. The American journal of pathology 162:69-80.

Jayo A, Parsons M (2010) Fascin: a key regulator of cytoskeletal dynamics. The international journal of biochemistry & cell biology 42:1614-1617.

Jayo A, Parsons M, Adams JC (2012) A novel Rho-dependent pathway that drives interaction of fascin-1 with p-Lin-11/Isl-1/Mec-3 kinase (LIMK) 1/2 to promote fascin-1/actin binding and filopodia stability. BMC biology 10:72.

Jin K, Wang X, Xie L, Mao XO, Zhu W, Wang Y, Shen J, Mao Y, Banwait S, Greenberg DA (2006) Evidence for stroke-induced neurogenesis in the human brain. Proceedings of the National Academy of Sciences of the United States of America 103:13198-13202.

Jin K, Xie L, Kim SH, Parmentier-Batteur S, Sun Y, Mao XO, Childs J, Greenberg DA (2004) Defective adult neurogenesis in CB1 cannabinoid receptor knockout mice. Molecular pharmacology 66:204-208.

Jin K, Zhu Y, Sun Y, Mao XO, Xie L, Greenberg DA (2002) Vascular endothelial growth factor (VEGF) stimulates neurogenesis in vitro and in vivo. Proceedings of the National Academy of Sciences of the United States of America 99:11946-11950.

Johansson CB, Momma S, Clarke DL, Risling M, Lendahl U, Frisen J (1999) Identification of a neural stem cell in the adult mammalian central nervous system. Cell 96:25-34.

Jorgensen JR, Fransson A, Fjord-Larsen L, Thompson LH, Houchins JP, Andrade N, Torp M, Kalkkinen N, Andersson E, Lindvall O, Ulfendahl M, Brunak S, Johansen TE, Wahlberg LU (2012) Cometin is a novel neurotrophic factor that promotes neurite outgrowth and neuroblast migration in vitro and supports survival of spiral ganglion neurons in vivo. Experimental neurology 233:172-181.

Kam M, Curtis MA, McGlashan SR, Connor B, Nannmark U, Faull RL (2009) The cellular composition and morphological organization of the rostral migratory stream in the adult human brain. Journal of chemical neuroanatomy 37:196-205.

Kane RE (1975) Preparation and purification of polymerized actin from sea urchin egg extracts. The Journal of cell biology 66:305-315.

Kaneko N, Marin O, Koike M, Hirota Y, Uchiyama Y, Wu JY, Lu Q, Tessier-Lavigne M, Alvarez-Buylla A, Okano H, Rubenstein JL, Sawamoto K (2010) New neurons clear the path of astrocytic processes for their rapid migration in the adult brain. Neuron 67:213-223.

Kaneko N, Sawamoto K (2009) Adult neurogenesis and its alteration under pathological conditions. Neuroscience research 63:155-164.

Kaplan MS, Hinds JW (1977) Neurogenesis in the adult rat: electron microscopic analysis of light radioautographs. Science 197:1092-1094.

Kawauchi T, Chihama K, Nabeshima Y, Hoshino M (2006) Cdk5 phosphorylates and stabilizes p27kip1 contributing to actin organization and cortical neuronal migration. Nature cell biology 8:17-26.

Kawauchi T, Sekine K, Shikanai M, Chihama K, Tomita K, Kubo K, Nakajima K, Nabeshima Y, Hoshino M (2010) Rab GTPases-dependent endocytic pathways regulate neuronal migration and maturation through N-cadherin trafficking. Neuron 67:588-602.

Kazanietz MG, Areces LB, Bahador A, Mischak H, Goodnight J, Mushinski JF, Blumberg PM (1993) Characterization of ligand and substrate specificity for the calcium-dependent and calcium-independent protein kinase C isozymes. Molecular pharmacology 44:298-307.

Kazanis I, Lathia JD, Vadakkan TJ, Raborn E, Wan R, Mughal MR, Eckley DM, Sasaki T, Patton B, Mattson MP, Hirschi KK, Dickinson ME, ffrench-Constant C (2010) Quiescence and activation of stem and precursor cell populations in the subependymal zone of the mammalian brain are associated with distinct cellular and extracellular matrix signals. The Journal of neuroscience : the official journal of the Society for Neuroscience 30:9771-9781.

Kee N, Sivalingam S, Boonstra R, Wojtowicz JM (2002) The utility of Ki-67 and BrdU as proliferative markers of adult neurogenesis. Journal of neuroscience methods 115:97-105.

Keon BH, Jedrzejewski PT, Paul DL, Goodenough DA (2000) Isoform specific expression of the neuronal F-actin binding protein, drebrin, in specialized cells of stomach and kidney epithelia. Journal of cell science 113 Pt 2:325-336.

Kerever A, Schnack J, Vellinga D, Ichikawa N, Moon C, Arikawa-Hirasawa E, Efird JT, Mercier F (2007) Novel extracellular matrix structures in the neural stem cell niche capture the neurogenic factor fibroblast growth factor 2 from the extracellular milieu. Stem cells 25:2146-2157.

Khlghatyan J, Saghatelyan A (2012) Time-lapse imaging of neuroblast migration in acute slices of the adult mouse forebrain. Journal of visualized experiments : JoVE e4061.

Kim J, Isokawa M, Ledent C, Alger BE (2002) Activation of muscarinic acetylcholine receptors enhances the release of endogenous cannabinoids in the hippocampus. The Journal of neuroscience : the official journal of the Society for Neuroscience 22:10182-10191.

Kim SJ, Choi IJ, Cheong TC, Lee SJ, Lotan R, Park SH, Chun KH (2010) Galectin-3 increases gastric cancer cell motility by up-regulating fascin-1 expression. Gastroenterology 138:1035-1045 e1031-1032.

Kim Y, Comte I, Szabo G, Hockberger P, Szele FG (2009) Adult mouse subventricular zone stem and progenitor cells are sessile and epidermal growth factor receptor negatively regulates neuroblast migration. PloS one 4:e8122.

Kobayashi R, Sekino Y, Shirao T, Tanaka S, Ogura T, Inada K, Saji M (2004) Antisense knockdown of drebrin A, a dendritic spine protein, causes stronger preference, impaired pre-pulse inhibition, and an increased sensitivity to psychostimulant. Neuroscience research 49:205-217.

Koizumi H, Higginbotham H, Poon T, Tanaka T, Brinkman BC, Gleeson JG (2006) Doublecortin maintains bipolar shape and nuclear translocation during migration in the adult forebrain. Nature neuroscience 9:779-786.

Kojima N, Kato Y, Shirao T, Obata K (1988) Nucleotide sequences of two embryonic drebrins, developmentally regulated brain proteins, and developmental change in their mRNAs. Brain research 464:207-215.

Kojima N, Shirao T (2007) Synaptic dysfunction and disruption of postsynaptic drebrin-actin complex: a study of neurological disorders accompanied by cognitive deficits. Neuroscience research 58:1-5.

Kojima N, Shirao T, Obata K (1993) Molecular cloning of a developmentally regulated brain protein, chicken drebrin A and its expression by alternative splicing of the drebrin gene. Brain research Molecular brain research 19:101-114.

Kokoeva MV, Yin H, Flier JS (2005) Neurogenesis in the hypothalamus of adult mice: potential role in energy balance. Science 310:679-683.

Korobova F, Svitkina T (2008) Arp2/3 complex is important for filopodia formation, growth cone motility, and neuritogenesis in neuronal cells. Molecular biology of the cell 19:1561-1574.

Kosaka T, Kosaka K (2005) Intraglomerular dendritic link connected by gap junctions and chemical synapses in the mouse main olfactory bulb: electron microscopic serial section analyses. Neuroscience 131:611-625.

Kraft R, Escobar MM, Narro ML, Kurtis JL, Efrat A, Barnard K, Restifo LL (2006) Phenotypes of Drosophila brain neurons in primary culture reveal a role for fascin in neurite shape and trajectory. The Journal of neuroscience : the official journal of the Society for Neuroscience 26:8734-8747.

Kreis P, Hendricusdottir R, Kay L, Papageorgiou IE, van Diepen M, Mack T, Ryves J, Harwood A, Leslie NR, Kann O, Parsons M, Eickholt BJ (2013) Phosphorylation of the actin binding protein Drebrin at S647 is regulated by neuronal activity and PTEN. PloS one 8:e71957.

Kureishy N, Sapountzi V, Prag S, Anilkumar N, Adams JC (2002) Fascins, and their roles in cell structure and function. BioEssays : news and reviews in molecular, cellular and developmental biology 24:350-361.

Lalli G (2009) RalA and the exocyst complex influence neuronal polarity through PAR-3 and aPKC. Journal of cell science 122:1499-1506.

Lalli G (2014) Extracellular signals controlling neuroblast migration in the postnatal brain. Advances in experimental medicine and biology 800:149-180.

Lambert de Rouvroit C, Goffinet AM (2001) Neuronal migration. Mechanisms of development 105:47-56.

Lappalainen P, Kessels MM, Cope MJ, Drubin DG (1998) The ADF homology (ADF-H) domain: a highly exploited actin-binding module. Molecular biology of the cell 9:1951-1959.

Lawler J (2000) The functions of thrombospondin-1 and-2. Current opinion in cell biology 12:634-640.

Lazarini F, Lledo PM (2011) Is adult neurogenesis essential for olfaction? Trends in neurosciences 34:20-30.

Lazarini F, Mouthon MA, Gheusi G, de Chaumont F, Olivo-Marin JC, Lamarque S, Abrous DN, Boussin FD, Lledo PM (2009) Cellular and behavioral effects of cranial irradiation of the subventricular zone in adult mice. PloS one 4:e7017.

Lee K, Gallop JL, Rambani K, Kirschner MW (2010) Self-assembly of filopodia-like structures on supported lipid bilayers. Science 329:1341-1345.

Lee SR, Kim HY, Rogowska J, Zhao BQ, Bhide P, Parent JM, Lo EH (2006) Involvement of matrix metalloproteinase in neuroblast cell migration from the subventricular zone after stroke. The Journal of neuroscience : the official journal of the Society for Neuroscience 26:3491-3495.

Lendahl U, Zimmerman LB, McKay RD (1990) CNS stem cells express a new class of intermediate filament protein. Cell 60:585-595.

Leventhal C, Rafii S, Rafii D, Shahar A, Goldman SA (1999) Endothelial trophic support of neuronal production and recruitment from the adult mammalian subependyma. Molecular and cellular neurosciences 13:450-464.

Li A, Dawson JC, Forero-Vargas M, Spence HJ, Yu X, Konig I, Anderson K, Machesky LM (2010) The actin-bundling protein fascin stabilizes actin in invadopodia and potentiates protrusive invasion. Current biology : CB 20:339-345.

Lim DA, Alvarez-Buylla A (1999) Interaction between astrocytes and adult subventricular zone precursors stimulates neurogenesis. Proceedings of the National Academy of Sciences of the United States of America 96:7526-7531.

Lim DA, Tramontin AD, Trevejo JM, Herrera DG, Garcia-Verdugo JM, Alvarez-Buylla A (2000) Noggin antagonizes BMP signaling to create a niche for adult neurogenesis. Neuron 28:713-726.

Lledo PM, Alonso M, Grubb MS (2006) Adult neurogenesis and functional plasticity in neuronal circuits. Nature reviews Neuroscience 7:179-193.

Lledo PM, Merkle FT, Alvarez-Buylla A (2008) Origin and function of olfactory bulb interneuron diversity. Trends in neurosciences 31:392-400.

Lois C, Alvarez-Buylla A (1994) Long-distance neuronal migration in the adult mammalian brain. Science 264:1145-1148.

Lois C, Garcia-Verdugo JM, Alvarez-Buylla A (1996) Chain migration of neuronal precursors. Science 271:978-981.

Louissaint A, Jr., Rao S, Leventhal C, Goldman SA (2002) Coordinated interaction of neurogenesis and angiogenesis in the adult songbird brain. Neuron 34:945-960.

Luskin MB (1993) Restricted proliferation and migration of postnatally generated neurons derived from the forebrain subventricular zone. Neuron 11:173-189.

Macara IG (2004) Parsing the polarity code. Nature reviews Molecular cell biology 5:220-231.

Macas J, Nern C, Plate KH, Momma S (2006) Increased generation of neuronal progenitors after ischemic injury in the aged adult human forebrain. The Journal of neuroscience : the official journal of the Society for Neuroscience 26:13114-13119.

Mackowiak M, Chocyk A, Markowicz-Kula K, Wedzony K (2004) Neurogenesis in the adult brain. Polish journal of pharmacology 56:673-687.

Mammoto A, Sasaki T, Asakura T, Hotta I, Imamura H, Takahashi K, Matsuura Y, Shirao T, Takai Y (1998) Interactions of drebrin and gephyrin with profilin. Biochemical and biophysical research communications 243:86-89.

Marin O, Plump AS, Flames N, Sanchez-Camacho C, Tessier-Lavigne M, Rubenstein JL (2003) Directional guidance of interneuron migration to the cerebral cortex relies on subcortical Slit1/2-independent repulsion and cortical attraction. Development 130:1889-1901.

Marin O, Valiente M, Ge X, Tsai LH (2010) Guiding neuronal cell migrations. Cold Spring Harbor perspectives in biology 2:a001834.

Mason HA, Ito S, Corfas G (2001) Extracellular signals that regulate the tangential migration of olfactory bulb neuronal precursors: inducers, inhibitors, and repellents. The Journal of neuroscience : the official journal of the Society for Neuroscience 21:7654-7663.

Mason I (2007) Initiation to end point: the multiple roles of fibroblast growth factors in neural development. Nature reviews Neuroscience 8:583-596.

Matsuda LA, Lolait SJ, Brownstein MJ, Young AC, Bonner TI (1990) Structure of a cannabinoid receptor and functional expression of the cloned cDNA. Nature 346:561-564.

Mattila PK, Lappalainen P (2008) Filopodia: molecular architecture and cellular functions. Nature reviews Molecular cell biology 9:446-454.

Mayanil CS, George D, Freilich L, Miljan EJ, Mania-Farnell B, McLone DG, Bremer EG (2001) Microarray analysis detects novel Pax3 downstream target genes. The Journal of biological chemistry 276:49299-49309.

McAnuff MA, Rettig GR, Rice KG (2007) Potency of siRNA versus shRNA mediated knockdown in vivo. Journal of pharmaceutical sciences 96:2922-2930.

McCaig CD, Rajnicek AM, Song B, Zhao M (2005) Controlling cell behavior electrically: current views and future potential. Physiological reviews 85:943-978.

Mechoulam R, Parker LA (2013) The endocannabinoid system and the brain. Annual review of psychology 64:21-47.

Megiorni F, Indovina P, Mora B, Mazzilli MC (2005) Minor expression of fascin-1 gene (FSCN1) in NTera2 cells depleted of CREB-binding protein. Neuroscience letters 381:169-174.

Mejia-Gervacio S, Murray K, Sapir T, Belvindrah R, Reiner O, Lledo PM (2012) MARK2/Par-1 guides the directionality of neuroblasts migrating to the olfactory bulb. Molecular and cellular neurosciences 49:97-103.

Mercer JC, Qi Q, Mottram LF, Law M, Bruce D, Iyer A, Morales JL, Yamazaki H, Shirao T, Peterson BR, August A (2010) Chemico-genetic identification of drebrin as a regulator of calcium responses. The international journal of biochemistry & cell biology 42:337-345.

Mercier F, Arikawa-Hirasawa E (2012) Heparan sulfate niche for cell proliferation in the adult brain. Neuroscience letters 510:67-72.

Mercier F, Kitasako JT, Hatton GI (2002) Anatomy of the brain neurogenic zones revisited: fractones and the fibroblast/macrophage network. The Journal of comparative neurology 451:170-188.

Merkle FT, Fuentealba LC, Sanders TA, Magno L, Kessaris N, Alvarez-Buylla A (2014) Adult neural stem cells in distinct microdomains generate previously unknown interneuron types. Nature neuroscience 17:207-214.

Merkle FT, Tramontin AD, Garcia-Verdugo JM, Alvarez-Buylla A (2004) Radial glia give rise to adult neural stem cells in the subventricular zone. Proceedings of the National Academy of Sciences of the United States of America 101:17528-17532.

Merriam EB, Millette M, Lumbard DC, Saengsawang W, Fothergill T, Hu X, Ferhat L, Dent EW (2013) Synaptic regulation of microtubule dynamics in dendritic spines by calcium, F-actin, and drebrin. The Journal of neuroscience : the official journal of the Society for Neuroscience 33:16471-16482.

Mirzadeh Z, Merkle FT, Soriano-Navarro M, Garcia-Verdugo JM, Alvarez-Buylla A (2008) Neural stem cells confer unique pinwheel architecture to the ventricular surface in neurogenic regions of the adult brain. Cell stem cell 3:265-278.

Mission JP, Takahashi T, Caviness VS, Jr. (1991) Ontogeny of radial and other astroglial cells in murine cerebral cortex. Glia 4:138-148.

Miyakoshi LM, Todeschini AR, Mendez-Otero R, Hedin-Pereira C (2012) Role of the 9-O-acetyl GD3 in subventricular zone neuroblast migration. Molecular and cellular neurosciences 49:240-249.

Mizui T, Kojima N, Yamazaki H, Katayama M, Hanamura K, Shirao T (2009) Drebrin E is involved in the regulation of axonal growth through actin-myosin interactions. Journal of neurochemistry 109:611-622.

Mizui T, Takahashi H, Sekino Y, Shirao T (2005) Overexpression of drebrin A in immature neurons induces the accumulation of F-actin and PSD-95 into dendritic filopodia, and the formation of large abnormal protrusions. Molecular and cellular neurosciences 30:630-638.

Mobley AK, McCarty JH (2011) beta8 integrin is essential for neuroblast migration in the rostral migratory stream. Glia 59:1579-1587.

Mobley AK, Tchaicha JH, Shin J, Hossain MG, McCarty JH (2009) Beta8 integrin regulates neurogenesis and neurovascular homeostasis in the adult brain. Journal of cell science 122:1842-1851.

Monje ML, Mizumatsu S, Fike JR, Palmer TD (2002) Irradiation induces neural precursor-cell dysfunction. Nature medicine 8:955-962.

Moreno MM, Linster C, Escanilla O, Sacquet J, Didier A, Mandairon N (2009) Olfactory perceptual learning requires adult neurogenesis. Proceedings of the National Academy of Sciences of the United States of America 106:17980-17985.

Morshead CM, Garcia AD, Sofroniew MV, van Der Kooy D (2003) The ablation of glial fibrillary acidic protein-positive cells from the adult central nervous system results in the loss of forebrain neural stem cells but not retinal stem cells. The European journal of neuroscience 18:76-84.

Mosialos G, Birkenbach M, Ayehunie S, Matsumura F, Pinkus GS, Kieff E, Langhoff E (1996) Circulating human dendritic cells differentially express high levels of a 55-kd actin-bundling protein. The American journal of pathology 148:593-600.

Mosialos G, Yamashiro S, Baughman RW, Matsudaira P, Vara L, Matsumura F, Kieff E, Birkenbach M (1994) Epstein-Barr virus infection induces expression in B lymphocytes of a novel gene encoding an evolutionarily conserved 55-kilodalton actin-bundling protein. Journal of virology 68:7320-7328.

Motulsky H (1998) GraphPad Software, InStat guide to choosing and interpreting statistical tests. Inc., San Diego California USA.

Munro S, Thomas KL, Abu-Shaar M (1993) Molecular characterization of a peripheral receptor for cannabinoids. Nature 365:61-65.

Murase S, Cho C, White JM, Horwitz AF (2008) ADAM2 promotes migration of neuroblasts in the rostral migratory stream to the olfactory bulb. The European journal of neuroscience 27:1585-1595.

Murase S, Horwitz AF (2002) Deleted in colorectal carcinoma and differentially expressed integrins mediate the directional migration of neural precursors in the rostral migratory stream. The Journal of neuroscience : the official journal of the Society for Neuroscience 22:3568-3579.

Nagel J, Delandre C, Zhang Y, Forstner F, Moore AW, Tavosanis G (2012) Fascin controls neuronal class-specific dendrite arbor morphology. Development 139:2999-3009.

Nam SC, Kim Y, Dryanovski D, Walker A, Goings G, Woolfrey K, Kang SS, Chu C, Chenn A, Erdelyi F, Szabo G, Hockberger P, Szele FG (2007) Dynamic features of postnatal subventricular zone cell motility: a two-photon time-lapse study. The Journal of comparative neurology 505:190-208.

Nemethova M, Auinger S, Small JV (2008) Building the actin cytoskeleton: filopodia contribute to the construction of contractile bundles in the lamella. The Journal of cell biology 180:1233-1244.

Ng KL, Li JD, Cheng MY, Leslie FM, Lee AG, Zhou QY (2005) Dependence of olfactory bulb neurogenesis on prokineticin 2 signaling. Science 308:1923-1927.

Nguyen Ba-Charvet KT, Brose K, Marillat V, Kidd T, Goodman CS, Tessier-Lavigne M, Sotelo C, Chedotal A (1999) Slit2-Mediated chemorepulsion and collapse of developing forebrain axons. Neuron 22:463-473.

Nguyen L, Malgrange B, Breuskin I, Bettendorff L, Moonen G, Belachew S, Rigo JM (2003) Autocrine/paracrine activation of the GABA(A) receptor inhibits the proliferation of neurogenic polysialylated neural cell adhesion molecule-positive (PSA-NCAM+) precursor cells from postnatal striatum. The Journal of neuroscience : the official journal of the Society for Neuroscience 23:3278-3294.

Nguyen-Ba-Charvet KT, Picard-Riera N, Tessier-Lavigne M, Baron-Van Evercooren A, Sotelo C, Chedotal A (2004) Multiple roles for slits in the control of cell migration in the rostral migratory stream. The Journal of neuroscience : the official journal of the Society for Neuroscience 24:1497-1506.

Nguyen-Ba-Charvet KT, Plump AS, Tessier-Lavigne M, Chedotal A (2002) Slit1 and slit2 proteins control the development of the lateral olfactory tract. The Journal of neuroscience : the official journal of the Society for Neuroscience 22:5473-5480.

Nie K, Molnar Z, Szele FG (2010) Proliferation but not migration is associated with blood vessels during development of the rostral migratory stream. Developmental neuroscience 32:163-172.

Niethammer M, Smith DS, Ayala R, Peng J, Ko J, Lee MS, Morabito M, Tsai LH (2000) NUDEL is a novel Cdk5 substrate that associates with LIS1 and cytoplasmic dynein. Neuron 28:697-711.

Noctor SC, Flint AC, Weissman TA, Dammerman RS, Kriegstein AR (2001) Neurons derived from radial glial cells establish radial units in neocortex. Nature 409:714-720.

Noctor SC, Martinez-Cerdeno V, Kriegstein AR (2007) Contribution of intermediate progenitor cells to cortical histogenesis. Archives of neurology 64:639-642.

Nolz JC, Gomez TS, Zhu P, Li S, Medeiros RB, Shimizu Y, Burkhardt JK, Freedman BD, Billadeau DD (2006) The WAVE2 complex regulates actin cytoskeletal reorganization and CRAC-mediated calcium entry during T cell activation. Current biology : CB 16:24-34.

O'Shea KS, Liu LH, Dixit VM (1991) Thrombospondin and a 140 kd fragment promote adhesion and neurite outgrowth from embryonic central and peripheral neurons and from PC12 cells. Neuron 7:231-237.

O'Shea KS, Liu LH, Kinnunen LH, Dixit VM (1990) Role of the extracellular matrix protein thrombospondin in the early development of the mouse embryo. The Journal of cell biology 111:2713-2723.

Ocbina PJ, Dizon ML, Shin L, Szele FG (2006) Doublecortin is necessary for the migration of adult subventricular zone cells from neurospheres. Molecular and cellular neurosciences 33:126-135.

Ohab JJ, Fleming S, Blesch A, Carmichael ST (2006) A neurovascular niche for neurogenesis after stroke. The Journal of neuroscience : the official journal of the Society for Neuroscience 26:13007-13016.

Ohshima T, Ward JM, Huh CG, Longenecker G, Veeranna, Pant HC, Brady RO, Martin LJ, Kulkarni AB (1996) Targeted disruption of the cyclin-dependent kinase 5 gene results in abnormal corticogenesis, neuronal pathology and perinatal death. Proceedings of the National Academy of Sciences of the United States of America 93:11173-11178.

Ono K, Tomasiewicz H, Magnuson T, Rutishauser U (1994) N-CAM mutation inhibits tangential neuronal migration and is phenocopied by enzymatic removal of polysialic acid. Neuron 13:595-609.

Ono S, Yamakita Y, Yamashiro S, Matsudaira PT, Gnarra JR, Obinata T, Matsumura F (1997) Identification of an actin binding region and a protein kinase C phosphorylation site on human fascin. The Journal of biological chemistry 272:2527-2533.

Ooe N, Saito K, Mikami N, Nakatuka I, Kaneko H (2004) Identification of a novel basic helix-loop-helix-PAS factor, NXF, reveals a Sim2 competitive, positive regulatory role in dendritic-cytoskeleton modulator drebrin gene expression. Molecular and cellular biology 24:608-616.

Orona E, Scott JW, Rainer EC (1983) Different granule cell populations innervate superficial and deep regions of the external plexiform layer in rat olfactory bulb. The Journal of comparative neurology 217:227-237.

Otto JJ, Kane RE, Bryan J (1979) Formation of filopodia in coelomocytes: localization of fascin, a 58,000 dalton actin cross-linking protein. Cell 17:285-293.

Oudin MJ, Gajendra S, Williams G, Hobbs C, Lalli G, Doherty P (2011) Endocannabinoids regulate the migration of subventricular zone-derived neuroblasts in the postnatal brain. The Journal of neuroscience : the official journal of the Society for Neuroscience 31:4000-4011.

Palazuelos J, Aguado T, Egia A, Mechoulam R, Guzman M, Galve-Roperh I (2006) Non-psychoactive CB2 cannabinoid agonists stimulate neural progenitor proliferation. FASEB journal : official publication of the Federation of American Societies for Experimental Biology 20:2405-2407.

Palmer TD, Takahashi J, Gage FH (1997) The adult rat hippocampus contains primordial neural stem cells. Molecular and cellular neurosciences 8:389-404.

Palmer TD, Willhoite AR, Gage FH (2000) Vascular niche for adult hippocampal neurogenesis. The Journal of comparative neurology 425:479-494.

Panganiban G, Rubenstein JL (2002) Developmental functions of the Distal-less/Dlx homeobox genes. Development 129:4371-4386.

Paratcha G, Ibanez CF, Ledda F (2006) GDNF is a chemoattractant factor for neuronal precursor cells in the rostral migratory stream. Molecular and cellular neurosciences 31:505-514.

Park HT, Wu J, Rao Y (2002) Molecular control of neuronal migration. BioEssays : news and reviews in molecular, cellular and developmental biology 24:821-827.

Parrish-Aungst S, Shipley MT, Erdelyi F, Szabo G, Puche AC (2007) Quantitative analysis of neuronal diversity in the mouse olfactory bulb. The Journal of comparative neurology 501:825-836.

Parsons M, Adams JC (2008) Rac regulates the interaction of fascin with protein kinase C in cell migration. Journal of cell science 121:2805-2813.

Parsons M, Vojnovic B, Ameer-Beg S (2004) Imaging protein-protein interactions in cell motility using fluorescence resonance energy transfer (FRET). Biochemical Society transactions 32:431-433.

Pastrana E, Cheng LC, Doetsch F (2009) Simultaneous prospective purification of adult subventricular zone neural stem cells and their progeny. Proceedings of the National Academy of Sciences of the United States of America 106:6387-6392.

Peitsch WK, Bulkescher J, Spring H, Hofmann I, Goerdt S, Franke WW (2006) Dynamics of the actin-binding protein drebrin in motile cells and definition of a juxtanuclear drebrin-enriched zone. Experimental cell research 312:2605-2618.

Peitsch WK, Grund C, Kuhn C, Schnolzer M, Spring H, Schmelz M, Franke WW (1999) Drebrin is a widespread actin-associating protein enriched at junctional plaques, defining a specific microfilament anchorage system in polar epithelial cells. European journal of cell biology 78:767-778.

Peitsch WK, Hofmann I, Bulkescher J, Hergt M, Spring H, Bleyl U, Goerdt S, Franke WW (2005) Drebrin, an actin-binding, cell-type characteristic protein: induction and localization in epithelial skin tumors and cultured keratinocytes. The Journal of investigative dermatology 125:761-774.

Peitsch WK, Hofmann I, Pratzel S, Grund C, Kuhn C, Moll I, Langbein L, Franke WW (2001) Drebrin particles: components in the ensemble of proteins regulating actin dynamics of lamellipodia and filopodia. European journal of cell biology 80:567-579.

Pelosi G, Pasini F, Fraggetta F, Pastorino U, Iannucci A, Maisonneuve P, Arrigoni G, De Manzoni G, Bresaola E, Viale G (2003) Independent value of fascin immunoreactivity for predicting lymph node metastases in typical and atypical pulmonary carcinoids. Lung cancer 42:203-213.

Peraud A, Mondal S, Hawkins C, Mastronardi M, Bailey K, Rutka JT (2003) Expression of fascin, an actin-bundling protein, in astrocytomas of varying grades. Brain tumor pathology 20:53-58.

Peretto P, Giachino C, Aimar P, Fasolo A, Bonfanti L (2005) Chain formation and glial tube assembly in the shift from neonatal to adult subventricular zone of the rodent forebrain. The Journal of comparative neurology 487:407-427.

Pertwee RG (2006) The pharmacology of cannabinoid receptors and their ligands: an overview. International journal of obesity 30 Suppl 1:S13-18.

Petreanu L, Alvarez-Buylla A (2002) Maturation and death of adult-born olfactory bulb granule neurons: role of olfaction. The Journal of neuroscience : the official journal of the Society for Neuroscience 22:6106-6113.

Platel JC, Dave KA, Bordey A (2008a) Control of neuroblast production and migration by converging GABA and glutamate signals in the postnatal forebrain. The Journal of physiology 586:3739-3743.

Platel JC, Dave KA, Gordon V, Lacar B, Rubio ME, Bordey A (2010) NMDA receptors activated by subventricular zone astrocytic glutamate are critical for neuroblast survival prior to entering a synaptic network. Neuron 65:859-872.

Platel JC, Heintz T, Young S, Gordon V, Bordey A (2008b) Tonic activation of GLUK5 kainate receptors decreases neuroblast migration in whole-mounts of the subventricular zone. The Journal of physiology 586:3783-3793.

Platel JC, Lacar B, Bordey A (2007) GABA and glutamate signaling: homeostatic control of adult forebrain neurogenesis. Journal of molecular histology 38:602-610.

Polleux F, Whitford KL, Dijkhuizen PA, Vitalis T, Ghosh A (2002) Control of cortical interneuron migration by neurotrophins and PI3-kinase signaling. Development 129:3147-3160.

Ponting CP, Russell RB (2000) Identification of distant homologues of fibroblast growth factors suggests a common ancestor for all beta-trefoil proteins. Journal of molecular biology 302:1041-1047.

Porteus MH, Bulfone A, Liu JK, Puelles L, Lo LC, Rubenstein JL (1994) DLX-2, MASH-1, and MAP-2 expression and bromodeoxyuridine incorporation define molecularly distinct cell populations in the embryonic mouse forebrain. The Journal of neuroscience : the official journal of the Society for Neuroscience 14:6370-6383.

Prosser HM, Bradley A, Caldwell MA (2007) Olfactory bulb hypoplasia in Prokr2 null mice stems from defective neuronal progenitor migration and differentiation. The European journal of neuroscience 26:3339-3344.

Puverel S, Nakatani H, Parras C, Soussi-Yanicostas N (2009) Prokineticin receptor 2 expression identifies migrating neuroblasts and their subventricular zone transient-amplifying progenitors in adult mice. The Journal of comparative neurology 512:232-242.

Quinones-Hinojosa A, Sanai N, Soriano-Navarro M, Gonzalez-Perez O, Mirzadeh Z, Gil-Perotin S, Romero-Rodriguez R, Berger MS, Garcia-Verdugo JM, Alvarez-Buylla A (2006) Cellular composition and cytoarchitecture of the adult human subventricular zone: a niche of neural stem cells. The Journal of comparative neurology 494:415-434.

Quintavalle M, Elia L, Condorelli G, Courtneidge SA (2010) MicroRNA control of podosome formation in vascular smooth muscle cells in vivo and in vitro. The Journal of cell biology 189:13-22.

Rakic P (1985) Limits of neurogenesis in primates. Science 227:1054-1056.

Rao DD, Vorhies JS, Senzer N, Nemunaitis J (2009) siRNA vs. shRNA: similarities and differences. Advanced drug delivery reviews 61:746-759.

Rehm K, Panzer L, van Vliet V, Genot E, Linder S (2013) Drebrin preserves endothelial integrity by stabilizing nectin at adherens junctions. Journal of cell science 126:3756-3769.

Reiner O, Sapir T (2009) Polarity regulation in migrating neurons in the cortex. Molecular neurobiology 40:1-14.

Reynolds BA, Weiss S (1992) Generation of neurons and astrocytes from isolated cells of the adult mammalian central nervous system. Science 255:1707-1710.

Ricca BL, Rock RS (2010) The stepping pattern of myosin X is adapted for processive motility on bundled actin. Biophysical journal 99:1818-1826.

Ridley AJ, Schwartz MA, Burridge K, Firtel RA, Ginsberg MH, Borisy G, Parsons JT, Horwitz AR (2003) Cell migration: integrating signals from front to back. Science 302:1704-1709.

Riedl J, Crevenna AH, Kessenbrock K, Yu JH, Neukirchen D, Bista M, Bradke F, Jenne D, Holak TA, Werb Z, Sixt M, Wedlich-Soldner R (2008) Lifeact: a versatile marker to visualize F-actin. Nature methods 5:605-607.

Robin AM, Zhang ZG, Wang L, Zhang RL, Katakowski M, Zhang L, Wang Y, Zhang C, Chopp M (2006) Stromal cell-derived factor 1alpha mediates neural progenitor cell motility after focal cerebral ischemia. Journal of cerebral blood flow and metabolism : official journal of the International Society of Cerebral Blood Flow and Metabolism 26:125-134.

Rolando C, Parolisi R, Boda E, Schwab ME, Rossi F, Buffo A (2012) Distinct roles of Nogo-a and Nogo receptor 1 in the homeostatic regulation of adult neural stem cell function and neuroblast migration. The Journal of neuroscience : the official journal of the Society for Neuroscience 32:17788-17799.

Roma AA, Prayson RA (2005) Fascin expression in 90 patients with glioblastoma multiforme. Annals of diagnostic pathology 9:307-311.

Ross TD, Coon BG, Yun S, Baeyens N, Tanaka K, Ouyang M, Schwartz MA (2013) Integrins in mechanotransduction. Current opinion in cell biology 25:613-618.

Rosse C, Formstecher E, Boeckeler K, Zhao Y, Kremerskothen J, White MD, Camonis JH, Parker PJ (2009) An aPKC-exocyst complex controls paxillin phosphorylation and migration through localised JNK1 activation. PLoS biology 7:e1000235.

Rousselot P, Lois C, Alvarez-Buylla A (1995) Embryonic (PSA) N-CAM reveals chains of migrating neuroblasts between the lateral ventricle and the olfactory bulb of adult mice. The Journal of comparative neurology 351:51-61.

Rutishauser U, Watanabe M, Silver J, Troy FA, Vimr ER (1985) Specific alteration of NCAM-mediated cell adhesion by an endoneuraminidase. The Journal of cell biology 101:1842-1849.

Saghatelyan A, de Chevigny A, Schachner M, Lledo PM (2004) Tenascin-R mediates activity-dependent recruitment of neuroblasts in the adult mouse forebrain. Nature neuroscience 7:347-356.

Saha B, Ypsilanti AR, Boutin C, Cremer H, Chedotal A (2012) Plexin-B2 regulates the proliferation and migration of neuroblasts in the postnatal and adult subventricular zone. The Journal of neuroscience : the official journal of the Society for Neuroscience 32:16892-16905.

Sanai N, Berger MS, Garcia-Verdugo JM, Alvarez-Buylla A (2007) Comment on "Human neuroblasts migrate to the olfactory bulb via a lateral ventricular extension". Science 318:393; author reply 393.

Sanai N, Nguyen T, Ihrie RA, Mirzadeh Z, Tsai HH, Wong M, Gupta N, Berger MS, Huang E, Garcia-Verdugo JM, Rowitch DH, Alvarez-Buylla A (2011) Corridors of

migrating neurons in the human brain and their decline during infancy. Nature 478:382-386.

Sanai N, Tramontin AD, Quinones-Hinojosa A, Barbaro NM, Gupta N, Kunwar S, Lawton MT, McDermott MW, Parsa AT, Manuel-Garcia Verdugo J, Berger MS, Alvarez-Buylla A (2004) Unique astrocyte ribbon in adult human brain contains neural stem cells but lacks chain migration. Nature 427:740-744.

Sancho-Tello M, Valles S, Montoliu C, Renau-Piqueras J, Guerri C (1995) Developmental pattern of GFAP and vimentin gene expression in rat brain and in radial glial cultures. Glia 15:157-166.

Sasaki Y, Hayashi K, Shirao T, Ishikawa R, Kohama K (1996) Inhibition by drebrin of the actin-bundling activity of brain fascin, a protein localized in filopodia of growth cones. Journal of neurochemistry 66:980-988.

Sawamoto K, Wichterle H, Gonzalez-Perez O, Cholfin JA, Yamada M, Spassky N, Murcia NS, Garcia-Verdugo JM, Marin O, Rubenstein JL, Tessier-Lavigne M, Okano H, Alvarez-Buylla A (2006) New neurons follow the flow of cerebrospinal fluid in the adult brain. Science 311:629-632.

Schaar BT, McConnell SK (2005) Cytoskeletal coordination during neuronal migration. Proceedings of the National Academy of Sciences of the United States of America 102:13652-13657.

Schliwa M, Euteneuer U, Graf R, Ueda M (1999) Centrosomes, microtubules and cell migration. Biochemical Society symposium 65:223-231.

Schmechel DE, Rakic P (1979) A Golgi study of radial glial cells in developing monkey telencephalon: morphogenesis and transformation into astrocytes. Anatomy and embryology 156:115-152.

Scholzen T, Gerdes J (2000) The Ki-67 protein: from the known and the unknown. Journal of cellular physiology 182:311-322.

Sedeh RS, Fedorov AA, Fedorov EV, Ono S, Matsumura F, Almo SC, Bathe M (2010) Structure, evolutionary conservation, and conformational dynamics of Homo sapiens fascin-1, an F-actin crosslinking protein. Journal of molecular biology 400:589-604.

Seki T, Arai Y (1993) Distribution and possible roles of the highly polysialylated neural cell adhesion molecule (NCAM-H) in the developing and adult central nervous system. Neuroscience research 17:265-290.

Sekino Y, Kojima N, Shirao T (2007) Role of actin cytoskeleton in dendritic spine morphogenesis. Neurochemistry international 51:92-104.

Sekino Y, Tanaka S, Hanamura K, Yamazaki H, Sasagawa Y, Xue Y, Hayashi K, Shirao T (2006) Activation of N-methyl-D-aspartate receptor induces a shift of drebrin

distribution: disappearance from dendritic spines and appearance in dendritic shafts. Molecular and cellular neurosciences 31:493-504.

Seri B, Garcia-Verdugo JM, Collado-Morente L, McEwen BS, Alvarez-Buylla A (2004) Cell types, lineage, and architecture of the germinal zone in the adult dentate gyrus. The Journal of comparative neurology 478:359-378.

Seri B, Garcia-Verdugo JM, McEwen BS, Alvarez-Buylla A (2001) Astrocytes give rise to new neurons in the adult mammalian hippocampus. The Journal of neuroscience : the official journal of the Society for Neuroscience 21:7153-7160.

Shen Q, Goderie SK, Jin L, Karanth N, Sun Y, Abramova N, Vincent P, Pumiglia K, Temple S (2004) Endothelial cells stimulate self-renewal and expand neurogenesis of neural stem cells. Science 304:1338-1340.

Shepherd GM (1972) Synaptic organization of the mammalian olfactory bulb. Physiological reviews 52:864-917.

Shepherd GM (2004) The human sense of smell: are we better than we think? PLoS biology 2:E146.

Shieh JC, Schaar BT, Srinivasan K, Brodsky FM, McConnell SK (2011) Endocytosis regulates cell soma translocation and the distribution of adhesion proteins in migrating neurons. PloS one 6:e17802.

Shim KS, Lubec G (2002) Drebrin, a dendritic spine protein, is manifold decreased in brains of patients with Alzheimer's disease and Down syndrome. Neuroscience letters 324:209-212.

Shinohara R, Thumkeo D, Kamijo H, Kaneko N, Sawamoto K, Watanabe K, Takebayashi H, Kiyonari H, Ishizaki T, Furuyashiki T, Narumiya S (2012) A role for mDia, a Rho-regulated actin nucleator, in tangential migration of interneuron precursors. Nature neuroscience 15:373-380, S371-372.

Shiraishi-Yamaguchi Y, Sato Y, Sakai R, Mizutani A, Knopfel T, Mori N, Mikoshiba K, Furuichi T (2009) Interaction of Cupidin/Homer2 with two actin cytoskeletal regulators, Cdc42 small GTPase and Drebrin, in dendritic spines. BMC neuroscience 10:25.

Shirao T (1995) The roles of microfilament-associated proteins, drebrins, in brain morphogenesis: a review. Journal of biochemistry 117:231-236.

Shirao T, Hayashi K, Ishikawa R, Isa K, Asada H, Ikeda K, Uyemura K (1994) Formation of thick, curving bundles of actin by drebrin A expressed in fibroblasts. Experimental cell research 215:145-153.

Shirao T, Kojima N, Kato Y, Obata K (1988) Molecular cloning of a cDNA for the developmentally regulated brain protein, drebrin. Brain research 464:71-74.

Shirao T, Kojima N, Terada S, Obata K (1990) Expression of three drebrin isoforms in the developing nervous system. Neuroscience research Supplement : the official journal of the Japan Neuroscience Society 13:S106-111.

Shonukan O, Bagayogo I, McCrea P, Chao M, Hempstead B (2003) Neurotrophin-induced melanoma cell migration is mediated through the actin-bundling protein fascin. Oncogene 22:3616-3623.

Smith DS, Niethammer M, Ayala R, Zhou Y, Gambello MJ, Wynshaw-Boris A, Tsai LH (2000) Regulation of cytoplasmic dynein behaviour and microtubule organization by mammalian Lis1. Nature cell biology 2:767-775.

Snapyan M, Lemasson M, Brill MS, Blais M, Massouh M, Ninkovic J, Gravel C, Berthod F, Gotz M, Barker PA, Parent A, Saghatelyan A (2009) Vasculature guides migrating neuronal precursors in the adult mammalian forebrain via brain-derived neurotrophic factor signaling. The Journal of neuroscience : the official journal of the Society for Neuroscience 29:4172-4188.

Solecki DJ, Model L, Gaetz J, Kapoor TM, Hatten ME (2004) Par6alpha signaling controls glial-guided neuronal migration. Nature neuroscience 7:1195-1203.

Sonego M, Gajendra S, Parsons M, Ma Y, Hobbs C, Zentar MP, Williams G, Machesky LM, Doherty P, Lalli G (2013a) Fascin regulates the migration of subventricular zone-derived neuroblasts in the postnatal brain. The Journal of neuroscience : the official journal of the Society for Neuroscience 33:12171-12185.

Sonego M, Zhou Y, Oudin MJ, Doherty P, Lalli G (2013b) In vivo Postnatal Electroporation and Time-lapse Imaging of Neuroblast Migration in Mouse Acute Brain Slices. Journal of visualized experiments : JoVE.

Song H, Stevens CF, Gage FH (2002) Astroglia induce neurogenesis from adult neural stem cells. Nature 417:39-44.

Song M, Kojima N, Hanamura K, Sekino Y, Inoue HK, Mikuni M, Shirao T (2008) Expression of drebrin E in migrating neuroblasts in adult rat brain: coincidence between drebrin E disappearance from cell body and cessation of migration. Neuroscience 152:670-682.

Spalding KL, Bergmann O, Alkass K, Bernard S, Salehpour M, Huttner HB, Bostrom E, Westerlund I, Vial C, Buchholz BA, Possnert G, Mash DC, Druid H, Frisen J (2013) Dynamics of hippocampal neurogenesis in adult humans. Cell 153:1219-1227.

Spalding KL, Bhardwaj RD, Buchholz BA, Druid H, Frisen J (2005) Retrospective birth dating of cells in humans. Cell 122:133-143.

Spassky N, Merkle FT, Flames N, Tramontin AD, Garcia-Verdugo JM, Alvarez-Buylla A (2005) Adult ependymal cells are postmitotic and are derived from radial glial cells during embryogenesis. The Journal of neuroscience : the official journal of the Society for Neuroscience 25:10-18.

Spradling A, Drummond-Barbosa D, Kai T (2001) Stem cells find their niche. Nature 414:98-104.

Steffen A, Faix J, Resch GP, Linkner J, Wehland J, Small JV, Rottner K, Stradal TE (2006) Filopodia formation in the absence of functional WAVE- and Arp2/3-complexes. Molecular biology of the cell 17:2581-2591.

Stewart RR, Hoge GJ, Zigova T, Luskin MB (2002) Neural progenitor cells of the neonatal rat anterior subventricular zone express functional GABA(A) receptors. Journal of neurobiology 50:305-322.

Sugiura T, Kondo S, Sukagawa A, Nakane S, Shinoda A, Itoh K, Yamashita A, Waku K (1995) 2-Arachidonoylglycerol: a possible endogenous cannabinoid receptor ligand in brain. Biochemical and biophysical research communications 215:89-97.

Suh Y, Obernier K, Holzl-Wenig G, Mandl C, Herrmann A, Worner K, Eckstein V, Ciccolini F (2009) Interaction between DLX2 and EGFR regulates proliferation and neurogenesis of SVZ precursors. Molecular and cellular neurosciences 42:308-314.

Suhonen JO, Peterson DA, Ray J, Gage FH (1996) Differentiation of adult hippocampus-derived progenitors into olfactory neurons in vivo. Nature 383:624-627.

Sultan S, Mandairon N, Kermen F, Garcia S, Sacquet J, Didier A (2010) Learning-dependent neurogenesis in the olfactory bulb determines long-term olfactory memory. FASEB journal : official publication of the Federation of American Societies for Experimental Biology 24:2355-2363.

Svitkina TM, Bulanova EA, Chaga OY, Vignjevic DM, Kojima S, Vasiliev JM, Borisy GG (2003) Mechanism of filopodia initiation by reorganization of a dendritic network. The Journal of cell biology 160:409-421.

Takahashi H, Mizui T, Shirao T (2006) Down-regulation of drebrin A expression suppresses synaptic targeting of NMDA receptors in developing hippocampal neurones. Journal of neurochemistry 97 Suppl 1:110-115.

Takahashi H, Sekino Y, Tanaka S, Mizui T, Kishi S, Shirao T (2003) Drebrin-dependent actin clustering in dendritic filopodia governs synaptic targeting of postsynaptic density-95 and dendritic spine morphogenesis. The Journal of neuroscience : the official journal of the Society for Neuroscience 23:6586-6595.

Tattersfield AS, Croon RJ, Liu YW, Kells AP, Faull RL, Connor B (2004) Neurogenesis in the striatum of the quinolinic acid lesion model of Huntington's disease. Neuroscience 127:319-332.

Terakawa Y, Agnihotri S, Golbourn B, Nadi M, Sabha N, Smith CA, Croul SE, Rutka JT (2013) The role of drebrin in glioma migration and invasion. Experimental cell research 319:517-528.

Thored P, Arvidsson A, Cacci E, Ahlenius H, Kallur T, Darsalia V, Ekdahl CT, Kokaia Z, Lindvall O (2006) Persistent production of neurons from adult brain stem cells during recovery after stroke. Stem cells 24:739-747.

Toda M, Shirao T, Minoshima S, Shimizu N, Toya S, Uyemura K (1993) Molecular cloning of cDNA encoding human drebrin E and chromosomal mapping of its gene. Biochemical and biophysical research communications 196:468-472.

Tomasiewicz H, Ono K, Yee D, Thompson C, Goridis C, Rutishauser U, Magnuson T (1993) Genetic deletion of a neural cell adhesion molecule variant (N-CAM-180) produces distinct defects in the central nervous system. Neuron 11:1163-1174.

Tsai LH, Gleeson JG (2005) Nucleokinesis in neuronal migration. Neuron 46:383-388.

Tubb B, Mulholland DJ, Vogl W, Lan ZJ, Niederberger C, Cooney A, Bryan J (2002) Testis fascin (FSCN3): a novel paralog of the actin-bundling protein fascin expressed specifically in the elongate spermatid head. Experimental cell research 275:92-109.

Urban E, Jacob S, Nemethova M, Resch GP, Small JV (2010) Electron tomography reveals unbranched networks of actin filaments in lamellipodia. Nature cell biology 12:429-435.

Valiente M, Marin O (2010) Neuronal migration mechanisms in development and disease. Current opinion in neurobiology 20:68-78.

Valley MT, Mullen TR, Schultz LC, Sagdullaev BT, Firestein S (2009) Ablation of mouse adult neurogenesis alters olfactory bulb structure and olfactory fear conditioning. Frontiers in neuroscience 3:51.

van Praag H, Schinder AF, Christie BR, Toni N, Palmer TD, Gage FH (2002) Functional neurogenesis in the adult hippocampus. Nature 415:1030-1034.

Vignjevic D, Kojima S, Aratyn Y, Danciu O, Svitkina T, Borisy GG (2006) Role of fascin in filopodial protrusion. The Journal of cell biology 174:863-875.

Vignjevic D, Schoumacher M, Gavert N, Janssen KP, Jih G, Lae M, Louvard D, Ben-Ze'ev A, Robine S (2007) Fascin, a novel target of beta-catenin-TCF signaling, is expressed at the invasive front of human colon cancer. Cancer research 67:6844-6853.

Vignjevic D, Yarar D, Welch MD, Peloquin J, Svitkina T, Borisy GG (2003) Formation of filopodia-like bundles in vitro from a dendritic network. The Journal of cell biology 160:951-962.

Voigt T (1989) Development of glial cells in the cerebral wall of ferrets: direct tracing of their transformation from radial glia into astrocytes. The Journal of comparative neurology 289:74-88.

Wang Z, Andrade N, Torp M, Wattananit S, Arvidsson A, Kokaia Z, Jorgensen JR, Lindvall O (2012) Meteorin is a chemokinetic factor in neuroblast migration and

promotes stroke-induced striatal neurogenesis. Journal of cerebral blood flow and metabolism : official journal of the International Society of Cerebral Blood Flow and Metabolism 32:387-398.

Ward M, McCann C, DeWulf M, Wu JY, Rao Y (2003) Distinguishing between directional guidance and motility regulation in neuronal migration. The Journal of neuroscience : the official journal of the Society for Neuroscience 23:5170-5177.

Ward ME, Rao Y (2005) Investigations of neuronal migration in the central nervous system. Methods in molecular biology 294:137-156.

Webb DJ, Asmussen H, Murase S, Horwitz AF (2002) Cell migration in slice cultures. Methods in cell biology 69:341-358.

Whitman MC, Fan W, Rela L, Rodriguez-Gil DJ, Greer CA (2009) Blood vessels form a migratory scaffold in the rostral migratory stream. The Journal of comparative neurology 516:94-104.

Wichterle H, Garcia-Verdugo JM, Alvarez-Buylla A (1997) Direct evidence for homotypic, glia-independent neuronal migration. Neuron 18:779-791.

Wilkinson SE, Parker PJ, Nixon JS (1993) Isoenzyme specificity of bisindolylmaleimides, selective inhibitors of protein kinase C. The Biochemical journal 294 (Pt 2):335-337.

Williams EJ, Walsh FS, Doherty P (2003) The FGF receptor uses the endocannabinoid signaling system to couple to an axonal growth response. The Journal of cell biology 160:481-486.

Williams G, Zentar MP, Gajendra S, Sonego M, Doherty P, Lalli G (2013) Transcriptional Basis for the Inhibition of Neural Stem Cell Proliferation and Migration by the TGFbeta-Family Member GDF11. PloS one 8:e78478.

Winner B, Cooper-Kuhn CM, Aigner R, Winkler J, Kuhn HG (2002) Long-term survival and cell death of newly generated neurons in the adult rat olfactory bulb. The European journal of neuroscience 16:1681-1689.

Winner B, Couillard-Despres S, Geyer M, Aigner R, Bogdahn U, Aigner L, Kuhn HG, Winkler J (2008) Dopaminergic lesion enhances growth factor-induced striatal neuroblast migration. Journal of neuropathology and experimental neurology 67:105-116.

Wittko IM, Schanzer A, Kuzmichev A, Schneider FT, Shibuya M, Raab S, Plate KH (2009) VEGFR-1 regulates adult olfactory bulb neurogenesis and migration of neural progenitors in the rostral migratory stream in vivo. The Journal of neuroscience : the official journal of the Society for Neuroscience 29:8704-8714.

Worth DC, Daly CN, Geraldo S, Oozeer F, Gordon-Weeks PR (2013) Drebrin contains a cryptic F-actin-bundling activity regulated by Cdk5 phosphorylation. The Journal of cell biology 202:793-806.

Worth DC, Parsons M (2010) Advances in imaging cell-matrix adhesions. Journal of cell science 123:3629-3638.

Wu W, Wong K, Chen J, Jiang Z, Dupuis S, Wu JY, Rao Y (1999) Directional guidance of neuronal migration in the olfactory system by the protein Slit. Nature 400:331-336.

Yamakita Y, Matsumura F, Yamashiro S (2009) Fascin1 is dispensable for mouse development but is favorable for neonatal survival. Cell motility and the cytoskeleton 66:524-534.

Yamakita Y, Ono S, Matsumura F, Yamashiro S (1996) Phosphorylation of human fascin inhibits its actin binding and bundling activities. The Journal of biological chemistry 271:12632-12638.

Yamashiro-Matsumura S, Matsumura F (1985) Purification and characterization of an F-actin-bundling 55-kilodalton protein from HeLa cells. The Journal of biological chemistry 260:5087-5097.

Yamashiro-Matsumura S, Matsumura F (1986) Intracellular localization of the 55-kD actin-bundling protein in cultured cells: spatial relationships with actin, alpha-actinin, tropomyosin, and fimbrin. The Journal of cell biology 103:631-640.

Yamashita T, Ninomiya M, Hernandez Acosta P, Garcia-Verdugo JM, Sunabori T, Sakaguchi M, Adachi K, Kojima T, Hirota Y, Kawase T, Araki N, Abe K, Okano H, Sawamoto K (2006) Subventricular zone-derived neuroblasts migrate and differentiate into mature neurons in the post-stroke adult striatum. The Journal of neuroscience : the official journal of the Society for Neuroscience 26:6627-6636.

Yan YP, Sailor KA, Lang BT, Park SW, Vemuganti R, Dempsey RJ (2007) Monocyte chemoattractant protein-1 plays a critical role in neuroblast migration after focal cerebral ischemia. Journal of cerebral blood flow and metabolism : official journal of the International Society of Cerebral Blood Flow and Metabolism 27:1213-1224.

Yuan TF, Arias-Carrion O (2011) Adult neurogenesis in the hypothalamus: evidence, functions, and implications. CNS & neurological disorders drug targets 10:433-439.

Zanet J, Jayo A, Plaza S, Millard T, Parsons M, Stramer B (2012) Fascin promotes filopodia formation independent of its role in actin bundling. The Journal of cell biology 197:477-486.

Zanet J, Stramer B, Millard T, Martin P, Payre F, Plaza S (2009) Fascin is required for blood cell migration during Drosophila embryogenesis. Development 136:2557-2565.

Zhang H, Vutskits L, Pepper MS, Kiss JZ (2003) VEGF is a chemoattractant for FGF-2-stimulated neural progenitors. The Journal of cell biology 163:1375-1384.

Zhang J, Fonovic M, Suyama K, Bogyo M, Scott MP (2009) Rab35 controls actin bundling by recruiting fascin as an effector protein. Science 325:1250-1254.

Zhang RL, LeTourneau Y, Gregg SR, Wang Y, Toh Y, Robin AM, Zhang ZG, Chopp M (2007) Neuroblast division during migration toward the ischemic striatum: a study of dynamic migratory and proliferative characteristics of neuroblasts from the subventricular zone. The Journal of neuroscience : the official journal of the Society for Neuroscience 27:3157-3162.

Zhao C, Deng W, Gage FH (2008) Mechanisms and functional implications of adult neurogenesis. Cell 132:645-660.

Zhou J, Shrikhande G, Xu J, McKay RM, Burns DK, Johnson JE, Parada LF (2011) Tsc1 mutant neural stem/progenitor cells exhibit migration deficits and give rise to subependymal lesions in the lateral ventricle. Genes & development 25:1595-1600.

Zigova T, Pencea V, Wiegand SJ, Luskin MB (1998) Intraventricular administration of BDNF increases the number of newly generated neurons in the adult olfactory bulb. Molecular and cellular neurosciences 11:234-245.

Zitt C, Strauss B, Schwarz EC, Spaeth N, Rast G, Hatzelmann A, Hoth M (2004) Potent inhibition of Ca2+ release-activated Ca2+ channels and T-lymphocyte activation by the pyrazole derivative BTP2. The Journal of biological chemistry 279:12427-12437.